

**PERFORMANCE EVALUATION OF CONTROL METHODS ON
THE WATER SIDE OF DRUM BOILERS**

A Thesis
Submitted to
the Temple University Graduate Board

in Partial Fulfillment
of the Requirements for the Degree of
Master of Science in Electrical Engineering

by
Robert A. Borzellieri, P.E.
December 2019

Thesis Committee
Dr. Saroj Biswas Department of ECE, Temple University
Dr. Li Bai Department of ECE, Temple University
Dr. Liang Du Department of ECE, Temple University
Dr. Greg Anderson Naval Surface Warfare Center Philadelphia

©

by

Robert A. Borzelleri, P.E.

December 2019

All Rights Reserved

ABSTRACT

Performance Evaluation of Control Methods on the Water Side of Drum Boilers

Robert A. Borzellieri, P.E.

Master of Science in Electrical Engineering

Temple University, December 2019

Dr Saroj K. Biswas, Chair

This thesis evaluates control strategies for a drum boiler unit. Drum Boilers are a highly nonlinear system, as there are non-minimum phase shrink-and-swell effects to account for. A more complex control strategy may prove to be a better option than what is used in industry today. The goal is to showcase different control strategies on the nonlinear system given specified design constraints, from three element cascade control with a feed forward, to using a Linear Quadratic Regulator (LQR), to the more contemporary Model Predictive Control (MPC).

The process is built around the Åström-Bell non-linear complex drum-boiler model, and is extended with super-heater and turbine dynamics using other known results. The model involves simplification of controlling heat flux instead of modeling the heat transfer and fuel combustion from the air side of the boiler. The implementation of the complete system is carried out in MatLab.

Simulation results are presented for the three element control method, the linear quadratic regulator (LQR) applied to a nonlinear system, and a model predictive control (MPC) algorithm to use on nonlinear systems. The simulation results are focused on automatic control operation and finding satisfactory response behaviors. The LQR and MPC approach assume full state feedback without the use of an observer.

The research shows that all of the controllers can meet the design criterion, however secondary effects cause both the Three element cascade PID controller and the LQR controllers to be less desirable than the MPC approach. A heuristic trial and error approach to tuning was used in all methods due to the highly coupled nature of the system. This evaluation of the types of controllers showcasing tuning to a specified design criterion proves that the controller type is more important than optimal tuning.

TABLE OF CONTENTS

ABSTRACT	iv
LIST OF FIGURES	ix
LIST OF TABLES	xiv
CHAPTERS	
1 INTRODUCTION	1
1.1 Overview of Steam Drum Control	1
1.2 Literature Review	2
1.3 Goals and Objectives of proposed research	3
1.4 Outline of the Thesis	4
2 CONTROL METHODS FOR NONLINEAR SYSTEMS	5
2.1 Three Element Level Control	6
2.1.1 Application in Boiler Controls	8
2.2 Linear Quadratic Regulator	8
2.3 Model Predictive Control	10
2.3.1 Discrete Time MPC Theory	10
2.3.2 Discrete Time MPC for Nonlinear Systems	14
2.4 Controller Comparison Methods	17
3 SYSTEM MODELING	19
3.1 Steam Property Modeling	19
3.2 Åström and Bell Model	22
3.2.1 Global Mass and Energy Balance	22
3.2.2 Distribution of Steam in Risers and Drum	23
3.3 Simulation of Åström and Bell Model	25
3.3.1 Equilibrium Values	27
3.3.2 Comparison of simulation and Åström and Bell's previous work	28

3.4	Expanded Model	62
3.4.1	Input Simplifications	62
3.4.2	Expanded Model with Simplified Inputs	64
3.4.3	Equilibrium Values	65
3.4.4	Open Loop Step Responses to Expanded Model	65
4	THREE ELEMENT CONTROL	78
4.1	Controller Design	78
4.2	Simulation Results	80
4.2.1	Level Step Increase Figures 4.1 - 4.3	81
4.2.2	Level Step Decrease Figures 4.4 - 4.6	86
4.2.3	Pressure Step Increase Figures 4.7 - 4.9	91
4.2.4	Pressure Step Decrease Figures 4.10 - 4.12	96
4.3	Controller Performance	101
5	LINEAR QUADRATIC REGULATOR	103
5.1	Controller Design	103
5.2	Simulation Results	108
5.2.1	Level Step Increase Figures 5.3-5.4	110
5.2.2	Level Step Decrease Figures 5.5-5.6	115
5.2.3	Pressure Step Increase Figures 5.7-5.8	120
5.2.4	Pressure Step Decrease Figures 5.9-5.10	125
5.3	Controller Performance	130
6	MODEL PREDICTIVE CONTROL	132
6.1	Controller Design	132
6.2	Simulation Results	138
6.2.1	Level Step Increase Figures 6.1 - 6.2	139
6.2.2	Level Step Decrease Figures 6.3 - 6.4	144
6.2.3	Pressure Step Increase Figures 6.5 - 6.6	149
6.2.4	Pressure Step Decrease Figures 6.7 - 6.8	154
6.3	Controller Performance	159
7	COMPARISON OF CONTROL METHODS	161
7.1	Simulation Results	161
7.1.1	Level Step Increase Figures	163
7.1.2	Level Step Decrease Figures	168
7.1.3	Pressure Step Increase Figures	173
7.1.4	Pressure Step Decrease Figures	178
7.2	Controller Performance	183

8 CONCLUSIONS	187
8.1 Summary of Results	187
8.2 Further Research	189
REFERENCES	191
APPENDICES	
A ADDITIONAL INFORMATION FROM SOURCES	194
B CONTROLLER COMPARISON GRAPHICS	198
C MATLAB FILES	215

LIST OF FIGURES

1.1	Drum Boiler Schematic [8]	2
2.1	Three Element Control [3]	6
2.2	Alternative Three Element Control [3]	7
3.1	Curve Fitting Steam Åström-Bell	20
3.2	Curve Fitting Steam	21
3.3	Drum Water Level Response to a step corresponding to 10 MW in fuel flow rate	29
3.4	Water Level Contribution to a step corresponding to 10 MW in fuel flow rate	30
3.5	Steam Level Contribution to a step corresponding to 10 MW in fuel flow rate	31
3.6	Drum Pressure Response to a step corresponding to 10 MW in fuel flow rate	32
3.7	Steam Volume Ratio Response to a step corresponding to 10 MW in fuel flow rate	33
3.8	Steam Quality Response to a step corresponding to 10 MW in fuel flow rate	34
3.9	Total Water Volume Response to a step corresponding to 10 MW in fuel flow rate	35
3.10	Volume of Steam in Drum Response to a step corresponding to 10 MW in fuel flow rate	36
3.11	Riser and Downcomer Flow Response to a step corresponding to 10 MW in fuel flow rate	37
3.12	Condensation Flow Response to a step corresponding to 10 MW in fuel flow rate	38
3.13	Drum Water Level Response to a step change of 10 kg/s in steam flow rate	39
3.14	Water Level Contribution to a step change of 10 kg/s in steam flow rate	40

3.15	Steam Level Contribution to a step change of 10 kg/s in steam flow rate	41
3.16	Drum Pressure Response to a step change of 10 kg/s in steam flow rate	42
3.17	Steam Volume Ratio Response to a step change of 10 kg/s in steam flow rate	43
3.18	Steam Quality Response to a step change of 10 kg/s in steam flow rate	44
3.19	Total Water Volume Response to a step change of 10 kg/s in steam flow rate	45
3.20	Volume of Steam in Drum Response to a step change of 10 kg/s in steam flow rate	46
3.21	Riser and Downcomer Flow Response to a step change of 10 kg/s in steam flow rate	47
3.22	Condensation Flow Response to a step change of 10 kg/s in steam flow rate	48
3.23	Drum Water Level Response to a step corresponding to 10 kg/s in feed water flow rate	49
3.24	Water Level Contribution to a step corresponding to 10 kg/s in feed water flow rate	50
3.25	Steam Level Contribution to a step corresponding to 10 kg/s in feed water flow rate	51
3.26	Drum Pressure Response to a step corresponding to 10 kg/s in feed water flow rate	52
3.27	Steam Volume Ratio Response to a step corresponding to 10 kg/s in feed water flow rate	53
3.28	Steam Quality Response to a step corresponding to 10 kg/s in feed water flow rate	54
3.29	Drum Water Level Response to a step corresponding to 10 ^O C Feed Water Temperature	55
3.30	Water Level Contribution to a step corresponding to 10 ^O C Feed Water Temperature	56
3.31	Steam Level Contribution to a step corresponding to 10 ^O C Feed Water Temperature	57
3.32	Drum Pressure Response to a step corresponding to 10 ^O C Feed Water Temperature	58
3.33	Steam Volume Ratio Response to a step corresponding to 10 ^O C Feed Water Temperature	59
3.34	Steam Quality Response to a step corresponding to 10 ^O C Feed Water Temperature	60
3.35	Drum Water Level Response to a step corresponding to 10 MW in fuel flow rate	67

3.36	Drum Pressure Response to a step corresponding to 10 MW in fuel flow rate	68
3.37	Volume of Total Water Response to a step corresponding to 10 MW in fuel flow rate	69
3.38	Steam Quality Response to a step corresponding to 10 MW in fuel flow rate	70
3.39	Volume of Steam in the Drum Response to a step corresponding to 10 MW in fuel flow rate	71
3.40	Drum Water Level Response to a step corresponding to 10 kg/s feed water flow rate	72
3.41	Drum Pressure Response to a step corresponding to 10 kg/s feed water flow rate	73
3.42	Volume of Total Water Response to a step corresponding to 10 kg/s feed water flow rate	74
3.43	Steam Quality Response to a step corresponding to 10 kg/s feed water flow rate	75
3.44	Volume of Steam in the Drum Response to a step corresponding to 10 kg/s feed water flow rate	76
4.1	Controlled Variables PID Response to Drum Level step of 0.1	82
4.2	Controller Inputs PID Response to Drum Level step of 0.1	84
4.3	Cascaded PID Controller Response to Drum Level step of 0.1	85
4.4	Controlled Variables PID Response to Drum Level step of -0.1	87
4.5	Controller Inputs PID Response to Drum Level step of -0.1	89
4.6	Cascaded PID Controller Response to Drum Level step of -0.1	90
4.7	Controlled Variables PID Response to Drum Pressure step of 0.1	92
4.8	Controller Inputs PID Response to Drum Pressure step of 0.1	94
4.9	Cascaded PID Controller Response to Drum Pressure step of 0.1	95
4.10	Controlled Variables PID Response to Drum Pressure step of -0.1	97
4.11	Controller Inputs PID Response to Drum Pressure step of -0.1	99
4.12	Cascaded PID Controller Response to Drum Pressure step of -0.1	100
5.1	LQR Block Diagram [10]	104
5.2	Linear-Quadratic-Integral (LQI) Block Diagram [10]	106
5.3	Controlled Variables LQR Response to Drum Level step of 0.1	111
5.4	Controller Inputs LQR Response to Drum Level step of 0.1	113
5.5	Controlled Variables LQR Response to Drum Level step of -0.1	116
5.6	Controller Inputs LQR Response to Drum Level step of -0.1	118
5.7	Controlled Variables LQR Response to Drum Pressure step of 0.1	121
5.8	Controller Inputs LQR Response to Drum Pressure step of 0.1	123
5.9	Controlled Variables LQR Response to Drum Pressure step of -0.1	126

5.10	Controller Inputs LQR Response to Drum Pressure step of -0.1	128
6.1	Controlled Variables MPC Response to Drum Level step of 0.1	140
6.2	Controller Inputs MPC Response to Drum Level step of 0.1	142
6.3	Controlled Variables MPC Response to Drum Level step of -0.1	145
6.4	Controller Inputs MPC Response to Drum Level step of -0.1	147
6.5	Controlled Variables MPC Response to Drum Pressure step of 0.1	150
6.6	Controller Inputs MPC Response to Drum Pressure step of 0.1	152
6.7	Controlled Variables MPC Response to Drum Pressure step of -0.1	155
6.8	Controller Inputs MPC Response to Drum Pressure step of -0.1	157
7.1	Controlled Variables Response to Drum Level step of 0.1 at High Load	164
7.2	Controller Input Response to Drum Level step of 0.1 at High Load	166
7.3	Controlled Variables Response to Drum Level step of -0.1 at High Load	169
7.4	Controller Input Response to Drum Level step of -0.1 at High Load	171
7.5	Controlled Variables Response to Drum Pressure step of 0.1 at High Load	174
7.6	Controller Input Response to Drum Pressure step of 0.1 at High Load	176
7.7	Controlled Variables Response to Drum Pressure step of -0.1 at High Load	179
7.8	Controller Input Response to Drum Pressure step of -0.1 at High Load	181
B.1	Controlled Variables Response to Drum Level step of 0.1 at Low Load	199
B.2	Controller Input Response to Drum Level step of 0.1 at Low Load	200
B.3	Controlled Variables Response to Drum Level step of -0.1 at Low Load	201
B.4	Controller Input Response to Drum Level step of -0.1 at Low Load	202
B.5	Controlled Variables Response to Drum Pressure step of 0.1	203
B.6	Controller Input Response to Drum Pressure step of 0.1 at Low Load	204
B.7	Controlled Variables Response to Drum Pressure step of -0.1 at Low Load	205

B.8	Controller Input Response to Drum Pressure step of -0.1 at Low Load	206
B.9	Controlled Variables Response to Drum Level step of 0.1 at Medium Load	207
B.10	Controller Input Response to Drum Level step of 0.1 at Medium Load	208
B.11	Controlled Variables Response to Drum Level step of 0.1 at Medium Load	209
B.12	Controller Input Response to Drum Level step of -0.1 at Medium Load	210
B.13	Controlled Variables Response to Drum Pressure step of 0.1 at Medium Load	211
B.14	Controller Input Response to Drum Pressure step of 0.1 at Medium Load	212
B.15	Controlled Variables Response to Drum Pressure step of 0.1 at Medium Load	213
B.16	Controller Input Response to Drum Pressure step of -0.1 at Medium Load	214

LIST OF TABLES

3.1	Original Steam Table Models	20
3.2	Expanded Steam Table Models	21
4.1	PID Controller Performance Parameters: Level Step Increase .	83
4.2	PID Controller Input Performance Parameters: Level Step Increase	85
4.3	PID Controller Performance Parameters: Level Step Decrease	88
4.4	PID Controller Input Performance Parameters: Level Step Decrease	90
4.5	PID Controller Performance Parameters: Pressure Step Increase	93
4.6	PID Controller Input Performance Parameters: Pressure Step Increase	95
4.7	PID Controller Performance Parameters: Pressure Step Increase	98
4.8	PID Controller Input Performance Parameters: Pressure Step Increase	100
4.9	PID Controller Percent Overshoot	101
4.10	PID Controller Settling Time	101
4.11	PID Controlled Variable Energy	101
4.12	PID Controller Inputs Energy	102
4.13	PID State Variable Energy	102
5.1	LQR Controller Performance Parameters: Level Step Increase	112
5.2	LQR Controller Input Performance Parameters: Level Step Increase	114
5.3	LQR Controller Performance Parameters: Level Step Decrease	117
5.4	LQR Controller Input Performance Parameters: Level Step Decrease	119
5.5	LQR Controller Performance Parameters: Pressure Step Increase	122
5.6	LQR Controller Input Performance Parameters: Pressure Step Increase	124
5.7	LQR Controller Performance Parameters: Pressure Step Increase	127

5.8	LQR Controller Input Performance Parameters: Pressure Step Increase	129
5.9	LQR Controller Percent Overshoot	130
5.10	LQR Controller Settling Time	130
5.11	LQR Controlled Variable Energy	131
5.12	LQR Controller Inputs Energy	131
5.13	LQR State Variable Energy	131
6.1	MPC Controller Performance Parameters: Level Step Increase	141
6.2	MPC Controller Input Performance Parameters: Level Step Increase	143
6.3	MPC Controller Performance Parameters: Level Step Decrease	146
6.4	MPC Controller Input Performance Parameters: Level Step Decrease	148
6.5	MPC Controller Performance Parameters: Pressure Step Increase	151
6.6	MPC Controller Input Performance Parameters: Pressure Step Increase	153
6.7	MPC Controller Performance Parameters: Pressure Step Increase	156
6.8	MPC Controller Input Performance Parameters: Pressure Step Increase	158
6.9	MPC Controller Percent Overshoot	159
6.10	MPC Controller Settling Time	159
6.11	MPC Controlled Variable Energy	159
6.12	MPC Controller Inputs Energy	160
6.13	MPC State Variable Energy	160
7.1	Controller Performance Parameters: Level Step Increase . . .	165
7.2	Controller Input Performance Parameters: Level Step Increase	167
7.3	Controller Performance Parameters: Level Step Decrease . . .	170
7.4	Controller Input Performance Parameters: Pressure Step Decrease	172
7.5	Controller Performance Parameters: Pressure Step Increase . .	175
7.6	Controller Input Performance Parameters: Pressure Step Increase	177
7.7	Controller Performance Parameters: Pressure Step Decrease .	180
7.8	Controller Input Performance Parameters: Pressure Step Decrease	182
7.9	MPC Controller Percent Overshoot	183
7.10	MPC Controller Settling Time	183
7.11	Controlled Variable Energy	184
7.12	Controller Inputs Energy	184
7.13	Controller State Variables Energy	185

CHAPTER 1

INTRODUCTION

1.1 Overview of Steam Drum Control

Industrial Boiler systems are used for many purposes, from supplying steam to various locations like hospitals to propulsion systems to the more common power generation. Boilers are now operating at higher pressure and are being built smaller than they were, and causes faster process control responses [5]. Because of high pressure operation, boilers must have an adequate level of control to stay safe. Due to the phenomena of minimum phase behavior and the shrink and swell effect, the boiler drum level control initially reacts in direct opposition to what is required for process stability. Shrink and swell refers to a phenomenon that when the drum pressure drops, some water in the tubes flashes, and those steam bubbles push water in the tubes above them up into the drum, temporarily raising the drum level. Then when the system stabilizes and those steam bubbles either collapse or reach the drum, the tubes rapidly refill with water from the drum, dropping its level. The effect is asymmetrical - when drum pressure rises due to falling steam demand, it temporarily suppresses the production of steam in the tubes but the effect is more subtle. [3] This effect must then be accounted for if the system is to be properly controlled. A Drum Boiler Schematic can be seen in Figure 1.1.

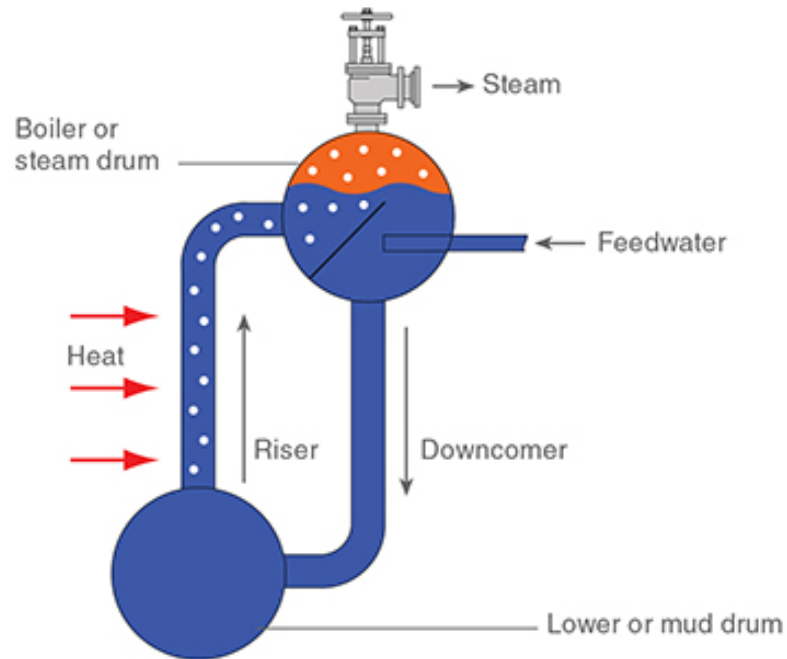


Figure 1.1: Drum Boiler Schematic [8]

1.2 Literature Review

Mathematical models for a Boiler-Turbine system exist in the literature, however most are simplified to not include the dynamics of the drum's water level nor the shrink and swell effect. The model developed by Åström and Bell [7] provides sufficient detail to model these parameters. An extension of this model was developed by Iacob and Andreescu [13] which provides modeling for the feed-water valve, fuel flow valve, steam valve, throttle pressure, and power output.

Steam boiler is a highly nonlinear system which poses significant complexities in its control system design and analysis. Conventional control method is known as *three element control* in the industry, which is effectively a PID type control system that regulates three measured quantities in the boiler, such as liquid level in the drum, feed water flow, and steam flow leaving the drum. The three-element control is based on linearized dynamics of the

boiler that provides the required boiler performance when the deviation of the state variables remains relatively small with respect to the nominal state. This research investigates design of boiler control system that is expected to provide a better system performance when large variations of the system state may occur.

1.3 Goals and Objectives of proposed research

The broad objective of this research is to investigate performance of drum boilers under different control applications. In particular, we investigate three control methods: conventional three-element control, Linear Quadratic Regulator (LQR), and Model Predictive control (MPC). Conventional three-element control and linearized LQR control methods rely on a linearized model of the boiler. Both have limited performance as the boiler must operate near the nominal operating point of the system. This research explores the application of the Model Predictive Control (MPC) for the design of the boiler control system. In recent years, MPC control method has found significant attention in industry [17, 12, 2, 16] and academia [9, 15, 18] alike with excellent performance. There are several advantages of the MPC control system that make it an ideal candidate for its application to the boiler control, such as 1) it does not require that the system operate near a nominal operating point, 2) it is easy to include various constraints in the control design, and 3) it is possible to design a controller even when the system model is not precisely known.

The goals of this thesis are

- Review mathematical model of the steam boiler
- Investigate limitations of conventional control systems, such as PID and LQR
- Apply model predictive control system to the steam boiler and analyze

its performance

The developed control system will be evaluated by simulation only as there are no experimental facilities available. For the mathematical model of the boiler, we will consider the Åström and Bell [7] model which is quite well known in the literature. The closed loop system will be analyzed in Matlab/Simulink environment under various operating conditions.

1.4 Outline of the Thesis

This following is an outline of the rest of this thesis proposal: Chapter 2 presents the basics of the three-element control and the LQR control which will be followed by details of Model Predictive Control design method. In Chapter 3 we present the Åström and Bell [7] model of the steam boiler and the model validation. Chapter 4 presents the formulation and simulation results of three-element control. Chapter 5 presents LQR control methods, including reference tracking, and LQR simulation results. Chapter 6 presents MPC control formulation, the nonlinear control algorithm, and simulation results. Chapter 7 aggregates the simulation results from Chapters 5, 6, and 7. Chapter 8 presents the conclusions and outlines plans for further research.

CHAPTER 2

CONTROL METHODS FOR NONLINEAR SYSTEMS

The boiler system is inherently nonlinear so that an adequate control method must be implemented for its safe and efficient operation. Common industry practice in this respect is to implement the three-element control, which is fundamentally the PID control structure which is first discussed. Then we also present the linear quadratic control (LRQ) which is a powerful control method used in many industrial applications, which however has its limitations when applied to nonlinear systems. In fact, both PID and LQR control methods cannot be used for nonlinear systems unless the system model is linearized. As is well known, the linearized model is valid only if the process operates in a small neighborhood with respect to the nominal operating state. For large variations in the operating state, it is necessary that a nonlinear control method be utilized. The Model Predictive Control (MPC) is one of the powerful, yet simple, methods for controlling nonlinear systems, and has attracted the attention of engineers in the profession. This chapter introduces the fundamentals of the MPC control method, which will be used in this thesis for controlling the steam boiler.

2.1 Three Element Level Control

Three Element Control refers to the number of measurements or Process Variables (PV) that are used in the control calculation. These measured elements are:

- l - Liquid Level in the Drum
- q_f - Feed-water Flow into the Drum
- q_s - Steam Flow leaving the Drum

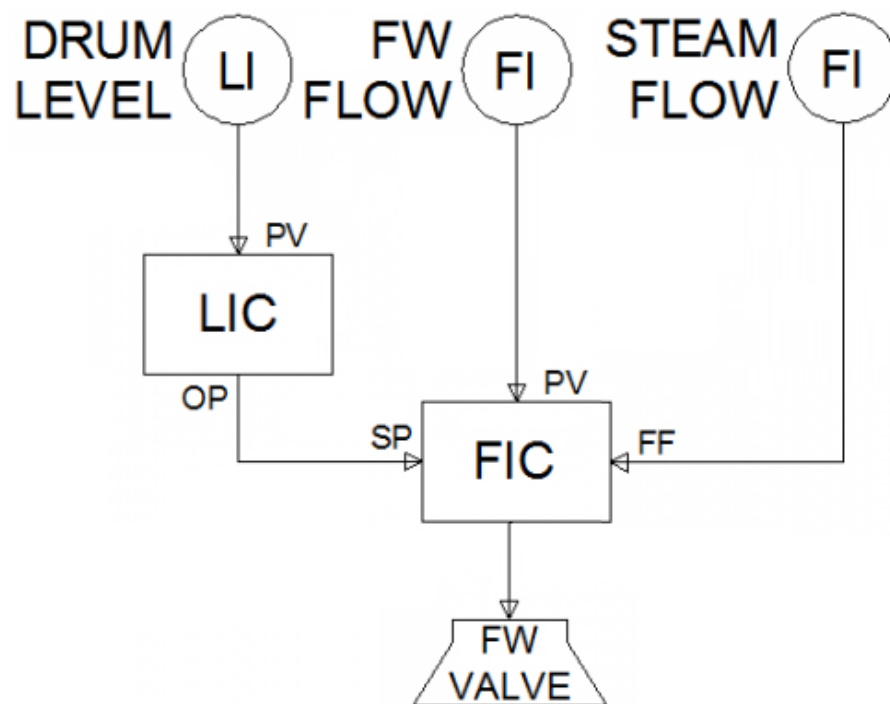


Figure 2.1: Three Element Control [3]

Three Element Control [3] consists of two PI(D) loops in cascade control, and a feed forward control. This can be seen in Figure 2.1. The two loops in cascade are a fast acting internal loop for feed-water and a slower external loop for drum level. In a cascade control scenario, the external loop's output

(OP) is used as the Set Point (SP) for the inner loop. The feed forward (FF) of steam flow is applied to the internal loop. An alternative, and less popular configuration can have the feed forward on the outer loop, as seen in Figure 2.2. It should be noted that a cascaded control setup has several drawbacks, including integral windup due to the inner loop being at a physical limit but the outer loop still attempting to control.

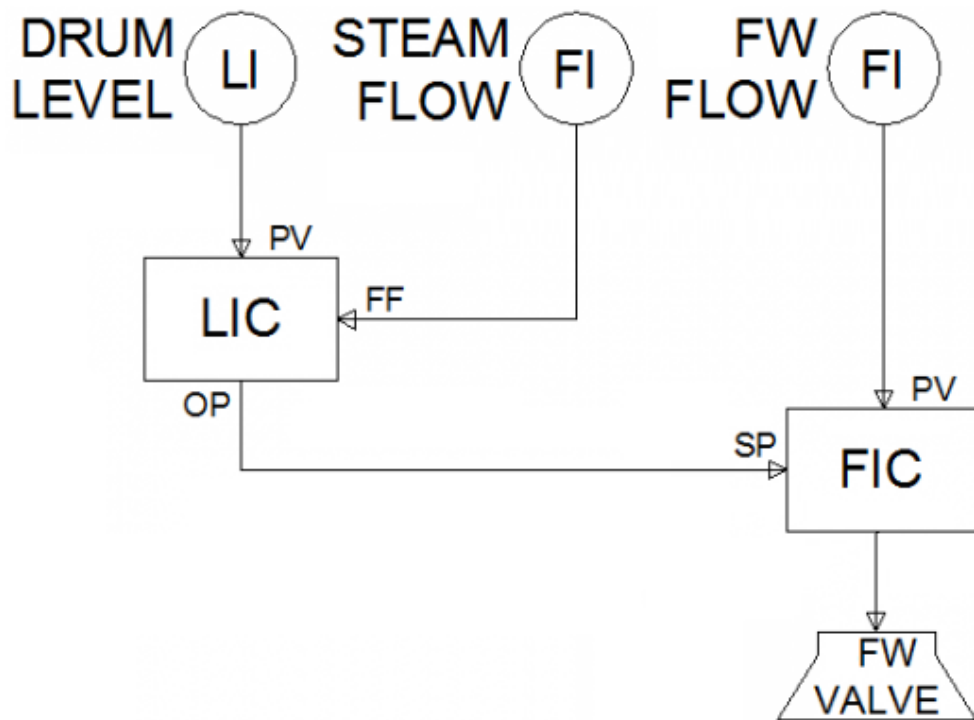


Figure 2.2: Alternative Three Element Control [3]

Single Element and Two Element control are used at lower feed-water flows or lower load, where the shrink and swell effects are not as prevalent. Single Element control is a PI(D) Level control loop, and Two Element control is the same as Three Element control, without the feed forward.

In this control mode, Throttle Pressure is usually controlled by a simple PI(D) loop. Total power output may be controlled instead of throttle pressure. The turbine is often modeled as a first order system with the input of Throttle

Pressure and the output of mechanical power [5].

2.1.1 Application in Boiler Controls

By design, the PID control is used to minimize error with respect to a desired operating reference using specific tuning parameters. It does not allow any optimization of the process operation, such as minimization of fuel consumption (or control energy), nor does it account for any boundary conditions. Industry experts also use adaptive tuning controllers due to the fact that the tuning parameters can vary with load. Optimization of process operation could be achieved using optimal and robust control methods as presented next.

2.2 Linear Quadratic Regulator

The Linear Quadratic Regulator (LQR) is a powerful method for optimizing process operation. In this method, the system performance is defined in terms of a cost function which is a measure of cost of state error and cost of control. The objective is to find a control that minimizes the cost function. For a discrete time linear system,

$$x(k+1) = Ax(k) + Bu(k) \quad (2.1)$$

where x_k is the state vector and u_k is the control vector, and the state and control matrices A and B are of compatible dimension. The cost function is taken as

$$J = \sum_0^{\infty} (x_k^T Q x_k + u_k^T R u_k) \quad (2.2)$$

where Q is a positive semidefinite matrix and R is a positive definite matrix. Here the first term of the cost function represents the cost due to state error with respect to the reference (which is taken as zero in this case), and the cost

of control. The optimal control sequence that minimizes the cost function is given by the discrete time Riccati equation

$$\begin{aligned}
 P &= A^T P A - (A^T P B)(R + B^T P B)^{-1}(B^T P A) + Q \\
 K_{lqr} &= (R + B^T P B^{-1})(B^T P A) \\
 u_k &= -K_{lqr} x_k
 \end{aligned} \tag{2.3}$$

By solving the Riccati equation, one obtains the matrix P which is a positive symmetric definite matrix, which is then used to find the feedback gain K_{lqr} for the control loop. In this method, the Riccati matrix P can be computed before the control loop initiates. From the design perspective, one must choose the appropriate weighting matrices Q and R matrices so as to obtain the desired closed loop performance.

It is important to note that the linear quadratic regulator as discussed above applies to linear systems only. However there are many practical systems, including the steam boiler discussed in the thesis, are described by nonlinear system model. For nonlinear systems, one can linearize the system model and then apply the LQR theory. However the drawback is that this approach works well only when the actual nonlinear system operates within a small neighborhood of the operating point. For large variations of the system state, the results are usually not acceptable.

There is some research in applying LQR methodologies to nonlinear systems using the State-Dependent Riccati Equation [11]. In this method, the one derives the Riccati equation in which the system model matrices is actually dependent on the current system state. So fundamentally, this means that the Riccati equation must be solved in real time for each sampling time before the control input is computed. This is not a trivial job as it takes significant computing resources to solve the Riccati differential equations.

2.3 Model Predictive Control

Model predictive control (MPC) [17] is a popular control method that has found many applications in chemical industries. MPC is an advanced control method that optimizes the current state satisfying process constraints while at the same time using predicted information of system state in future time slots. MPC control strategies are characterized by an explicitly and separately identifiable model of the controlled system. This model is used to calculate the behavior of the plant with the future control signal as adjustable variables.

MPC has direct links to the classical linear quadratic regulator (LQR) in continuous time and discrete time when using a long prediction horizon. The key difference between MPC and LQR is that the MPC solves the optimization problem using a moving time horizon window and optimized along the entire time horizon, while LQR solves the same problem within a fixed window and solves for a single optimal solution.

2.3.1 Discrete Time MPC Theory

The MPC control method is a receding horizon control method in which one first finds the optimal solution for a predicted time horizon, but apply the control for only one time step. The process is then repeated for future time slots. Consider the linear system in discrete time

$$\begin{aligned}x(k+1) &= Ax(k) + Bu(k) \\ y(k) &= Cx(k)\end{aligned}\tag{2.4}$$

Denote the control signals for the entire control horizon starting from time slot k_i as

$$U(k_i) = \{u(k_i), u(k_i + 1), \dots, u(k_i + N_c + 1)\}\tag{2.5}$$

where N_c is the Control Horizon (or the number of steps the controller will use for optimal control each cycle). Then future system States can be denoted as:

$$\begin{aligned}
x(k_i + 1|k_i) &= Ax(k_i) + Bu(k_i) \\
x(k_i + 2|k_i) &= Ax(k_i + 1|k_i) + Bu(k_i + 1) \\
&= A^2x(k_i) + ABu(k_i) + Bu(k_i + 1) \\
x(k_i + 3|k_i) &= Ax(k_i + 2|k_i) + Bu(k_i + 2) \\
&= A^3x(k_i) + A^2Bu(k_i) + ABu(k_i + 1) + Bu(k_i + 2) \\
x(k_i + N_p|k_i) &= A^{N_p}x(k_i) + A^{N_p-1}Bu(k_i + 1 - 1) + \dots \\
&\quad \dots + A^{N_p-N_c}Bu(k_i + N_c - 1)
\end{aligned} \tag{2.6}$$

where N_p is the Prediction Horizon (or the number of samples the model will look into the future).

Using the above equation, future Controlled Outputs can be computed as:

$$\begin{aligned}
y(k_i) &= Cx(k_i) \\
y(k_i + 1|k_i) &= CAx(k_i) + CBu(k_i) \\
y(k_i + 2|k_i) &= CA^2x(k_i) + CABu(k_i) + CBu(k_i + 1) \\
y(k_i + 3|k_i) &= CA^3x(k_i) + CA^2Bu(k_i) + CABu(k_i + 1) + CBu(k_i + 2) \\
y(k_i + N_p|k_i) &= CA^{N_p}x(k_i) + CA^{N_p-1}Bu(k_i + 1 - 1) + \dots \\
&\quad \dots + CA^{N_p-N_c}Bu(k_i + N_c - 1)
\end{aligned} \tag{2.7}$$

The control horizon N_c is chosen to be less than (or equal to) the prediction horizon N_p . The control horizon is usually chosen to be less than the prediction horizon for processing speed. It should be noted that all predicted variables are calculated from the current state, future control movements, and the model information. The above equations then can be expressed in matrix form as:

$$Y = Fx(k_i) + \Phi U(k_i) \tag{2.8}$$

where

$$Y = \begin{bmatrix} y(k_i + 1|k_i) \\ y(k_i + 2|k_i) \\ \vdots \\ y(k_i + N_p|k_i) \end{bmatrix},$$

$$U = \begin{bmatrix} u(k_i) \\ u(k_i + 1) \\ \vdots \\ u(k_i + N_c - 1) \end{bmatrix}$$

$$F = \begin{bmatrix} CA \\ CA^2 \\ \vdots \\ CA^{N_p} \end{bmatrix}$$

(2.9)

$$\Phi = \begin{bmatrix} CB & 0 & 0 & \dots & 0 \\ CAB & CB & 0 & \dots & 0 \\ CA^2B & CAB & CB & \dots & 0 \\ \vdots & \vdots & \vdots & \ddots & \vdots \\ CA^{N_p-1}B & CA^{N_p-2}B & CA^{N_p-3}B & \dots & CA^{N_p-N_c}B \end{bmatrix}$$

Suppose the control objective is for the system output $y(k_i)$, $y(k_i + 1)$, \dots , $y(k_i + N_p)$ to follow a desired output. Define the set-point desired reference as

$$R_s = \overline{R}_s r(k_i)$$

$$\overline{R}_s^T = \overbrace{\begin{bmatrix} \underbrace{\text{size}(r)}_I & I & \dots & I \end{bmatrix}}^{N_p} \quad (2.10)$$

i.e., \overline{R}_s is a repeated block matrix of N_p identity matrices. The identity matrices are sized based off of the number of reference inputs.

To minimize the tracking error, define the cost function

$$J(U) = \frac{1}{2}(R_s - Y)^T Q(R_s - Y) + \frac{1}{2}U^T R U \quad (2.11)$$

where Q and R are positive definite weighting matrices. Clearly, the first term minimizes the set-point tracking error and the second term minimizes the cost of control. The cost function is then minimized subject to the constraint (2.8).

Substituting equation (2.8) in the above equation, and differentiating with respect to U , we obtain

$$\frac{\partial J}{\partial U} = -\Phi^T Q(R_s - Fx(k_i)) + (\Phi^T Q\Phi + R)U = 0$$

which gives the optimal tracking control sequence as

$$U(k_i) = (\Phi^T Q\Phi + R)^{-1} \Phi^T Q(R_s - Fx(k_i)) \quad (2.12)$$

For closed loop MPC control method, a receding horizon concept is used, and only the first element of the control vector U is used at time slot k_i , i.e.,

$$\begin{aligned} u(k_i) &= \overbrace{\begin{bmatrix} I & 0 & \dots & 0 \end{bmatrix}}^{N_c} U(k_i) \\ &= \overbrace{\begin{bmatrix} I & 0 & \dots & 0 \end{bmatrix}}^{N_c} (\Phi^T Q\Phi + R)^{-1} \Phi^T Q(\bar{R}_s r(k_i) - Fx(k_i)) \\ &= K_y r(k_i) - K_{mpc} x(k_i) \end{aligned} \quad (2.13)$$

where:

$$K_y = \overbrace{\begin{bmatrix} I & 0 & \dots & 0 \end{bmatrix}}^{N_c} (\Phi^T Q\Phi + R)^{-1} \Phi^T Q \bar{R}_s \quad (2.14)$$

$$K_{mpc} = \overbrace{\begin{bmatrix} I & 0 & \dots & 0 \end{bmatrix}}^{N_c} (\Phi^T Q\Phi + R)^{-1} \Phi^T Q F \quad (2.15)$$

Substituting the above control in the system model (2.4), we obtain

$$\begin{aligned} x(k+1) &= Ax(k) + B(K_y r(k_i) - K_{mpc} x(k_i)) \\ &= (A - BK_{mpc})x(k_i) + BK_y r(k_i) \\ &= A_{closed} x(k) + B_{closed} r(k_i) \end{aligned} \quad (2.16)$$

where

$$\begin{aligned} A_{closed} &= A - BK_{mpc} \\ B_{closed} &= BK_y \end{aligned} \tag{2.17}$$

The process is then repeated for every time slot in the control horizon. This completes the MPC control concept for the discrete time linear system.

2.3.2 Discrete Time MPC for Nonlinear Systems

The MPC control described above can be extended for nonlinear systems. The basic idea is to linearize the nonlinear system with respect to the current state, and then use the MPC control for one time slot using the method described in the previous section. Then for the next time slot, the nonlinear system is linearized again using the updated system state, which is followed by a new computation of MPC control. The process is continued till the end of desired control horizon.

Consider the nonlinear system given by

$$\begin{aligned} \dot{x}(t) &= f(x(t), u(t)) \\ y(t) &= g(x(t), u(t)) \end{aligned} \tag{2.18}$$

The nonlinear system is then linearized at the current time slot k_i using $\{x(k_i), u(k_i)\}$ to obtain

$$\begin{aligned} \frac{\partial \Delta x(t)}{dt} &= A_i^c \Delta x(t) + B_i^c \Delta u(t) \\ \Delta y(t) &= C_i^c \Delta x(t) + D_i^c \Delta u(t) \end{aligned} \tag{2.19}$$

where

$$\begin{aligned}
A_i^c &= \left. \frac{\partial f(x(t), u(t))}{\partial x} \right|_{x(t), u(t)} \\
B_i^c &= \left. \frac{\partial f(x(t), u(t))}{\partial u} \right|_{x(t), u(t)} \\
C_i^c &= \left. \frac{\partial g(x(t), u(t))}{\partial x} \right|_{x(t), u(t)} \\
D_i^c &= \left. \frac{\partial g(x(t), u(t))}{\partial u} \right|_{x(t), u(t)}
\end{aligned} \tag{2.20}$$

The above linearized system is then expressed as a discrete time equation as

$$\begin{aligned}
\Delta x(k_i + 1) &= A_i \Delta x(k_i) + B_i \Delta u(k_i) \\
\Delta y(k_i) &= C_i \Delta x(k_i) + D_i \Delta u(k_i) \\
\Delta x(k_i + 1) &= \Delta x(t + T_s)
\end{aligned} \tag{2.21}$$

where the various matrices are

$$\begin{aligned}
A_i &= e^{A_i^c T_s} \\
B_i &= \left(\int_0^{T_s} e^{A_i^c \tau} d\tau \right) B_i^c \\
C_i &= C_i^c \\
D_i &= D_i^c
\end{aligned} \tag{2.22}$$

Note that the system matrices in the above equation will vary for each time slot, and must be updated within the control loop.

At this point the MPC algorithm described in the previous section are applied to the linearized system (2.21), and the calculated control signal is applied for one time step. The process is then repeated until the end of the control horizon.

The algorithm can be summarized as follows:

Algorithm 2.1 *Implementation of MPC on Nonlinear Systems*

1. Linearize the continuous time system with respect to the current state $\{x(t), u(t)\}$.

- $\dot{x} = f(x(t), u(t)) \rightarrow \frac{\partial \Delta x(t)}{dt} = A_{ic}^c \Delta x(t) + B_{ic}^c \Delta u(t)$

2. Find the discrete time model of the linearized system at slot k_i .

- $\frac{\partial \Delta x(t)}{dt} = A_{ic}^c \Delta x(t) + B_{ic}^c \Delta u(t) \rightarrow \Delta x(k_i + 1) = A_i \Delta x(k_i) + B_i \Delta u(k_i)$

3. Compute the predicted control path and optimal control signals

- $A_i, B_i, C_i \rightarrow \Phi_i, F_i, R_{s_i}$

4. Compute the MPC gains using Φ_i , F_i , and R_{s_i} and a finite horizon.

- $\Phi_i, F_i, R_{s_i} \rightarrow U(k_i) \rightarrow u(k_i) = \overbrace{\begin{bmatrix} I & 0 & \dots & 0 \end{bmatrix}}^{N_c} U(k_i)$

- $K_{y_i} = \begin{bmatrix} I & 0 & \dots & 0 \end{bmatrix} (\Phi_i^T Q \Phi_i + R)^{-1} \Phi_i^T Q \bar{R}_s$

- $K_{mpc_i} = \begin{bmatrix} I & 0 & \dots & 0 \end{bmatrix} (\Phi_i^T Q \Phi_i + R)^{-1} \Phi_i^T Q F_i$

- *Note: N_p , N_c , Q , and R are design constants and do not change during each linearization.*

5. Calculate and apply the control signal $u(k_i)$.

- $u(k_i) = K_{y_i} r(k_i) - K_{mpc_i} x(k_i)$

6. Measure the updated system response $x(k_i + 1)$

- $x(k_i + 1) = x(t + Ts) = x(k_i) + f(x(k_i), u(k_i))Ts$

7. Repeat from Step 1.

It is clear from the above that MPC control for nonlinear systems involves significant amount of computation that must be completed within the sampling time. This includes linearization of the system at the current time slot and computation of MPC feedback gains and computation of the control signal for the next time slot. Although it requires additional computing power, the MPC method has been successfully implemented in many process control applications. The reason is that the method is fundamentally simple and can be used to optimize the system performance even when the system model is not accurately known.

2.4 Controller Comparison Methods

Controller performance will be defined using percent overshoot, settling time, and signal energy. These metrics will be used to compare the various controller types in a later chapter.

Percent Overshoot and Settling Time as defined can only be calculated when a change in reference is made. While the output (Y) may have more than one element, only the element that has its corresponding reference (R) changed as a step function can have these parameters calculated. This is due to defining the parameters with respect to the change in reference.

Percent overshoot will be calculated as seen in Equation (2.23):

$$\%Overshoot = \frac{\max(y_{step}) - \max(r_{step})}{\max(r_{step}) - \min(r_{step})} \quad (2.23)$$

Settling Time will be calculated as seen in Equation (2.24):

$$t_{settle} = \min(t) \begin{cases} y_{step}(t) \geq 1.02(\max(r_{step}) - \min(r_{step})) + \max(r_{step}) \\ y_{step}(t) \leq 0.98(\max(r_{step}) - \min(r_{step})) + \max(r_{step}) \end{cases} \quad (2.24)$$

As defined there is no way to calculate Percent Overshoot or Settling time for the controlled output when it deviates from a constant set point, which may happen when a coupled variable causes a disturbance. The concept of

Signal Energy can be borrowed from the field of signal processing, as it is a method to characterize a signal. This is an abstract concept, and should not be confused with kinetic or potential energy. Signal Energy is defined as:

$$E_\gamma = \langle \gamma [n], \gamma [n] \rangle = \sum |\gamma [n]|^2 \quad (2.25)$$

Signal Energy for Controlled Variables Deviation will be calculated as

$$E_y = \sum |err [n]|^2 = \sum |y [n] - r [n]|^2 \quad (2.26)$$

Signal Energy for Control Inputs will be calculated as:

$$E_u = \sum |u [n]|^2 = \sum |u [n] - u [0]|^2 \quad (2.27)$$

Signal Energy for Control States will be calculated as:

$$E_x = \sum |x [n]|^2 = \sum |x [n] - x [0]|^2 \quad (2.28)$$

Input Energy and State Energy (2.27)-(2.28) have a $\gamma[0]$ term to allow for comparisons across different loads.

The controller gains will be designed to the following parameters:

- 15% Overshoot for a Drum Level step at High load
- 450 seconds of Settling Time for a Drum Level step at High Load
- Drum Pressure will remain stable
- Drum Level will remain stable for other disturbances (such as a Drum Pressure Step)

The control system methodologies will then be compared in in the following manor, all using the same gains designed above:

- Compare the effects of different loads to the controller (Chapters 4, 5, 6)
- Compare the % overshoot and settling time for the step function of other controlled variables (Chapters 4, 5, 6)
- Compare various controller performance in terms of energy used (Chapter 7)

CHAPTER 3

SYSTEM MODELING

To simulate a steam drum and boiler, a model must be created. A highly praised model used in other research is the Åström-Bell non-linear drum-boiler model [7]. This model can be expanded upon as it uses an approximation of steam properties. Expanding the Åström-Bell second order model to a more accurately fit model increases both the accuracy and the computational complexity. The Åström-Bell model can then be extended using Jacob and Andreescu's methods [13] to create a reduced order model. Further reductions can be made with a specific set of assumptions and conditions. It can be assumed that several inputs will remain near constant. Also, first order differential equations will be used to approximate the physical dynamics of valves.

3.1 Steam Property Modeling

The simulation of a drum boiler requires an understanding of the thermodynamic properties of saturated steam. Saturation temperature, density (specific volume), and enthalpy are all functions of pressure, and the experimental data was modeled using the water and steam properties according to IAPWS IF-97 [4]. The Åström-Bell model uses quadratic functions to model these properties which are in table 3.1 [7]. A quadratic function was used because

the derivatives of these functions will be used in future calculations, and linear or constant derivatives are produced from quadratic models. Figure 3.1 shows how these equations compare to the physical properties. Note how at lower pressures there is a high degree of variation.

	Original Model Equation
Saturated Steam Temperature	$T(p) = C_1p^2 + B_1p + A_1$
Saturated Vapor Enthalpy	$h_s(p) = C_2p^2 + B_2p + A_2$
Saturated Vapor Density	$\rho_s(p) = C_3p^2 + B_3p + A_3$
Saturated Liquid Enthalpy	$h_w(p) = C_4p^2 + B_4p + A_4$
Saturated Liquid Density	$\rho_w(p) = C_5p^2 + B_5p + A_5$

Table 3.1: Original Steam Table Models

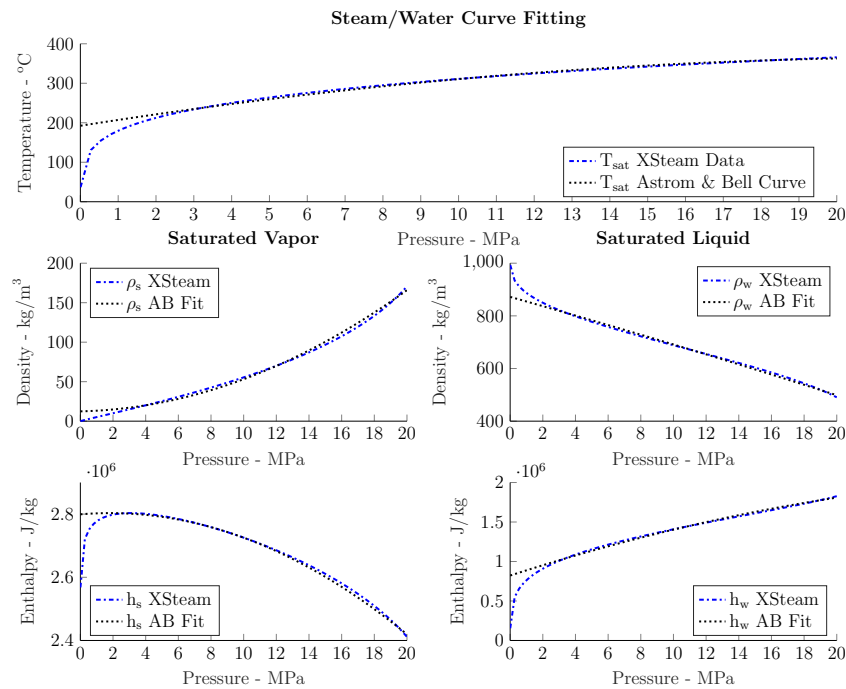


Figure 3.1: Curve Fitting Steam Åström-Bell

A more elaborate model can be used, and a curve fitting process can be applied to the tables of physical properties. The advantage of using a more elaborate model is that the operating parameters can be further expanded outside of the range of where the quadratic model breaks down. The various

model types are defined in Table 3.2. Exponential and cubic equations were used for a more accurate fit. Figure 3.2 shows the steam properties table, the quadratic model, and an expanded model.

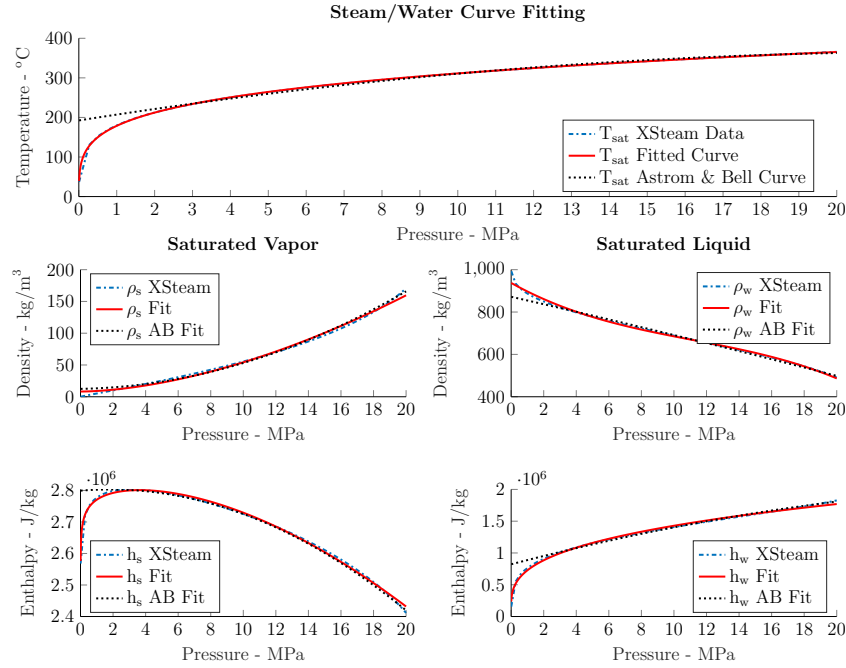


Figure 3.2: Curve Fitting Steam

	Original Model Equation	Expanded Model Equation
Saturated Steam Temperature	$T(p) = C_1p^2 + B_1p + A_1$	$T(p) = B_6p^{C_6} + A_6$
Saturated Vapor Enthalpy	$h_s(p) = C_2p^2 + B_2p + A_2$	$h_s(p) = D_7p^{E_7} + B_7p^{C_7} + A_7$
Saturated Vapor Density	$\rho_s(p) = C_3p^2 + B_3p + A_3$	$\rho_s(p) = B_8p^{C_8} + A_8$
Saturated Liquid Enthalpy	$h_w(p) = C_4p^2 + B_4p + A_4$	$h_w(p) = B_9p^{C_9} + A_9$
Saturated Liquid Density	$\rho_w(p) = C_5p^2 + B_5p + A_5$	$\rho_w(p) = D_{10}p^3 + C_{10}p^2 + B_{10}p + A_{10}$

Table 3.2: Expanded Steam Table Models

It is clear from Figure 3.2 that the more complex exponential models are a better fit than the quadratic modeling, as the model does not break down in the lower pressure ranges. While the original quadratic model makes the math much simpler when performing the partial derivatives the use of computational tools (MatLab's Symbolic Toolbox) makes this a rewarding design trade off

when compared to the expanded pressure ranges that the new model can operate at and the trivial nature of calculating these partial derivatives.

3.2 Åström and Bell Model

Åström and Bell's goal in creating a model was to find a moderately complex nonlinear model that captured the key properties of shrink and swell for drum boiler level. A first order model can be used if drum level is considered well controlled. The first order model ignores the drum level and therefore cannot be used for the purposes of this research [7].

3.2.1 Global Mass and Energy Balance

The steam boiler model is derived using mass and energy balance. The global Mass balance equation is [7]:

$$\frac{d}{dt} [\rho_s(p) V_{st} + \rho_w(p) V_{wt}] = q_f - q_s \quad (3.1)$$

(Where $\rho_s(p)$ and $\rho_w(p)$ are functions of p as seen in Table 3.2.) This can be placed into words as the sum of the change in the mass of the steam and water in the system (calculated as $m = \rho V$) must be equal to the sum of the mass flow rate of the steam flow out of the system and feed-water flow into the system. This is the principle of the conservation of mass. Various symbols in the above equation and rest of this chapter are listed in *List of Nomenclature* at the beginning of this thesis.

Noting that ρ is a function of pressure, p , the global mass balance (equation 3.1) can be placed into a matrix form [7] as

$$\begin{bmatrix} e_{11}(p) & e_{12}(p) \end{bmatrix} \frac{d}{dt} \begin{bmatrix} V_{wt} \\ p \end{bmatrix} = q_f - q_s \quad (3.2)$$

In equation (3.2), the coefficients are defined as follows:

$$\begin{aligned} e_{11}(p) &= \rho_w(p) - \rho_s(p) \\ e_{12}(p) &= V_{wt} \frac{\partial \rho_w(p)}{\partial p} - V_{st} \frac{\partial \rho_s(p)}{\partial p} \end{aligned}$$

The global energy balance as derived in [7] is given by

$$\begin{aligned} \frac{d}{dt} [\rho_s(p) h_s(p) V_{st} + \rho_w(p) h_w(p) V_{wt} - pV_t + m_t C_p t_s(p)] \\ = Q + q_f h_f(p) - q_s h_s(p) \end{aligned} \quad (3.3)$$

(Where $\rho_s(p)$, $\rho_w(p)$, $h_s(p)$, $h_w(p)$, $h_f(p)$, and $t_s(p)$ are functions of p as seen in Table 3.2.) This can be placed into words as the change of internal energy in both steam and water and the change of energy due to the change in volume and the temperature of the metal must equal the sum of the heat transfer in, the energy the steam brings, and the energy the feed-water brings.

The global energy balance (equation 3.3) can be simplified [7] as:

$$\begin{bmatrix} e_{21}(p) & e_{22}(p) \end{bmatrix} \frac{d}{dt} \begin{bmatrix} V_{wt} \\ p \end{bmatrix} = Q + q_f h_f(p, t_f) - q_s h_s(p) \quad (3.4)$$

where the coefficients are defined as follows:

$$\begin{aligned} e_{21}(p) &= \rho_w(p) h_w(p) - \rho_s(p) h_s(p) \\ e_{22}(p) &= V_{wt} \left(h_w(p) \frac{\partial \rho_w(p)}{\partial p} + \rho_w(p) \frac{\partial h_w(p)}{\partial p} \right) + \\ &\quad + V_{st} \left(h_s(p) \frac{\partial \rho_s(p)}{\partial p} + \rho_s(p) \frac{\partial h_s(p)}{\partial p} \right) - V_t + m_t C_p \frac{\partial t_s(p)}{\partial p} \end{aligned}$$

3.2.2 Distribution of Steam in Risers and Drum

The energy balance for the riser section [7]:

$$\begin{aligned} \frac{d}{dt} [\rho_s(p) h_s(p) \bar{\alpha}_v V_r + \rho_w(p) h_w(p) (1 - \bar{\alpha}_v) V_r - pV_r + m_r C_p t_s(p)] \\ = Q + q_{dc} h_w(p) - (\alpha_r h_c(p) + h_w(p)) q_r \end{aligned} \quad (3.5)$$

(Where $\rho_s(p)$, $\rho_w(p)$, $h_s(p)$, $h_w(p)$, $h_c(p)$, and $t_s(p)$ are functions of p as seen in Table 3.2.) This can be placed into words as the change of internal energy in both steam and water in the risers and the change of energy due to the change in volume and the temperature of the metal of the risers must equal the sum of the heat transfer in, the energy the risers loses, and the

energy the water in the down comers brings. $\bar{\alpha}_v$ is the average steam volume ratio.

The riser section energy balance (equation 3.5) can be simplified [7] as

$$\begin{bmatrix} e_{32}(p) & e_{33}(p) \end{bmatrix} \frac{d}{dt} \begin{bmatrix} p \\ \alpha_r \end{bmatrix} = Q + \alpha_r h_c(p) q_{dc} \quad (3.6)$$

In equation (3.6) the coefficients are defined as follows:

$$\begin{aligned} e_{32}(p) &= \left(\rho_w(p) \frac{\partial h_w(p)}{\partial p} + \rho_s(p) \frac{\partial h_s(p)}{\partial p} \right) (1 - \bar{\alpha}_v) V_r \\ &\quad + \left((1 - \alpha_r) h_c(p) \frac{\partial \rho_s(p)}{\partial p} + \rho_s(p) \frac{\partial h_s(p)}{\partial p} \right) \bar{\alpha}_v V_r \\ &\quad + (\rho_s(p) + (\rho_w(p) - \rho_s(p)) \alpha_r) h_c(p) V_r \frac{\partial \bar{\alpha}_v}{\partial p} - V_r + m_r C_p \frac{\partial t_s(p)}{\partial p} \\ e_{33}(p) &= ((1 - \alpha_r) \rho_s(p) + \alpha_r \rho_w(p)) h_c(p) V_r \frac{\partial \bar{\alpha}_v}{\partial \alpha_r} \end{aligned}$$

The mass balance for the riser section is given by [7]

$$\frac{d}{dt} [\rho_s(p) \bar{\alpha}_v V_r + \rho_w(p) (1 - \bar{\alpha}_v) V_r] = q_{dc} - q_r \quad (3.7)$$

(Where $\rho_s(p)$ and $\rho_w(p)$ are functions of p as seen in Table 3.2.) This can be placed into words as the change in density and volume of both steam and water in the risers must be equal to the mass flow rate of the sum of the mass flow rates into the down comers and out of the risers.

The riser section mass balance (equation 3.7) can be simplified to become:

$$\begin{bmatrix} e_{42}(p) & e_{43}(p) & e_{44}(p) \end{bmatrix} \frac{d}{dt} \begin{bmatrix} p \\ \alpha_r \\ V_{sd} \end{bmatrix} = \frac{\rho_s(p)}{T_d} (V_{sd}^0 - V_{sd}) + \frac{h_f(p, t_f) - h_w(p)}{h_c(p)} q_f \quad (3.8)$$

where the coefficients are defined as follows [7]:

$$\begin{aligned}
e_{42}(p) &= V_{sd} \frac{\partial \rho_s(p)}{\partial p} + \frac{1}{h_c(p)} \left(\rho_s(p) V_{sd} \frac{\partial h_s(p)}{\partial p} + \rho_w(p) V_{wd} \frac{\partial h_w(p)}{\partial p} \right) \\
&\quad + \frac{1}{h_c(p)} \left(m_d C_p \frac{\partial t_s(p)}{\partial p} - V_{sd} - V_{wd} \right) \\
&\quad + \alpha_r (1 + \beta) V_r \left((\rho_s(p) - \rho_w(p)) \frac{\partial \bar{\alpha}_v}{\partial p} \right) \\
&\quad + \alpha_r (1 + \beta) V_r \left(\bar{\alpha}_v \frac{\partial \rho_s(p)}{\partial p} + (1 - \bar{\alpha}_v) \frac{\partial \rho_w(p)}{\partial p} \right) \\
e_{43}(p) &= \alpha_r (1 + \beta) (\rho_s(p) - \rho_w(p)) V_r \frac{\partial \bar{\alpha}_v}{\partial p} \\
e_{44}(p) &= \rho_s(p)
\end{aligned}$$

3.3 Simulation of Åström and Bell Model

Equations (3.2), (3.4), (3.6), and (3.8) can be combined to give the following equation:

$$\begin{aligned}
\begin{bmatrix} e_{11}(p) & e_{12}(p) & 0 & 0 \\ e_{21}(p) & e_{22}(p) & 0 & 0 \\ 0 & e_{32}(p) & e_{33}(p) & 0 \\ 0 & e_{42}(p) & e_{43}(p) & e_{44}(p) \end{bmatrix} \frac{d}{dt} \begin{bmatrix} V_{wt} \\ p \\ \alpha_r \\ V_{sd} \end{bmatrix} &= \begin{bmatrix} q_f - q_s \\ Q + q_f h_f(p, t_f) - q_s h_s(p) \\ Q + \alpha_r h_c(p) q_{dc}(p) \\ \frac{\rho_s(p)}{T_d} (V_{sd}^0 - V_{sd}) + \frac{h_f(p, t_f) - h_w(p)}{h_c(p)} q_f \end{bmatrix} \\
\frac{d}{dt} \begin{bmatrix} V_{wt} \\ p \\ \alpha_r \\ V_{sd} \end{bmatrix} &= \begin{bmatrix} e_{11}(p) & e_{12}(p) & 0 & 0 \\ e_{21}(p) & e_{22}(p) & 0 & 0 \\ 0 & e_{32}(p) & e_{33}(p) & 0 \\ 0 & e_{42}(p) & e_{43}(p) & e_{44}(p) \end{bmatrix}^{-1} \begin{bmatrix} q_f - q_s \\ Q + q_f h_f(p, t_f) - q_s h_s(p) \\ Q + \alpha_r h_c(p) q_{dc}(p) \\ \frac{\rho_s(p)}{T_d} (V_{sd}^0 - V_{sd}) + \frac{h_f(p, t_f) - h_w(p)}{h_c(p)} q_f \end{bmatrix} \\
&\quad (3.9)
\end{aligned}$$

which is a nonlinear state space model of the form

$$\dot{x}(t) = F(x(t), u(t))$$

where equation (3.9) uses the following as state variables:

$$V_{wt} \quad p \quad \alpha_r \quad V_{sd}$$

and the following as control inputs:

$$q_f \quad q_s \quad Q \quad t_f$$

Several functions are dependant on p and will be evaluated at a pressure before the derivative is taken when simulations are processed.

For purposes of boiler control, the two requested outputs to be predicted are drum level and drum pressure, both of which may be measured directly using simple sensors. The Nonlinear State Space output equation takes the following form:

$$y(t) = G(x(t), u(t))$$

where the control outputs can be calculated as seen in Equation (3.10), where V_{wd} is a known function of the states and inputs and A_d is a constant.

$$y(t) = \begin{bmatrix} l \\ p \end{bmatrix} = \begin{bmatrix} \frac{V_{sd} + V_{wd}(V_{wt}, p, \alpha_r)}{A_d} - l_{nom} \\ p \end{bmatrix} = \begin{bmatrix} \frac{x_4 + V_{wd}(x_1, x_2, x_3)}{A_d} - l_{nom} \\ x_2 \end{bmatrix} \quad (3.10)$$

Where:

$$l_{nom} = \frac{V_r + V_{dc}}{2A_d}$$

If access to all of the states is possible, it allows for calculations of far more outputs. These include: the level contributions from both steam and water, riser and down comer mass flow rate, total water volume, volume of steam in the drum, condensation flow rate, and the average steam volume ratio. These values are of interest, as they give insight into the boiler dynamics, however they are not required for control. The expanded output equations can be seen below:

$$y_{exp}(t) = \left[y(t)^T \quad l_w \quad l_s \quad q_r \quad \alpha_v \quad q_{dc} \quad \alpha_r \quad V_{wt} \quad V_{sd} \quad q_{ct} \right]^T$$

3.3.1 Equilibrium Values

To find the equilibrium point of the system, equation (3.9) is set to 0 to and the following state values obtain the following control and output values:

	<i>Medium</i>	<i>High</i>	<i>units</i>	
V_{wt0}	= 57.1	57.1	m^3	
p_0	= 8.5	8.5	MPa	
α_{r0}	= 0.0516	0.0876	–	
V_{sd0}	= 4.983	4.983	m^3	
Q_0	= 85	170	MW	(3.11)
q_{f0}	= 50	100	kg/s	
t_{f0}	= 249.65	249.65	$^{\circ}K$	
q_{s0}	= 50	100	kg/s	
l_0	= 0.0258	0.2285	Δm	

It should be noted that t_{f0} is $-23.5^{\circ}C$ which is below freezing for water. This operating point was chosen by evaluating the Figures 4 from [7]. If V_{sd} is increased the steady state values for t_f will fall within reasonable bounds. For this research the Åström and Bell values will be used to allow for comparison to [7]. Further research with experimental data is advised.

3.3.2 Comparison of simulation and Åström and Bell's previous work

Validation of the reproduced Åström and Bell model was done by simulating step inputs of the model used in Eq. (3.9) and comparing the results to that of Åström and Bell [7]. Although Åström and Bell provides details of their simulation results, they do not provide many of the relevant parameters which makes it difficult to reproduce the results.

The following figures were taken from Åström and Bell's [7], section 5. These are used to directly compare the model generated matches the model, as not all parameters were given. The equilibrium point (3.11) was used to make direct comparisons to the figures presented.

10 MW fuel flow Step Responses: Figures 3.3 - 3.12

10 kg/s in steam flow Step Responses: Figures 3.13 - 3.22

10 kg/s in feed water flow Step Responses: Figures 3.23-3.28

10°C Feed Water Step Responses: Figures 3.29-3.34

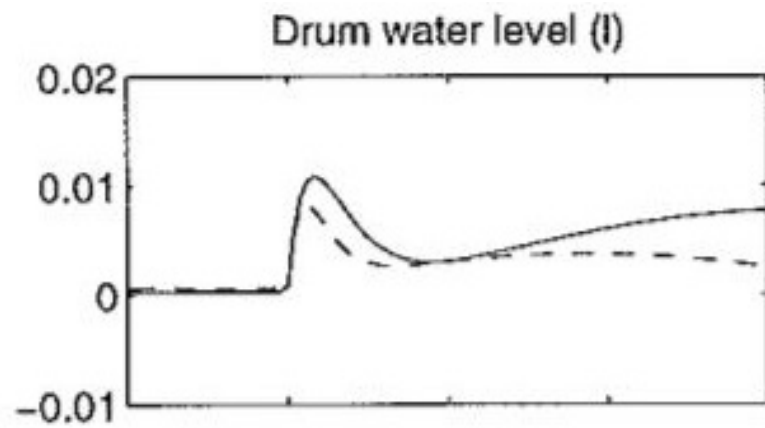
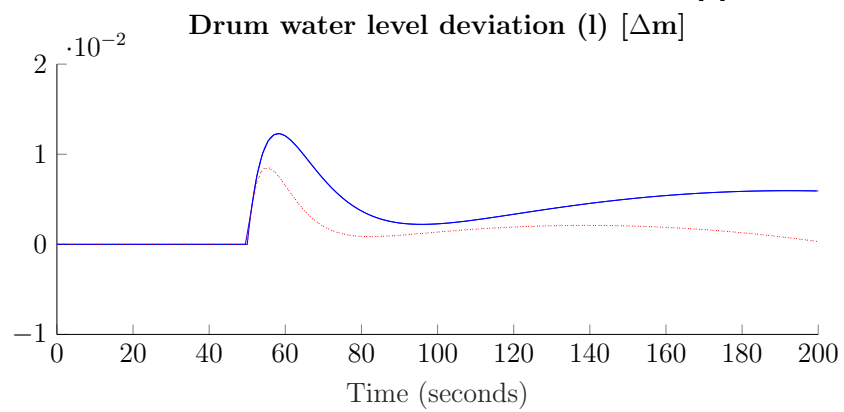


Figure 6 from Åström and Bell, section 5 [7]



Simulation Results using Model from Eq (3.9)

Figure 3.3: Drum Water Level Response to a step corresponding to 10 MW in fuel flow rate

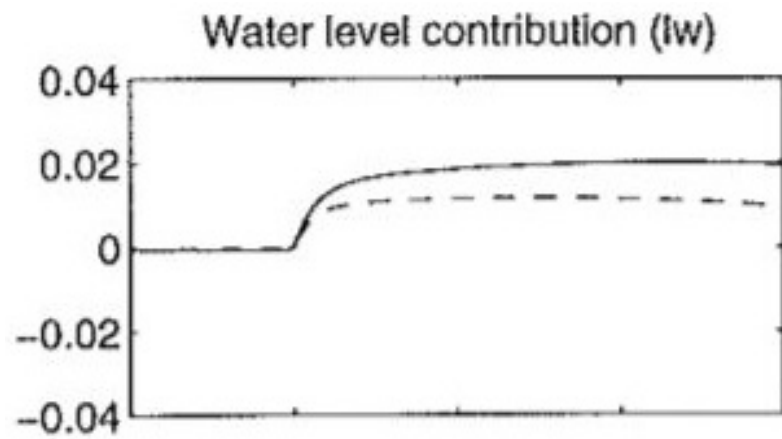
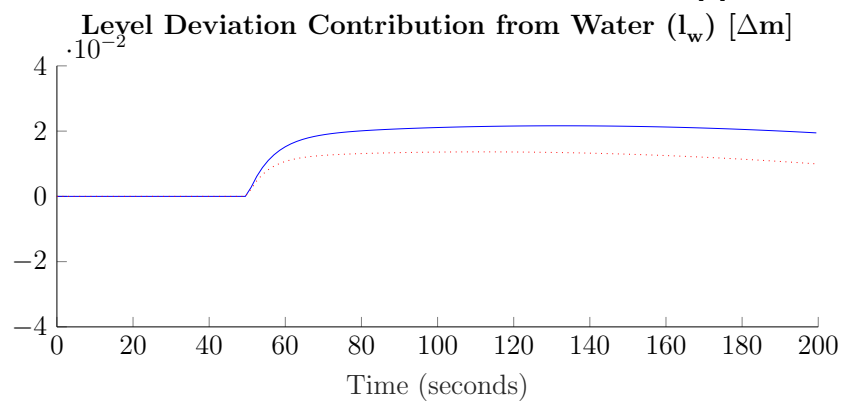


Figure 6 from Åström and Bell, section 5 [7]



Simulation Results using Model from Eq (3.9)

Figure 3.4: Water Level Contribution to a step corresponding to 10 MW in fuel flow rate

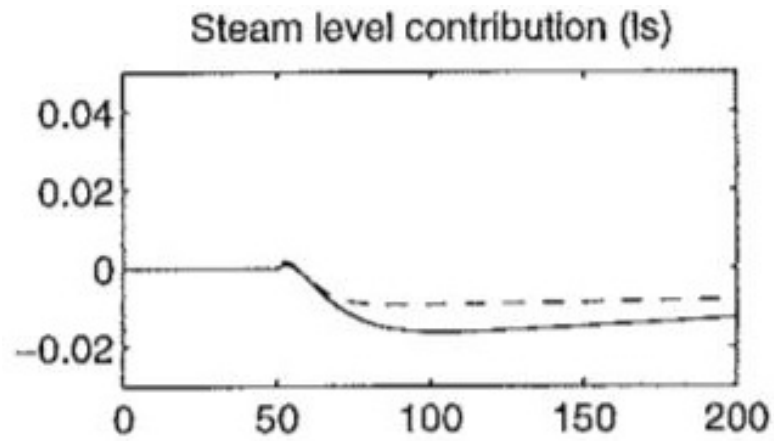
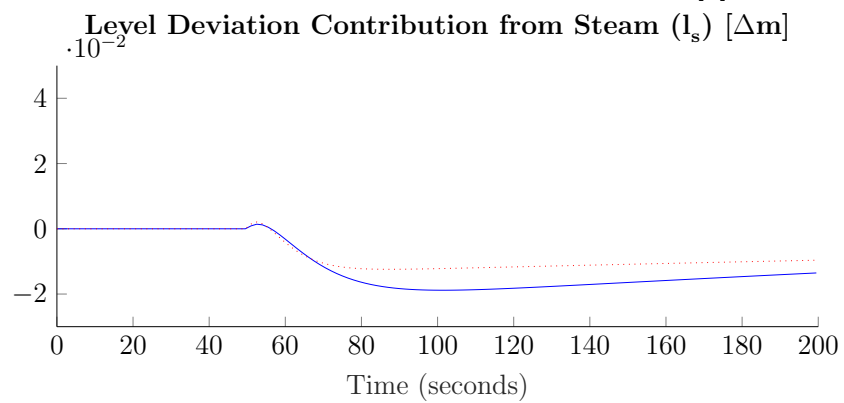


Figure 6 from Åström and Bell, section 5 [7]



Simulation Results using Model from Eq (3.9)

Figure 3.5: Steam Level Contribution to a step corresponding to 10 MW in fuel flow rate

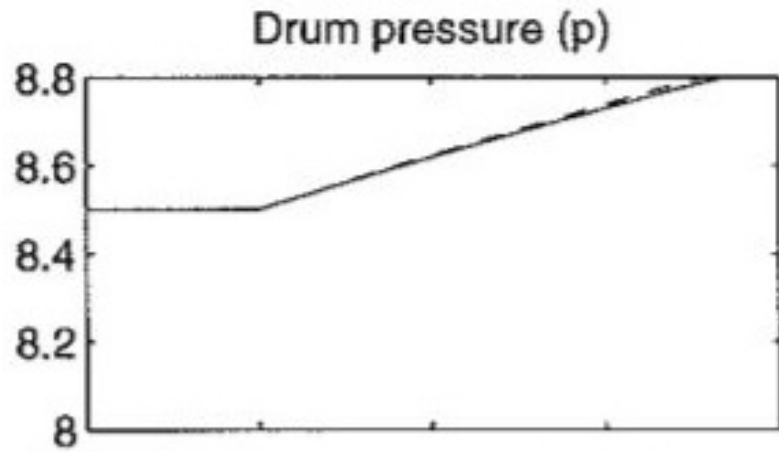
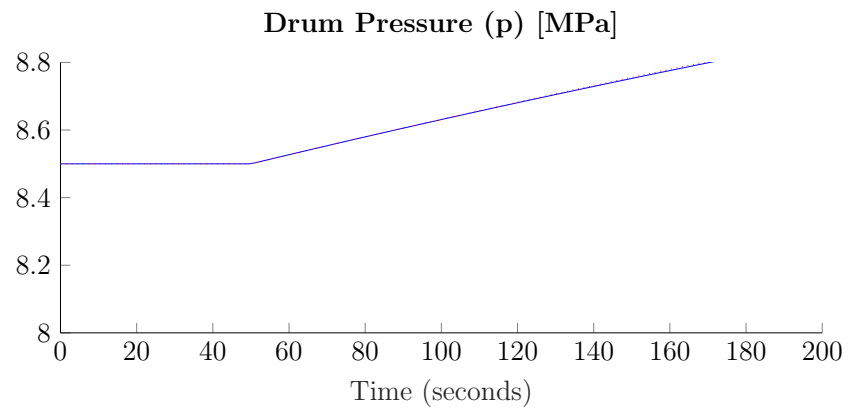


Figure 6 from Åström and Bell, section 5 [7]



Simulation Results using Model from Eq (3.9)

Figure 3.6: Drum Pressure Response to a step corresponding to 10 MW in fuel flow rate

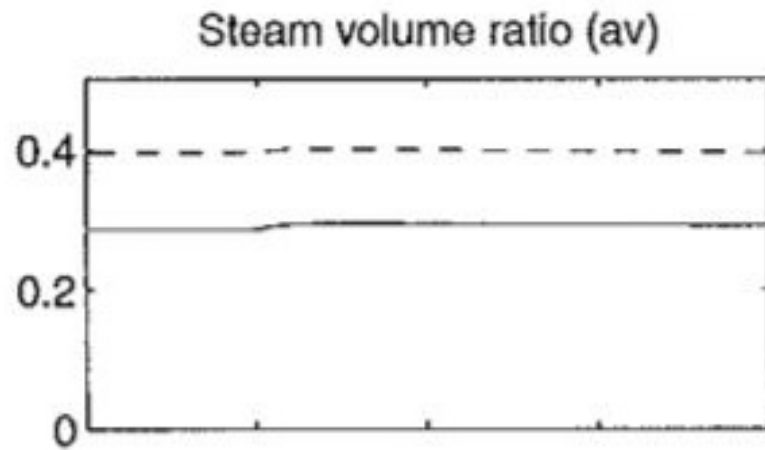
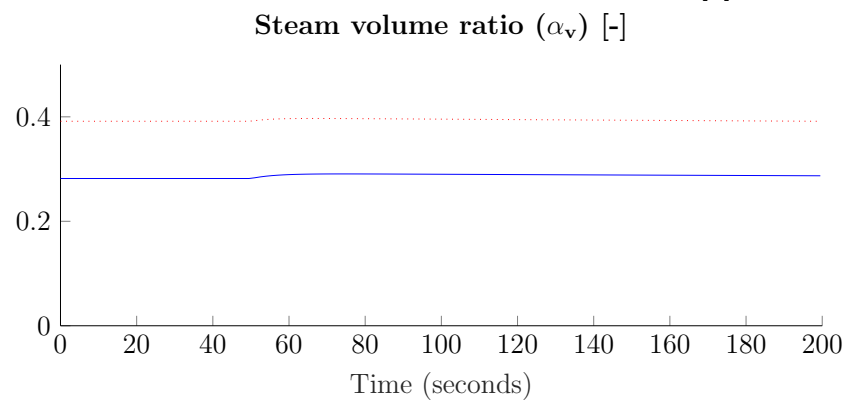


Figure 6 from Åström and Bell, section 5 [7]



Simulation Results using Model from Eq (3.9)

Figure 3.7: Steam Volume Ratio Response to a step corresponding to 10 MW in fuel flow rate

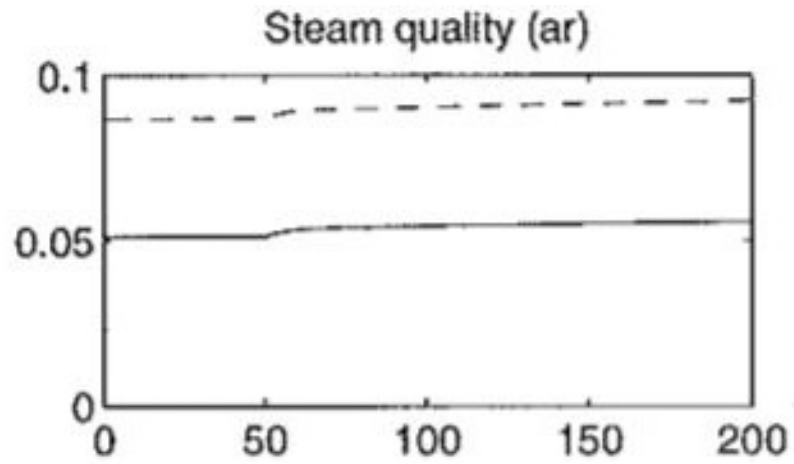
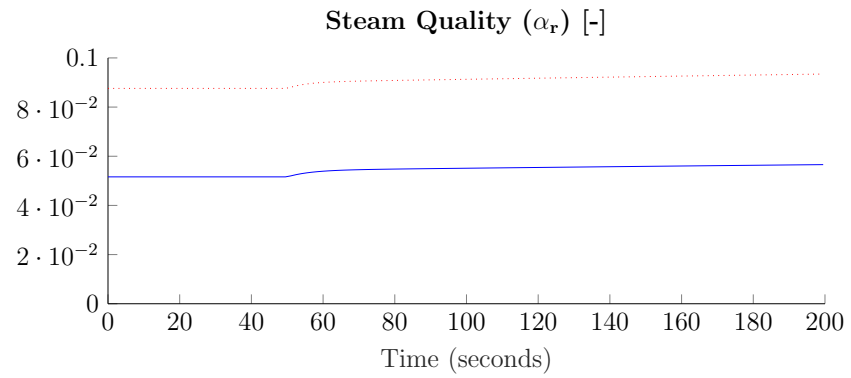


Figure 6 from Åström and Bell, section 5 [7]



Simulation Results using Model from Eq (3.9)

Figure 3.8: Steam Quality Response to a step corresponding to 10 MW in fuel flow rate

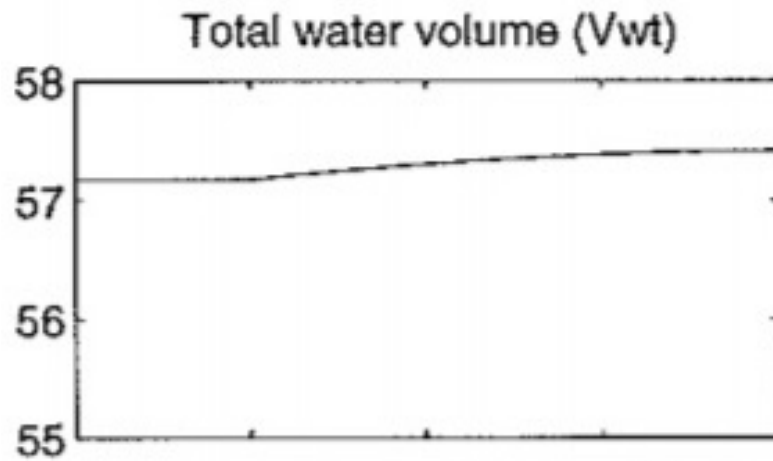
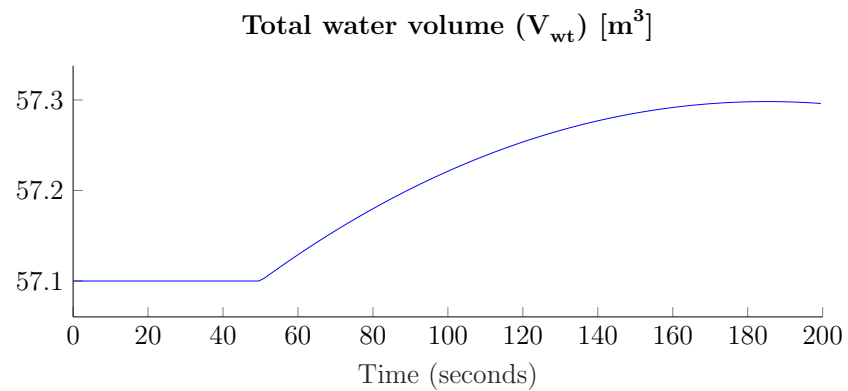


Figure 4 from Åström and Bell, section 5 [7]



Simulation Results using Model from Eq (3.9)

Figure 3.9: Total Water Volume Response to a step corresponding to 10 MW in fuel flow rate

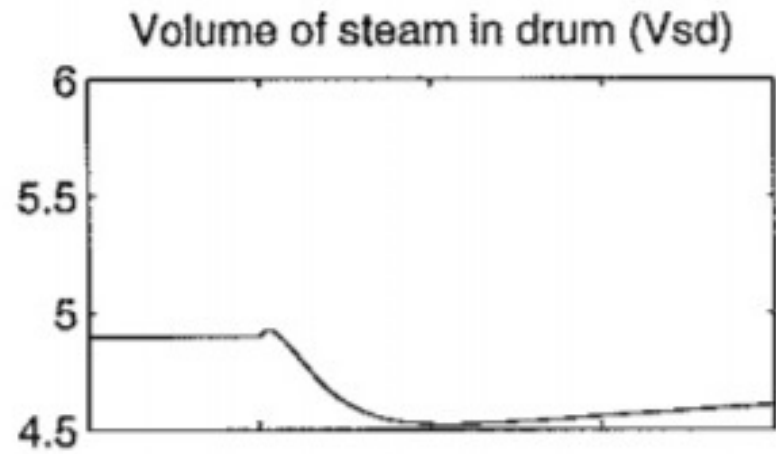
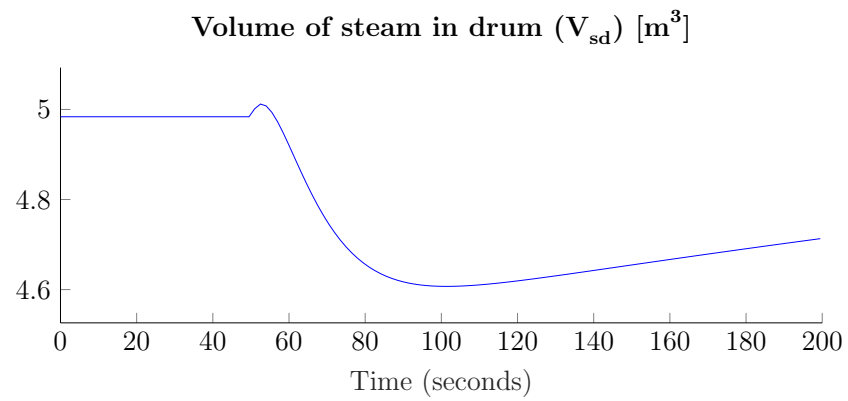


Figure 4 from Åström and Bell, section 5 [7]



Simulation Results using Model from Eq (3.9)

Figure 3.10: Volume of Steam in Drum Response to a step corresponding to 10 MW in fuel flow rate

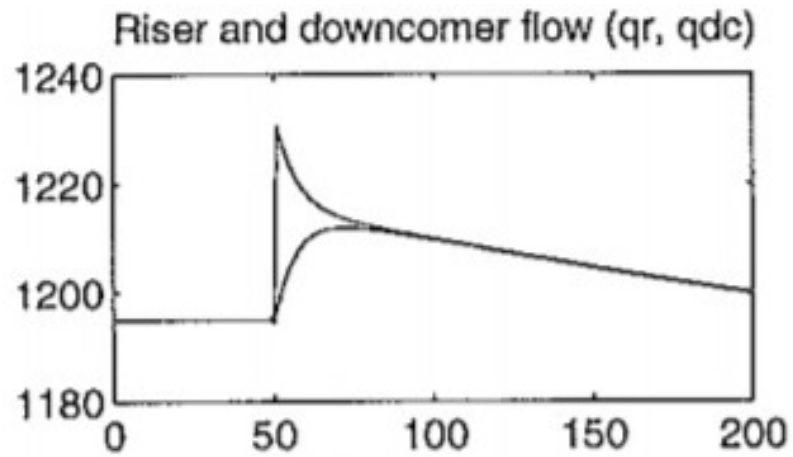
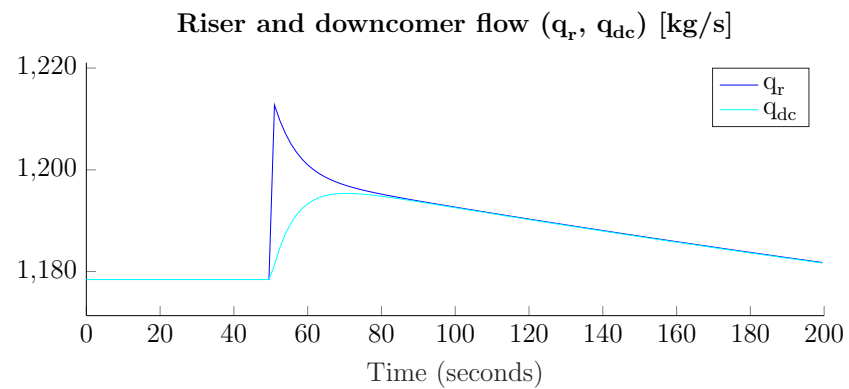


Figure 4 from Åström and Bell, section 5 [7]



Simulation Results using Model from Eq (3.9)

Figure 3.11: Riser and Downcomer Flow Response to a step corresponding to 10 MW in fuel flow rate

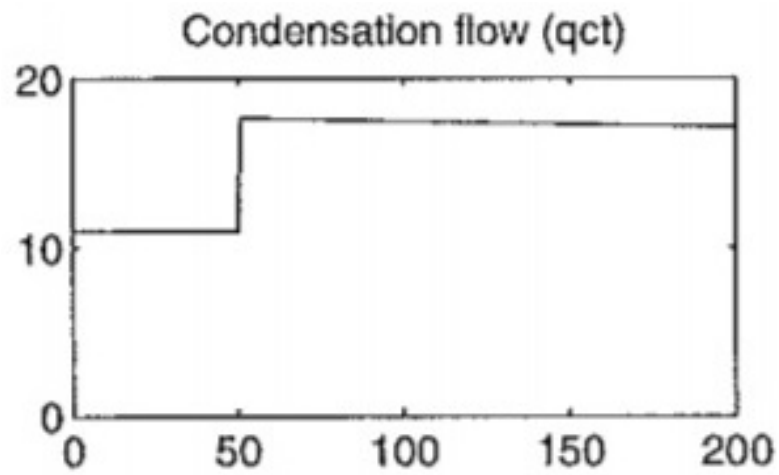
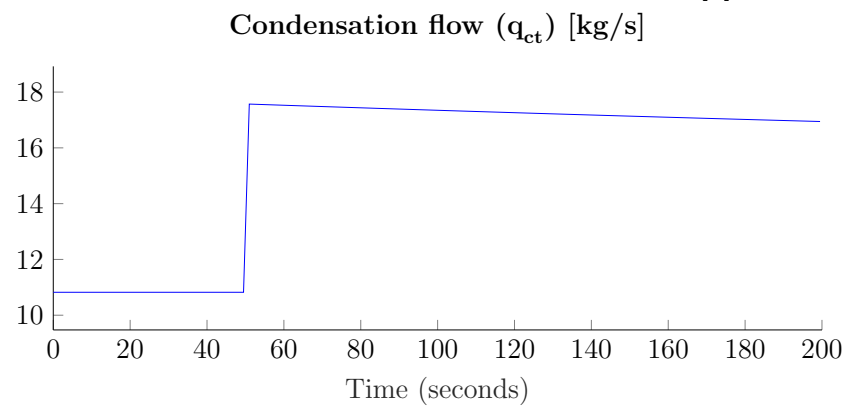


Figure 4 from Åström and Bell, section 5 [7]



Simulation Results using Model from Eq (3.9)

Figure 3.12: Condensation Flow Response to a step corresponding to 10 MW in fuel flow rate

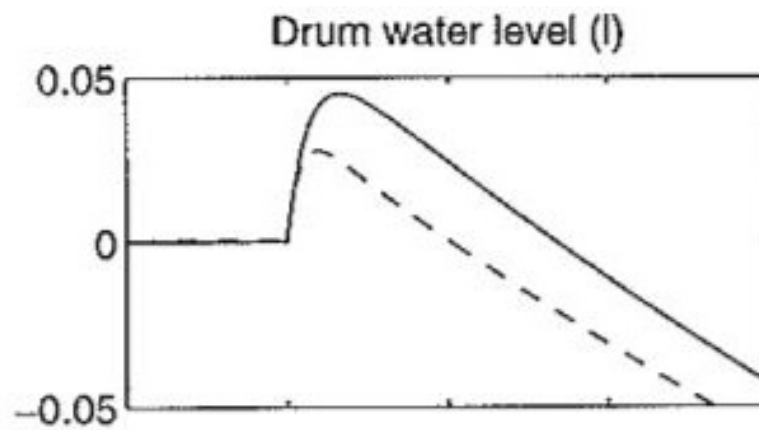
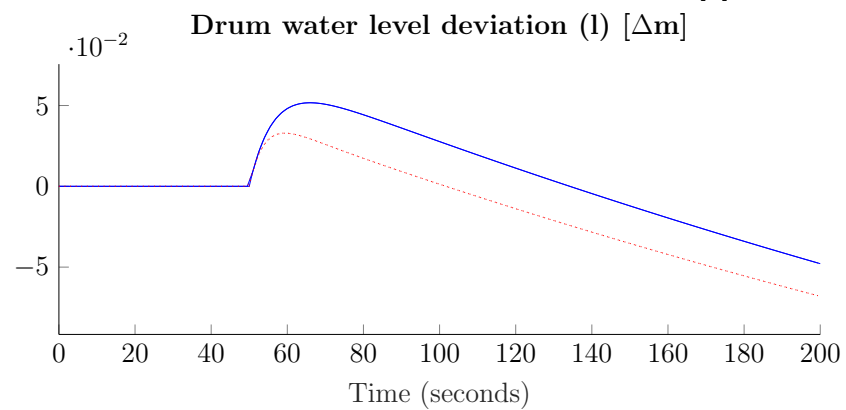


Figure 7 from Åström and Bell, section 5 [7]



Simulation Results using Model from Eq (3.9)

Figure 3.13: Drum Water Level Response to a step change of 10 kg/s in steam flow rate

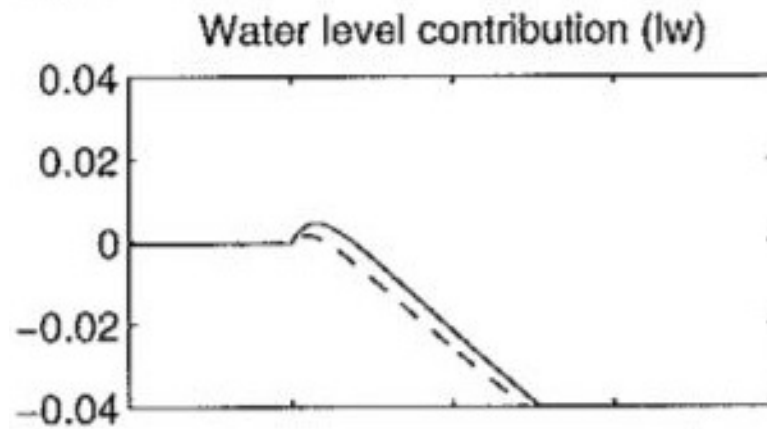
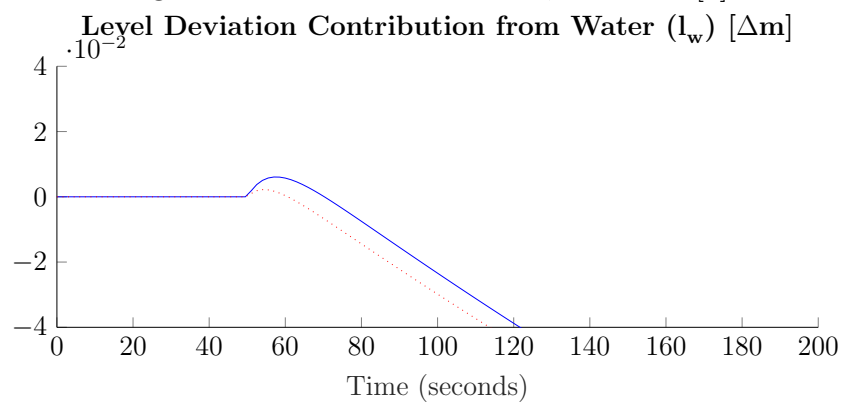


Figure 7 from Åström and Bell, section 5 [7]



Simulation Results using Model from Eq (3.9)

Figure 3.14: Water Level Contribution to a step change of 10 kg/s in steam flow rate

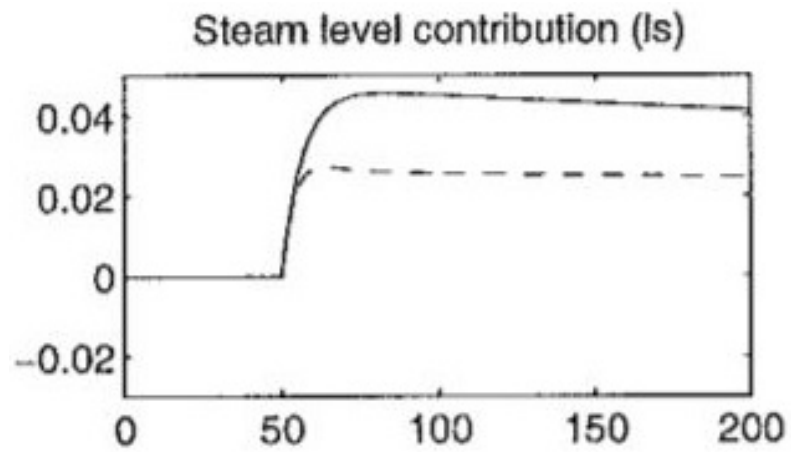
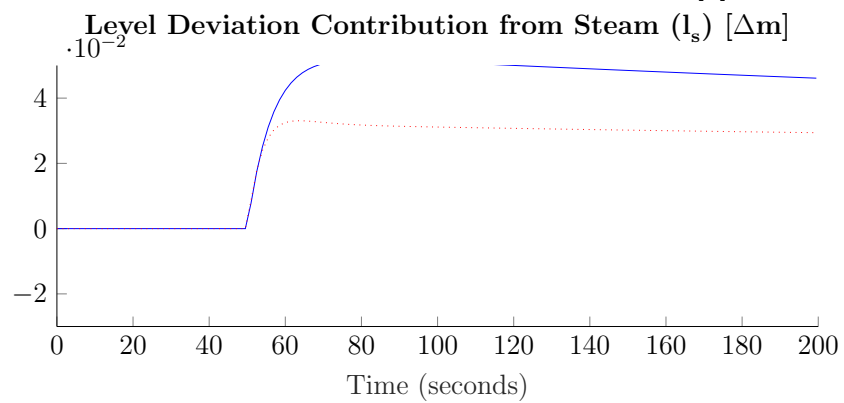


Figure 7 from Åström and Bell, section 5 [7]



Simulation Results using Model from Eq (3.9)

Figure 3.15: Steam Level Contribution to a step change of 10 kg/s in steam flow rate

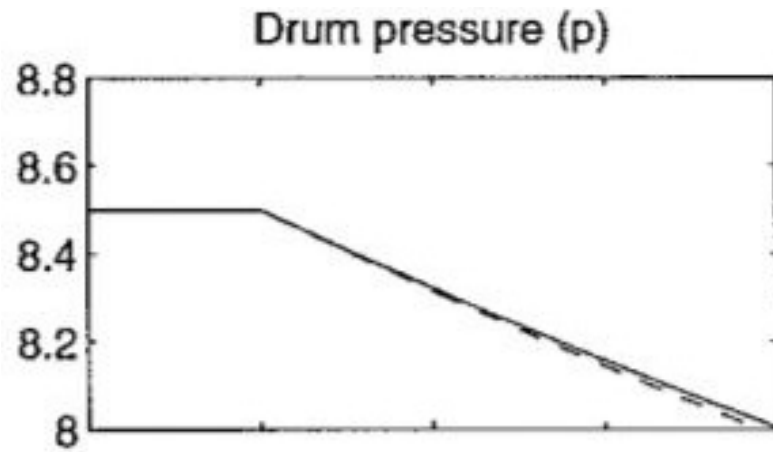
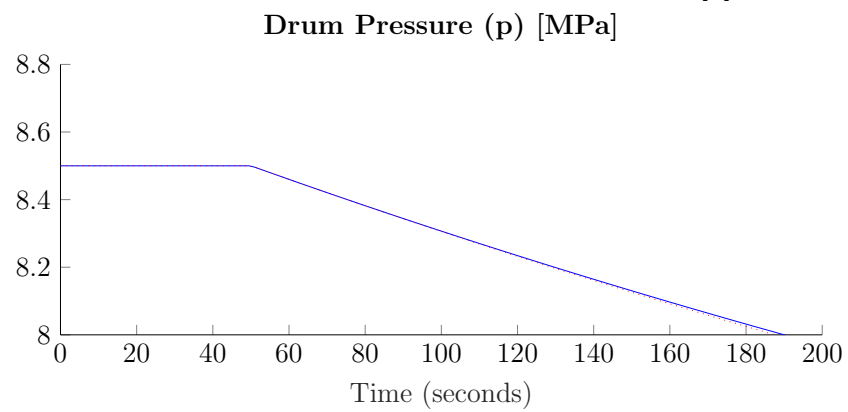


Figure 7 from Åström and Bell, section 5 [7]



Simulation Results using Model from Eq (3.9)

Figure 3.16: Drum Pressure Response to a step change of 10 kg/s in steam flow rate

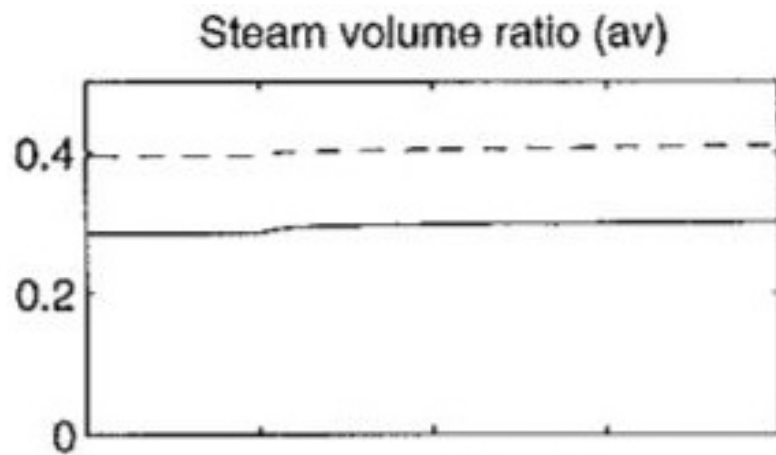
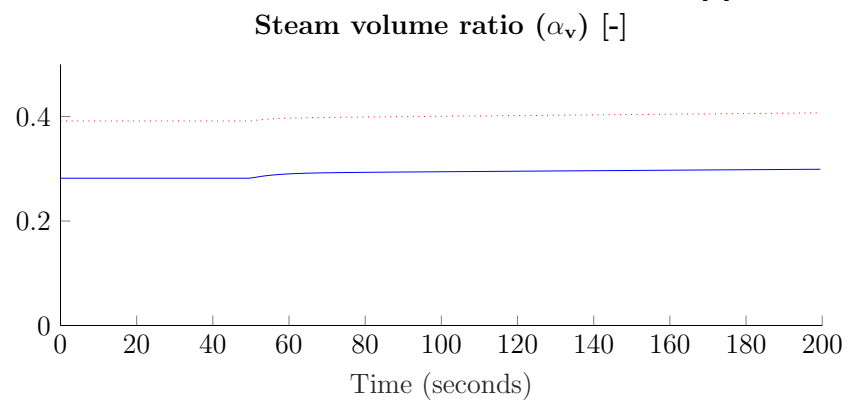


Figure 7 from Åström and Bell, section 5 [7]



Simulation Results using Model from Eq (3.9)

Figure 3.17: Steam Volume Ratio Response to a step change of 10 kg/s in steam flow rate

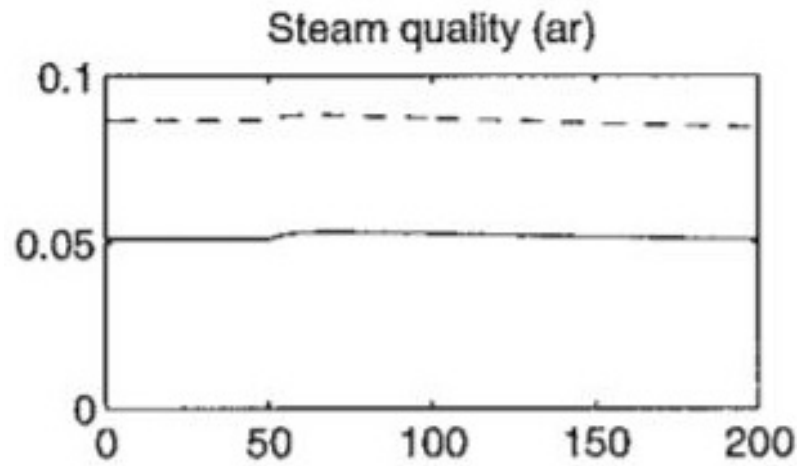
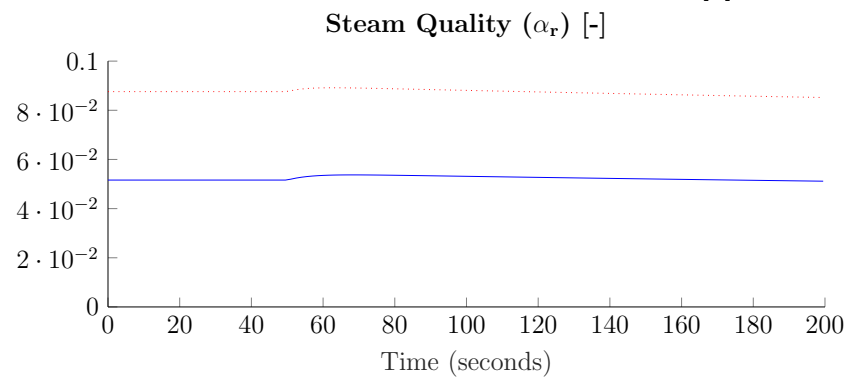


Figure 7 from Åström and Bell, section 5 [7]



Simulation Results using Model from Eq (3.9)

Figure 3.18: Steam Quality Response to a step change of 10 kg/s in steam flow rate

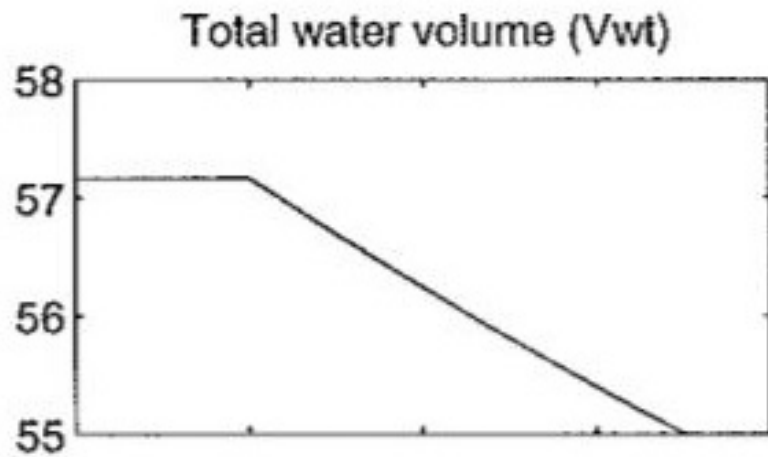
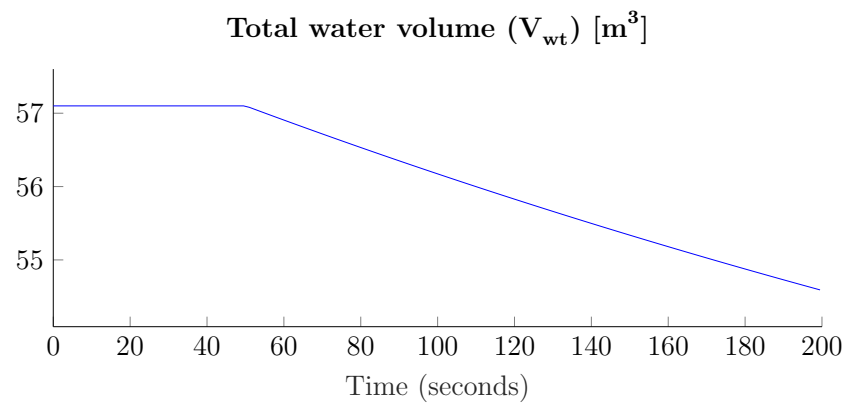


Figure 5 from Åström and Bell, section 5 [7]



Simulation Results using Model from Eq (3.9)

Figure 3.19: Total Water Volume Response to a step change of 10 kg/s in steam flow rate

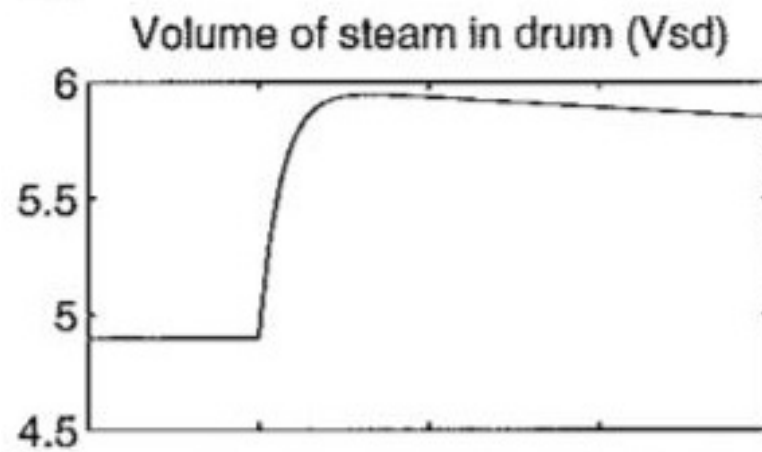
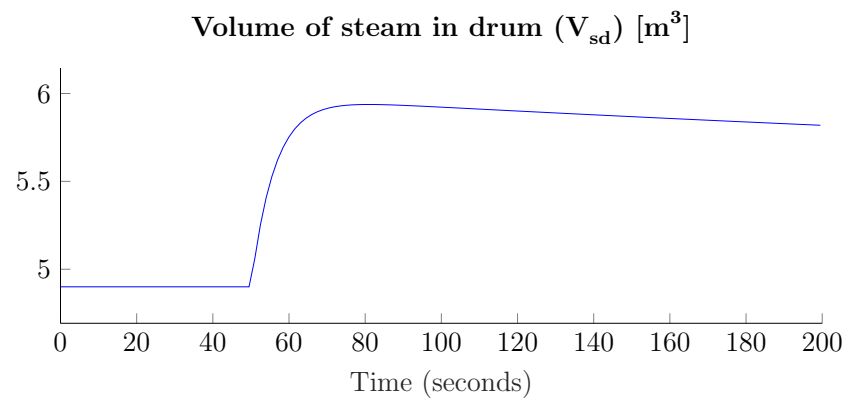


Figure 5 from Åström and Bell, section 5 [7]



Simulation Results using Model from Eq (3.9)

Figure 3.20: Volume of Steam in Drum Response to a step change of 10 kg/s in steam flow rate

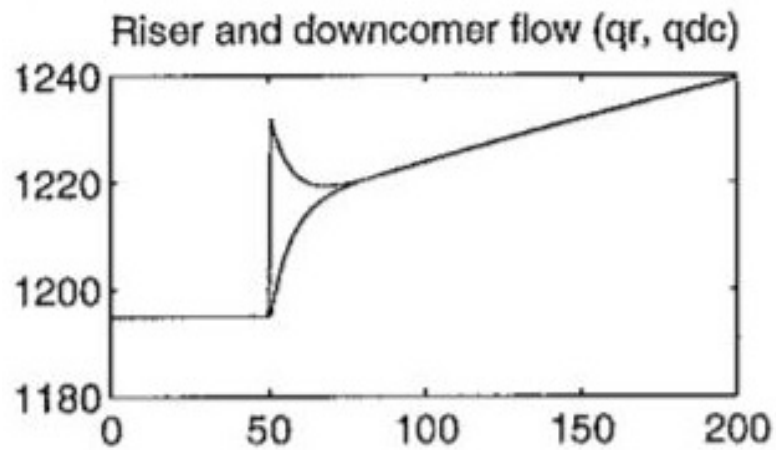
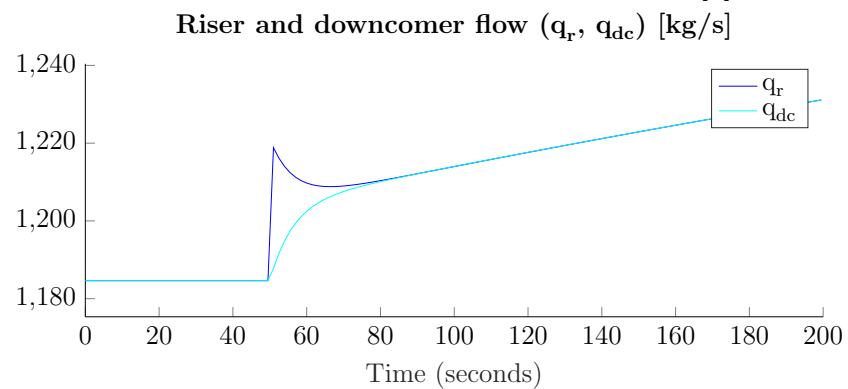


Figure 5 from Åström and Bell, section 5 [7]



Simulation Results using Model from Eq (3.9)

Figure 3.21: Riser and Downcomer Flow Response to a step change of 10 kg/s in steam flow rate

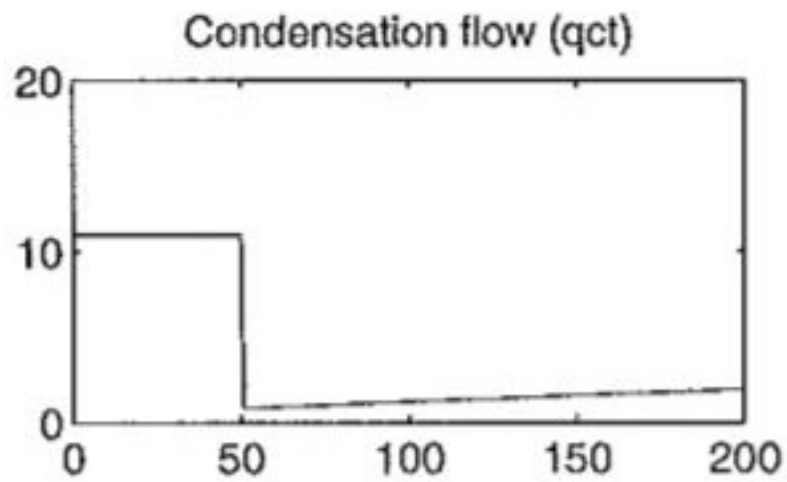
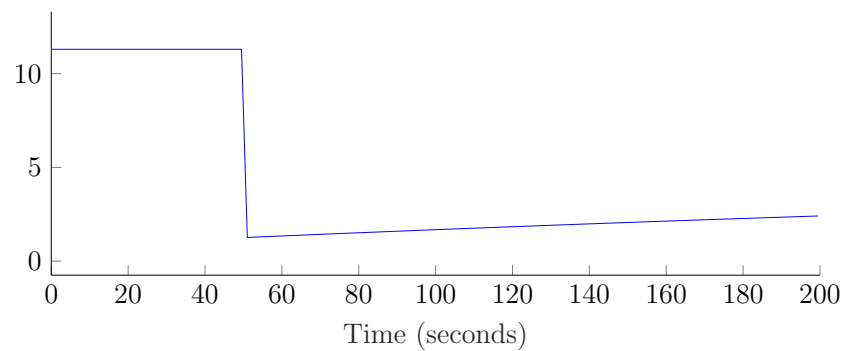


Figure 5 from Åström and Bell, section 5 [7]
Condensation flow (q_{ct}) [kg/s]



Simulation Results using Model from Eq (3.9)

Figure 3.22: Condensation Flow Response to a step change of 10 kg/s in steam flow rate

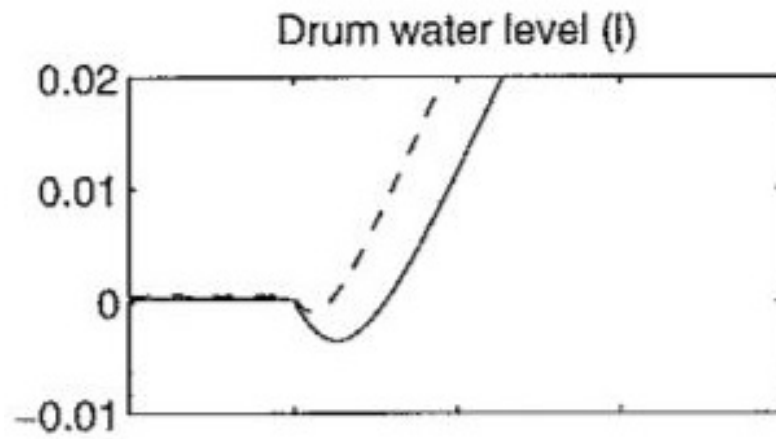
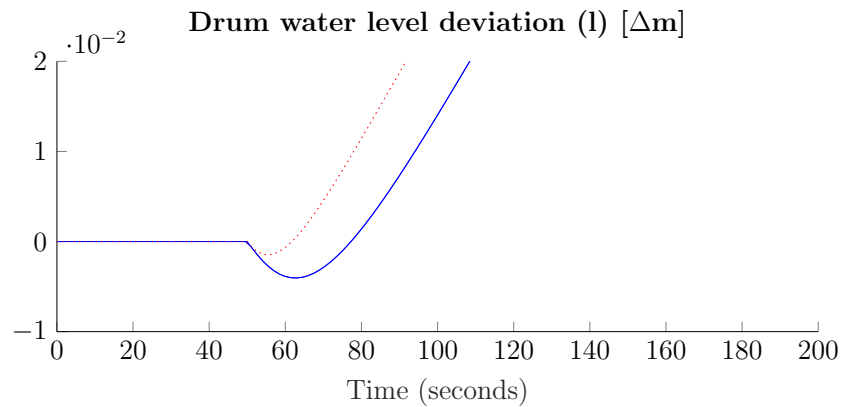


Figure 8 from Åström and Bell, section 5 [7]



Simulation Results using Model from Eq (3.9)

Figure 3.23: Drum Water Level Response to a step corresponding to 10 kg/s in feed water flow rate

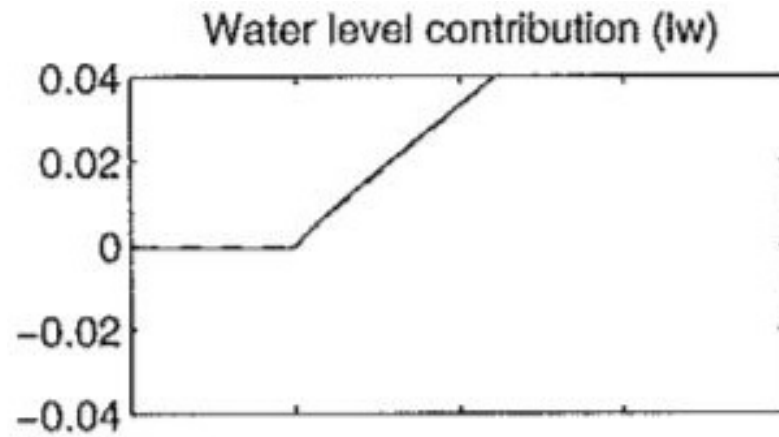
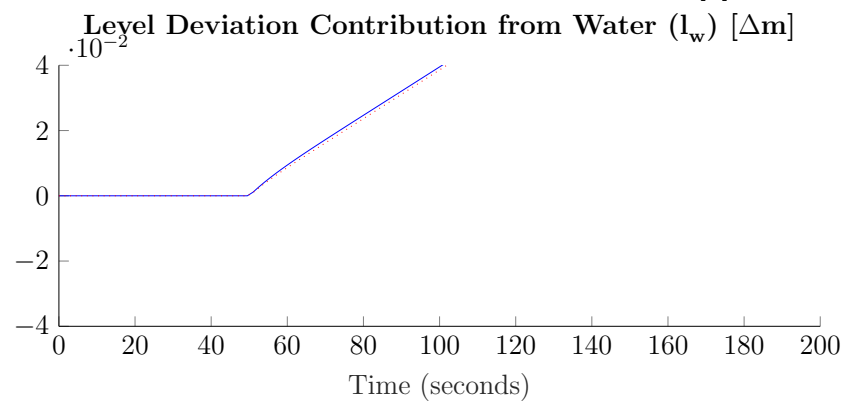


Figure 8 from Åström and Bell, section 5 [7]



Simulation Results using Model from Eq (3.9)

Figure 3.24: Water Level Contribution to a step corresponding to 10 kg/s in feed water flow rate

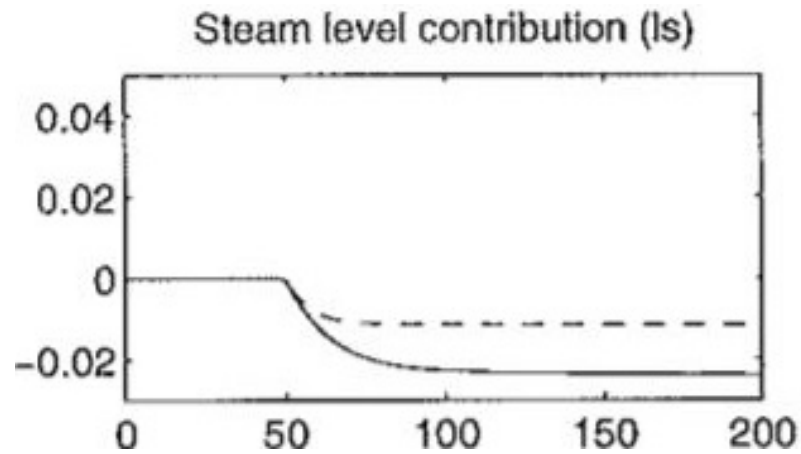
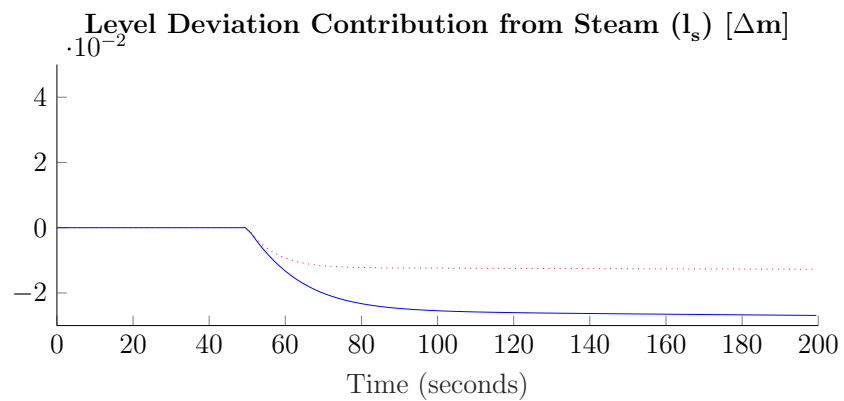


Figure 8 from Åström and Bell, section 5 [7]



Simulation Results using Model from Eq (3.9)

Figure 3.25: Steam Level Contribution to a step corresponding to 10 kg/s in feed water flow rate

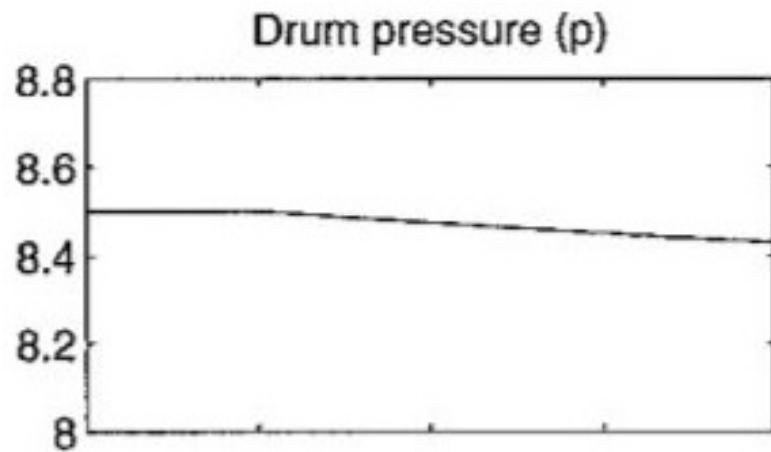
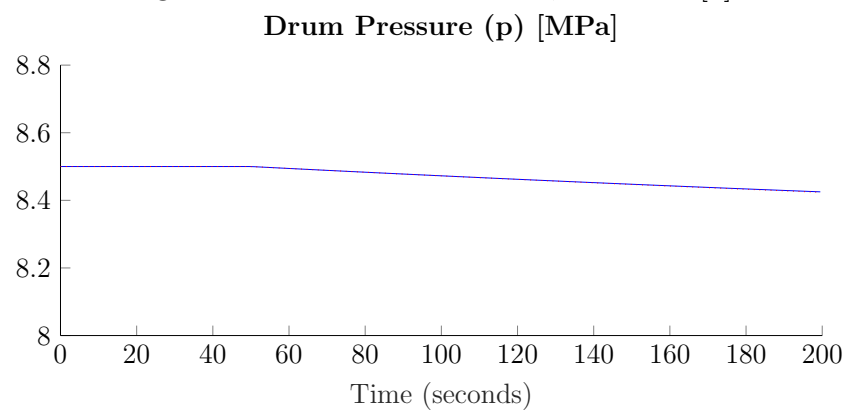


Figure 8 from Åström and Bell, section 5 [7]



Simulation Results using Model from Eq (3.9)

Figure 3.26: Drum Pressure Response to a step corresponding to 10 kg/s in feed water flow rate

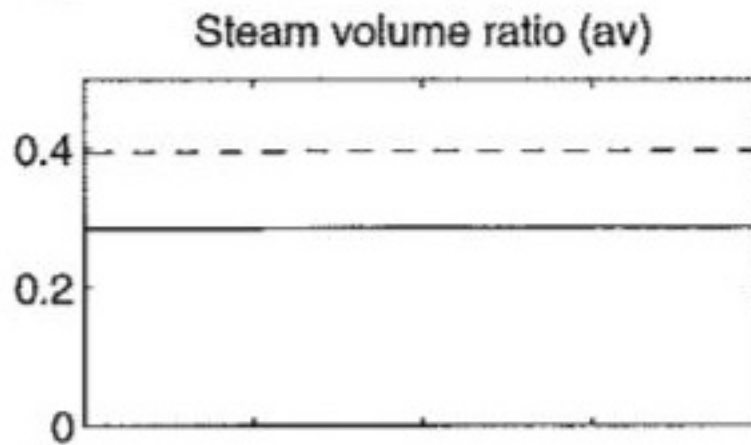
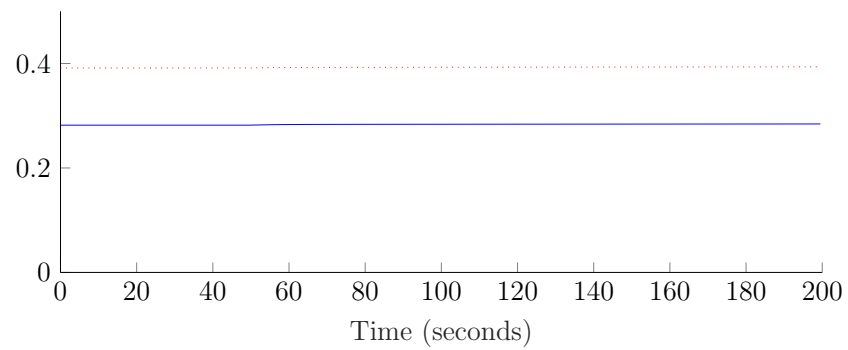


Figure 8 from Åström and Bell, section 5 [7]
 Steam volume ratio (α_v) [-]



Simulation Results using Model from Eq (3.9)

Figure 3.27: Steam Volume Ratio Response to a step corresponding to 10 kg/s in feed water flow rate

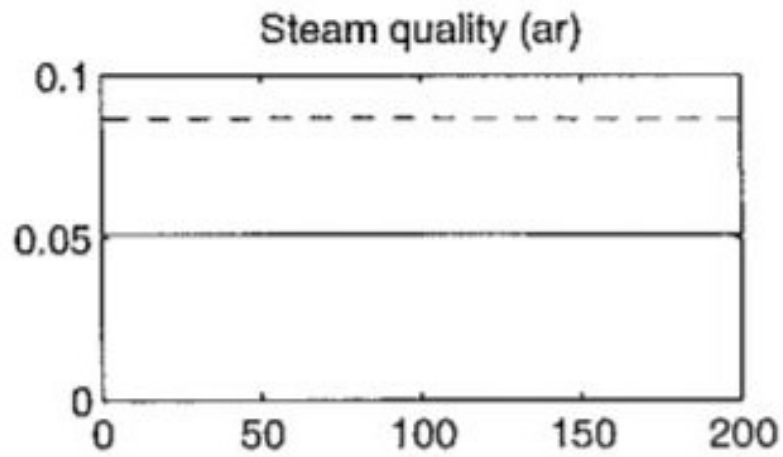
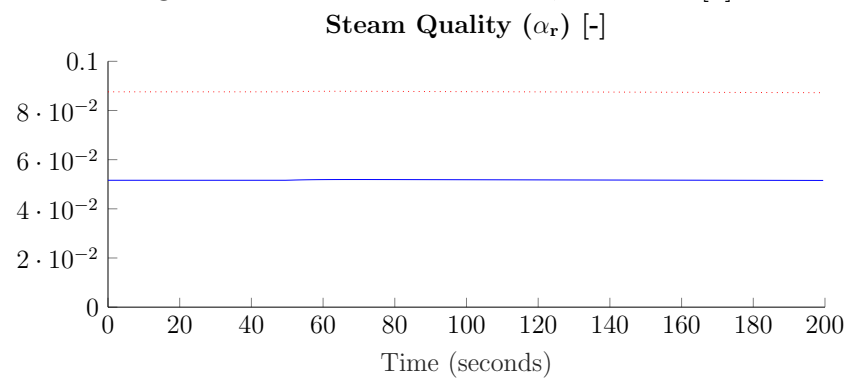


Figure 8 from Åström and Bell, section 5 [7]



Simulation Results using Model from Eq (3.9)

Figure 3.28: Steam Quality Response to a step corresponding to 10 kg/s in feed water flow rate

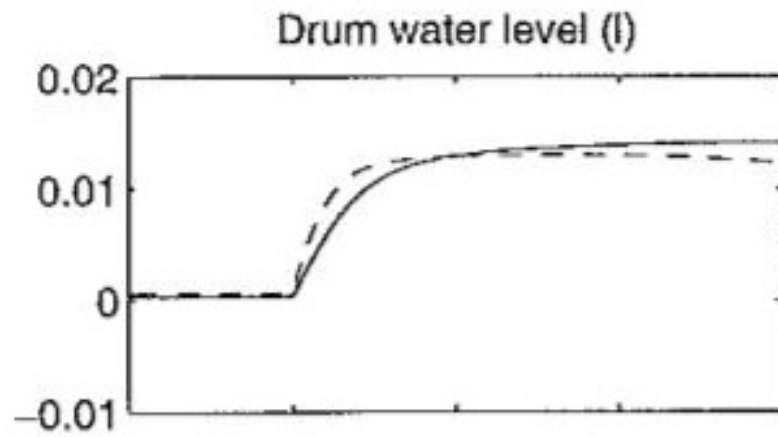
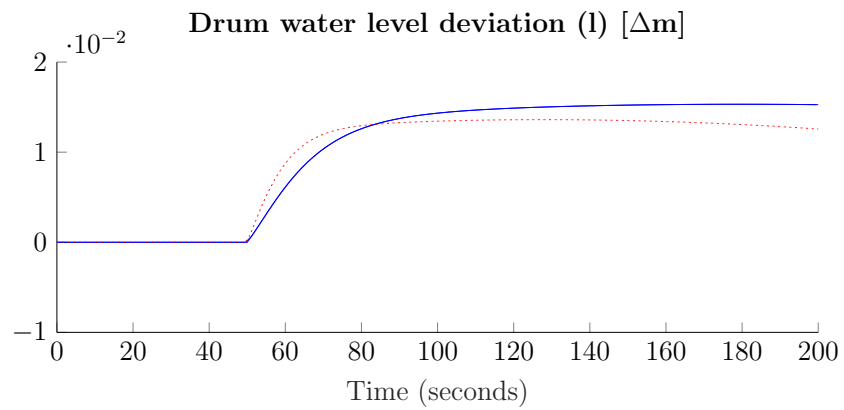


Figure 9 from Åström and Bell, section 5 [7]



Simulation Results using Model from Eq (3.9)

Figure 3.29: Drum Water Level Response to a step corresponding to 10°C Feed Water Temperature

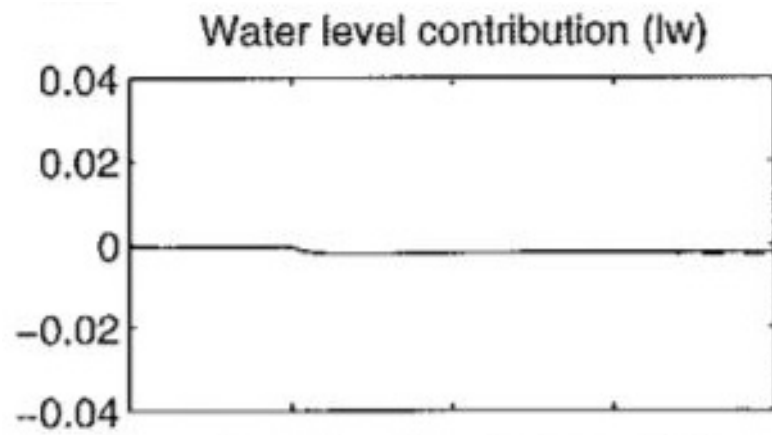
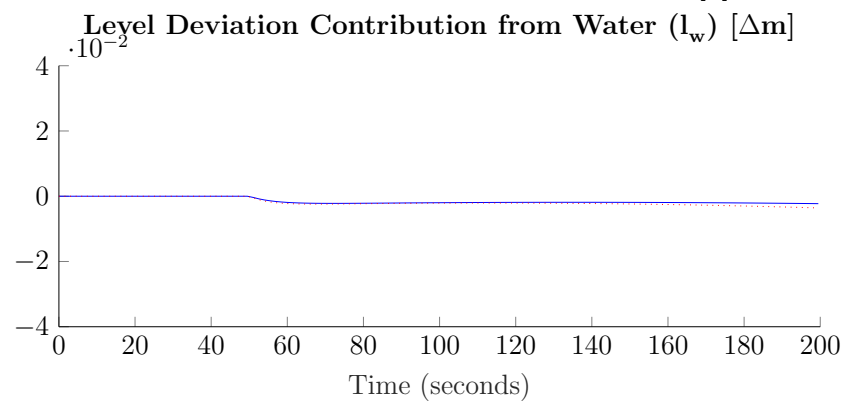


Figure 9 from Åström and Bell, section 5 [7]



Simulation Results using Model from Eq (3.9)

Figure 3.30: Water Level Contribution to a step corresponding to 10°C Feed Water Temperature

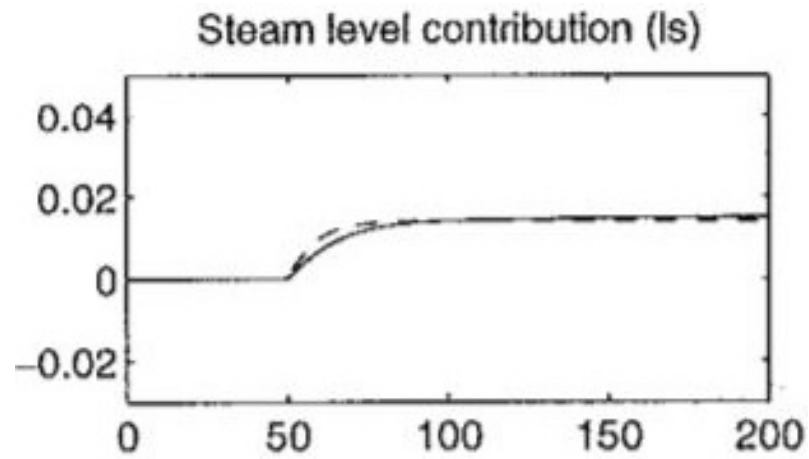
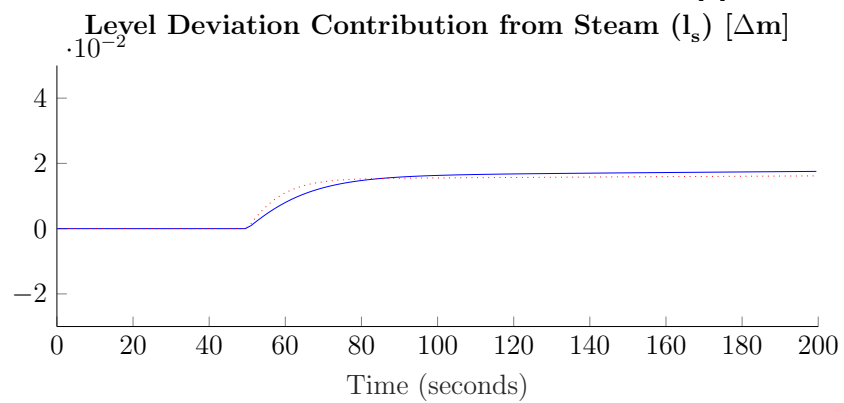


Figure 9 from Åström and Bell, section 5 [7]



Simulation Results using Model from Eq (3.9)

Figure 3.31: Steam Level Contribution to a step corresponding to 10°C Feed Water Temperature

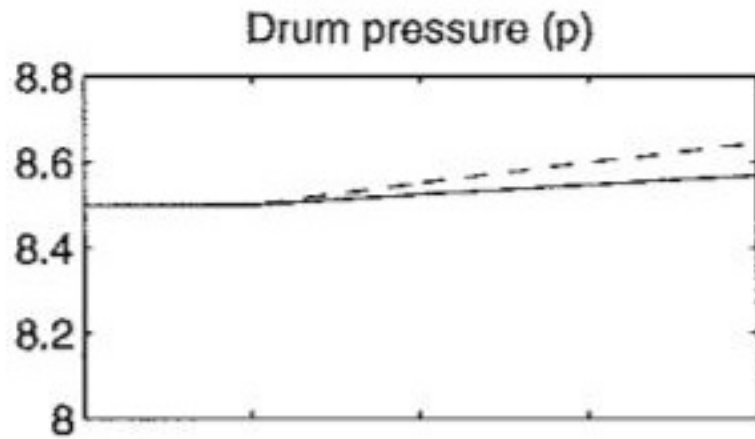
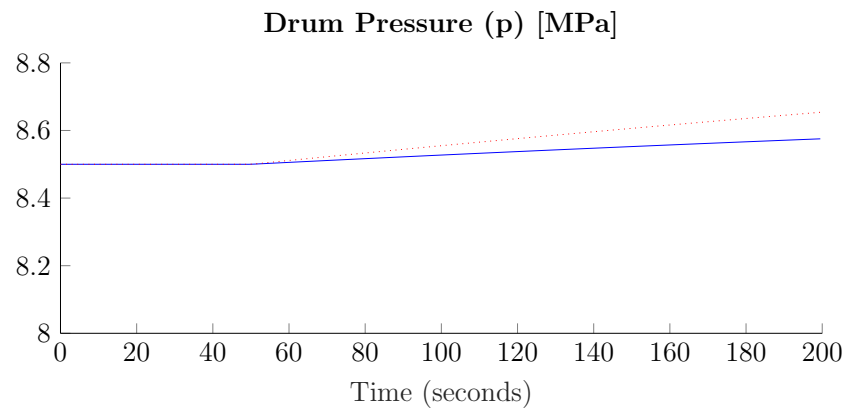


Figure 9 from Åström and Bell, section 5 [7]



Simulation Results using Model from Eq (3.9)

Figure 3.32: Drum Pressure Response to a step corresponding to 10°C Feed Water Temperature

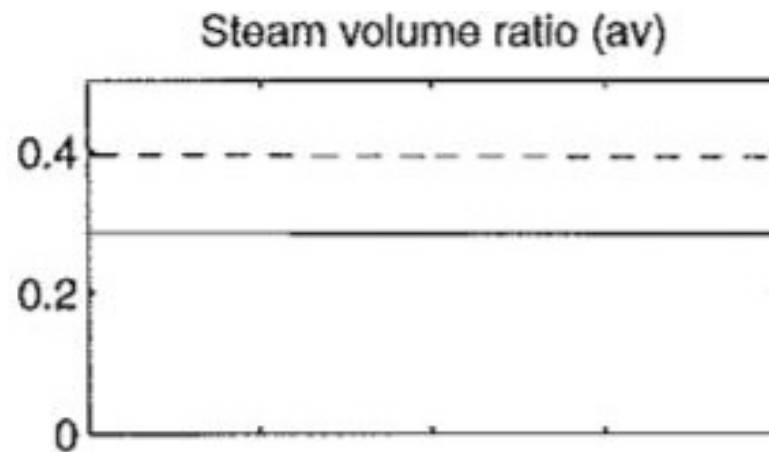
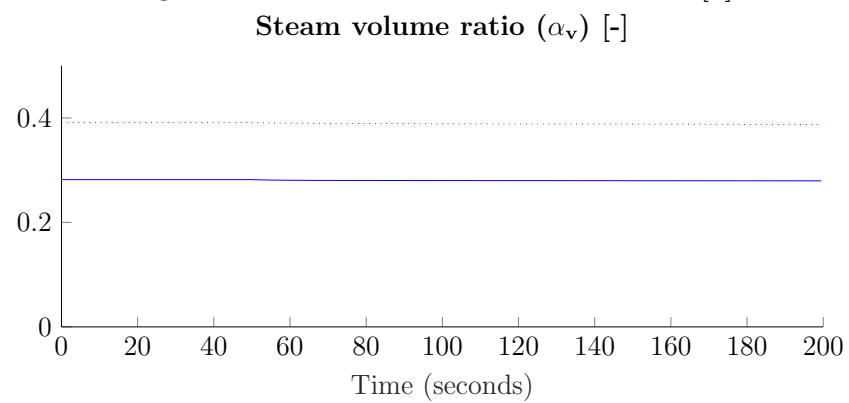


Figure 9 from Åström and Bell, section 5 [7]



Simulation Results using Model from Eq (3.9)

Figure 3.33: Steam Volume Ratio Response to a step corresponding to 10°C Feed Water Temperature

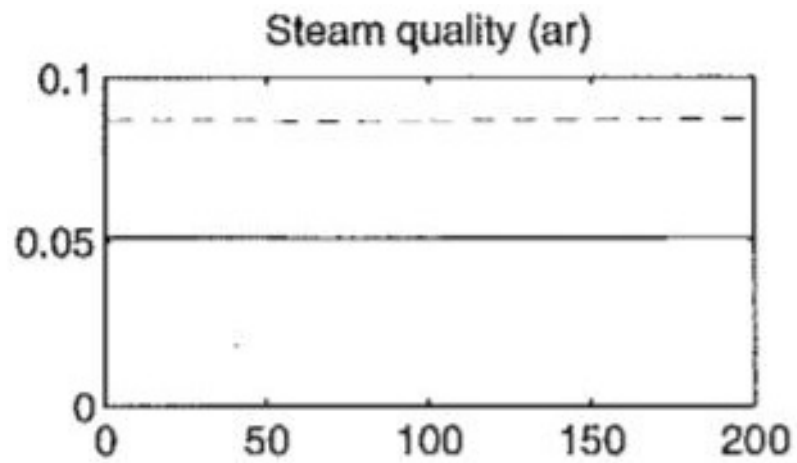
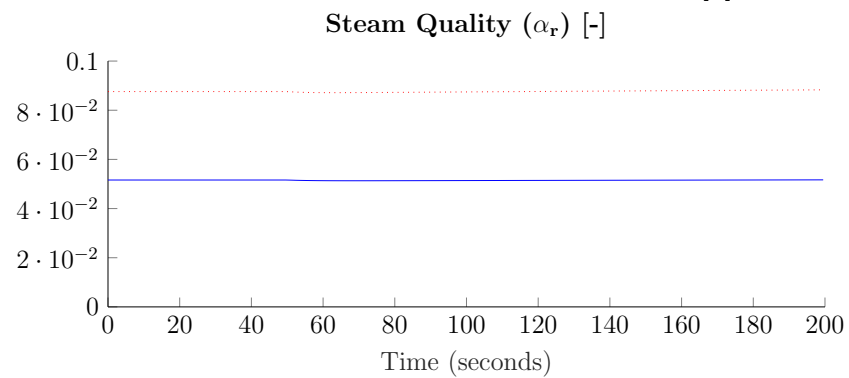


Figure 9 from Åström and Bell, section 5 [7]



Simulation Results using Model from Eq (3.9)

Figure 3.34: Steam Quality Response to a step corresponding to 10°C Feed Water Temperature

Using Figures 3.3 - 3.12 to compare the shape and scale of the graphed outputs from the simulated model and the corresponding output from Åström and Bell, it can be concluded that for a 10 MW fuel flow step increase, the system responses behave similarly. While the specific values may not match exactly due to a difference in calculated Initial Conditions, the same trends are shown on all of the simulation results.

Remark 3.1 *For $u(3) = Q$ the simulated model (3.9) has the same step response as the Åström and Bell model.*

Using Figures 3.13 - 3.22 to compare the shape and scale of the graphed outputs from the simulated model and the corresponding output from Åström and Bell, it can be concluded that for a 10 kg/s in steam flow step increase, the system responses behave similarly. While the specific values may not match exactly due to a difference in calculated Initial Conditions, the same trends are shown on all of the curves.

Remark 3.2 *For $u(2) = q_s$ the simulated model (3.9) has the same step response as the Åström and Bell model.*

Using Figures 3.23 - 3.28 to compare the shape and scale of the graphed outputs from the simulated model and the corresponding output from Åström and Bell, it can be concluded that for a 10 kg/s in feed water flow step increase, the system responses behave similarly. While the specific values may not match exactly due to a difference in calculated Initial Conditions, the same trends are shown on all of the curves.

Remark 3.3 *For $u(1) = q_f$ the simulated model (3.9) has the same step response as the Åström and Bell model.*

Using Figures 3.29 - 3.34 to compare the shape and scale of the graphed outputs from the simulated model and the corresponding output from Åström and Bell, it can be concluded that for a 10°C Feed Water temperature step increase, the system responses behave similarly. While the specific values may

not match exactly due to a difference in calculated Initial Conditions, the same trends are shown on all of the curves.

Remark 3.4 *For $u(4) = t_f$ the simulated model (3.9) has the same step response as the Åström and Bell model.*

If Remarks 3.1 - 3.4 are true, and all of the inputs to the model (3.9) have been tested then at the specified initial conditions it can be concluded that the model matches the Åström and Bell model.

3.4 Expanded Model

The Åström and Bell model uses 4 inputs, such as q_f , q_s , Q , t_f . Expansion upon this allows for a simpler control design. Basic assumptions and methods from previous works allow for the inputs to be lowered down to 2.

3.4.1 Input Simplifications

Feedwater

Feed-water temperature can usually be considered constant. Once an equilibrium value is found, this can reduce the number of inputs into the model.

$$t_f = t_{f0} = \text{constant}$$

This constant is then used to simplify the inputs from 4 to 3.

Steam Flow

Steam flow q_s is controlled by throttle valve and throttle pressure [13] which could be described by

$$p - p_t = K_{sh} \left(\frac{q_s}{k_v} \right)^2$$

$$q_s = \mu p_t$$

where k_v is the throttle valve coefficient that varies from 0 to 1. The throttle pressure can be estimated as being between 5% and 10% of the drum pressure [6], and K_{sh} and μ can be determined using this information and the above equations. For all simulations in this thesis, the throttle valve will be considered full open, and

$$K_{sh} = -0.0012 \quad \mu = 2.99 \quad k_v = 1$$

This then produces:

$$p = K_{sh}q_s^2 + \frac{q_s}{\mu}$$

$$q_s \implies q_s(p)$$

This function further simplifies the inputs from 3 (see Feedwater above) to 2, as q_s is now a direct function of p .

Valve Dynamics

The remaining inputs are controlled by valves, so first order approximations for the valve movement was added. Denoting T_{vQ} and T_{vfw} as the valve time constants, we have

$$\dot{Q} = \frac{(Q_{valve}-Q)}{T_{vQ}} \quad \dot{q}_f = \frac{(FW_{valve}-q_f)}{T_{vfw}}$$

which are expressed in the matrix form as:

$$\frac{d}{dt} \begin{bmatrix} Q \\ q_f \end{bmatrix} = \begin{bmatrix} \frac{(Q_{valve}-Q)}{T_{vQ}} \\ \frac{(FW_{valve}-q_f)}{T_{vfw}} \end{bmatrix} \quad (3.12)$$

These were then incorporated into the state equation, creating a 6 function nonlinear differential equation, with 6 states and 2 inputs.

State Variables: $V_{wt} \quad p \quad \alpha_r \quad V_{sd} \quad Q \quad q_{fw}$

Input Variables: $Q_{valve} \quad FW_{valve}$

3.4.2 Expanded Model with Simplified Inputs

Combining Equations (3.9) and (3.12) results in the following:

$$\frac{d}{dt} \begin{bmatrix} V_{wt} \\ p \\ \alpha_r \\ V_{sd} \\ Q \\ q_f \end{bmatrix} = \begin{bmatrix} e_{11} & e_{12} & 0 & 0 \\ e_{21} & e_{22} & 0 & 0 \\ 0 & e_{32} & e_{33} & 0 \\ 0 & e_{42} & e_{43} & e_{44} \end{bmatrix}^{-1} \begin{bmatrix} q_f - q_s(p) \\ Q + q_f h_f(p, t_{f0}) - q_s(p) h_s(p) \\ Q + \alpha_r h_c(p) q_{dc}(p) \\ \frac{\rho_s(p)}{T_d} (V_{sd}^0 - V_{sd}) + \frac{h_f(p, t_{f0}) - h_w(p)}{h_c(p)} q_f \\ \frac{(Q_{valve} - Q)}{T_{vQ}} \\ \frac{(FW_{valve} - q_{fw})}{T_{vfw}} \end{bmatrix} \quad (3.13)$$

Note: All shown e_{xy} are functions of $p \rightarrow e_{xy}(p)$

It should be noted that Equation (3.13) is in terms of

$$\dot{x} = f(x, u)$$

where:

$$x = \begin{bmatrix} V_{wt} & p & \alpha_r & V_{sd} & Q & q_f \end{bmatrix}^T$$

$$u = \begin{bmatrix} Q_{valve} & FW_{valve} \end{bmatrix}^T$$

This is a Nonlinear-Time-Invariant system model in the State Space form.

A list of simplifications made for the final model used (3.13) are as follows:

- Feed water Valve is treated as a first order system compared to Feed water Flow
- Fuel Valve is treated as a first order system compared to Heat transfer into the boiler. This is an oversimplification of the fuel flow dynamics, which consist of fuel flow and air flow. Air flow is normally controlled by excess flue oxygen and the stoichiometric ratio to fuel flow.
- Feed water Temperature is treated as constant
- Steam Flow is estimated based off of throttle pressure
- Properties of water are modeled based off of numerical evidence

3.4.3 Equilibrium Values

To find the equilibrium point of the system, equation (3.9) is set to 0 to and the following state values obtain the following control and output values at various equilibrium points. These were selected by using the medium equilibrium point in (3.11), specifically and varying p_0 . Equilibrium values were then found by solving for steady state. V_{wt0} and p_0 were selected first, and then from there Q_0 and q_f can be found, and then Q_{valve} and FW_{valve} are found from there. The remaining two values of α_{r0} and V_{sd0} can be determined.

		<i>Low</i>	<i>Medium</i>	<i>High</i>	<i>units</i>	
V_{wt0}	=	57.1	57.1	57.1	m^3	
p_0	=	6.8	8.5	10.2	MPa	
α_{r0}	=	0.0325	0.0435	0.0561	–	
V_{sd0}	=	5.213	4.984	4.854	m^3	
Q_0	=	57.11	67.65	76.84	MW	(3.14)
q_{f0}	=	33.07	39.79	46.12	kg/s	
Q_{valve}	=	57.11	67.65	76.84	MW	
FW_{valve}	=	33.07	39.79	46.12	kg/s	
l_0	=	-0.002	-0.032	-0.051	Δm	

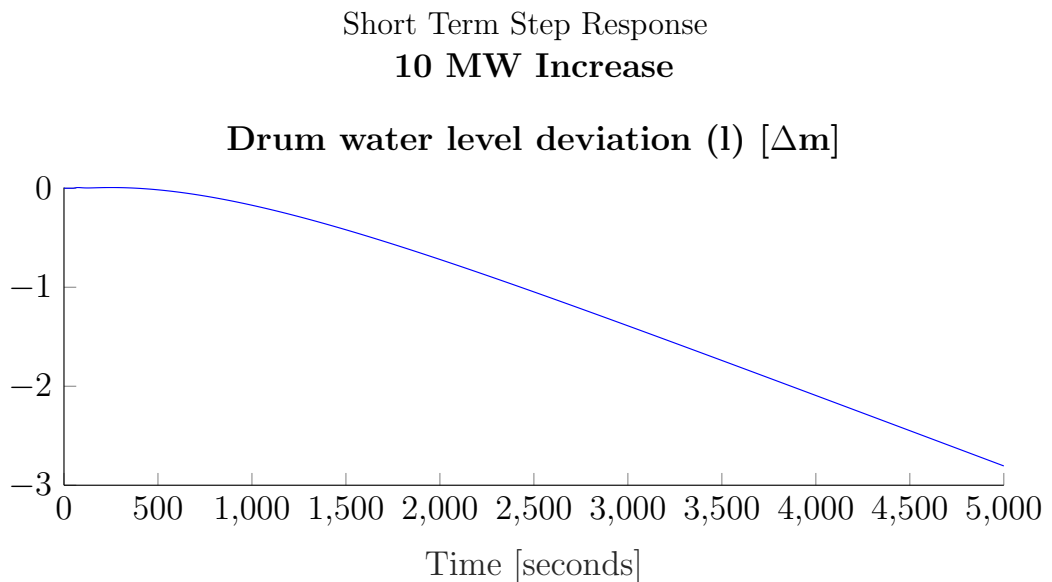
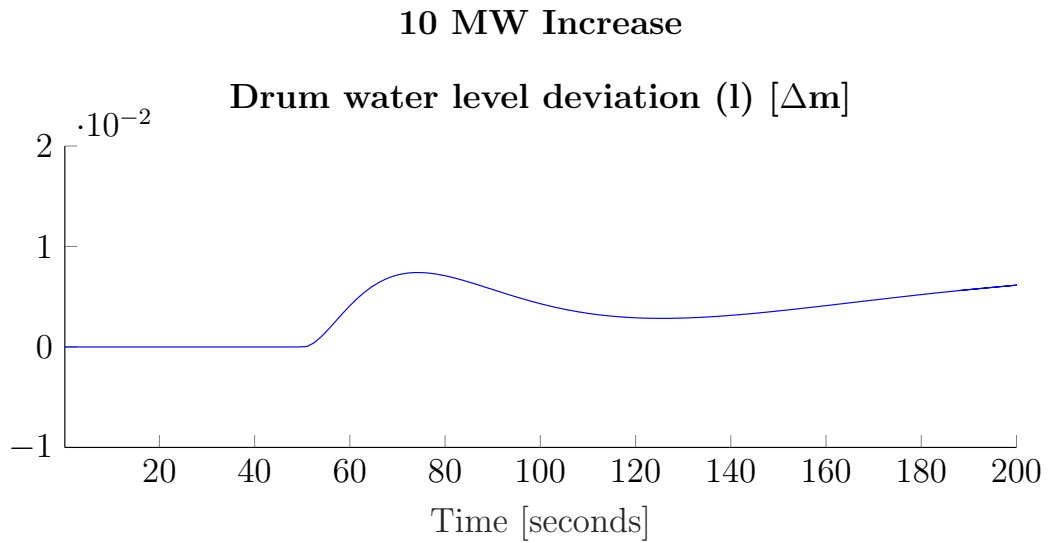
It should be noted that these Equilibrium values used the constant feed water temperature as shown in 3.11. The same concerns apply to these equilibrium points.

3.4.4 Open Loop Step Responses to Expanded Model

The system model given in equation (3.13) was simulated with step inputs, the results are the following figures. The Medium operating point was used, as it is the closest to the operating point in the previous simulations.

Figures 3.35 - 3.39 use the model (3.13), while Figures 3.3 - 3.8 uses the model (3.9). Both sets of figures use the same step input of $Q = 10$ MW, however the expanded model uses a first order dynamic delay.

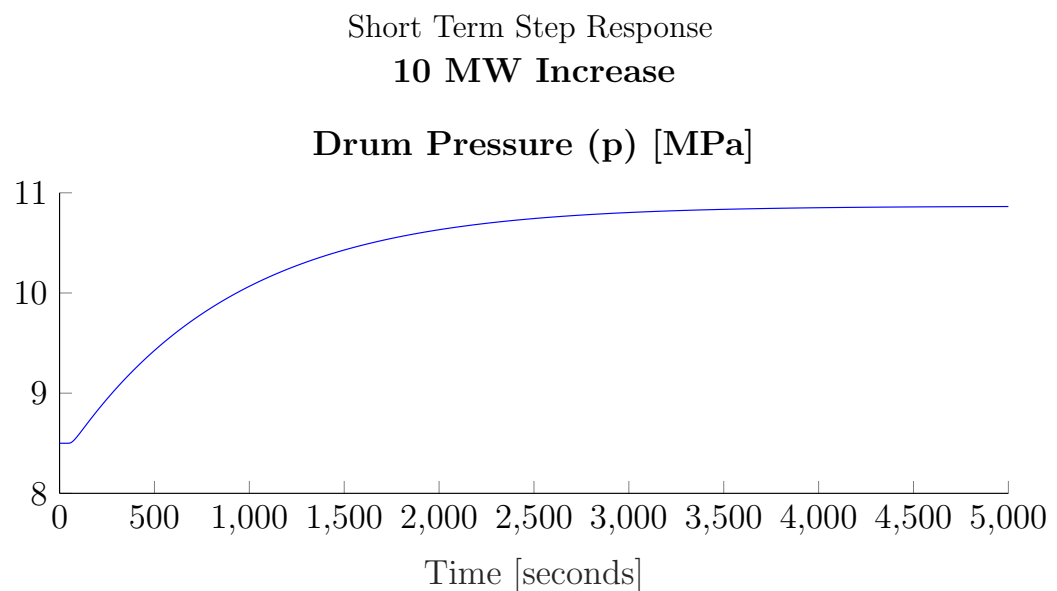
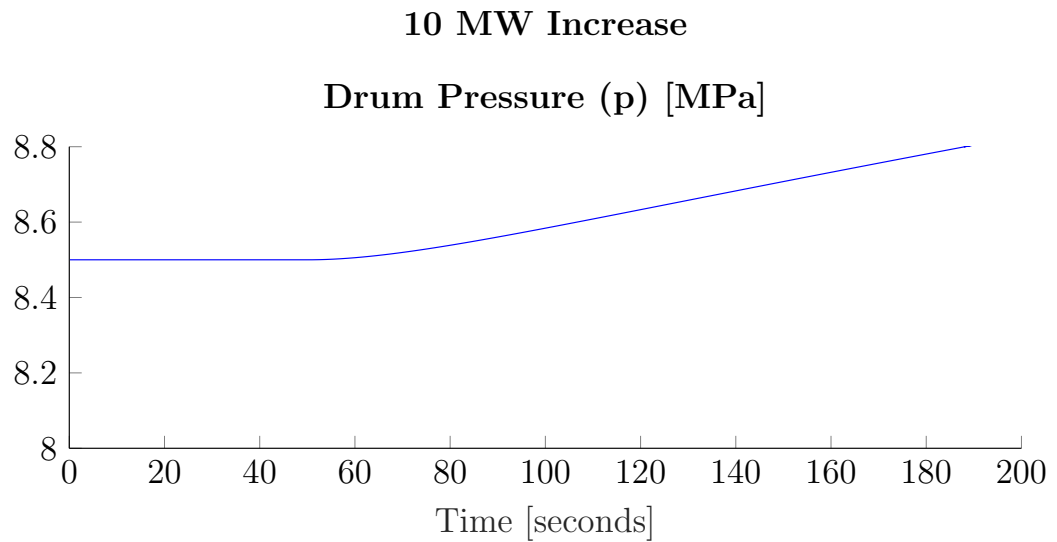
Figures 3.40 - 3.44 use the model (3.13), while Figures 3.23 - 3.28 uses the model (3.9). Both sets of figures use the same step input of $q_f = 10$ kg/s, however the expanded model uses a first order dynamic delay.



Long Term Step Response

Figure 3.35: Drum Water Level Response to a step corresponding to 10 MW in fuel flow rate

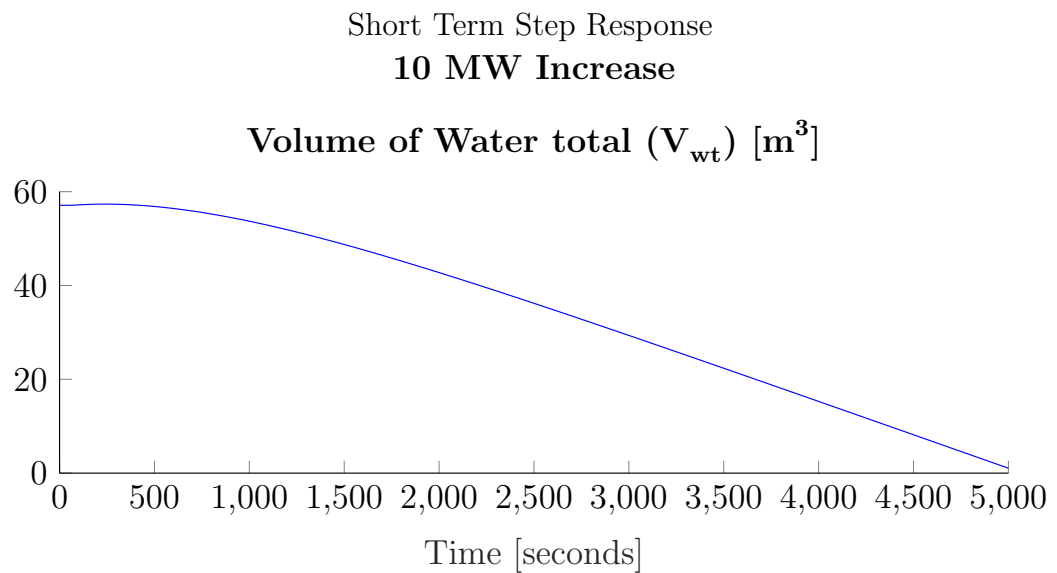
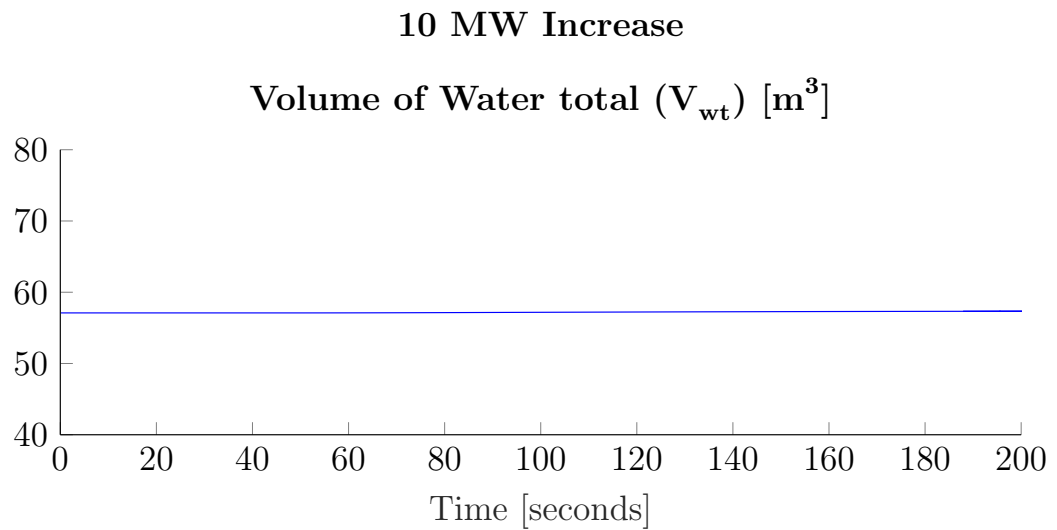
Figure 3.35 should be directly compared to Figure 3.3. This shows the shrink/swell effect, in how level initially reacts in one direction, however it ultimately trends to the opposite direction. The step response does not match Åström and Bell response due to the change in operating point.



Long Term Step Response

Figure 3.36: Drum Pressure Response to a step corresponding to 10 MW in fuel flow rate

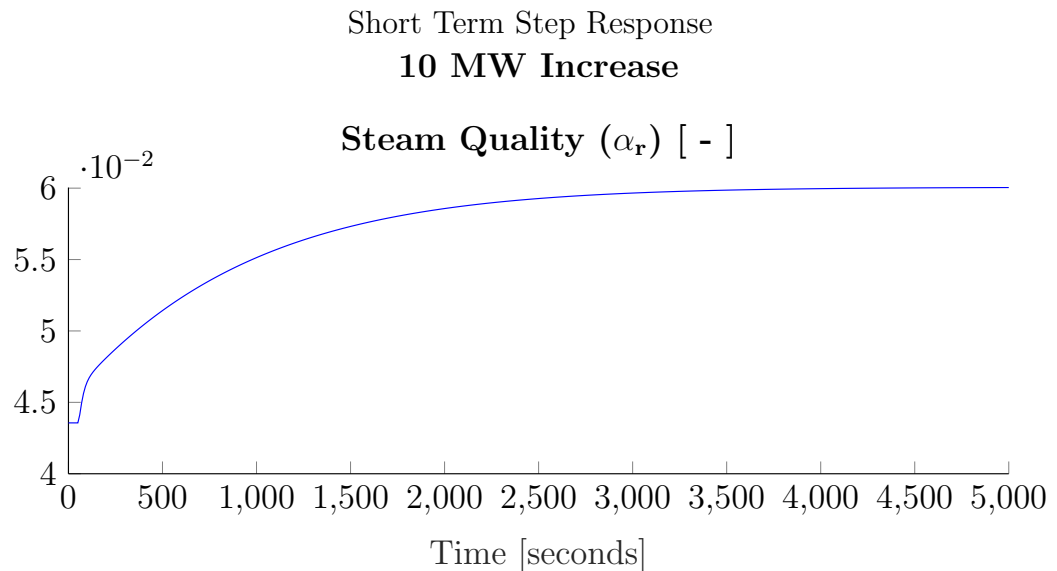
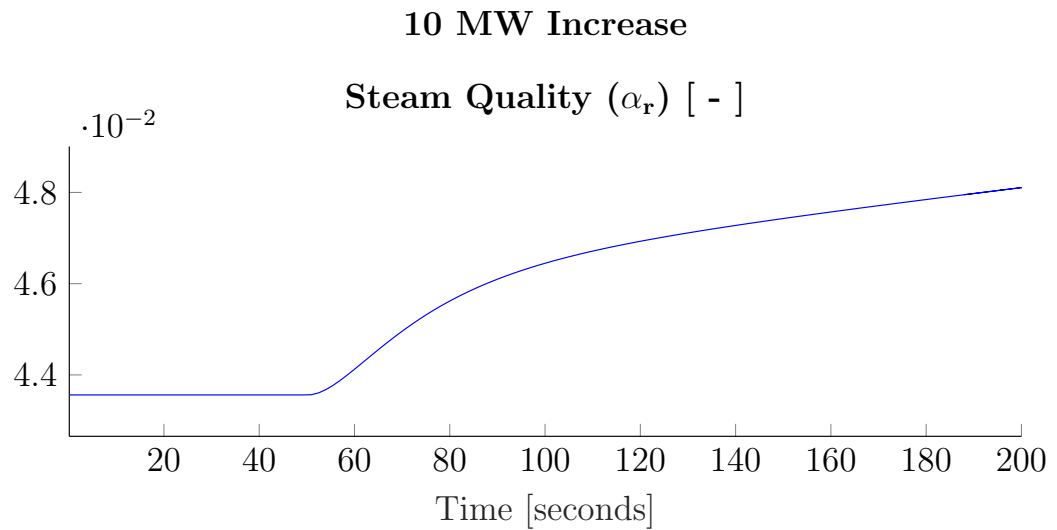
Figure 3.36 should be directly compared to Figure 3.6, the initial response matches what was seen in Åström and Bell and pressure eventually reaches a stable settling point.



Long Term Step Response

Figure 3.37: Volume of Total Water Response to a step corresponding to 10 MW in fuel flow rate

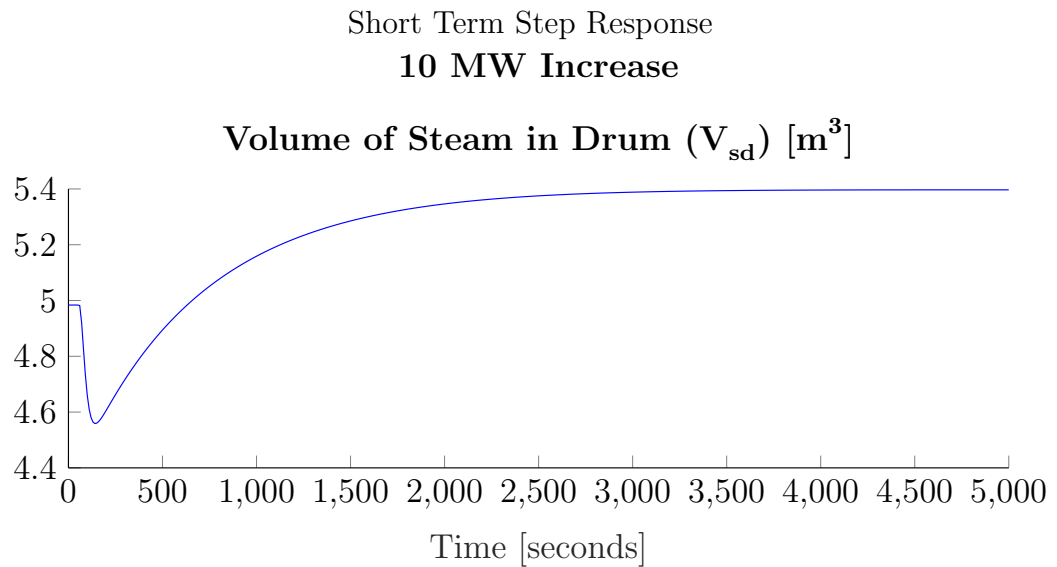
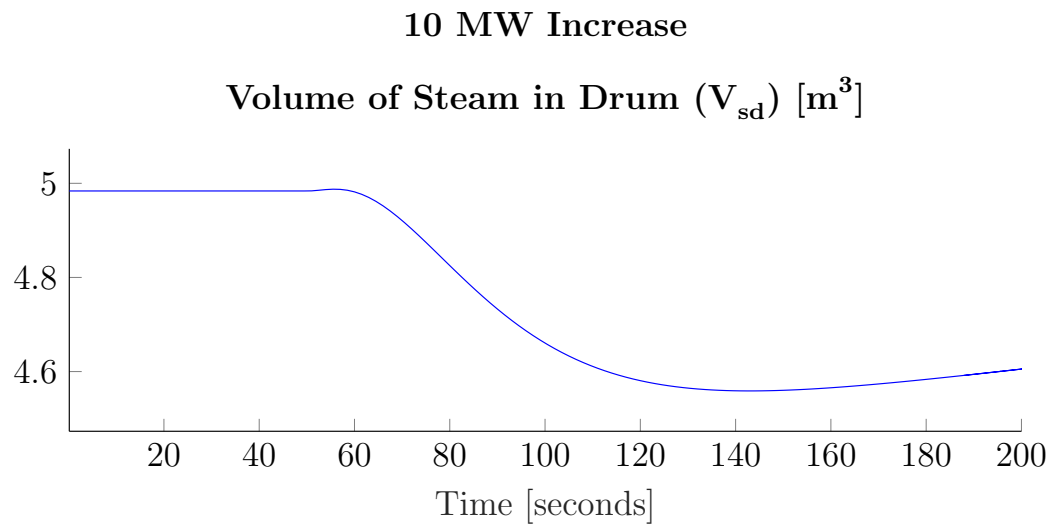
Figure 3.37 is not directly comparable to a figure from Åström and Bell, however it makes sense that if the feed water valve is held constant but more heat is added that water will eventually leave the system in the form of steam.



Long Term Step Response

Figure 3.38: Steam Quality Response to a step corresponding to 10 MW in fuel flow rate

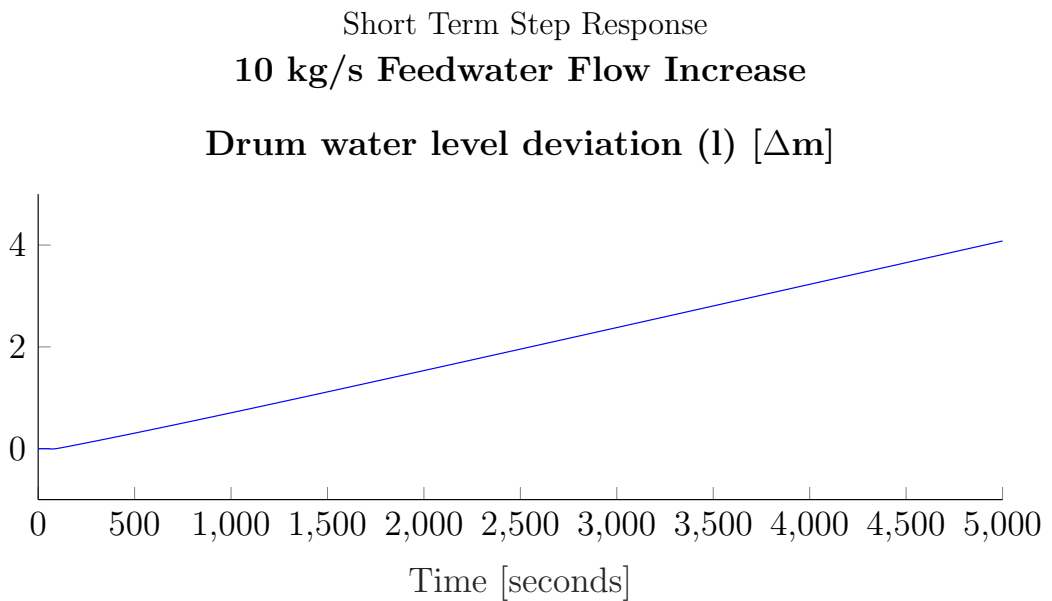
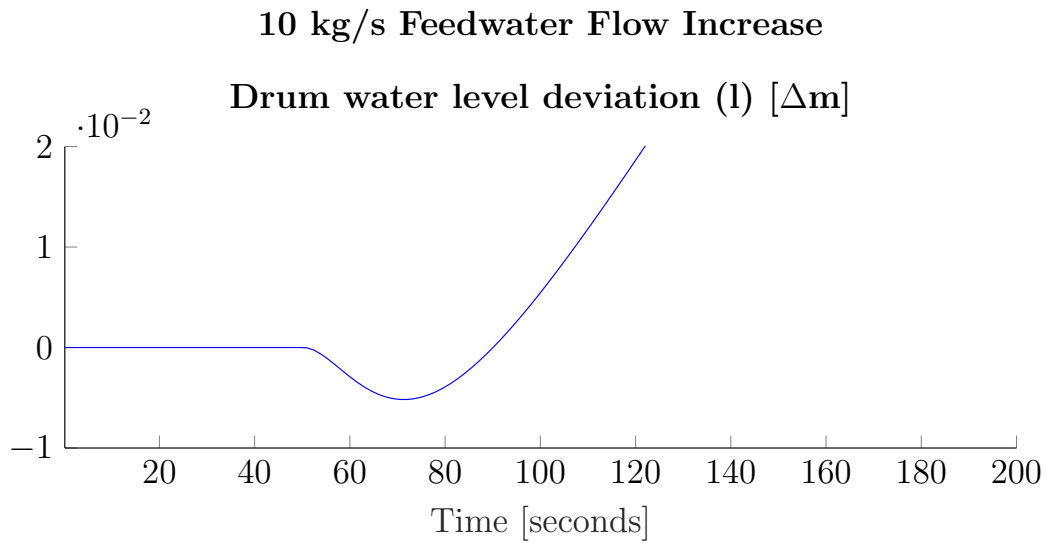
Figure 3.38 should be directly compared to Figure 3.8, the initial response matches what was seen in Åström and Bell and steam quality eventually reaches a stable settling point. The value changes are due to the change in operating point specified above.



Long Term Step Response

Figure 3.39: Volume of Steam in the Drum Response to a step corresponding to 10 MW in fuel flow rate

Figure 3.39 should be directly compared to Figure 3.5, as the volume of steam in the drum is directly proportional to the steam level contribution. The initial response does not show the shrink/swell effect due to the change in operating point specified above.



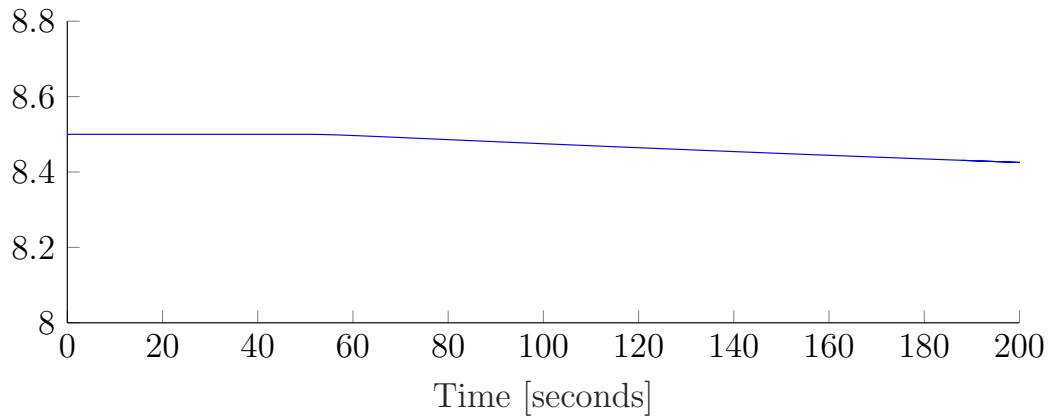
Long Term Step Response

Figure 3.40: Drum Water Level Response to a step corresponding to 10 kg/s feed water flow rate

Figure 3.40 should be directly compared to Figure 3.23. The shrink/swell effect shown in 3.23 is not seen here due to the change in operating point.

10 kg/s Feedwater Flow Increase

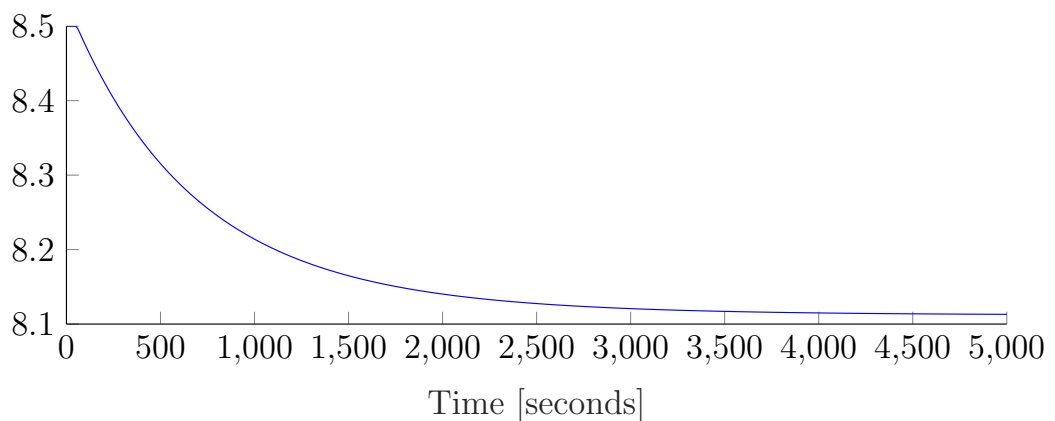
Drum Pressure (p) [MPa]



Short Term Step Response

10 kg/s Feedwater Flow Increase

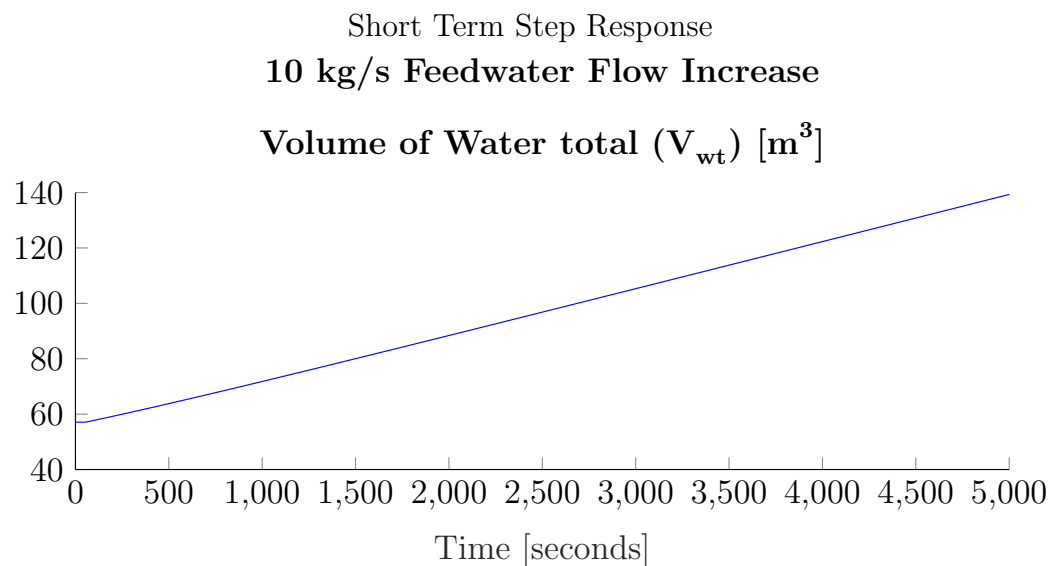
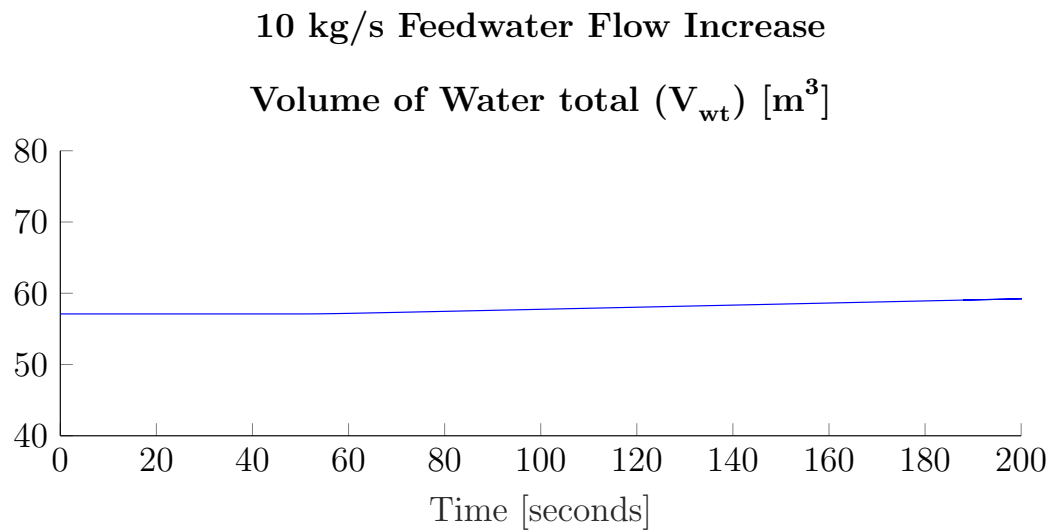
Drum Pressure (p) [MPa]



Long Term Step Response

Figure 3.41: Drum Pressure Response to a step corresponding to 10 kg/s feed water flow rate

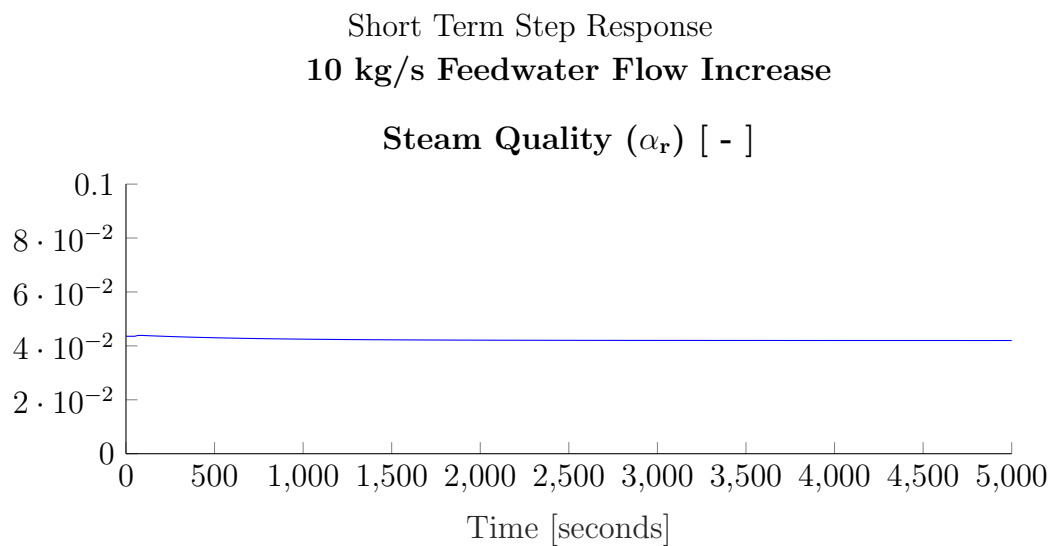
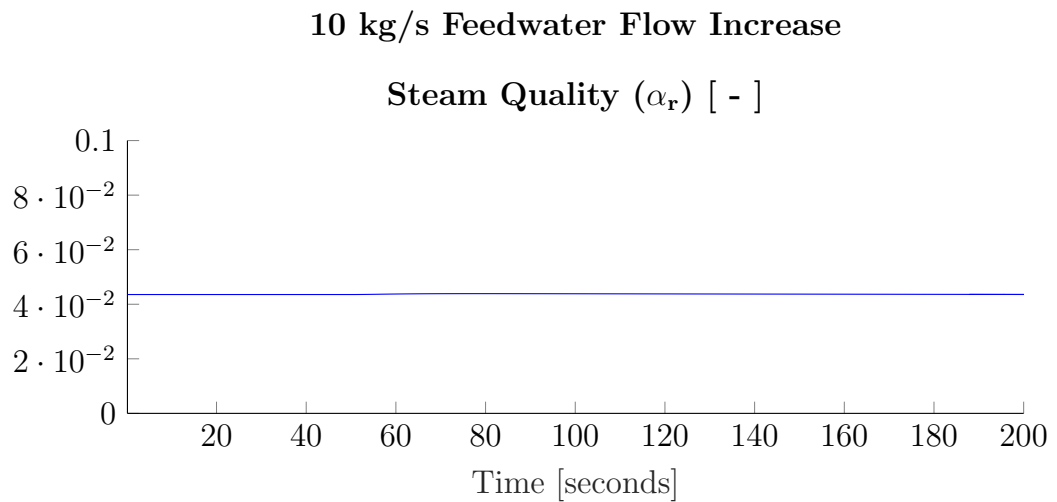
Figure 3.41 should be directly compared to Figure 3.26, the initial response does not match what was seen in Åström and Bell due to the change in operating point specified above.



Long Term Step Response

Figure 3.42: Volume of Total Water Response to a step corresponding to 10 kg/s feed water flow rate

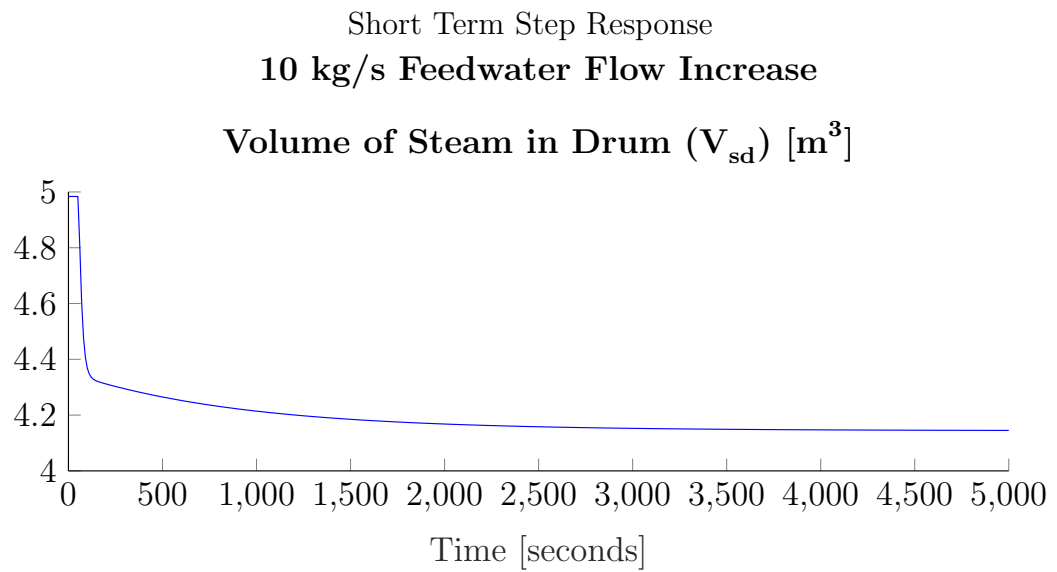
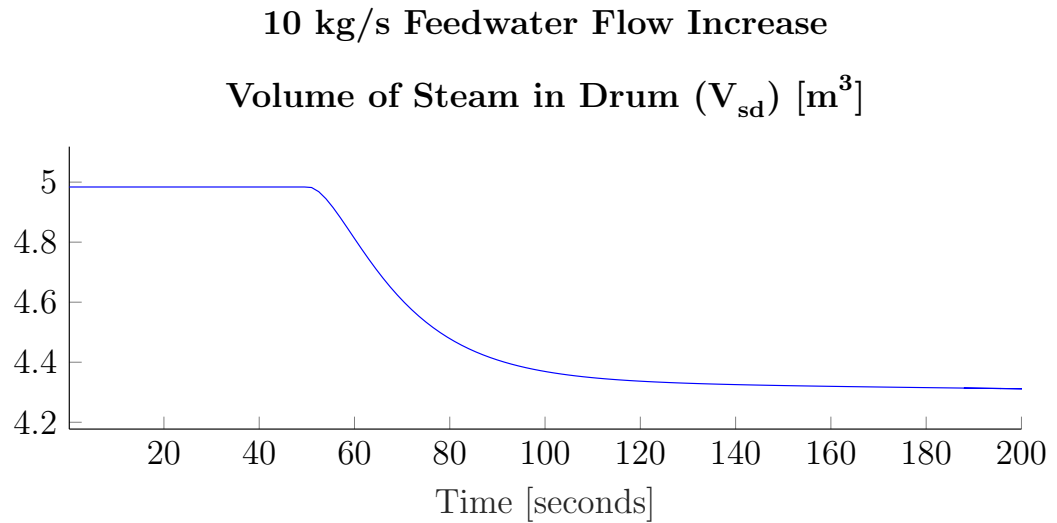
Figure 3.42 is not directly comparable to a figure from Åström and Bell, however it makes sense that if the feed water increased from a stable operating point and all other inputs are held constant, then more water will eventually fill the drum.



Long Term Step Response

Figure 3.43: Steam Quality Response to a step corresponding to 10 kg/s feed water flow rate

Figure 3.43 should be directly compared to Figure 3.28, the response matches what was seen in previous works and steam quality eventually reaches a stable settling point. Note the axis differences due to the load changes specified earlier.



Long Term Step Response

Figure 3.44: Volume of Steam in the Drum Response to a step corresponding to 10 kg/s feed water flow rate

Figure 3.44 should be directly compared to Figure 3.25, as the volume of steam in the drum is directly proportional to the steam level contribution.

These simulations do not take into account that the drum has a completely finite volume to fill nor does it take into account the possibility of bursting from high pressure. Future work could expand upon this, however this is not necessary for this research. The goal of these long term simulations was to determine that the shrink/swell effect was occurring and on what timescale would it be necessary to see those effects. Future simulations will be well within physical controllable ranges.

CHAPTER 4

THREE ELEMENT CONTROL

As discussed in Section 2.1, PID control is by design not optimized. It is however a proven tool used in industry and has been able to satisfactorily control boilers for decades. This chapter will discuss on the physical dynamics of how the PID strategy seen in Figure 2.1 can be used on the Expanded model, Eq. (3.13), without linearization. It should be noted that many power plants use adaptive controller gains in conjunction with this strategy.

4.1 Controller Design

The model in place requires control inputs to the Feed Water Valve and the Fuel Valve. The Fuel valve controls pressure directly, but due to the dynamics of the boiler, level control cannot be decoupled entirely, and the steam flow out becomes part of the three element controller. Due to the fact that the system cannot be decoupled, conventional PID tuning techniques are not applicable and a heuristic trial and error approach was used.

The Controller was tuned to be meet the design criterion of:

- 15% Overshoot for a Drum Level step at High load
- 450 seconds of Settling Time for a Drum Level step at High Load
- Drum Pressure will remain stable

- Drum Level will remain stable for other disturbances (such as a Drum Pressure Step)

The pressure controller is designed as a PI controller with the following gains:

$$K_{pQ} = 100 \quad K_{iQ} = 0.15$$

$$Q_{valve} = \left(K_{pQ} + K_{iQ} \frac{1}{s} \right) (p_{ref} - p) \quad (4.1)$$

The Three Element controller follows the format shown in Figure 2.2. The Level Controller has the following Gains:

$$K_{pl} = 255 \quad K_{il} = 0.098$$

$$q_{fwspl} = \left(K_{pl} + K_{il} \frac{1}{s} \right) (l_{ref} - l) \quad (4.2)$$

The Level Controller then feeds into the Feed Water Controller and the Feed Water Controller has a feed Forward. The following gains and equations apply:

$$K_{p_{qfw}} = 0.3 \quad K_{i_{qfw}} = 0.2 \quad K_{ff} = 1$$

$$FW_{valve} = \left(K_{p_{qfw}} + K_{i_{qfw}} \frac{1}{s} \right) (q_{fwspl} - q_{fw}) + K_{ff} q_s \quad (4.3)$$

The cascaded control is then calculated by combining (4.2) and (4.3) to get (4.4)

$$FW_{valve} = \left(K_{p_{qfw}} + K_{i_{qfw}} \frac{1}{s} \right) \left(\left(\left(K_{pl} + K_{il} \frac{1}{s} \right) (l_{ref} - l) \right) - q_{fw} \right) + K_{ff} q_s \quad (4.4)$$

These PID Controllers (4.1)-(4.4) were integrated into the Expanded Valve Model seen in Equation (3.13), which increased the number of states by 3 (one for each integral term in the PI Controllers). The new state variable for the PID closed loop system is as follows:

$$\left[V_{wt} \quad p \quad \alpha_r \quad V_{sd} \quad Q \quad q_f \quad (q_{fwspl} - q_{fw}) \quad (l_{ref} - l) \quad (p_{ref} - p) \right]^T$$

4.2 Simulation Results

The simulation using the PID controller can be calculated using the full nonlinear model without any linearization. The gains were chosen as seen in Section 4.1.

$$z(t) = \begin{bmatrix} x(t) \\ e(t) \end{bmatrix} \quad z(t_{n+1}) = z(t_n) + \dot{z}(t_n)T_s$$

$$t_n = 0, T_s, 2T_s, 3T_s, \dots, nT_s \quad T_s = 0.5s$$

It should be noted that the chosen gain values may not control properly over a large range, they were tested using trial and error via simulation.

The following simulations use the initial condition at the load setting as defined in (3.14). An initial reference signal is then created based off of the stable initial condition ($r_0 = y_0$).

$$x_0 = \begin{cases} V_{wt0} = 57.1 & 57.1 & 57.1 & m^3 \\ p_0 = 6.8 & 8.5 & 10.2 & MPa \\ \alpha_{r0} = 0.0325 & 0.0435 & 0.0561 & - \\ V_{sd0} = 5.213 & 4.984 & 4.854 & m^3 \\ Q_0 = Q_{valve} = 57.11 & 67.65 & 76.84 & MW \\ qf_0 = FW_{valve} = 33.07 & 39.79 & 46.12 & kg/s \end{cases}$$

$$r_0 = y_0 = \begin{cases} l_0 = -0.002 & -0.032 & -0.051 & \Delta m \\ p_0 = 6.8 & 8.5 & 10.2 & MPa \end{cases}$$

The reference signal $r(t)$ will be applied, and r_1 will vary based on the step command.

$$r(t) = \begin{cases} r_0 & \text{for } t < t_{step} \\ r_1 & \text{for } t > t_{step} \end{cases}$$

The controlled outputs are each compared to their reference as a step change is applied. This system has two controlled variables therefore four steps are required to show the controllers response; variable 1 (Drum Pressure) step up, variable 1 (Drum Pressure) step down, variable 2 (Drum Level Deviation) step up, variable 2 (Drum Level Deviation) step down. When one variable is being stepped the other has its reference held constant. The two variables are coupled together and when a reference is held constant it becomes a disturbance rejection response.

4.2.1 Level Step Increase Figures 4.1 - 4.3

The step command for this set of simulations is was calculated as follows:

$$r_1 = r_0 + \Delta r_{command} \quad \Delta r_{command} = \begin{bmatrix} \Delta l_{ref} \\ \Delta p_{ref} \end{bmatrix} = \begin{bmatrix} 0.1 \\ 0.0 \end{bmatrix}$$

$$r_1 = \begin{cases} & \textit{Low} & \textit{Medium} & \textit{High} & \textit{units} \\ l_{ref_0} & = & 0.098 & 0.068 & 0.049 & \Delta m \\ p_{ref_0} & = & 6.8 & 8.5 & 10.2 & MPa \end{cases}$$

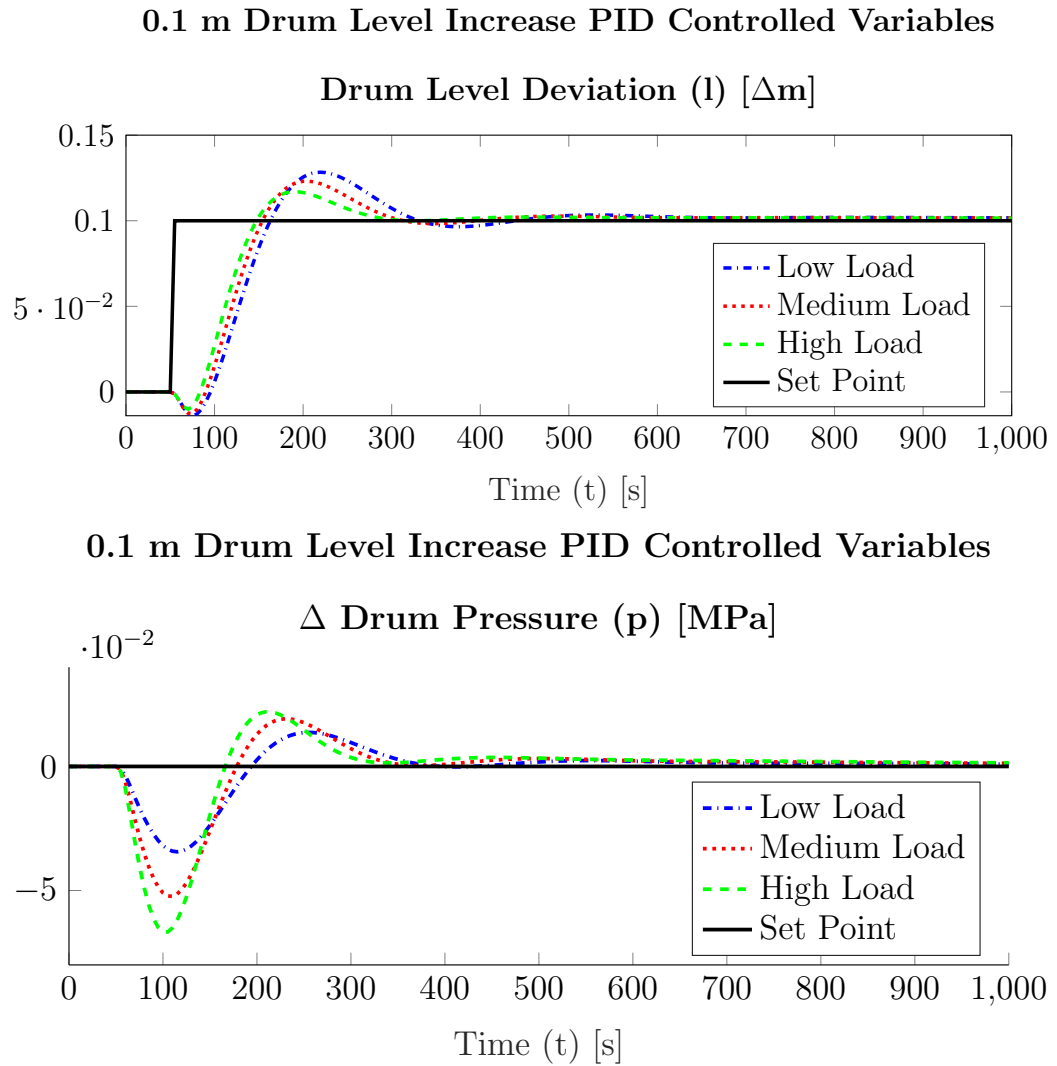


Figure 4.1: Controlled Variables PID Response to Drum Level step of 0.1

Note: This figure shows the change from the initial conditions, as the initial conditions vary across the load settings. This was done to compare the controller performance.

		Low Load	Medium Load	High Load	Average
Level	% Overshoot	26.89 %	21.76 %	15.68 %	21.45 %
Level	Settling Time	580 s	520 s	450.5 s	516.8 s
Level	Disturbance Rejection Energy	1.623	1.402	1.181	1.402
Pressure	Disturbance Rejection Energy	0.1864	0.3724	0.5285	0.3624

Table 4.1: PID Controller Performance Parameters: Level Step Increase

Figure 4.1 shows the simulation results using the specified step command and Table 4.2.1 shows the performance characteristics of this simulation as defined in Chapter 2.4. It can be seen that using these tuning parameters, the design goal is achieved. The Shrink/Swell effect can be seen on drum level deviation as well as the reduction of the Shrink/Swell effect as load increases (which is also a known phenomenon) .

The effects of different loads on this controller can be seen in two ways; as load increases the level controller performance parameters improve (decreased overshoot and settling time) while the pressure controller's performance degrades (energy increases). This can also be seen graphically as the amplitudes lower as load increase for drum level deviation, but the amplitudes increase for drum pressure.

It should be noted that there is what appears to be steady state error on both controlled variables, however this is due to the tuning. Increasing the integral component of the controllers (K_{iQ} , K_{iI}) will reduce this, however during this research it was not possible to find tuning parameters that both met the design criterion and quickly reduced this error component to zero.

Figure 4.1 does not have a comparable open loop simulation (like when comparing Figure 4.7 and Figure 3.36) because drum level is an integrative signal. A square wave or impulse command of FW_{valve} may show comparable open loop results.

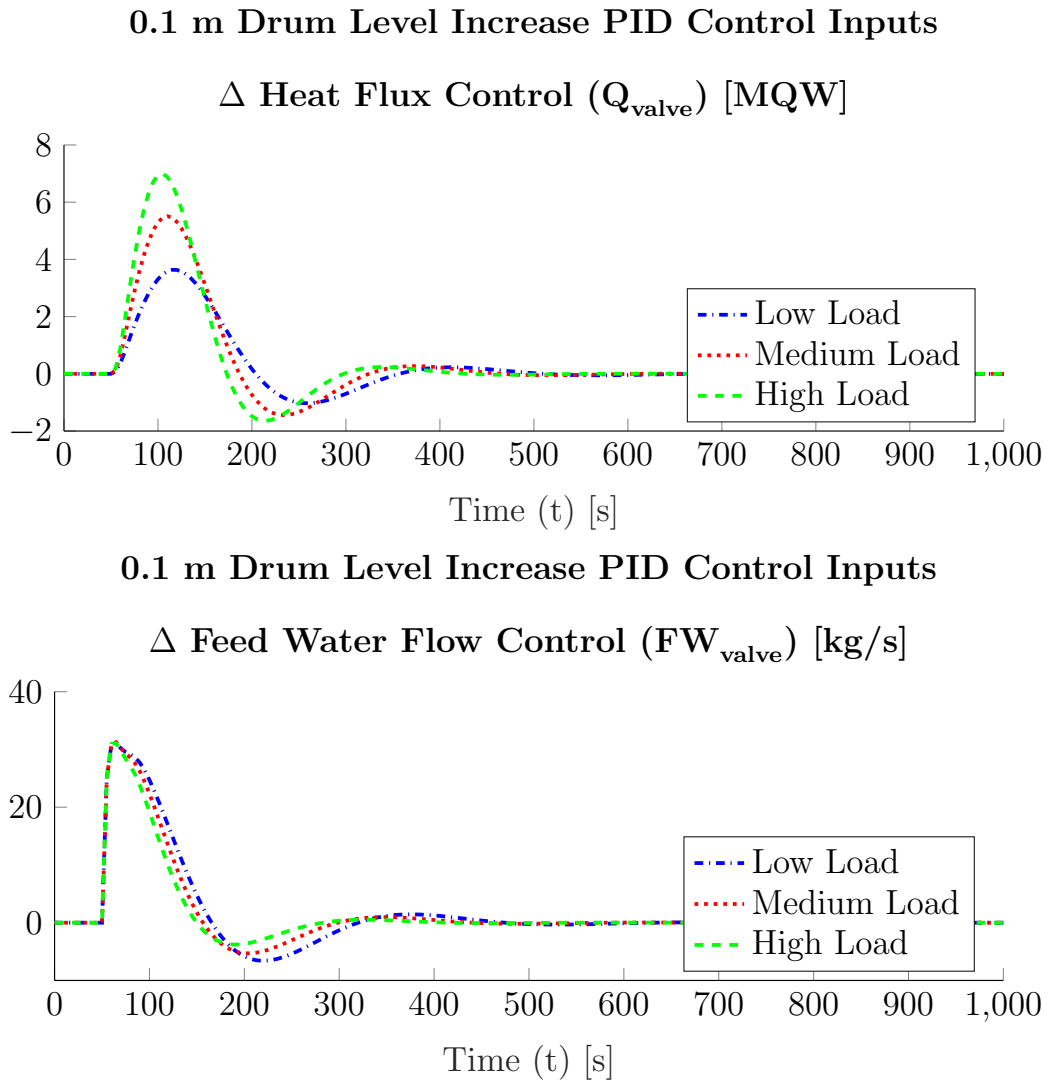


Figure 4.2: Controller Inputs PID Response to Drum Level step of 0.1

Note: This figure shows the change from the initial conditions, as the initial conditions vary across the load settings. This was done to compare the controller performance.

		Low Load	Medium Load	High Load	Average
Q_{valve}	Signal Energy	1958	3893	5512	3787
FW_{valve}	Signal Energy	1.1e+5	9.546e+4	8.089e+4	9.545e+4

Table 4.2: PID Controller Input Performance Parameters: Level Step Increase

Figure 4.2 shows the controller inputs and Table 4.2.1 shows the controller input energy for the simulations shown in Figure 4.1.

It can be seen that as load increases Heat flux requires more control action while feed water requires less. The energy shown by these signals increases for heat flux, but stays roughly the same for feed water.

0.1 m Drum Level Increase PID Cascade Control Error

Feed Water Flow - Feed Water Flow Reference $q_f - q_{ref}$ [kg/s]

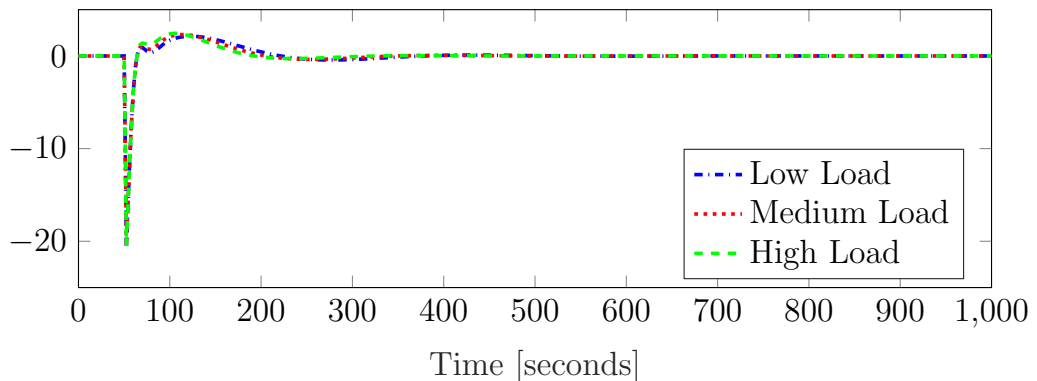


Figure 4.3: Cascaded PID Controller Response to Drum Level step of 0.1

Note: This figure shows the error from a cascaded set point. The set point varies in time and is not shown as a separate graph. This was done to compare the controller performance.

Figure 4.3 shows the error from the cascaded controller that is indicative of the three element design. It can be seen that there is a very quick response for all loads. As load increases the error decreases, however it is a negligible performance change.

4.2.2 Level Step Decrease Figures 4.4 - 4.6

The step command for this set of simulations is was calculated as follows:

$$r_1 = r_0 + \Delta r_{command} \quad \Delta r_{command} = \begin{bmatrix} \Delta l_{ref} \\ \Delta p_{ref} \end{bmatrix} = \begin{bmatrix} -0.1 \\ 0.0 \end{bmatrix}$$

$$r_1 = \begin{cases} & \begin{matrix} Low & Medium & High & units \end{matrix} \\ l_{ref0} & = & -0.102 & -0.132 & -0.151 & \Delta m \\ p_{ref0} & = & 6.8 & 8.5 & 10.2 & MPa \end{cases}$$

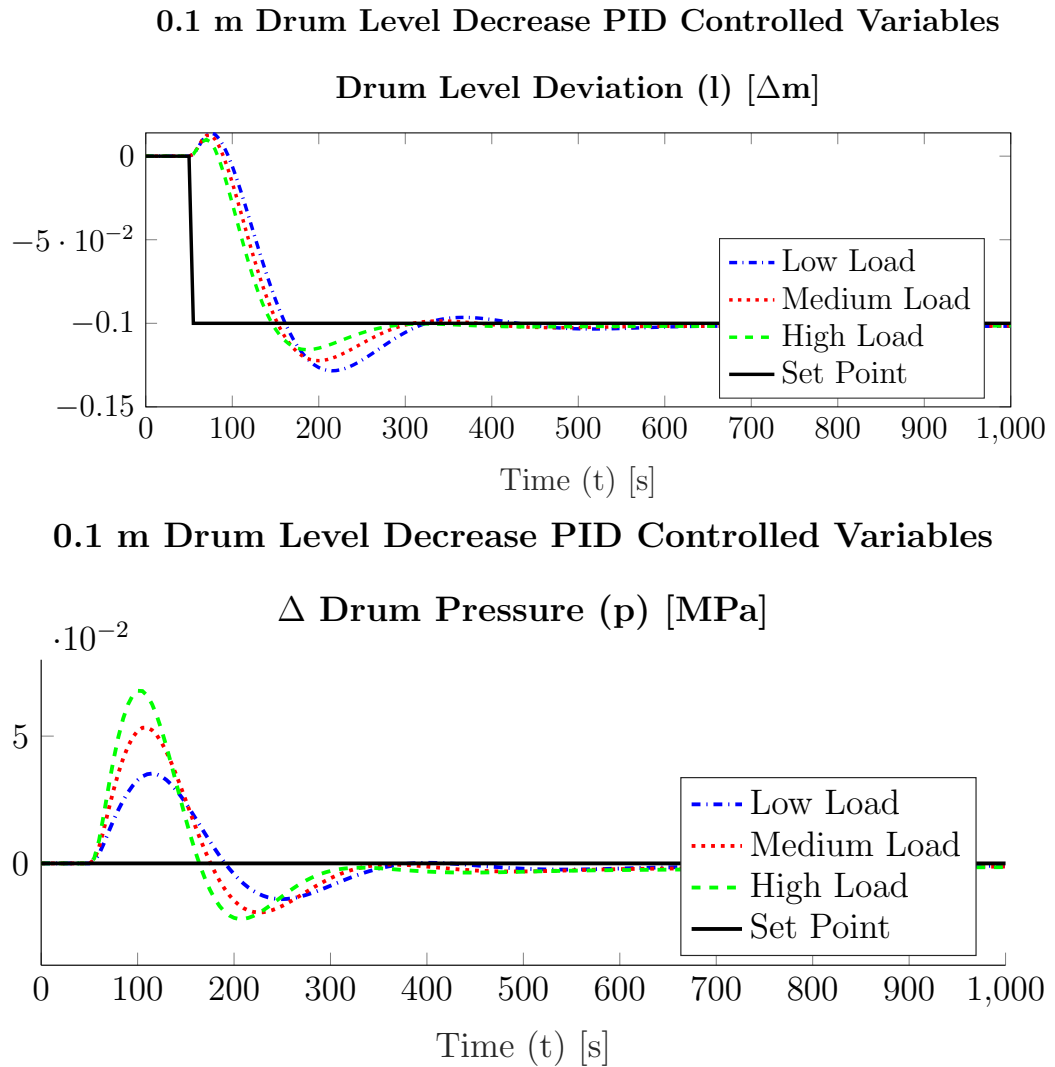


Figure 4.4: Controlled Variables PID Response to Drum Level step of -0.1

Note: This figure shows the change from the initial conditions, as the initial conditions vary across the load settings. This was done to compare the controller performance.

		Low Load	Medium Load	High Load	Average
Level	% Overshoot	26.96 %	20.99 %	14.5 %	20.82 %
Level	Settling Time	565.5 s	508.5 s	436.5 s	503.5 s
Level	Disturbance Rejection Energy	1.614	1.381	1.161	1.385
Pressure	Disturbance Rejection Energy	0.1909	0.3756	0.5292	0.3652

Table 4.3: PID Controller Performance Parameters: Level Step Decrease

Figure 4.4 shows a step from the same operating points as Figure 4.1, however in the opposite direction. Since the simulation is similar much of the same information can be gained.

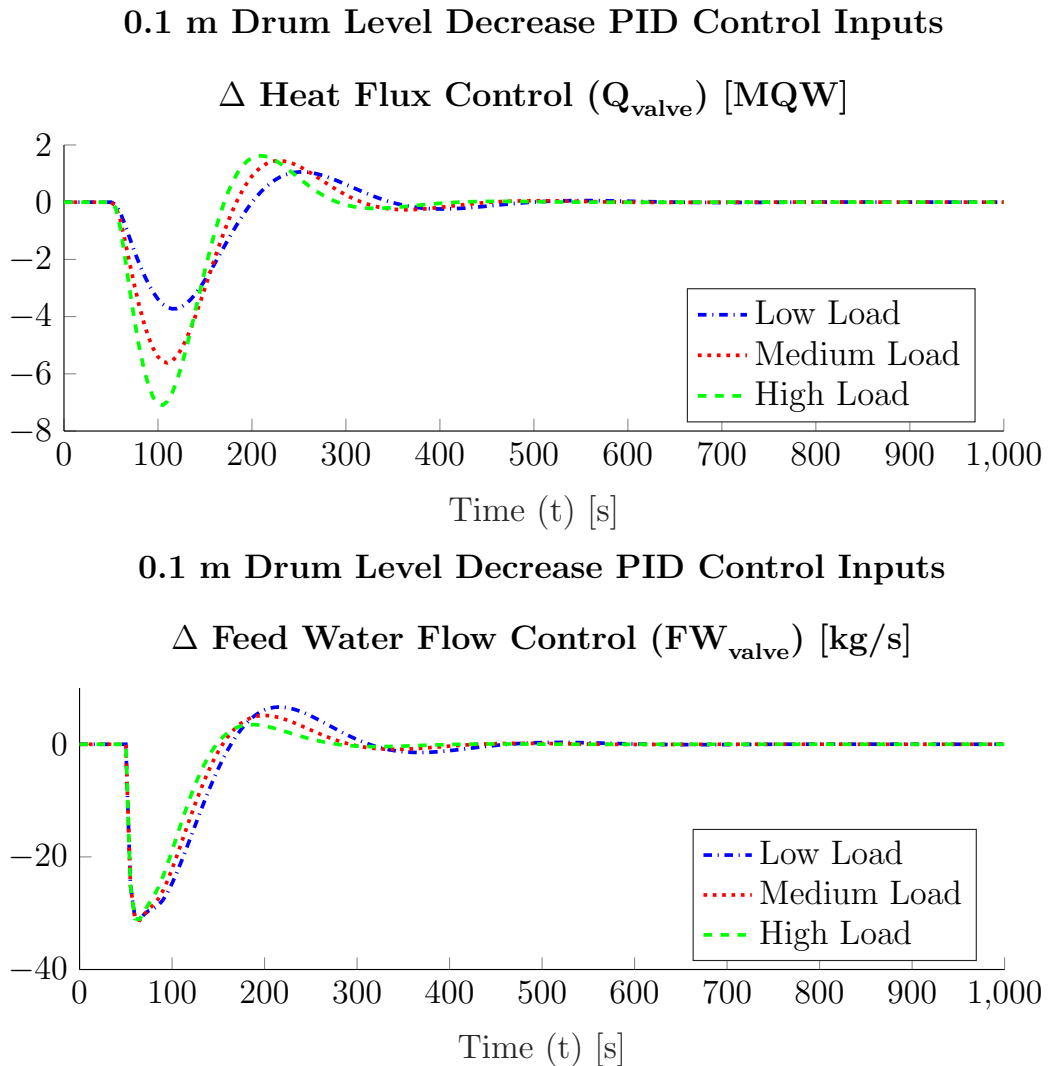


Figure 4.5: Controller Inputs PID Response to Drum Level step of -0.1

Note: This figure shows the change from the initial conditions, as the initial conditions vary across the load settings. This was done to compare the controller performance.

Figure 4.5 shows the controller inputs for the simulations shown in Figure 4.4. This is the controller inputs for a step from the same operating point as seen in Figures 4.1-4.2, however the step command is of opposite magnitude and similar conclusions can be drawn.

		Low Load	Medium Load	High Load	Average
Q_{valve}	Signal Energy	2003	3924	5517	3815
FW_{valve}	Signal Energy	1.094e+5	9.41e+4	7.955e+4	9.436e+4

Table 4.4: PID Controller Input Performance Parameters: Level Step Decrease

0.1 m Drum Level Decrease PID Cascade Control Error

Feed Water Flow - Feed Water Flow Reference $q_f - q_{ref}$ [kg/s]

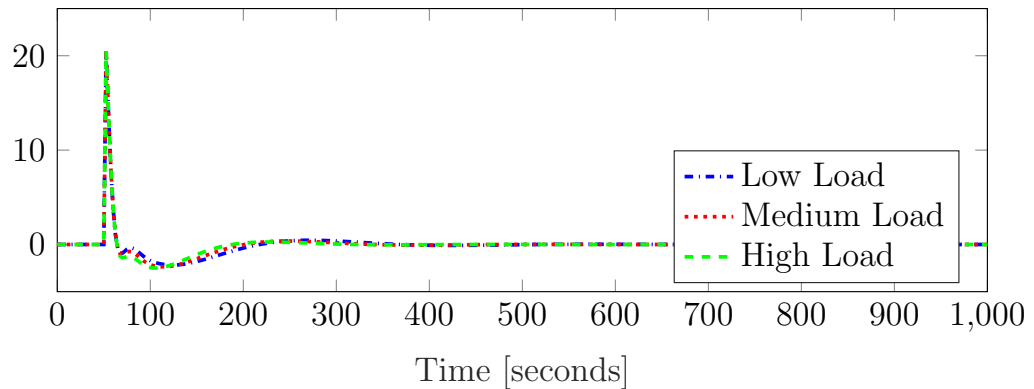


Figure 4.6: Cascaded PID Controller Response to Drum Level step of -0.1

Note: This figure shows the error from a cascaded set point. The set point varies in time and is not shown as a separate graph. This was done to compare the controller performance.

Figure 4.6 shows the error from the cascaded controller that is indicative of the three element design. This can be directly compared to Figure 4.3, however the cascaded set point is calculated from a PID with a step command in the opposite direction. As such much of the same information can be gained.

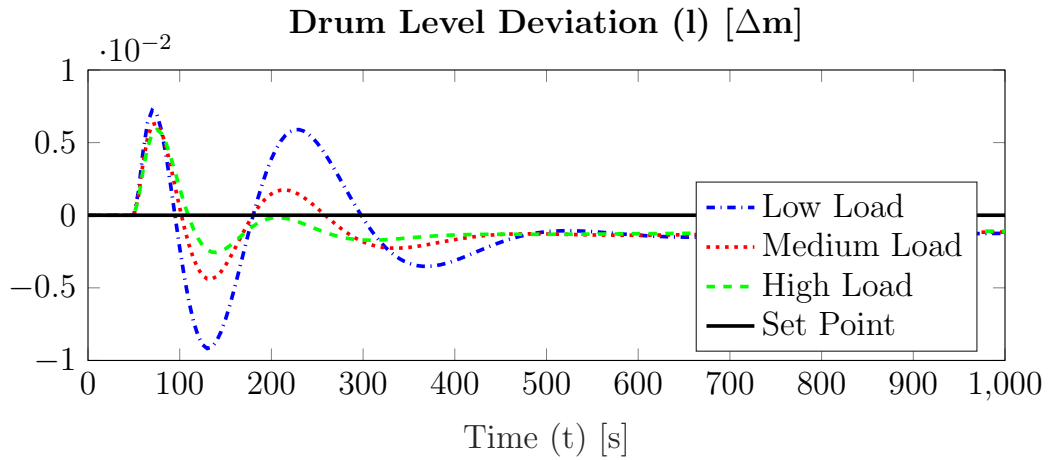
4.2.3 Pressure Step Increase Figures 4.7 - 4.9

The step command for this set of simulations is was calculated as follows:

$$r_1 = r_0 + \Delta r_{command} \quad \Delta r_{command} = \begin{bmatrix} \Delta l_{ref} \\ \Delta p_{ref} \end{bmatrix} = \begin{bmatrix} 0 \\ 0.1 \end{bmatrix}$$

$$r_1 = \begin{cases} & \begin{matrix} Low & Medium & High & units \end{matrix} \\ l_{ref0} & = & -0.002 & -0.032 & -0.051 & \Delta m \\ p_{ref0} & = & 6.9 & 8.6 & 10.3 & MPa \end{cases}$$

0.1 MPa Drum Pressure Increase PID Controlled Variables



0.1 MPa Drum Pressure Increase PID Controlled Variables

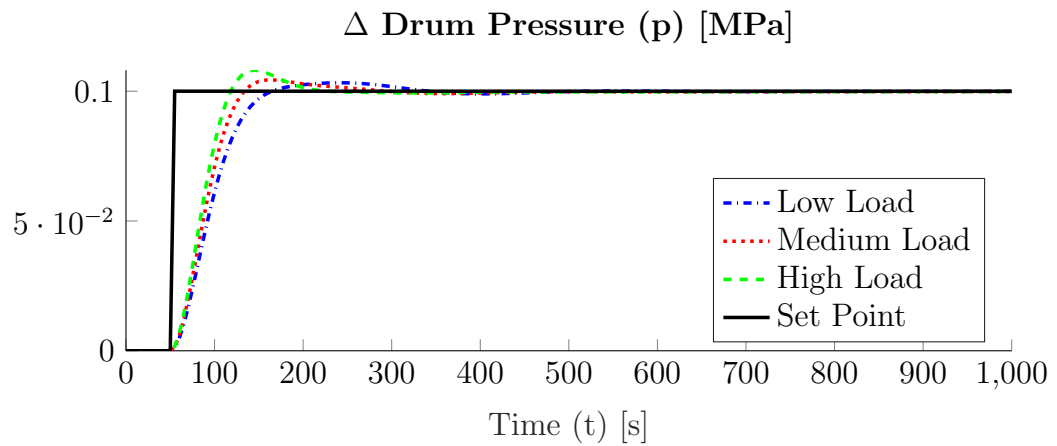


Figure 4.7: Controlled Variables PID Response to Drum Pressure step of 0.1

Note: This figure shows the change from the initial conditions, as the initial conditions vary across the load settings. This was done to compare the controller performance.

		Low Load	Medium Load	High Load	Average
Pressure	% Overshoot	3.275 %	4.437 %	8.151 %	5.288 %
Pressure	Settling Time	244 s	173 s	143.5 s	186.8 s
Pressure	Disturbance Rejection Energy	0.6238	0.5483	0.4979	0.5566
Level	Disturbance Rejection Energy	0.01878	0.007735	0.005868	0.01079

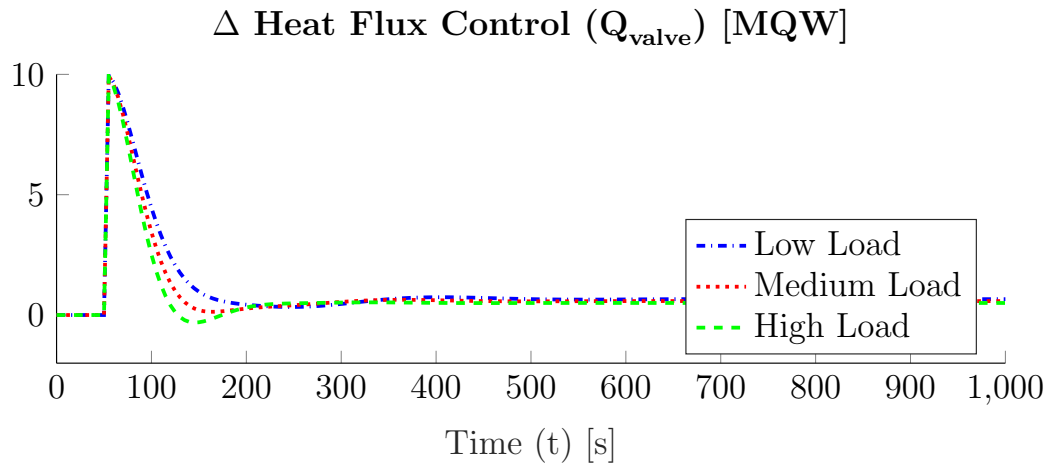
Table 4.5: PID Controller Performance Parameters: Pressure Step Increase

Figure 4.7 shows the simulation results using the specified step command and Table 4.2.3 shows the performance characteristics of this simulation as defined in Chapter 2.4.

The design goal was achieved as seen in Figure 4.1, however the tuning required to meet that goal resulted in nonzero error that is not cleared in a reasonable amount of time through the integral action of the level controller. Increasing the integral action causes the controller to deviate from the design.

The effects of different loads on this controller can be seen in near identical ways to Figure 4.1, level deviation control improves as load increase while drum pressure degrades.

0.1 MPa Drum Pressure Increase PID Control Inputs



0.1 MPa Drum Pressure Increase PID Control Inputs

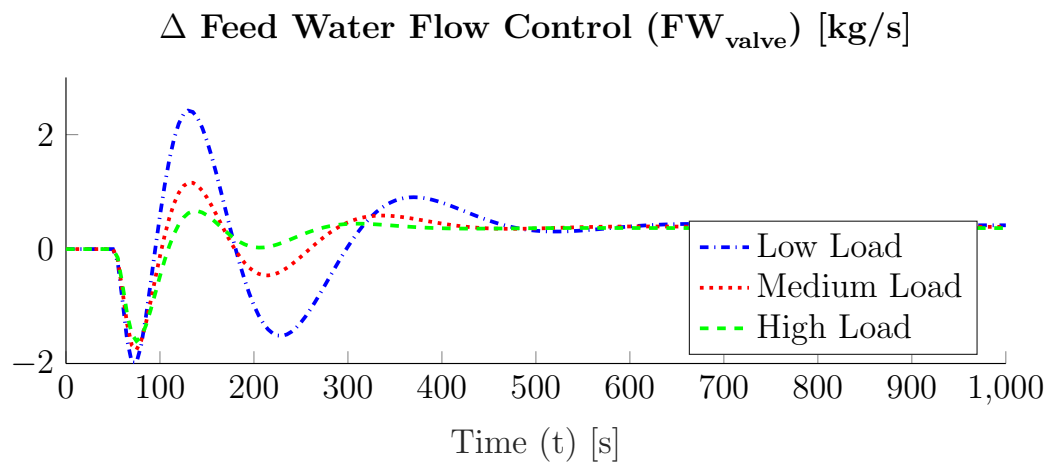


Figure 4.8: Controller Inputs PID Response to Drum Pressure step of 0.1

Note: This figure shows the change from the initial conditions, as the initial conditions vary across the load settings. This was done to compare the controller performance.

Figure 4.8 shows the controller inputs for the simulations shown in Figure 4.7.

The decoupled nature of the controllers can be seen as heat flux has a near step change in output, while feed water control is more gradual.

		Low Load	Medium Load	High Load	Average
Q_{valve}	Signal Energy	8006	6800	5959	6922
FW_{valve}	Signal Energy	1416	648.9	504.8	856.7

Table 4.6: PID Controller Input Performance Parameters: Pressure Step Increase

0.1 MPa Drum Pressure Increase PID Cascade Control Error

Feed Water Flow - Feed Water Flow Reference $q_f - q_{ref}$ [kg/s]

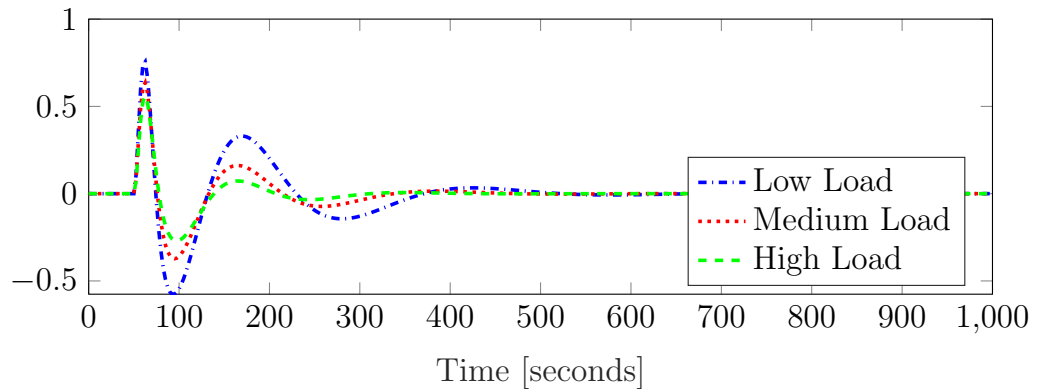


Figure 4.9: Cascaded PID Controller Response to Drum Pressure step of 0.1

Note: This figure shows the error from a cascaded set point. The set point varies in time and is not shown as a separate graph. This was done to compare the controller performance.

Figure 4.9 shows the error from the cascaded controller that is indicative of the three element design. It can be seen that as load increases the error decreases.

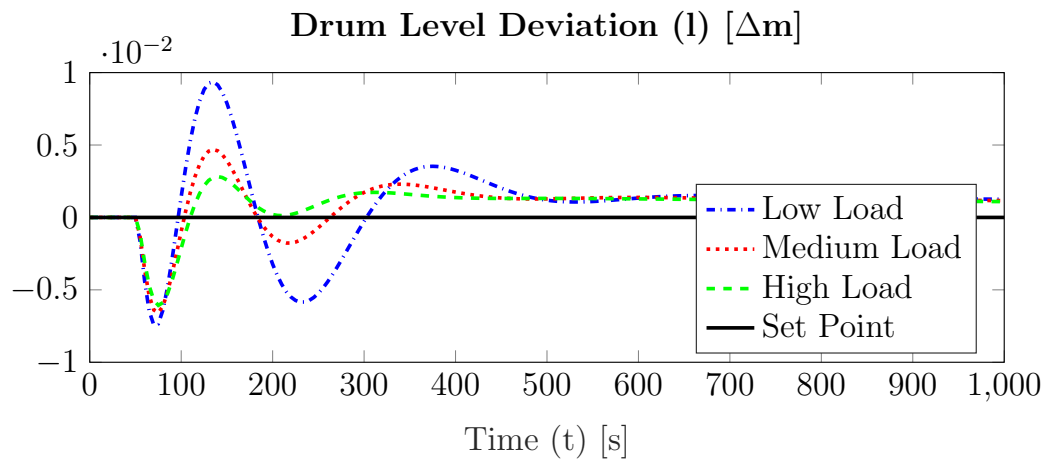
4.2.4 Pressure Step Decrease Figures 4.10 - 4.12

The step command for this set of simulations is was calculated as follows:

$$r_1 = r_0 + \Delta r_{command} \quad \Delta r_{command} = \begin{bmatrix} \Delta l_{ref} \\ \Delta p_{ref} \end{bmatrix} = \begin{bmatrix} 0 \\ -0.1 \end{bmatrix}$$

$$r_1 = \begin{cases} & \textit{Low} & \textit{Medium} & \textit{High} & \textit{units} \\ l_{ref0} & = & -0.002 & -0.032 & -0.051 & \Delta m \\ p_{ref0} & = & 6.7 & 8.4 & 10.1 & MPa \end{cases}$$

0.1 MPa Drum Pressure Decrease PID Controlled Variables



0.1 MPa Drum Pressure Decrease PID Controlled Variables

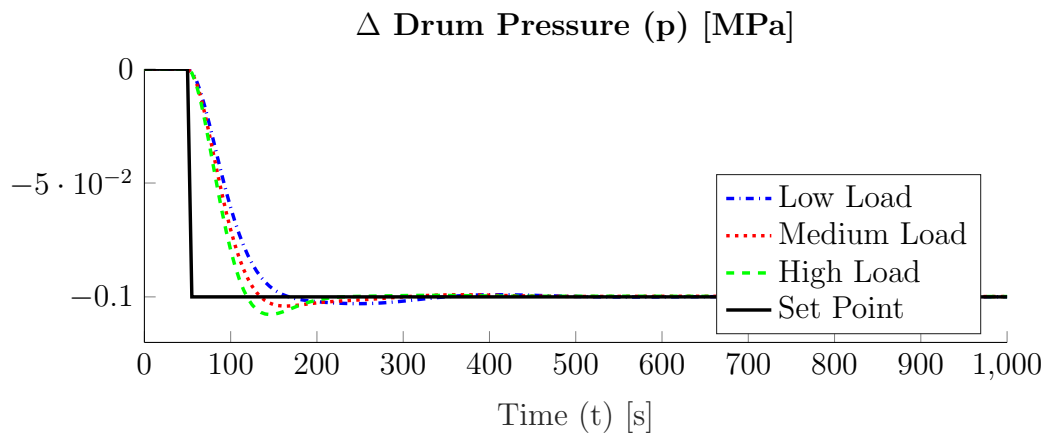


Figure 4.10: Controlled Variables PID Response to Drum Pressure step of -0.1

Note: This figure shows the change from the initial conditions, as the initial conditions vary across the load settings. This was done to compare the controller performance.

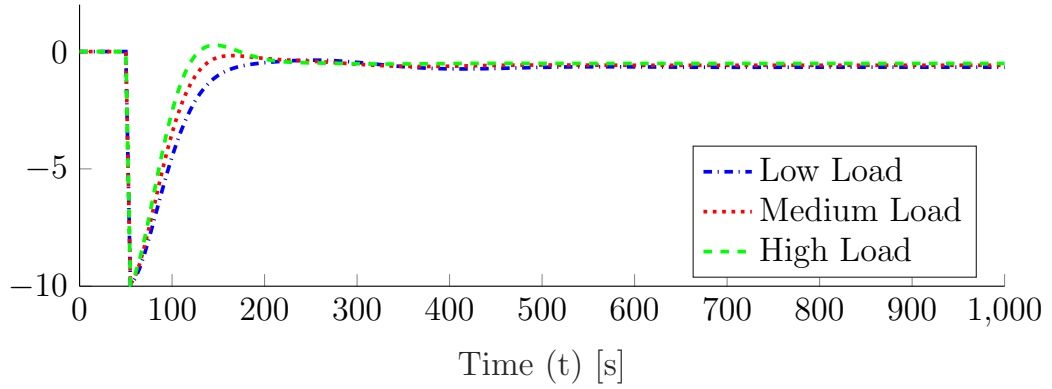
Figure 4.10 shows a step command in the opposite direction as seen in Figure 4.7. As such, many of the same conclusions can be inferred. The performance can be seen in Table 4.2.3.

		Low Load	Medium Load	High Load		Average
Pressure	% Overshoot	3.005 %	4.106 %	7.811 %		4.974 %
Pressure	Settling Time	246 s	169 s	143.5 s		186.2 s
Pressure	Disturbance Rejection Energy	0.6257	0.5495	0.4986		0.558
Level	Disturbance Rejection Energy	0.01949	0.008199	0.006146		0.01128

Table 4.7: PID Controller Performance Parameters: Pressure Step Increase

0.1 MPa Drum Pressure Decrease PID Control Inputs

Δ Heat Flux Control (Q_{valve}) [MQW]



0.1 MPa Drum Pressure Decrease PID Control Inputs

Δ Feed Water Flow Control (FW_{valve}) [kg/s]

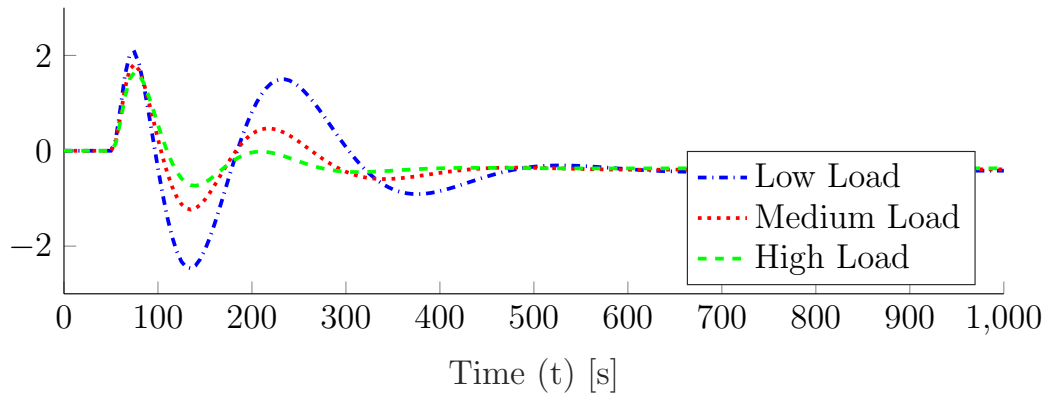


Figure 4.11: Controller Inputs PID Response to Drum Pressure step of -0.1

Note: This figure shows the change from the initial conditions, as the initial conditions vary across the load settings. This was done to compare the controller performance.

Figure 4.11 shows the controller inputs for the simulations shown in Figure 4.10. This is the controller inputs for a step from the same operating point as seen in Figures 4.7-4.8, however the step command is of opposite magnitude. The performance can be seen in Table 4.2.4.

		Low Load	Medium Load	High Load	Average
Q_{valve}	Signal Energy	8057	6836	5984	6959
FW_{valve}	Signal Energy	1464	680.8	524.2	889.8

Table 4.8: PID Controller Input Performance Parameters: Pressure Step Increase

0.1 MPa Drum Pressure Decrease PID Cascade Control Error

Feed Water Flow - Feed Water Flow Reference $q_f - q_{ref}$ [kg/s]

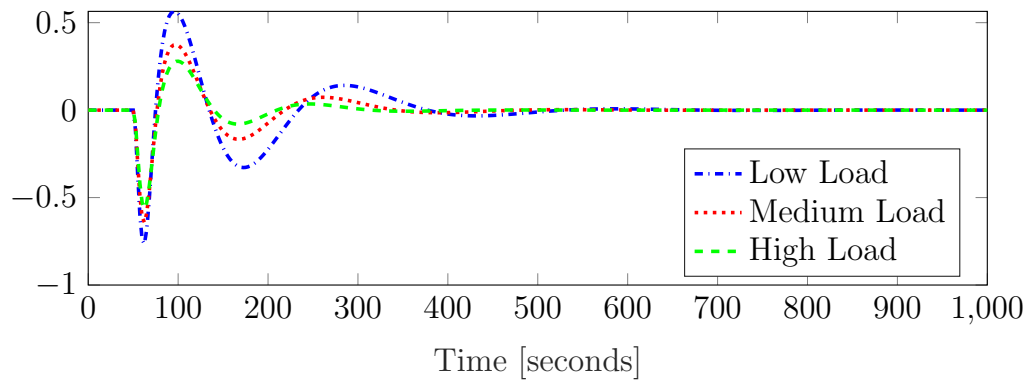


Figure 4.12: Cascaded PID Controller Response to Drum Pressure step of -0.1

Note: This figure shows the error from a cascaded set point. The set point varies in time and is not shown as a separate graph. This was done to compare the controller performance.

Figure 4.12 shows the error from the cascaded controller that is indicative of the three element design. This figure is similar to Figure 4.9.

4.3 Controller Performance

The following tables, Table 4.9-4.12, shows the controller performance as a result of the step functions. Percent overshoot, Settling Time, and Signal Energy are all listed below. Each of these values were shown with their proper figure in the previous section. The averages of the different load cases was also included.

Step Direction		Low Load		Medium Load		High Load		Average	
		Inc	Dec	Inc	Dec	Inc	Dec	Inc	Dec
Level Step	Level	26.89	26.96	21.76	20.99	15.68	14.5	21.45	20.82
Pressure Step	Pressure	3.275	3.005	4.437	4.106	8.151	7.811	5.288	4.974

Table 4.9: PID Controller Percent Overshoot

Step Direction		Low Load		Medium Load		High Load		Average	
		Inc	Dec	Inc	Dec	Inc	Dec	Inc	Dec
Level Step	Level	580	565.5	520	508.5	450.5	436.5	516.8	503.5
Pressure Step	Pressure	244	246	173	169	143.5	143.5	186.8	186.2

Table 4.10: PID Controller Settling Time

It should be noted that as load increases settling time improves for all cases by becoming smaller. This is due to the shrink/swell effect becoming less effective at the higher loads. For Pressure Steps the maximum percent overshoot increases as load increases, however the settling time improves so this is an acceptable trade off. The maximum percent overshoot for Level Steps improves as load increases.

Step Direction		Low Load		Medium Load		High Load	
		Inc	Dec	Inc	Dec	Inc	Dec
Level Step	Level	1.623	1.614	1.402	1.381	1.181	1.161
Level Step	Pressure	0.1864	0.1909	0.3724	0.3756	0.5285	0.5292
Pressure Step	Level	0.01878	0.01949	0.007735	0.008199	0.005868	0.006146
Pressure Step	Pressure	0.6238	0.6257	0.5483	0.5495	0.4979	0.4986

Table 4.11: PID Controlled Variable Energy

It should be noted that the signal energy for pressure during a level step change is the same for all loads. This is due to how level and pressure are coupled together and how the integral of pressure is a function being controlled. During pressure step functions the signal energy for the level function decreases as load increases.

		Low Load		Medium Load		High Load	
Step Direction		Inc	Dec	Inc	Dec	Inc	Dec
Level Step	Q_{valve}	1958	2003	3893	3924	5512	5517
Level Step	FW_{valve}	1.1e+5	1.094e+5	9.546e+4	9.41e+4	8.089e+4	7.955e+4
Pressure Step	Q_{valve}	8006	8057	6800	6836	5959	5984
Pressure Step	FW_{valve}	1416	1464	648.9	680.8	504.8	524.2

Table 4.12: PID Controller Inputs Energy

		Low Load		Medium Load		High Load	
Step Direction		Inc	Dec	Inc	Dec	Inc	Dec
Level Step	V_{wt}	1.598e+4	1.594e+4	1.58e+4	1.576e+4	1.564e+4	1.561e+4
Level Step	p	0.1864	0.1909	0.3724	0.3756	0.5285	0.5292
Level Step	α_r	0.0002076	0.000215	0.0004804	0.0004939	0.0008013	0.0008225
Level Step	V_{sd}	503.9	498.1	393.2	381.1	275.1	264.6
Level Step	Q	1698	1726	3272	3274	4488	4458
Level Step	q_f	1.068e+5	1.062e+5	9.221e+4	9.085e+4	7.767e+4	7.632e+4
Pressure Step	V_{wt}	6.382	6.526	0.76	0.7595	0.2998	0.2845
Pressure Step	p	27.89	27.88	28.04	28.03	28.2	28.19
Pressure Step	α_r	0.001432	0.001415	0.001741	0.001719	0.002175	0.002143
Pressure Step	V_{sd}	31.54	32.48	7.076	7.27	1.803	1.829
Pressure Step	Q	6110	6164	4895	4935	4035	4065
Pressure Step	q_f	1378	1425	631.6	662.6	493.9	512.7

Table 4.13: PID State Variable Energy

Controller input energy is held near constant for Q_{valve} during Pressure Steps and FW_{valve} during Level Steps. This is most likely due to the decoupled design of this controller with the Level being controlled by the FW_{valve} and with pressure being controlled by the Q_{valve} . As load increases on Level Steps Q_{valve} energy is reduced, while as load increases on Pressure Steps, FW_{valve} energy is increased.

CHAPTER 5

LINEAR QUADRATIC REGULATOR

As discussed in Section 2.2, the LQR controller is a powerful tool, however it is not designed for nonlinear systems. The LQR method has been successfully applied in many engineering applications, especially when the nonlinear system could be linearized with respect to an operating point. Recently, LQR controllers have been applied for boiler control [14]. This chapter presents how a LQR controller can be used on the Expanded model in Equation (3.13).

5.1 Controller Design

Standard LQR design finds a gain matrix for minimizing a certain cost function that represents quadratic cost of state error and the cost of control. In particular, the objective is to minimize the state error $\Delta x(t)$ and the cost of control over the control horizon. A block diagram of this can be seen in Figure 5.1

As discussed in Chapter 3, the mathematical model of the boiler is given by (3.13):

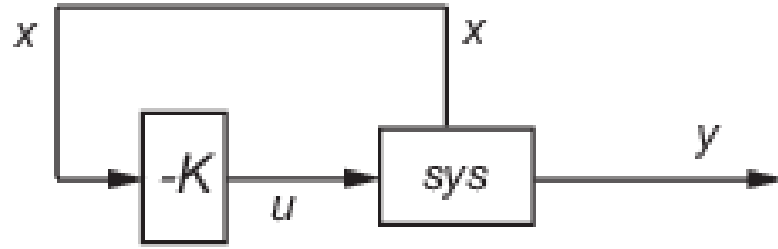


Figure 5.1: LQR Block Diagram [10]

$$\frac{d}{dt} \begin{bmatrix} V_{wt} \\ p \\ \alpha_r \\ V_{sd} \\ Q \\ q_f \end{bmatrix} = \begin{bmatrix} e_{11}(p) & e_{12}(p) & 0 & 0 \\ e_{21}(p) & e_{22}(p) & 0 & 0 \\ 0 & e_{32}(p) & e_{33}(p) & 0 \\ 0 & e_{42}(p) & e_{43}(p) & e_{44}(p) \end{bmatrix}^{-1} \begin{bmatrix} q_f - q_s(p) \\ Q + q_f h_f(t_{f_0}, p) - q_s(p) h_s(p) \\ Q + \alpha_r h_c(p) q_{dc}(p) \\ \frac{\rho_s(p)}{T_d} (V_{sd}^0 - V_{sd}) + \frac{h_f(t_{f_0}, p) - h_w(p)}{h_c(p)} q_f \\ \frac{(Q_{valve} - Q)}{T_{vQ}} \\ \frac{(FW_{valve} - q_f)}{T_{vfw}} \end{bmatrix}$$

which is a nonlinear model taking the form:

$$\dot{x}(t) = f(x(t), u(t))$$

The controlled outputs of the system as discussed in (3.10) are:

$$y(t) = \begin{bmatrix} l(V_{wt}, p, \alpha_r, V_{sd}) \\ p \end{bmatrix}$$

which is represented as

$$y(t) = g(x(t), u(t))$$

These nonlinear state space equations can be linearized with respect to the operating point $\{x^*, u^*\}$ as:

$$\begin{aligned} \frac{d\Delta x(t)}{dt} &= A_c \Delta x(t) + B_c \Delta u(t) \\ \Delta y(t) &= C_c \Delta x(t) + D_c \Delta u(t) \end{aligned}$$

where

$$\begin{aligned} A_c &= \left. \frac{\partial f(x(t), u(t))}{\partial x} \right|_{x^*, u^*} \\ B_c &= \left. \frac{\partial f(x(t), u(t))}{\partial u} \right|_{x^*, u^*} \\ C_c &= \left. \frac{\partial g(x(t), u(t))}{\partial x} \right|_{x^*, u^*} \\ D_c &= \left. \frac{\partial g(x(t), u(t))}{\partial u} \right|_{x^*, u^*} \end{aligned}$$

The linearization point chosen is the medium load from (3.14).

	<i>Medium</i>	<i>units</i>
V_{wt0}	= 57.1	m^3
p_0	= 8.5	MPa
α_{r0}	= 0.0295	—
V_{sd0}	= 8	m^3
Q_0	= 39.60	MW
q_{f0}	= 28.33	kg/s
Q_{valve}	= 39.60	MW
FW_{valve}	= 28.33	kg/s

The linearized system is then expressed as a discrete time equation as

$$\begin{aligned} \Delta x(k_i + 1) &= A_d \Delta x(k_i) + B_d \Delta u(k_i) \\ \Delta y(k_i) &= C_d \Delta x(k_i) + D_d \Delta u(k_i) \\ \Delta x(k_i + 1) &= \Delta x(t + T_s) \\ \Delta x(t) &= \dot{x}(t) T_s \end{aligned}$$

where the various matrices are

$$\begin{aligned} A_d &= e^{A_c T_s}, \quad B_d = \left(\int_0^{T_s} e^{A_c \tau} d\tau \right) B_c \\ C_d &= C_c, \quad D_d = D_c \end{aligned}$$

To find the feedback control $u(t)$, we use the LQR control method as discussed in Section 2.2. The optimal solution that minimizes the cost function

(2.2) is obtained through the use of the discrete time Riccati equation (2.3). These equations are repeated here for quick reference:

$$J = \sum_{k=0}^{\infty} (x_k^T Q_{lqr} x_k + u_k^T R_{lqr} u_k)$$

$$P_{lqr} = A_d^T P_{lqr} A_d - (A_d^T P_{lqr} B_d)(R_{lqr} + B_d^T P_{lqr} B_d)^{-1} (B_d^T P_{lqr} A_d) + Q_{lqr}$$

$$K_{lqr} = -(R + B_d^T P B_d^{-1})(B_d^T P A_d)$$

$$u_k = K_{lqr} x_k$$

To allow for reference tracking without an error, an integrator must be introduced in the loop. A block diagram of the system can be seen in Figure 5.2.

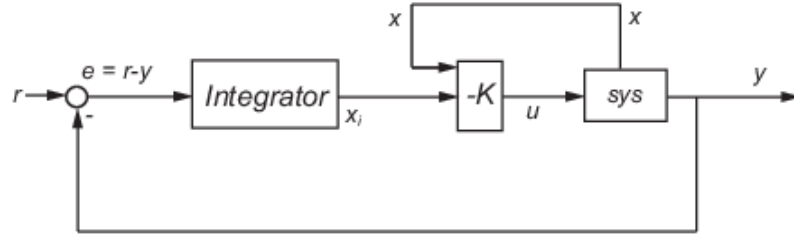


Figure 5.2: Linear-Quadratic-Integral (LQI) Block Diagram [10]

Note: LQI is specific form of LQR and will henceforth be referred to as LQR

For the control design, a new state variable for the reference tracking error must be introduced:

$$\begin{aligned} \epsilon(k_i + 1) &= \epsilon(k_i) + T_s(r(k_i) - y(k_i)) \\ &= \epsilon(k_i) + T_s(r(k_i) - C_d x(k_i)) \end{aligned} \quad (5.1)$$

The new state is then combined into the existing system [1]:

$$z(k_i + 1) = A_a z(k_i) + B_a \Delta u(k_i) + B_r r(k_i)$$

where

$$z(k_i) = \begin{bmatrix} \Delta x(k_i) \\ \epsilon(k_i) \end{bmatrix} \quad A_a = \begin{bmatrix} A_d & 0 \\ -C_d & I \end{bmatrix} \quad B_a = \begin{bmatrix} B_d \\ 0 \end{bmatrix} \quad B_r = \begin{bmatrix} 0 \\ I \end{bmatrix}$$

The LQR controller optimal state feedback is then calculated as:

$$\Delta u(t) = K_{LQR}z(t) = K_{feedback}\Delta x(t) + K_{reference}\epsilon(t)$$

Using the equations shown earlier on LQR gains (2.2)-(2.3), a gain can be calculated that not only minimized tracking error but is also stable.

$$J = \sum_0^{\infty} (z_k^T Q z_k + u_k^T R u_k)$$

$$P = A_a^T P A_a - (A_a^T P B_a)(R + B_a^T P B_a)^{-1}(B_a^T P A_a) + Q$$

$$K_{LQR} = -(R + B_a^T P B_a^{-1})(B_a^T P A_a)$$

The resulting gain matrix can be partitioned K_{LQR} to show a feedback portion on the states, $K_{LQR_{fbk}}$ and a gain for the controlled variable error, $K_{LQR_{ref}}$.

The Controller was tuned to be meet the design criterion of:

- 15% Overshoot for a Drum Level step at High load
- 450 seconds of Settling Time for a Drum Level step at High Load
- Drum Pressure will remain stable
- Drum Level will remain stable for other disturbances (such as a Drum Pressure Step)

Selecting the weighting matrices of Q and R are a crucial step in LQR design. Adopting cheap control methodology [14] and using a heuristic trial and error method, the values for Q and R matrices are selected as follows. Note that the weights can be partitioned as seen.

$$Q = \begin{bmatrix} \overbrace{0.1 & 0 & 0 & 0 & 0 & 0}^{\Delta x} & \overbrace{0 & 0}^{\epsilon} \\ 0 & 0.1 & 0 & 0 & 0 & 0 & 0 & 0 \\ 0 & 0 & 0.1 & 0 & 0 & 0 & 0 & 0 \\ 0 & 0 & 0 & 0.1 & 0 & 0 & 0 & 0 \\ 0 & 0 & 0 & 0 & 0.1 & 0 & 0 & 0 \\ 0 & 0 & 0 & 0 & 0 & 0.1 & 0 & 0 \\ 0 & 0 & 0 & 0 & 0 & 0 & 10 & 0 \\ 0 & 0 & 0 & 0 & 0 & 0 & 0 & 7.375 \end{bmatrix} \quad R = \begin{bmatrix} \overbrace{7.95 & 0}^{\Delta u} \\ 0 & 0.01 \end{bmatrix} \quad (5.2)$$

It should be noted that this controller uses full state feedback. It is unlikely that each of the states will be measurable. An observer must be designed for practical use in industry, however for the comparison of control methodologies a full state feedback is considered adequate.

5.2 Simulation Results

The simulation using the LQR controller can be calculated using the full nonlinear model without any linearization. The gain matrices were chosen at a single operating point, and then used to calculate the control signal $u(t)$ based on full state feedback.

$$\Delta x(k) = F(x(t), u(t))T_s$$

$$e(t) = y(t) - r(t) = G(x(t), u(t)) - r(t)$$

$$\Delta u(k) = K_{LQR_{fbk}} \Delta x(k) + K_{LQR_{ref}} e(k)$$

$$u(k+1) = u(t+T_s) = u(k) + \Delta u(k)$$

It should be noted that the chosen gain values may not control properly over a large range, as they are only optimal for a specific operating point.

The following simulations use the initial condition at the load setting as defined in (3.14). An initial reference signal is then created based off of the stable initial condition ($r_0 = y_0$).

$$\begin{aligned}
 \begin{matrix} x_0 \\ u_0 \end{matrix} &= \left\{ \begin{array}{lcllcl} & & \textit{Low} & \textit{Medium} & \textit{High} & \textit{units} \\ V_{wt0} & = & 57.1 & 57.1 & 57.1 & m^3 \\ p_0 & = & 6.8 & 8.5 & 10.2 & MPa \\ \alpha_{r0} & = & 0.0325 & 0.0435 & 0.0561 & - \\ V_{sd0} & = & 5.213 & 4.984 & 4.854 & m^3 \\ Q_0 = Q_{valve} & = & 57.11 & 67.65 & 76.84 & MW \\ q_{f0} = FW_{valve} & = & 33.07 & 39.79 & 46.12 & kg/s \end{array} \right. \\
 r_0 = y_0 &= \left\{ \begin{array}{lcllcl} & & \textit{Low} & \textit{Medium} & \textit{High} & \textit{units} \\ l_0 & = & -0.002 & -0.032 & -0.051 & \Delta m \\ p_0 & = & 6.8 & 8.5 & 10.2 & MPa \end{array} \right.
 \end{aligned}$$

The reference signal $r(t)$ will be applied, and r_1 will vary based on the step command.

$$r(t) = \begin{cases} r_0 & \textit{for } t < t_{step} \\ r_1 & \textit{for } t > t_{step} \end{cases}$$

The controlled outputs are each compared to their reference as a step change is applied. This system has two controlled variables therefore four steps are required to show the controllers response; variable 1 (Drum Pressure) step up, variable 1 (Drum Pressure) step down, variable 2 (Drum Level Deviation) step up, variable 2 (Drum Level Deviation) step down. When one variable is being stepped the other has its reference held constant. The two variables are coupled together and when a reference is held constant it becomes a disturbance rejection response.

Controller performance will be defined using percent overshoot, settling time, and signal energy, as defined in Section 2.4. These metrics will be used to compare the various controller types in a later chapter.

5.2.1 Level Step Increase Figures 5.3-5.4

The step command for this set of simulations is was calculated as follows:

$$r_1 = r_0 + \Delta r_{command} \quad \Delta r_{command} = \begin{bmatrix} \Delta l_{ref} \\ \Delta p_{ref} \end{bmatrix} = \begin{bmatrix} 0.1 \\ 0.0 \end{bmatrix}$$

$$r_1 = \begin{cases} & \begin{matrix} Low & Medium & High & units \end{matrix} \\ l_{ref0} & = & 0.098 & 0.068 & 0.049 & \Delta m \\ p_{ref0} & = & 6.8 & 8.5 & 10.2 & MPa \end{cases}$$

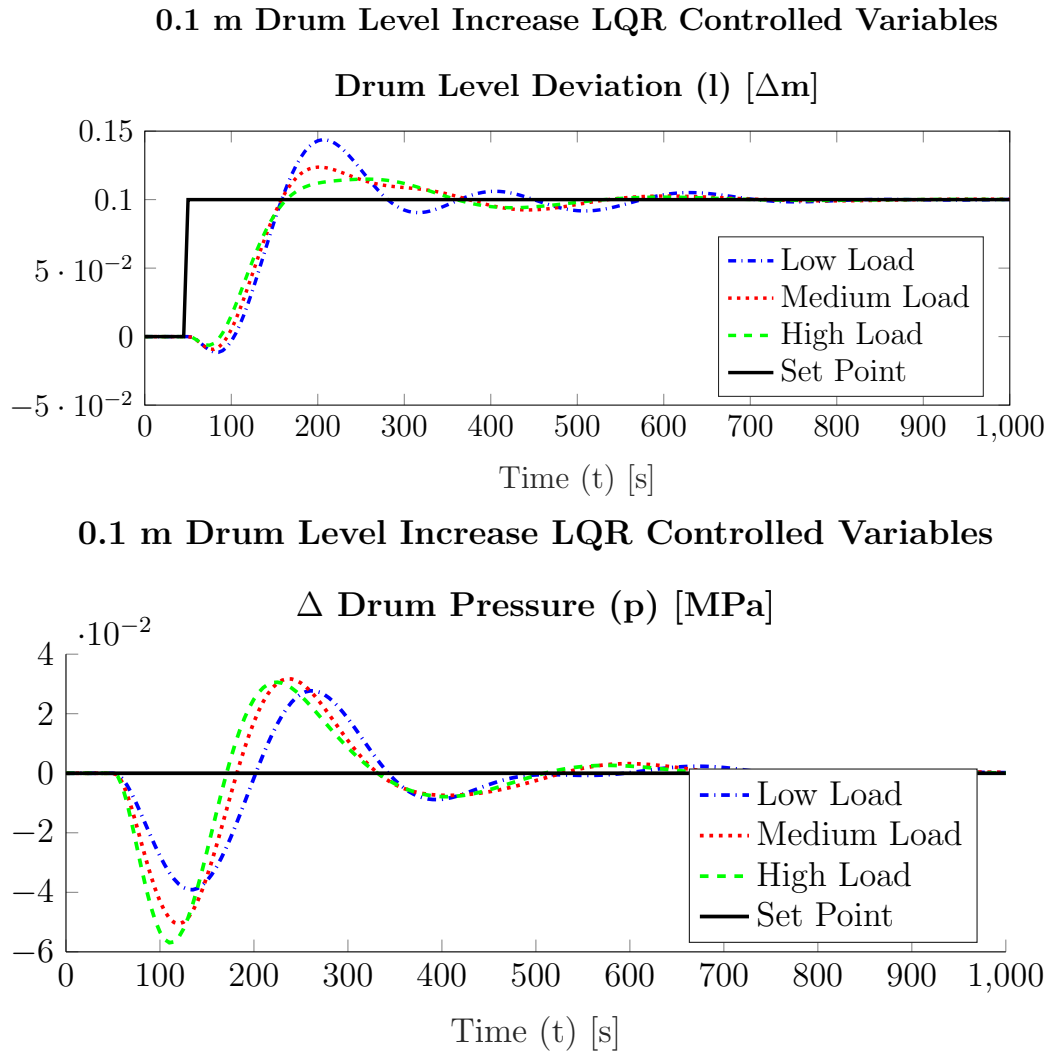


Figure 5.3: Controlled Variables LQR Response to Drum Level step of 0.1

Note: This figure shows the change from the initial conditions, as the initial conditions vary across the load settings. This was done to compare the controller performance.

		Low Load	Medium Load	High Load	Average
Level	% Overshoot	43.74 %	23.75 %	14.97 %	27.49 %
Level	Settling Time	632.5 s	595.5 s	450 s	559.3 s
Level	Disturbance Rejection Energy	1.865	1.54	1.338	1.581
Pressure	Disturbance Rejection Energy	0.3215	0.4458	0.4857	0.4177

Table 5.1: LQR Controller Performance Parameters: Level Step Increase

Figure 5.3 shows the simulation results using the specified step command and Table 5.2.1 shows the performance characteristics of this simulation as defined in Chapter 2.4. It can be seen that using these tuning parameters, the design goal is achieved. The Shrink/Swell effect can be seen on drum level deviation as well as the reduction of the Shrink/Swell effect as load increases (which is also a known phenomenon). It can be seen that both variables are adequately controlled by the designed LQR system as the transients are controlled.

The effects of different loads on this controller can be seen in two ways; as load increases the level controller performance parameters improve (decreased overshoot and settling time) while the pressure controller's performance degrades (energy increases). This can also be seen graphically as the amplitudes lower as load increase for drum level deviation, but the amplitudes increase for drum pressure.

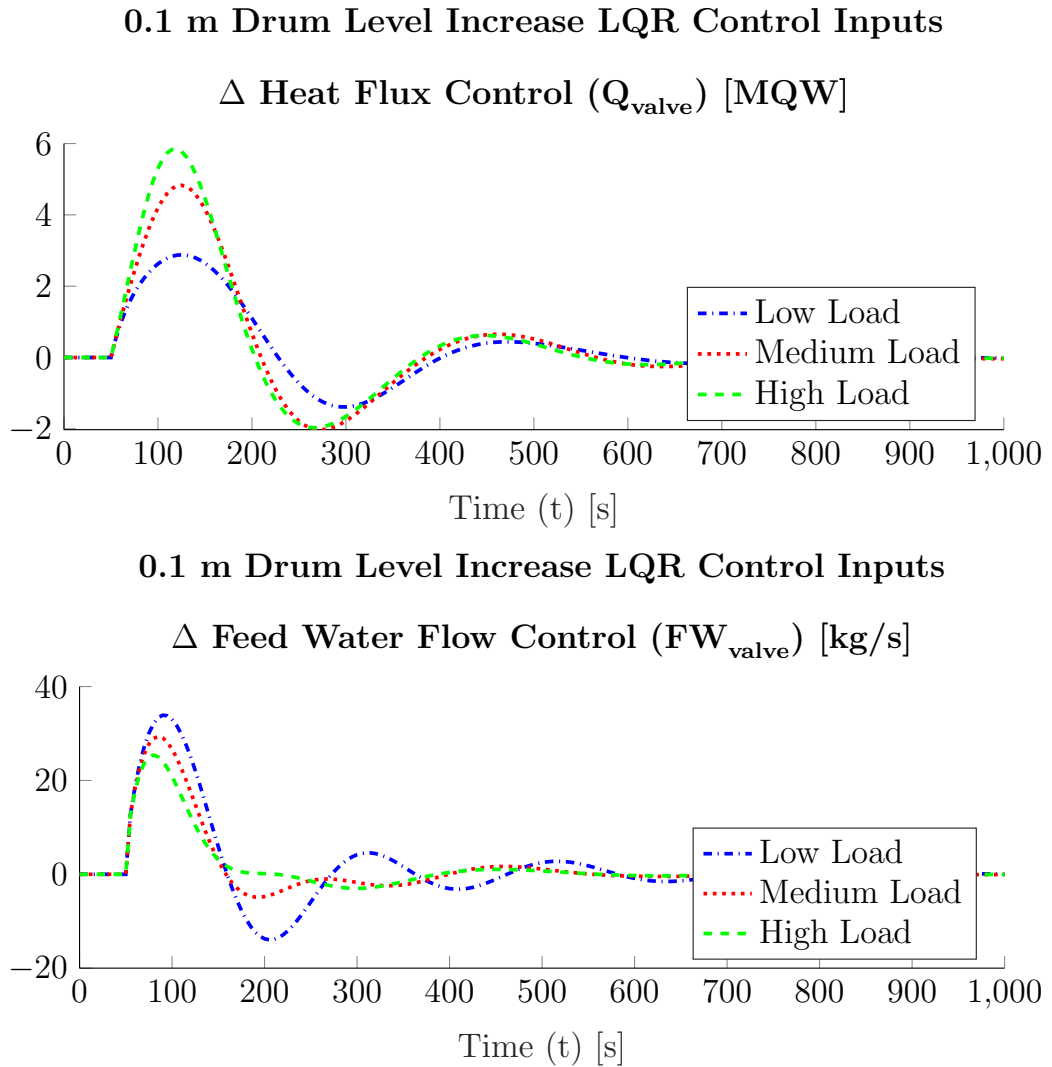


Figure 5.4: Controller Inputs LQR Response to Drum Level step of 0.1

Note: This figure shows the change from the initial conditions, as the initial conditions vary across the load settings. This was done to compare the controller performance.

		Low Load	Medium Load	High Load		Average
Q_{valve}	Signal Energy	1900	4315	5503		3906
FW_{valve}	Signal Energy	1.546e+05	9.241e+04	6.373e+04		1.036e+05

Table 5.2: LQR Controller Input Performance Parameters: Level Step Increase

Figure 5.4 shows the controller inputs and Table 5.2.1 shows the controller input energy for the simulations shown in Figure 5.3.

It can be seen that as load increases Heat flux requires more control action while feed water requires less. The energy shown by these signals increases for heat flux, but decreases for feed water.

5.2.2 Level Step Decrease Figures 5.5-5.6

The step command for this set of simulations is was calculated as follows:

$$r_1 = r_0 + \Delta r_{command} \quad \Delta r_{command} = \begin{bmatrix} \Delta l_{ref} \\ \Delta p_{ref} \end{bmatrix} = \begin{bmatrix} -0.1 \\ 0.0 \end{bmatrix}$$

$$r_1 = \begin{cases} & \begin{matrix} Low & Medium & High & units \end{matrix} \\ l_{ref0} & = & -0.102 & -0.132 & -0.151 & \Delta m \\ p_{ref0} & = & 6.8 & 8.5 & 10.2 & MPa \end{cases}$$

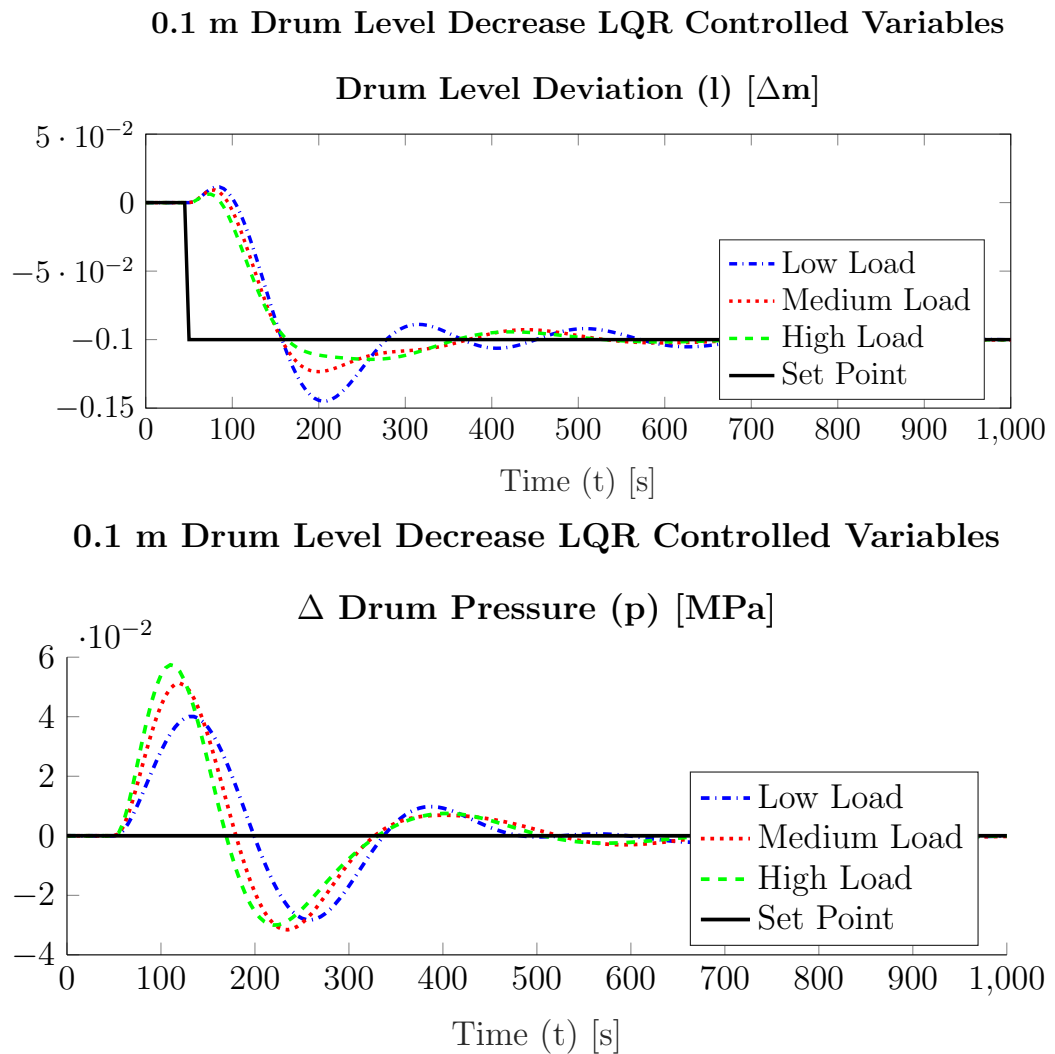


Figure 5.5: Controlled Variables LQR Response to Drum Level step of -0.1

Note: This figure shows the change from the initial conditions, as the initial conditions vary across the load settings. This was done to compare the controller performance.

		Low Load	Medium Load	High Load	Average
Level	% Overshoot	43.74 %	23.75 %	14.97 %	27.49 %
Level	Settling Time	632.5 s	595.5 s	450 s	559.3 s
Level	Disturbance Rejection Energy	1.874	1.522	1.32	1.572
Pressure	Disturbance Rejection Energy	0.3215	0.4458	0.4857	0.4177

Table 5.3: LQR Controller Performance Parameters: Level Step Decrease

Figure 5.3 shows the simulation results using the specified step command and Table 5.2.1 shows the performance characteristics of this simulation. This is a step from the same operating point but in the opposite direction as seen in Figure 5.3 and as such much of the same information can be gained.

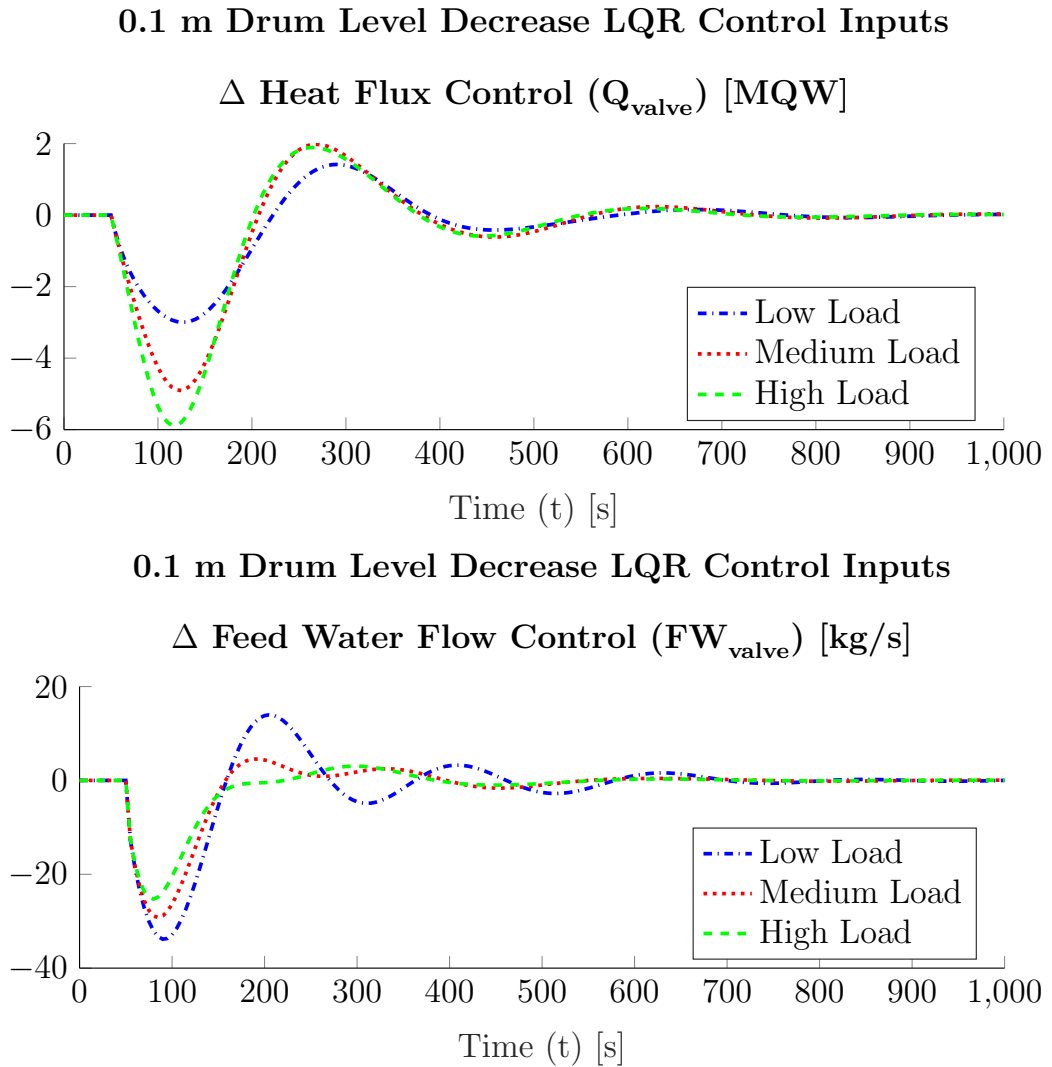


Figure 5.6: Controller Inputs LQR Response to Drum Level step of -0.1

Note: This figure shows the change from the initial conditions, as the initial conditions vary across the load settings. This was done to compare the controller performance.

		Low Load	Medium Load	High Load	Average
Q_{valve}	Signal Energy	1951	4274	5416	3880
FW_{valve}	Signal Energy	1.534e+05	9.026e+04	6.248e+04	1.02e+05

Table 5.4: LQR Controller Input Performance Parameters: Level Step Decrease

Figure 5.6 shows the simulation results using the specified step command and Table 5.2.2 shows the performance characteristics of this simulation. This is a step from the same operating point but in the opposite direction as seen in Figure 5.4 and as such much of the same information can be gained.

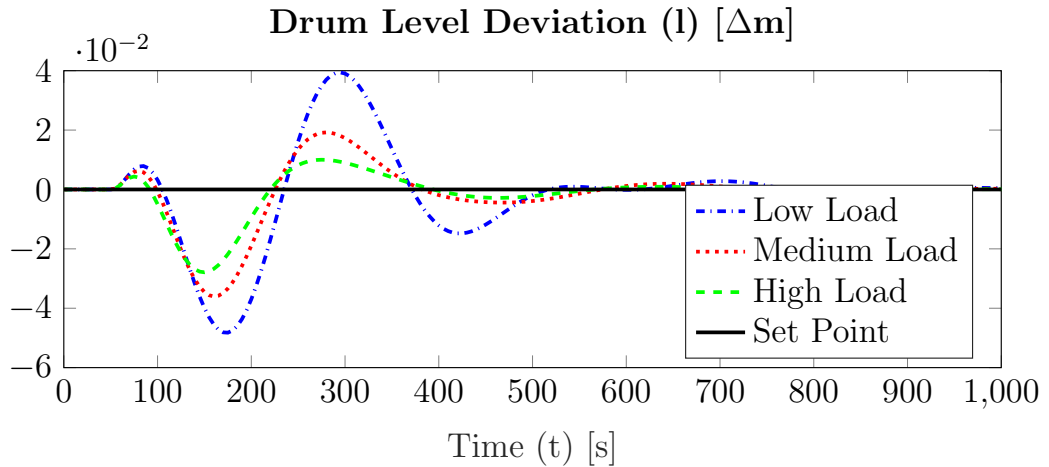
5.2.3 Pressure Step Increase Figures 5.7-5.8

The step command for this set of simulations is was calculated as follows:

$$r_1 = r_0 + \Delta r_{command} \quad \Delta r_{command} = \begin{bmatrix} \Delta l_{ref} \\ \Delta p_{ref} \end{bmatrix} = \begin{bmatrix} 0 \\ 0.1 \end{bmatrix}$$

$$r_1 = \begin{cases} & \begin{matrix} Low & Medium & High & units \end{matrix} \\ l_{ref0} & = & -0.002 & -0.032 & -0.051 & \Delta m \\ p_{ref0} & = & 6.9 & 8.6 & 10.3 & MPa \end{cases}$$

0.1 MPa Drum Pressure Increase LQR Controlled Variables



0.1 MPa Drum Pressure Increase LQR Controlled Variables

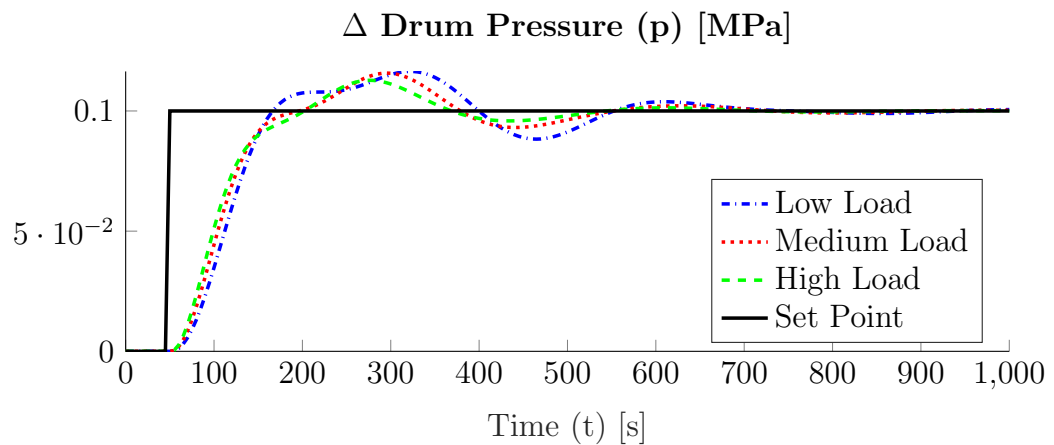


Figure 5.7: Controlled Variables LQR Response to Drum Pressure step of 0.1

Note: This figure shows the change from the initial conditions, as the initial conditions vary across the load settings. This was done to compare the controller performance.

		Low Load	Medium Load	High Load	Average
Pressure	% Overshoot	16.47 %	15.77 %	12.76 %	15 %
Pressure	Settling Time	619 s	599 s	450.5 s	556.2 s
Pressure	Disturbance Rejection Energy	1.023	0.8732	0.7804	0.8923
Level	Disturbance Rejection Energy	0.5229	0.2108	0.1089	0.2809

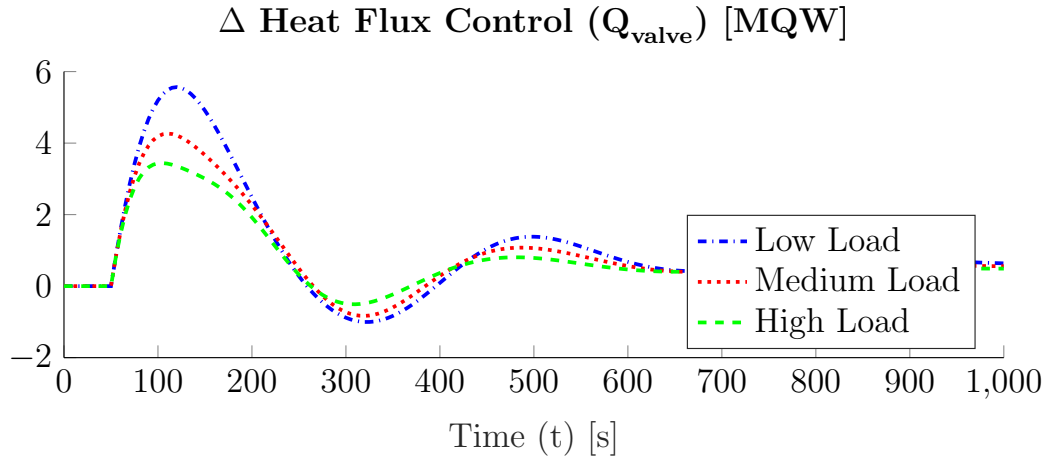
Table 5.5: LQR Controller Performance Parameters: Pressure Step Increase

Figure 5.3 shows the simulation results using the specified step command and Table 5.2.1 shows the performance characteristics of this simulation as defined in Chapter 2.4. These are the same tuning parameters used for the simulations in Figure 5.3, and as such the design goal was achieved. It can be seen that both variables are adequately controlled by the designed LQR system as the transients are controlled.

The effects of different loads on this controller can be seen in two ways; as load increases both the level and pressure controllers performance parameters improve, and the amplitudes decrease as load increases.

The effects of the different step command from the design criteria step show that this can properly control both variables.

0.1 MPa Drum Pressure Increase LQR Control Inputs



0.1 MPa Drum Pressure Increase LQR Control Inputs

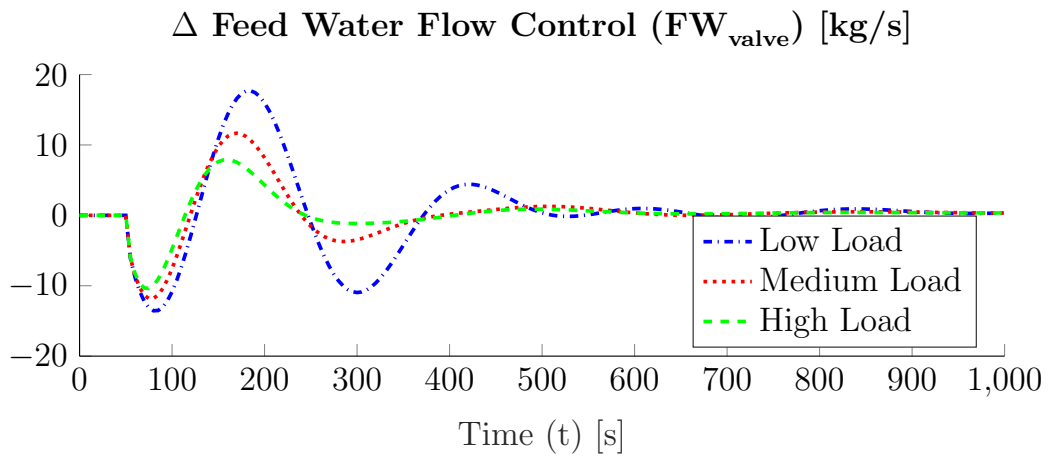


Figure 5.8: Controller Inputs LQR Response to Drum Pressure step of 0.1

Note: This figure shows the change from the initial conditions, as the initial conditions vary across the load settings. This was done to compare the controller performance.

		Low Load	Medium Load	High Load		Average
Q_{valve}	Signal Energy	7114	4666	3203		4995
FW_{valve}	Signal Energy	6.975e+04	2.83e+04	1.501e+04		3.769e+04

Table 5.6: LQR Controller Input Performance Parameters: Pressure Step Increase

Figure 5.8 shows the controller inputs for the simulations shown in Figure 5.7. It can be seen that as load increase the action required from the controller decreases. This may be caused by the system nonlinearities and the reduction of the Shrink/Swell effect.

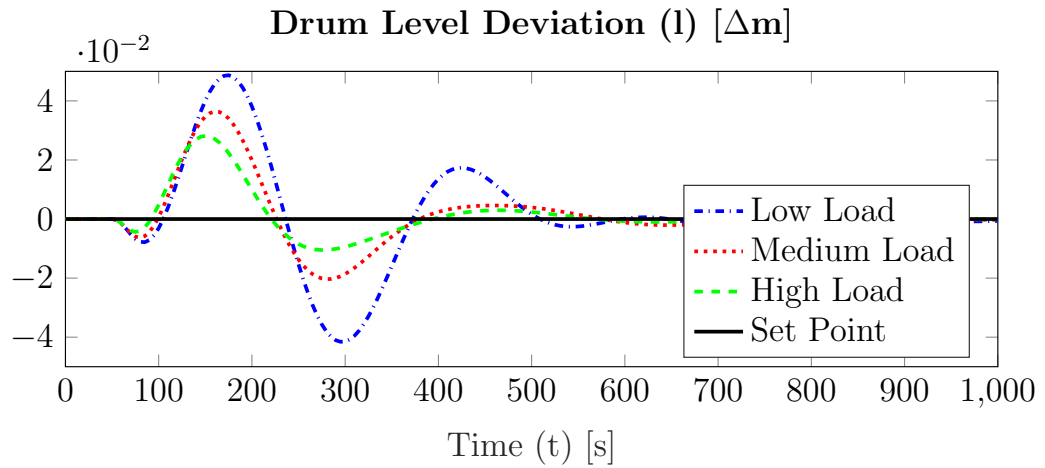
5.2.4 Pressure Step Decrease Figures 5.9-5.10

The step command for this set of simulations is was calculated as follows:

$$r_1 = r_0 + \Delta r_{command} \quad \Delta r_{command} = \begin{bmatrix} \Delta l_{ref} \\ \Delta p_{ref} \end{bmatrix} = \begin{bmatrix} 0 \\ -0.1 \end{bmatrix}$$

$$r_1 = \begin{cases} & \textit{Low} & \textit{Medium} & \textit{High} & \textit{units} \\ l_{ref0} & = & -0.002 & -0.032 & -0.051 & \Delta m \\ p_{ref0} & = & 6.7 & 8.4 & 10.1 & MPa \end{cases}$$

0.1 MPa Drum Pressure Decrease LQR Controlled Variables



0.1 MPa Drum Pressure Decrease LQR Controlled Variables

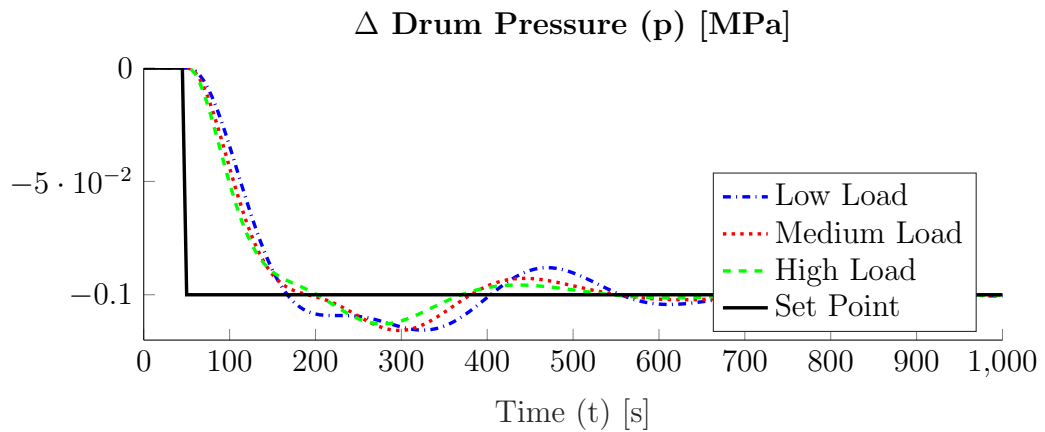


Figure 5.9: Controlled Variables LQR Response to Drum Pressure step of -0.1

Note: This figure shows the change from the initial conditions, as the initial conditions vary across the load settings. This was done to compare the controller performance.

As seen in Figure 5.7, this system is adequately controlled by the designed LQR system. This is a step from the same operating point in the opposite direction, and as such much of the same information can be gained.

		Low Load	Medium Load	High Load	Average
Pressure	% Overshoot	15.6 %	15.76 %	12.88 %	14.75 %
Pressure	Settling Time	621 s	605 s	453 s	559.7 s
Pressure	Disturbance Rejection Energy	1.032	0.8795	0.7845	0.8987
Level	Disturbance Rejection Energy	0.5669	0.2222	0.1127	0.3006

Table 5.7: LQR Controller Performance Parameters: Pressure Step Increase

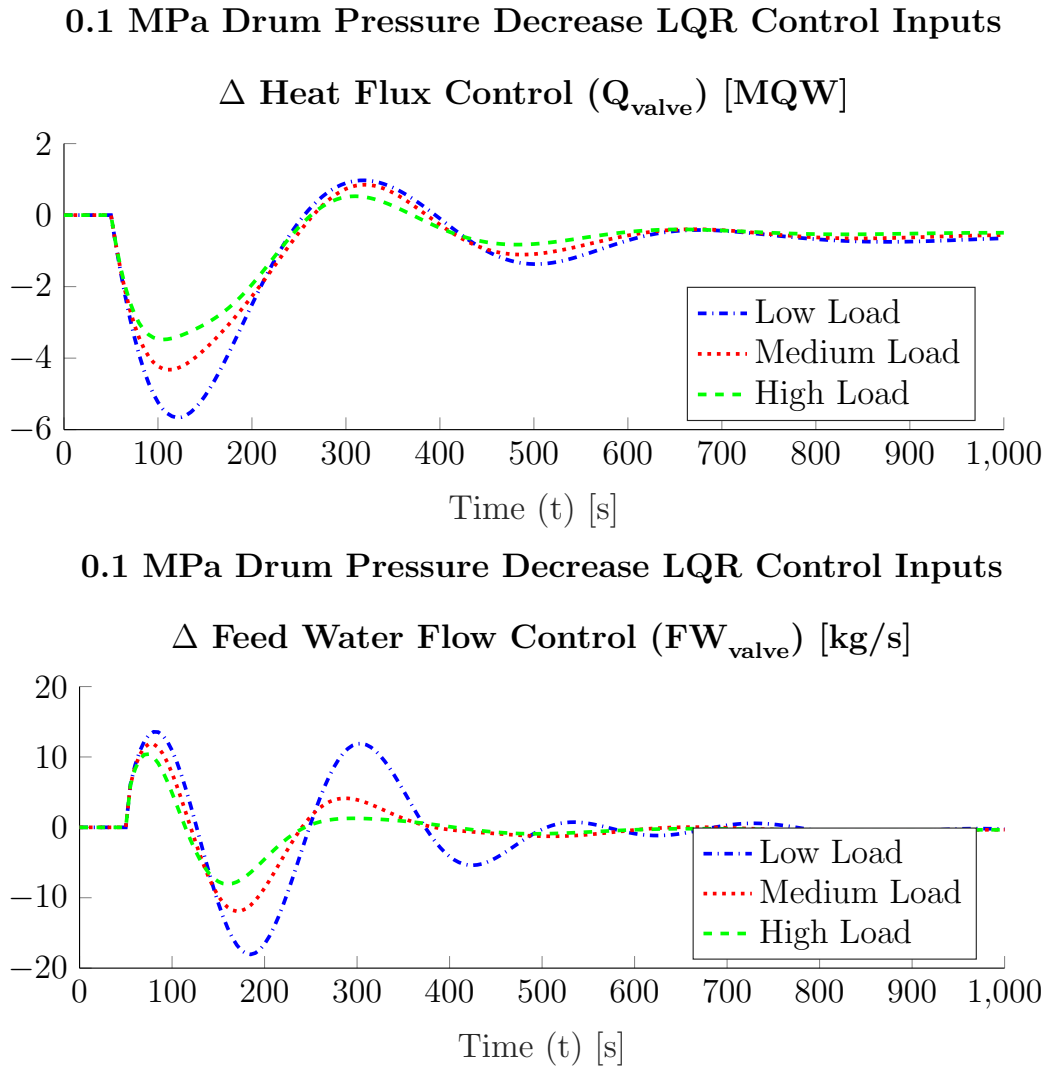


Figure 5.10: Controller Inputs LQR Response to Drum Pressure step of -0.1

Note: This figure shows the change from the initial conditions, as the initial conditions vary across the load settings. This was done to compare the controller performance.

Figure 5.10 shows the controller inputs for the simulations shown in Figure 5.9. This is the controller inputs for a step from the same operating point as seen in Figures 5.7-5.8, however the step command is of opposite magnitude. If inverted the graphs would be near identical.

		Low Load	Medium Load	High Load		Average
Q_{valve}	Signal Energy	7307	4788	3278		5124
FW_{valve}	Signal Energy	7.581e+04	2.962e+04	1.544e+04		4.029e+04

Table 5.8: LQR Controller Input Performance Parameters: Pressure Step Increase

5.3 Controller Performance

The following tables, Table 5.9-5.12, shows the controller performance as a result of the step functions. Percent overshoot, Settling Time, and Signal Energy are all listed below. Each of these values were shown with their proper figure in the previous section. The averages of the different load cases was also included.

Step Direction		Low Load		Medium Load		High Load		Average	
		Inc	Dec	Inc	Dec	Inc	Dec	Inc	Dec
Level Step	Level	43.74	44.94	23.75	23.42	14.97	14.43	27.49	27.6
Pressure Step	Pressure	16.47	15.6	15.77	15.76	12.76	12.88	15	14.75

Table 5.9: LQR Controller Percent Overshoot

Step Direction		Low Load		Medium Load		High Load		Average	
		Inc	Dec	Inc	Dec	Inc	Dec	Inc	Dec
Level Step	Level	632.5	627.5	595.5	582.5	450	447	559.3	552.3
Pressure Step	Pressure	619	621	599	605	450.5	453	556.2	559.7

Table 5.10: LQR Controller Settling Time

It should be noted that as load increases both percent overshoot and settling time improve by becoming smaller. This is due to the shrink/swell effect becoming less effective at the higher loads.

Signal energy for the other signals was included to show which controller has the best disturbance rejection and which controller uses less control energy or effort. In LQR terms, the higher the R matrix is the lower the signal energy would be for the control inputs. For all table entries, the lower the value is the better the system performance.

It should be noted that the signal energy for pressure during a level step change is the same for all loads. This is due to how level and pressure are coupled together and how the integral of pressure is a function being controlled. During pressure step functions the signal energy for the level function decreases as load increases.

		Low Load		Medium Load		High Load	
Step Direction		Inc	Dec	Inc	Dec	Inc	Dec
Level Step	Level	1.865	1.874	1.54	1.522	1.338	1.32
Level Step	Pressure	0.3215	0.3299	0.4458	0.4419	0.4857	0.4779
Pressure Step	Level	0.5229	0.5669	0.2108	0.2222	0.1089	0.1127
Pressure Step	Pressure	1.023	1.032	0.8732	0.8795	0.7804	0.7845

Table 5.11: LQR Controlled Variable Energy

		Low Load		Medium Load		High Load	
Step Direction		Inc	Dec	Inc	Dec	Inc	Dec
Level Step	Q_{valve}	1900	1951	4315	4274	5503	5416
Level Step	FW_{valve}	1.546e+05	1.534e+05	9.241e+04	9.026e+04	6.373e+04	6.248e+04
Pressure Step	Q_{valve}	7114	7307	4666	4788	3203	3278
Pressure Step	FW_{valve}	6.975e+04	7.581e+04	2.83e+04	2.962e+04	1.501e+04	1.544e+04

Table 5.12: LQR Controller Inputs Energy

		Low Load		Medium Load		High Load	
Step Direction		Inc	Dec	Inc	Dec	Inc	Dec
Level Step	V_{wt}	1.562e+04	1.557e+04	1.536e+04	1.532e+04	1.517e+04	1.515e+04
Level Step	p	0.3215	0.3299	0.4458	0.4419	0.4857	0.4779
Level Step	α_r	0.000213	0.000224	0.0005359	0.0005436	0.0008706	0.0008789
Level Step	V_{sd}	660.2	664.7	398	384	241.5	232
Level Step	Q	1714	1750	3813	3762	4815	4728
Level Step	q_f	1.517e+05	1.505e+05	9.045e+04	8.831e+04	6.222e+04	6.098e+04
Pressure Step	V_{wt}	243.9	263.7	106.4	111	60.48	62.07
Pressure Step	p	28.14	28.15	28.02	28.02	27.95	27.95
Pressure Step	α_r	0.001657	0.001645	0.001898	0.001881	0.002274	0.002247
Pressure Step	V_{sd}	364.5	404	121	130.7	49.07	51.9
Pressure Step	Q	6587	6763	4338	4451	2981	3051
Pressure Step	q_f	6.842e+04	7.44e+04	2.759e+04	2.89e+04	1.453e+04	1.496e+04

Table 5.13: LQR State Variable Energy

Controller input energy reduces as load goes up during a pressure step, but increases during a level step. This is most likely due to the weighting of the R or Q matrices.

CHAPTER 6

MODEL PREDICTIVE CONTROL

As discussed in Section 2.2, the MPC controller is a powerful tool, however it is not designed for nonlinear systems. Algorithm 2.1 shows how MPC can be used on a nonlinear system. This chapter will discuss on the physical dynamics of how a MPC controller can be used on the Expanded model in Equation (3.13) without linearization.

6.1 Controller Design

As described in the previous chapter stable feedback alone is not adequate for control, and to perform reference tracking an integrator must be introduced. When calculating a specific time step's gain a discrete time linearized system must be calculated. The integrator will be introduced once the discrete time linearized system is calculated. To calculate a specific time step's gains consider the system in question is the model discussed in (3.13).

$$\frac{d}{dt} \begin{bmatrix} V_{wt} \\ p \\ \alpha_r \\ V_{sd} \\ Q \\ q_f \end{bmatrix} = \begin{bmatrix} e_{11}(p) & e_{12}(p) & 0 & 0 \\ e_{21}(p) & e_{22}(p) & 0 & 0 \\ 0 & e_{32}(p) & e_{33}(p) & 0 \\ 0 & e_{42}(p) & e_{43}(p) & e_{44}(p) \end{bmatrix}^{-1} \begin{bmatrix} q_f - q_s(p) \\ Q + q_f h_f(t_{f_0}, p) - q_s(p) h_s(p) \\ Q + \alpha_r h_c(p) q_{dc}(p) \\ \frac{\rho_s(p)}{T_d} (V_{sd}^0 - V_{sd}) + \frac{h_f(t_{f_0}, p) - h_w(p)}{h_c(p)} q_f \\ \frac{(Q_{valve} - Q)}{T_{vQ}} \\ \frac{(FW_{valve} - q_f)}{T_{vfw}} \end{bmatrix}$$

Which take the form:

$$\dot{x}(t) = g(x(t), u(t))$$

The controlled outputs of the system as discussed in (3.10) are:

$$y(t) = \begin{bmatrix} l(V_{wt}, p, \alpha_r, V_{sd}) \\ p \end{bmatrix}$$

Which take the form:

$$y(t) = g(x(t), u(t))$$

These nonlinear state space equations can be linearized to take the following form:

$$\begin{aligned} \frac{d\Delta x(t)}{dt} &= A_i^c \Delta x(t) + B_i^c \Delta u(t) \\ \Delta y(t) &= C_i^c \Delta x(t) + D_i^c \Delta u(t) \end{aligned} \quad (6.1)$$

where

$$\begin{aligned} A_i^c &= \left. \frac{\partial f(x(t), u(t))}{\partial x} \right|_{x(t), u(t)} \\ B_i^c &= \left. \frac{\partial f(x(t), u(t))}{\partial u} \right|_{x(t), u(t)} \\ C_i^c &= \left. \frac{\partial g(x(t), u(t))}{\partial x} \right|_{x(t), u(t)} \\ D_i^c &= \left. \frac{\partial g(x(t), u(t))}{\partial u} \right|_{x(t), u(t)} \end{aligned}$$

It should be noted that this linearization is performed at every time step in the simulation. The linearization is performed at the current state control. This is noted by the subscript of i .

This state space system is then converted into a discrete time system.

$$\begin{aligned}\Delta x(k_i + 1) &= A_i^d \Delta x(k_i) + B_i^d \Delta u(k_i) \\ \Delta y(k_i) &= C_i^d \Delta x(k_i) + D_i^d \Delta u(k_i) \\ \Delta x(k_i + 1) &= \Delta x(t + T_s) \\ \Delta x(t) &= \dot{x}(t)/T_s\end{aligned}$$

where the various matrices are

$$\begin{aligned}A_i^d &= e^{A_i^c T_s} & B_i^d &= \left(\int_0^{T_s} e^{A_i^c \tau} d\tau \right) B_i^c \\ C_i^d &= C_i^c & D_i^d &= D_i^c\end{aligned}$$

The integrator is then implemented:

$$A_i^{MPC} = \begin{bmatrix} A_i^d & 0 \\ C_i^d A_i^d & I \end{bmatrix} \quad B_i^{MPC} = \begin{bmatrix} B_i^d \\ C_i^d B_i^d \end{bmatrix} \quad C_i^{MPC} = \begin{bmatrix} 0 \\ I \end{bmatrix} \quad (6.2)$$

$$\begin{aligned}\Delta x(k_i + 1) &= A_i^{MPC} \Delta x(k_i) + B_i^{MPC} \Delta u(k_i) \\ y(k_i) &= C_i^{MPC} \Delta x(k_i) \\ \Delta x(k_i + 1) &= \Delta x(t + T_s) \\ \Delta x(t) &= \dot{x}(t)T_s\end{aligned} \quad (6.3)$$

For shorthand, $A_i^{MPC} = A_i$, $B_i^{MPC} = B_i$, and $C_i^{MPC} = C_i$.

The MPC procedure was shown in Section 2.3. Equations (2.6) and (2.7) show how future states and outputs can be predicted if the current state, control, and model are known.

$$\begin{aligned}\Delta x(k_i + N_p | k_i) &= A_i^{N_p} \Delta x(k_i) + A_i^{N_p-1} B_i u(k_i + 1 - 1) + \dots \\ &\quad \dots + A_i^{N_p-N_c} B_i u(k_i + N_c - 1) \\ y(k_i + N_p | k_i) &= C_i A_i^{N_p} \Delta x(k_i) + C_i A_i^{N_p-1} B_i u(k_i + 1 - 1) + \dots \\ &\quad \dots + C_i A_i^{N_p-N_c} B_i u(k_i + N_c - 1)\end{aligned}$$

This is then arranged in a matrix equation:

$$Y = F_i x(k_i) + \Phi_i U(k_i)$$

$$Y = \begin{bmatrix} y(k_i + 1|k_i) \\ y(k_i + 2|k_i) \\ \vdots \\ y(k_i + N_p|k_i) \end{bmatrix}$$

$$U = \begin{bmatrix} u(k_i) \\ u(k_i + 1) \\ \vdots \\ u(k_i + N_c - 1) \end{bmatrix}$$

$$F_i = \begin{bmatrix} C_i A_i \\ C_i A_i^2 \\ \vdots \\ C_i A_i^{N_p} \end{bmatrix}$$

$$\Phi_i = \begin{bmatrix} C_i B_i & 0 & 0 & \cdots & 0 \\ C_i A_i B_i & C_i B_i & 0 & \cdots & 0 \\ C_i A_i^2 B_i & C_i A_i B_i & C_i B_i & \cdots & 0 \\ \vdots & \vdots & \vdots & \ddots & \vdots \\ C_i A_i^{N_p-1} B_i & C_i A_i^{N_p-2} B_i & C_i A_i^{N_p-3} B_i & \cdots & C_i A_i^{N_p-N_c} B_i \end{bmatrix}$$

To minimize the tracking error, define the cost function

$$J(U) = \frac{1}{2}(R_s - Y)^T Q (R_s - Y) + \frac{1}{2} U^T R U$$

where R_s is a reference signal matrix, defined in equation (2.10).

Minimizing the cost function and applying the receding horizon discussed in chapter 2 gives:

$$\begin{aligned}
U(k_i) &= (\Phi_i^T Q \Phi_i + R)^{-1} \Phi_i^T Q (\bar{R}_s r(k_i) - F_i x(k_i)) \\
u(k_i) &= \overbrace{\begin{bmatrix} I & 0 & \dots & 0 \end{bmatrix}}^{N_c} (\Phi_i^T Q \Phi_i + R)^{-1} \Phi_i^T Q (\bar{R}_s r(k_i) - F_i x(k_i)) \\
u(k_i) &= K_i^{MPC^{ref}} r(k_i) - K_i^{MPC^{fbk}} \Delta x(k_i) \\
K_i^{MPC^{ref}} &= \overbrace{\begin{bmatrix} I & 0 & \dots & 0 \end{bmatrix}}^{N_c} (\Phi_i^T Q \Phi_i + R)^{-1} \Phi_i^T Q \bar{R}_s \\
K_i^{MPC^{fbk}} &= \overbrace{\begin{bmatrix} I & 0 & \dots & 0 \end{bmatrix}}^{N_c} (\Phi_i^T Q \Phi_i + R)^{-1} \Phi_i^T Q F_i
\end{aligned}$$

The method above is used in Algorithm 2.1, to review:

1. Linearize the continuous time system with respect to the current state $\{x(t), u(t)\}$.
 - $\dot{x} = f(x(t), u(t)) \rightarrow \frac{\partial \Delta x(t)}{\partial t} = A_i^c \Delta x(t) + B_i^c \Delta u(t)$
2. Find the discrete time model of the linearized system at slot k_i .
 - $\frac{\partial \Delta x(t)}{\partial t} = A_i^c \Delta x(t) + B_i^c \Delta u(t) \rightarrow \Delta x(k_i + 1) = A_i^d \Delta x(k_i) + B_i^d \Delta u(k_i)$
 - $A_i^d, B_i^d, C_i^d \rightarrow A_i^{MPC}, B_i^{MPC}, C_i^{MPC}$
3. Compute the MPC gains $K_i^{MPC^{fbk}}$ and $K_i^{MPC^{ref}}$ using A_i^{MPC} , B_i^{MPC} , and C_i^{MPC} . Apply the control signal $u(k_i)$.
 - $u(k_i + 1) = u(k_i) + \Delta u(k_i) = u(k_i) + K_i^{MPC^{ref}} r(k_i) - K_i^{MPC^{fbk}} \Delta x(k_i)$
4. Measure the updated system response $x(k_i + 1)$
 - $x(k_i + 1) = x(t + Ts) = x(k_i) + f(x(k_i), u(k_i))Ts$
5. Repeat from Step 1.

The Controller was tuned to be meet the design criterion of

- 15% Overshoot for a Drum Level step at High load
- 450 seconds of Settling Time for a Drum Level step at High Load
- Drum Pressure will remain stable
- Drum Level will remain stable for other disturbances (such as a Drum Pressure Step)

The MPC design values are N_p , N_c , Q , and R . Q and R are designed similarly to LQR, and were tuned as follows:

$$Q = \begin{bmatrix} I_{N_p} & 0_{N_p} \\ 0_{N_p} & I_{N_p} \end{bmatrix}$$

$$R = K_\omega \begin{bmatrix} I_{N_c} & 0_{N_c} \\ 0_{N_c} & I_{N_c} \end{bmatrix}$$

$$K_\omega = 0.0925$$

K_ω was determined by trial and error, while still fitting the design criteria as best as possible.

N_p was determined by reviewing how long the open loop step responses take to show the shrink/swell effect and to be roughly three times longer than that. Inspecting Figure 3.3

$$\text{Step Start Time} = 50s$$

$$\text{Shrink/Swell End Time} = 90s$$

$$3(90 - 50) = 120s$$

$$N_p = \frac{120}{T_s} = 240s$$

N_c was determined to be the same as N_p , calculating the optimal control over the entire prediction horizon. N_c can be lowered to reduce the processing time, however it cannot be reduced indefinitely.

$$N_c = N_p$$

Both N_p and N_c were chosen and then proven via simulation and may not be optimal for processing time.

6.2 Simulation Results

The simulation using the MPC controller can be calculated using the full nonlinear model without any linearization. The gain matrices were chosen at a single operating point, and then used to calculate the control signal $u(t)$ based on full state feedback.

$$\Delta x(k) = F(x(t), u(t))T_s$$

$$e(t) = y(t) - r(t) = G(x(t), u(t)) - r(t)$$

$$\Delta u(k) = K_{LQI_{fbk}} \Delta x(k) + K_{LQI_{ref}} e(k)$$

$$u(k+1) = u(t+T_s) = u(k) + \Delta u(k)$$

It should be noted that the chosen gain values may not control properly over a large range, as they are only optimal for a specific operating point.

The following simulations use the initial condition at the load setting as defined in (3.14). An initial reference signal is then created based off of the stable initial condition ($r_0 = y_0$).

$$\begin{array}{l} x_0 \\ u_0 \end{array} = \left\{ \begin{array}{lllll} & & \textit{Low} & \textit{Medium} & \textit{High} & \textit{units} \\ V_{wt0} & = & 57.1 & 57.1 & 57.1 & m^3 \\ p_0 & = & 6.8 & 8.5 & 10.2 & MPa \\ \alpha_{r0} & = & 0.0325 & 0.0435 & 0.0561 & - \\ V_{sd0} & = & 5.213 & 4.984 & 4.854 & m^3 \\ Q_0 = Q_{valve} & = & 57.11 & 67.65 & 76.84 & MW \\ q_{f0} = FW_{valve} & = & 33.07 & 39.79 & 46.12 & kg/s \end{array} \right.$$

$$r_0 = y_0 = \begin{cases} & \textit{Low} & \textit{Medium} & \textit{High} & \textit{units} \\ l_0 & = & -0.002 & -0.032 & -0.051 & \Delta m \\ p_0 & = & 6.8 & 8.5 & 10.2 & MPa \end{cases}$$

The reference signal $r(t)$ will be applied, and r_1 will vary based on the step command.

$$r(t) = \begin{cases} r_0 & \textit{for } t < t_{step} \\ r_1 & \textit{for } t > t_{step} \end{cases}$$

The controlled outputs are each compared to their reference as a step change is applied. This system has two controlled variables therefore four steps are required to show the controllers response; variable 1 (Drum Pressure) step up, variable 1 (Drum Pressure) step down, variable 2 (Drum Level Deviation) step up, variable 2 (Drum Level Deviation) step down. When one variable is being stepped the other has its reference held constant. The two variables are coupled together and when a reference is held constant it becomes a disturbance rejection response.

6.2.1 Level Step Increase Figures 6.1 - 6.2

The step command for this set of simulations is was calculated as follows:

$$r_1 = r_0 + \Delta r_{command} \quad \Delta r_{command} = \begin{bmatrix} \Delta l_{ref} \\ \Delta p_{ref} \end{bmatrix} = \begin{bmatrix} 0.1 \\ 0.0 \end{bmatrix}$$

$$r_1 = \begin{cases} & \textit{Low} & \textit{Medium} & \textit{High} & \textit{units} \\ l_{ref0} & = & 0.098 & 0.068 & 0.049 & \Delta m \\ p_{ref0} & = & 6.8 & 8.5 & 10.2 & MPa \end{cases}$$

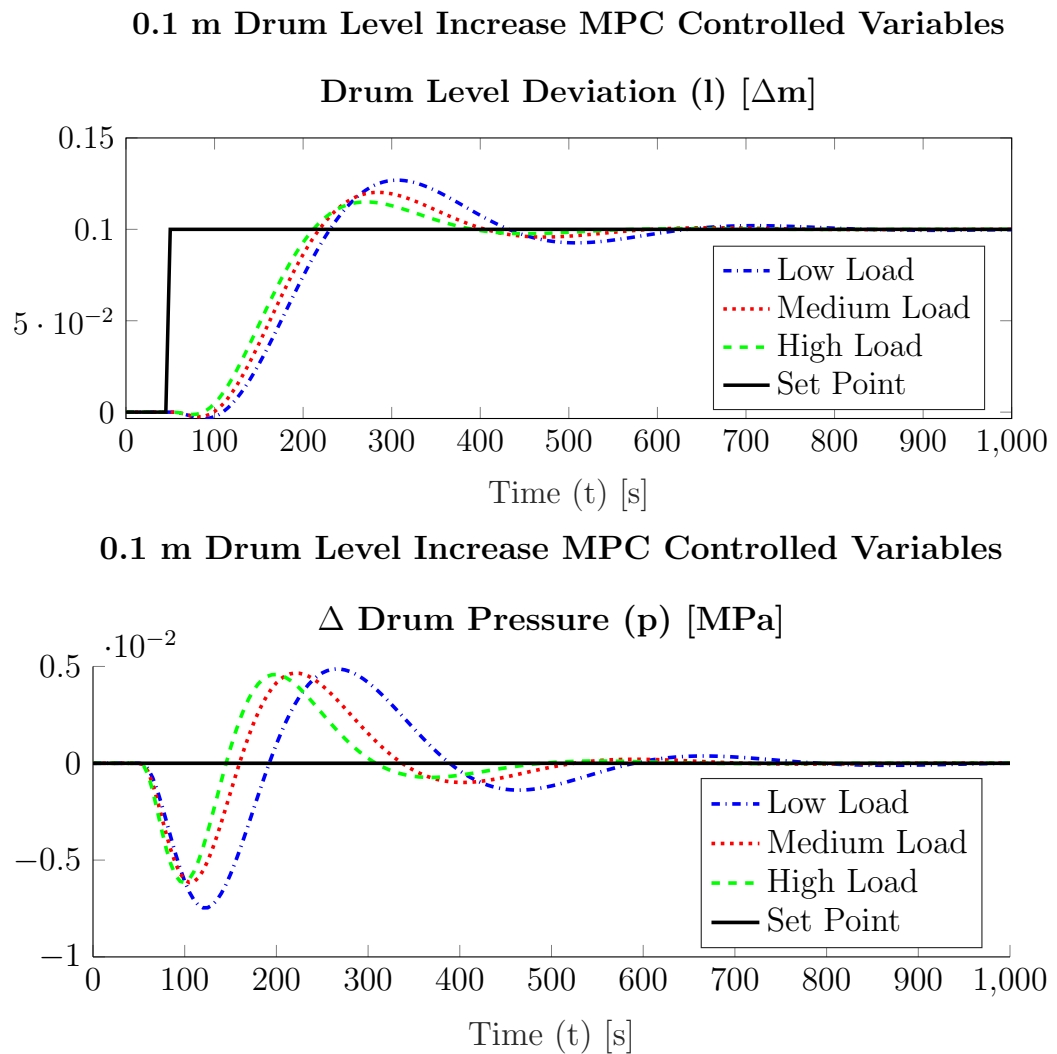


Figure 6.1: Controlled Variables MPC Response to Drum Level step of 0.1

Note: This figure shows the change from the initial conditions, as the initial conditions vary across the load settings. This was done to compare the controller performance.

		Low Load	Medium Load	High Load	Average
Level	% Overshoot	26.9 %	20.23 %	14.99 %	20.71 %
Level	Settling Time	669.5 s	492 s	433 s	531.5 s
Level	Disturbance Rejection Energy	2.314	1.986	1.733	2.011
Pressure	Disturbance Rejection Energy	0.01159	0.007251	0.006173	0.008339

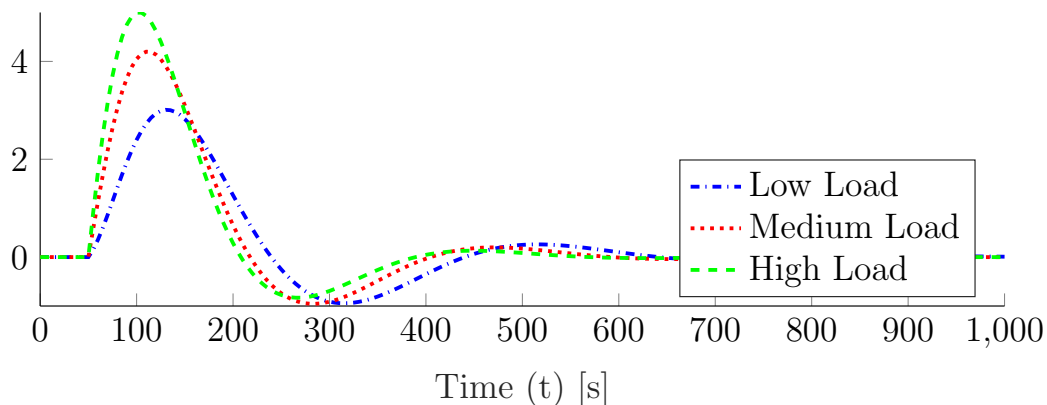
Table 6.1: MPC Controller Performance Parameters: Level Step Increase

Figure 6.1 shows the simulation results using the specified step command and Table 6.2.1 shows the performance characteristics of this simulation as defined in Chapter 2.4. It can be seen that using these tuning parameters, the design goal is achieved. The Shrink/Swell effect can be seen on drum level deviation as well as the reduction of the Shrink/Swell effect as load increases (which is also a known phenomenon). It can be seen that both variables are excellently controlled by the designed MPC system as the transients are controlled.

The effects of different loads on this controller can be seen in two ways; as load increases both the level and pressure controllers performance parameters improve, and the amplitudes decrease as load increases.

0.1 m Drum Level Increase MPC Control Inputs

Δ Heat Flux Control (Q_{valve}) [MQW]



0.1 m Drum Level Increase MPC Control Inputs

Δ Feed Water Flow Control (FW_{valve}) [kg/s]

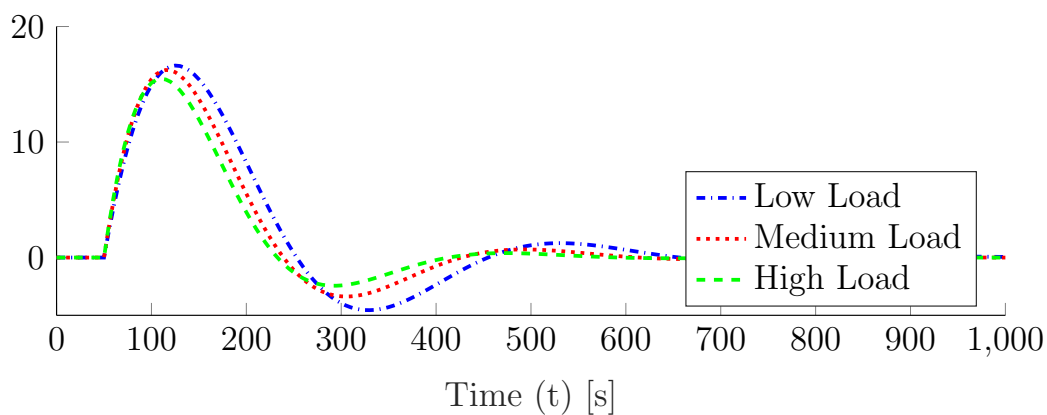


Figure 6.2: Controller Inputs MPC Response to Drum Level step of 0.1

Note: This figure shows the change from the initial conditions, as the initial conditions vary across the load settings. This was done to compare the controller performance.

		Low Load	Medium Load	High Load		Average
Q_{valve}	Signal Energy	1698	2821	3573		2697
FW_{valve}	Signal Energy	5.75e+04	4.827e+04	4.047e+04		4.874e+04

Table 6.2: MPC Controller Input Performance Parameters: Level Step Increase

Figure 6.2 shows the controller inputs for the simulations shown in Figure 6.1. It can be seen that as load increases heat flux requires more control action, while feed water requires less. This is the a different effect than what was seen when doing a drum pressure step change. It should be noted that the feed water control is near identical for all loads.

6.2.2 Level Step Decrease Figures 6.3 - 6.4

The step command for this set of simulations is was calculated as follows:

$$r_1 = r_0 + \Delta r_{command} \quad \Delta r_{command} = \begin{bmatrix} \Delta l_{ref} \\ \Delta p_{ref} \end{bmatrix} = \begin{bmatrix} -0.1 \\ 0.0 \end{bmatrix}$$

$$r_1 = \begin{cases} & \textit{Low} & \textit{Medium} & \textit{High} & \textit{units} \\ l_{ref0} & = & -0.102 & -0.132 & -0.151 & \Delta m \\ p_{ref0} & = & 6.8 & 8.5 & 10.2 & MPa \end{cases}$$

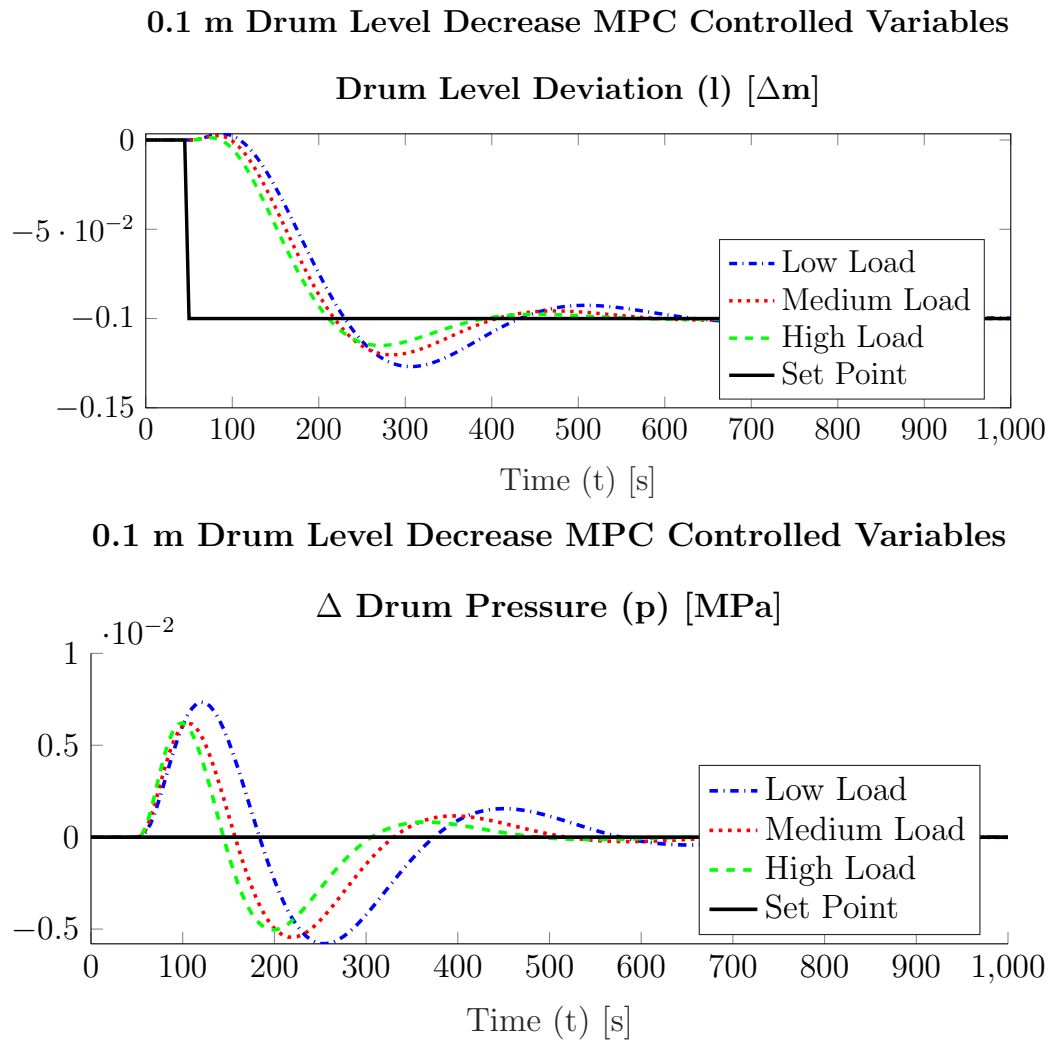


Figure 6.3: Controlled Variables MPC Response to Drum Level step of -0.1

Note: This figure shows the change from the initial conditions, as the initial conditions vary across the load settings. This was done to compare the controller performance.

		Low Load	Medium Load	High Load	Average
Level	% Overshoot	26.9 %	20.23 %	14.99 %	20.71 %
Level	Settling Time	669.5 s	492 s	433 s	531.5 s
Level	Disturbance Rejection Energy	2.305	1.976	1.724	2.002
Pressure	Disturbance Rejection Energy	0.01159	0.007251	0.006173	0.008339

Table 6.3: MPC Controller Performance Parameters: Level Step Decrease

Figure 6.3 is a simulation using a step from the same operating point but in the opposite direction as the simulation in Figure 6.1, much of the same information can be gained.

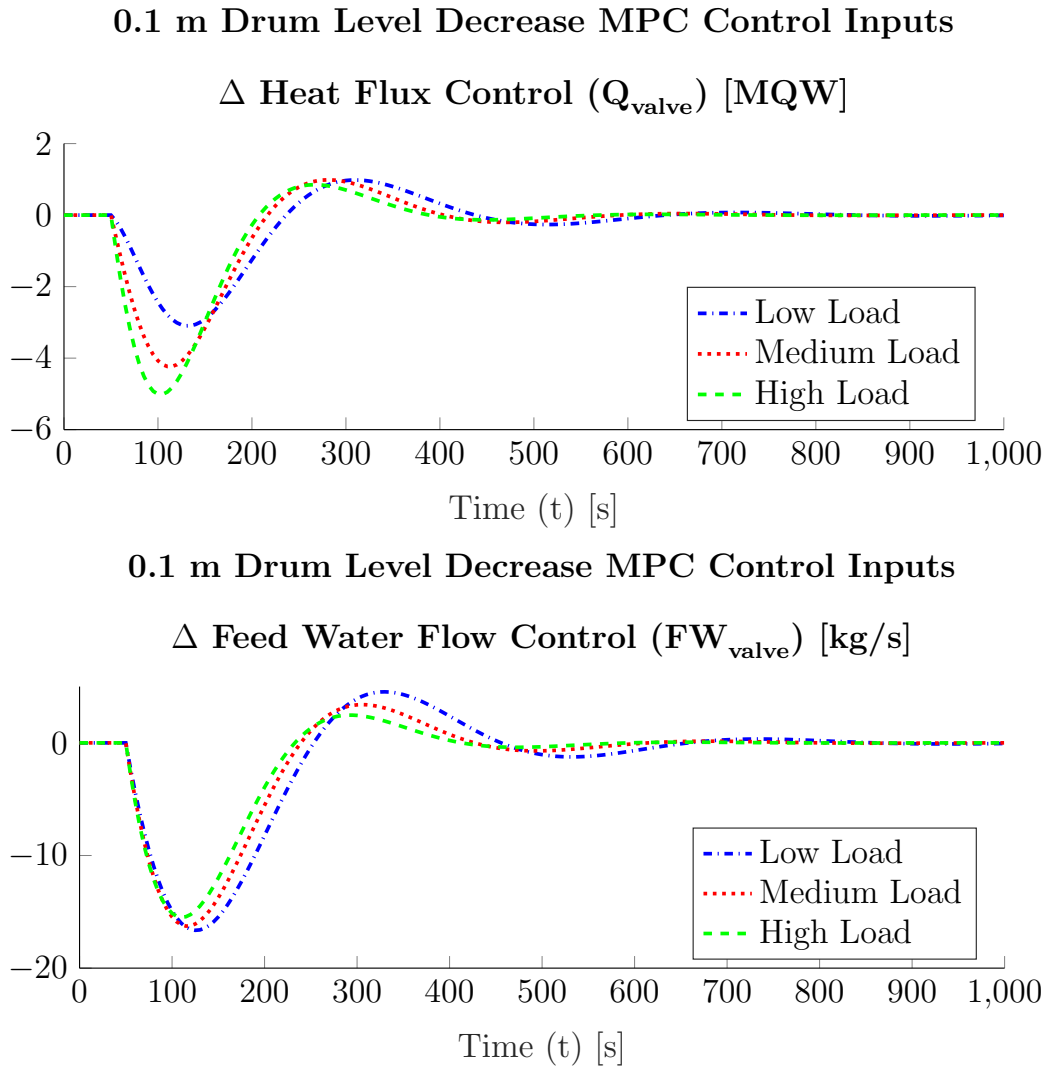


Figure 6.4: Controller Inputs MPC Response to Drum Level step of -0.1

Note: This figure shows the change from the initial conditions, as the initial conditions vary across the load settings. This was done to compare the controller performance.

		Low Load	Medium Load	High Load		Average
Q_{valve}	Signal Energy	1778	2877	3603		2753
FW_{valve}	Signal Energy	5.753e+04	4.845e+04	4.059e+04		4.886e+04

Table 6.4: MPC Controller Input Performance Parameters: Level Step Decrease

Figure 6.4 shows the controller inputs for the simulations shown in Figure 6.3. It can be seen that as load increases the action required from the controller varies. Heat flux requires more control action as load increases, while feed water requires less. This is the a different effect than what was seen when doing a drum pressure step change.

This is the controller inputs for a step from the same operating point as seen in Figures 6.1-6.2, however the step command is of opposite magnitude. If inverted the graphs would be near identical, except for the near negligible differences due to the nonlinear system.

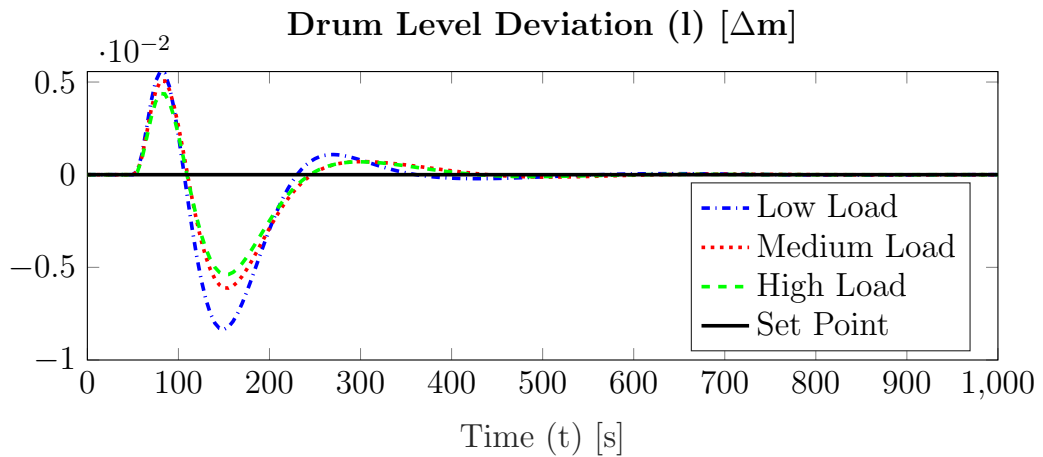
6.2.3 Pressure Step Increase Figures 6.5 - 6.6

The step command for this set of simulations is was calculated as follows:

$$r_1 = r_0 + \Delta r_{command} \quad \Delta r_{command} = \begin{bmatrix} \Delta l_{ref} \\ \Delta p_{ref} \end{bmatrix} = \begin{bmatrix} 0 \\ 0.1 \end{bmatrix}$$

$$r_1 = \begin{cases} & \begin{matrix} Low & Medium & High & units \end{matrix} \\ l_{ref0} & = & -0.002 & -0.032 & -0.051 & \Delta m \\ p_{ref0} & = & 6.9 & 8.6 & 10.3 & MPa \end{cases}$$

0.1 MPa Drum Pressure Increase MPC Controlled Variables



0.1 MPa Drum Pressure Increase MPC Controlled Variables

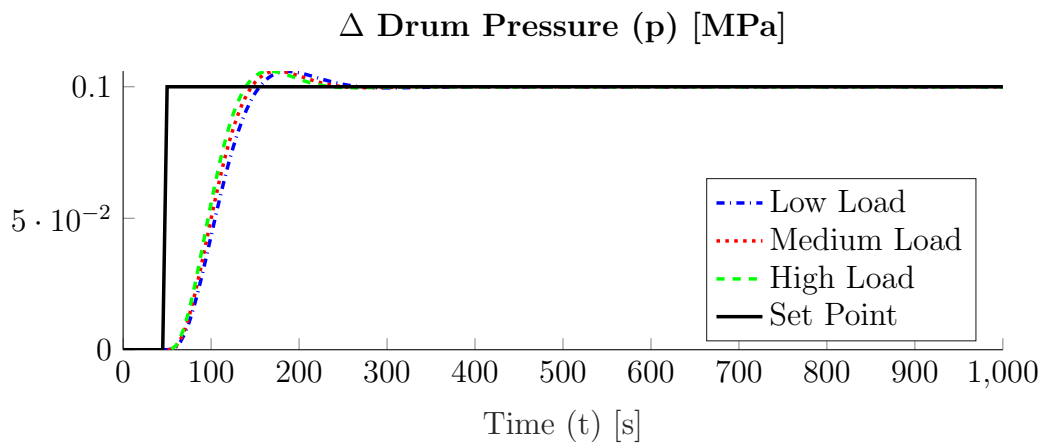


Figure 6.5: Controlled Variables MPC Response to Drum Pressure step of 0.1

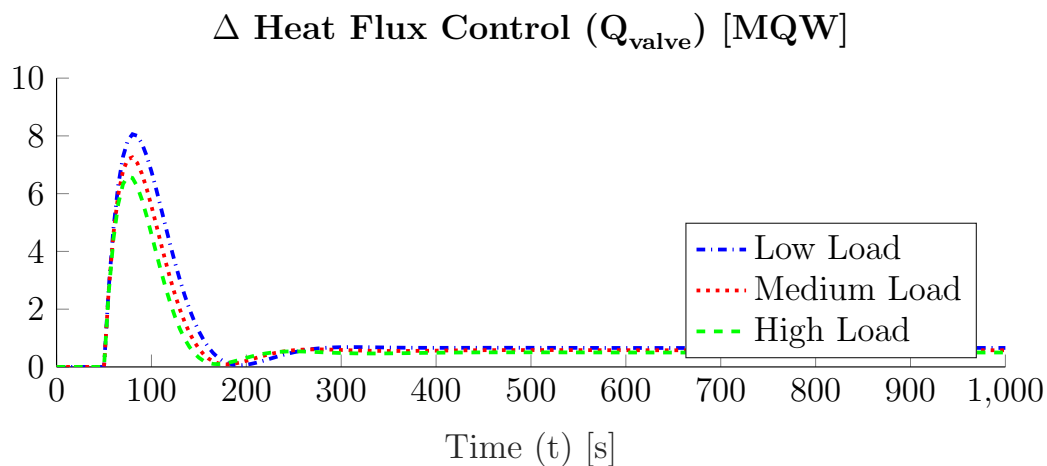
Note: This figure shows the change from the initial conditions, as the initial conditions vary across the load settings. This was done to compare the controller performance.

		Low Load	Medium Load	High Load	Average
Pressure	% Overshoot	5.837 %	5.93 %	5.977 %	5.915 %
Pressure	Settling Time	186 s	170 s	158 s	171.3 s
Pressure	Disturbance Rejection Energy	0.8489	0.7793	0.7247	0.7843
Level	Disturbance Rejection Energy	0.009109	0.00566	0.004351	0.006373

Table 6.5: MPC Controller Performance Parameters: Pressure Step Increase

Figure 6.5 shows the simulation results using the specified step command and Table 6.2.3 shows the performance characteristics of this simulation as defined in Chapter 2.4. This step uses the same gains as the controller that met the design goal, seen in Figure 6.1. It can be seen that both variables are excellently controlled by the designed MPC system as the transients are controlled in a much shorter time than the open loop as seen in Figure 3.36. It can be seen that as the load increases, the controller perform better overall, with lower settling times and lower disturbance rejection energy. The overshoot is near constant, but increases slightly with load.

0.1 MPa Drum Pressure Increase MPC Control Inputs



0.1 MPa Drum Pressure Increase MPC Control Inputs

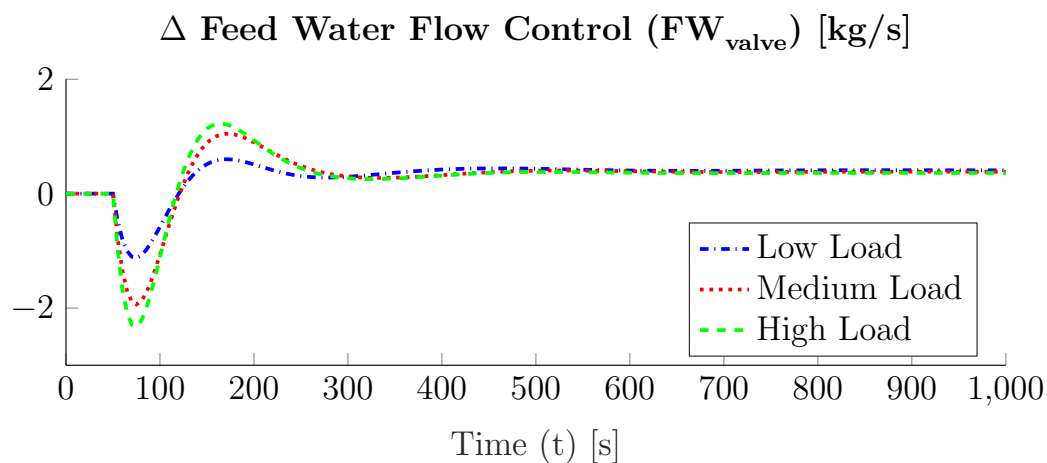


Figure 6.6: Controller Inputs MPC Response to Drum Pressure step of 0.1

Note: This figure shows the change from the initial conditions, as the initial conditions vary across the load settings. This was done to compare the controller performance.

		Low Load	Medium Load	High Load	Average
Q_{valve}	Signal Energy	7296	5441	4158	5631
FW_{valve}	Signal Energy	544.8	774.4	879.5	732.9

Table 6.6: MPC Controller Input Performance Parameters: Pressure Step Increase

Figure 6.6 shows the controller inputs for the simulations shown in Figure 6.5. It can be seen that as load increase the control action required from heat flux decreases, while the control action required from feed water increases as load increases. This may be caused by the system nonlinearities and the reduction of the Shrink/Swell effect.

6.2.4 Pressure Step Decrease Figures 6.7 - 6.8

The step command for this set of simulations is was calculated as follows:

$$r_1 = r_0 + \Delta r_{command} \quad \Delta r_{command} = \begin{bmatrix} \Delta l_{ref} \\ \Delta p_{ref} \end{bmatrix} = \begin{bmatrix} 0 \\ -0.1 \end{bmatrix}$$

$$r_1 = \begin{cases} & \begin{matrix} Low & Medium & High & units \end{matrix} \\ l_{ref0} & = & -0.002 & -0.032 & -0.051 & \Delta m \\ p_{ref0} & = & 6.7 & 8.4 & 10.1 & MPa \end{cases}$$

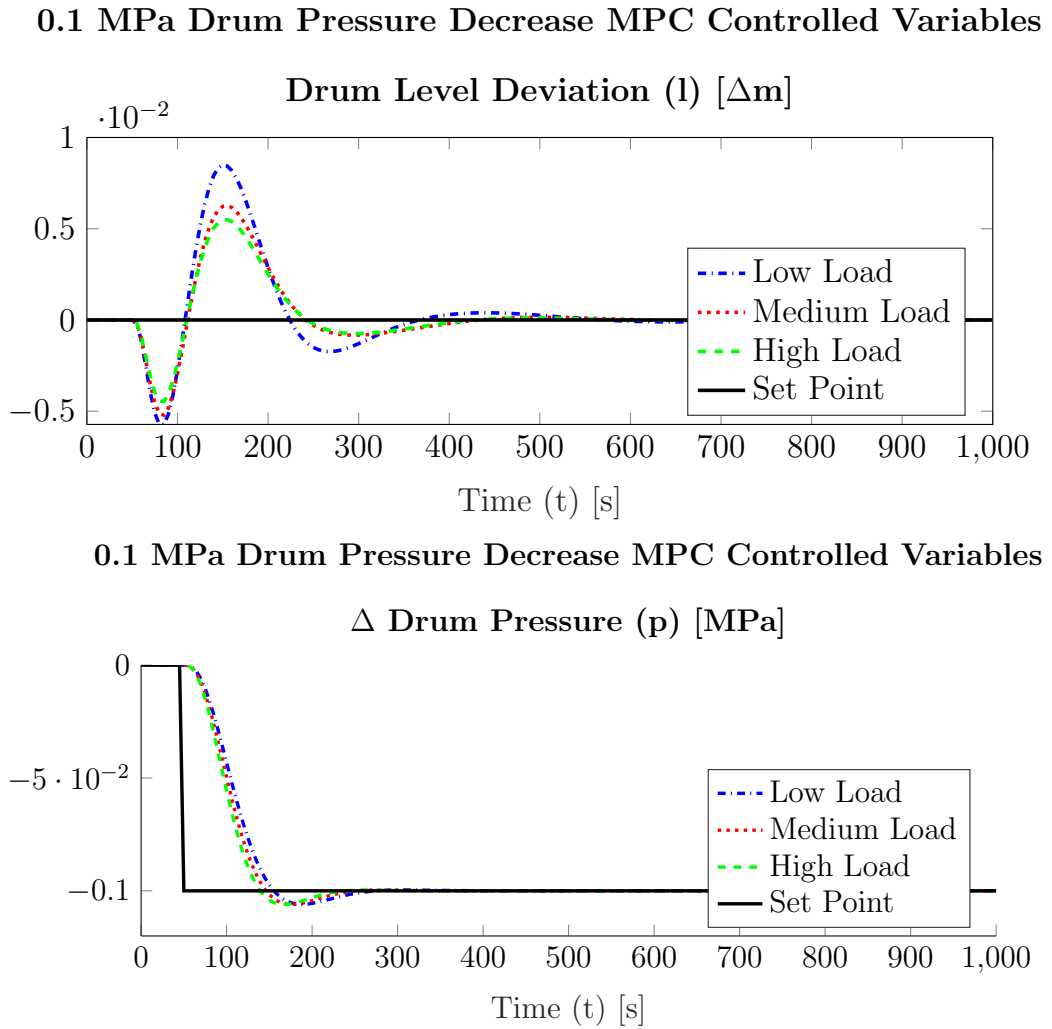


Figure 6.7: Controlled Variables MPC Response to Drum Pressure step of -0.1

Note: This figure shows the change from the initial conditions, as the initial conditions vary across the load settings. This was done to compare the controller performance.

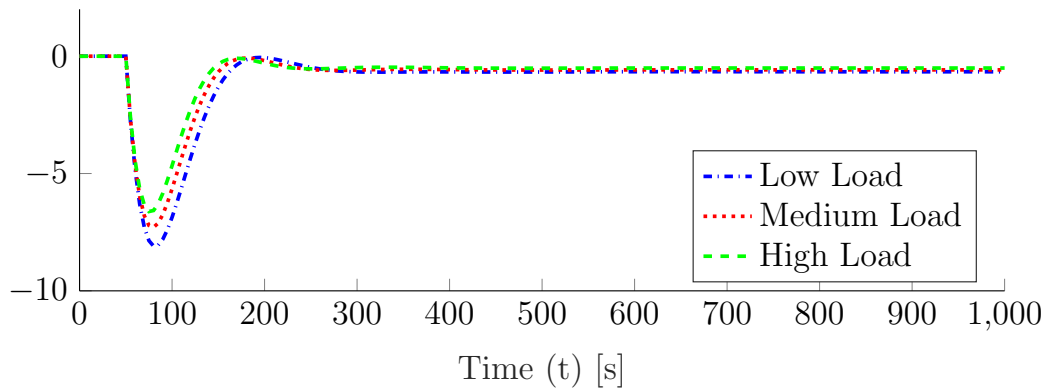
		Low Load	Medium Load	High Load	Average
Pressure	% Overshoot	5.993 %	6.051 %	6.087 %	6.044 %
Pressure	Settling Time	189 s	172 s	159.5 s	173.5 s
Pressure	Disturbance Rejection Energy	0.8503	0.7804	0.7256	0.7854
Level	Disturbance Rejection Energy	0.009546	0.00586	0.004503	0.006636

Table 6.7: MPC Controller Performance Parameters: Pressure Step Increase

Since Figure 6.7 is a simulation using a step from the same operating point but in the opposite direction as the simulation in Figure 6.5, much of the same information can be gained and this section will not have any new comments.

0.1 MPa Drum Pressure Decrease MPC Control Inputs

Δ Heat Flux Control (Q_{valve}) [MQW]



0.1 MPa Drum Pressure Decrease MPC Control Inputs

Δ Feed Water Flow Control (FW_{valve}) [kg/s]

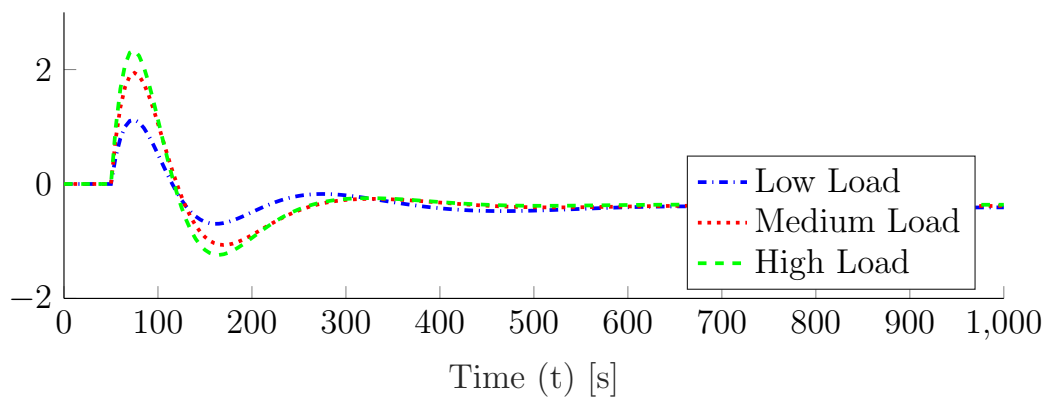


Figure 6.8: Controller Inputs MPC Response to Drum Pressure step of -0.1

Note: This figure shows the change from the initial conditions, as the initial conditions vary across the load settings. This was done to compare the controller performance.

		Low Load	Medium Load	High Load	Average
Q_{valve}	Signal Energy	7449	5540	4227	5739
FW_{valve}	Signal Energy	550.2	778.5	889.1	739.3

Table 6.8: MPC Controller Input Performance Parameters: Pressure Step Increase

Figure 6.8 shows the controller inputs for the simulations shown in Figure 6.7. This is the controller inputs for a step from the same operating point as seen in Figures 6.5-6.6, however the step command is of opposite magnitude. If inverted the graphs would be near identical, except for the near negligible differences due to the nonlinear system.

6.3 Controller Performance

The following tables, Table 6.9-6.12, shows the controller performance as a result of the step functions. Percent overshoot, Settling Time, and Signal Energy are all listed below. Each of these values were shown with their proper figure in the previous section. The averages of the different load cases was also included.

Step Direction		Low Load		Medium Load		High Load		Average	
		Inc	Dec	Inc	Dec	Inc	Dec	Inc	Dec
Level Step	Level	26.9	26.9	20.23	20.32	14.99	15.08	20.71	20.77
Pressure Step	Pressure	5.837	5.993	5.93	6.051	5.977	6.087	5.915	6.044

Table 6.9: MPC Controller Percent Overshoot

Step Direction		Low Load		Medium Load		High Load		Average	
		Inc	Dec	Inc	Dec	Inc	Dec	Inc	Dec
Level Step	Level	669.5	671.5	492	492.5	433	434	531.5	532.7
Pressure Step	Pressure	186	189	170	172	158	159.5	171.3	173.5

Table 6.10: MPC Controller Settling Time

It should be noted that as load increases percent overshoot increases for pressure and decreases for level. Settling time improves both level and pressure as load increases.

Signal energy for the other signals was included to show which controller has the best disturbance rejection and which controller uses less control energy or effort. For all table entries, the lower the value is the better the system performance.

Step Direction		Low Load		Medium Load		High Load	
		Inc	Dec	Inc	Dec	Inc	Dec
Level Step	Level	2.314	2.305	1.986	1.976	1.733	1.724
Level Step	Pressure	0.01159	0.01262	0.007251	0.008445	0.006173	0.006847
Pressure Step	Level	0.009109	0.009546	0.00566	0.00586	0.004351	0.004503
Pressure Step	Pressure	0.8489	0.8503	0.7793	0.7804	0.7247	0.7256

Table 6.11: MPC Controlled Variable Energy

It should be noted that the signal energy decreases as load increases for both controllers, showing the reduction of the Shrink/Swell effect.

		Low Load		Medium Load		High Load	
Step Direction		Inc	Dec	Inc	Dec	Inc	Dec
Level Step	Q_{valve}	1698	1778	2821	2877	3573	3603
Level Step	FW_{valve}	5.75e+04	5.753e+04	4.827e+04	4.845e+04	4.047e+04	4.059e+04
Pressure Step	Q_{valve}	7296	7449	5441	5540	4158	4227
Pressure Step	FW_{valve}	544.8	550.2	774.4	778.5	879.5	889.1

Table 6.12: MPC Controller Inputs Energy

		Low Load		Medium Load		High Load	
Step Direction		Inc	Dec	Inc	Dec	Inc	Dec
Level Step	V_{wt}	1.498e+04	1.498e+04	1.484e+04	1.484e+04	1.474e+04	1.474e+04
Level Step	p	0.01159	0.01262	0.007251	0.008445	0.006173	0.006847
Level Step	α_r	0.000237	0.0002481	0.0005121	0.0005283	0.0008241	0.000845
Level Step	V_{sd}	358.1	357.6	263	263.2	179.1	179.1
Level Step	Q	1541	1610	2508	2557	3126	3153
Level Step	q_f	5.716e+04	5.719e+04	4.792e+04	4.81e+04	4.014e+04	4.027e+04
Pressure Step	V_{wt}	5.64	6.424	2.365	2.497	1.785	1.829
Pressure Step	p	27.76	27.77	27.87	27.87	27.95	27.95
Pressure Step	α_r	0.001426	0.001416	0.001706	0.001689	0.002111	0.002084
Pressure Step	V_{sd}	22.82	25.39	5.346	5.901	1.908	2.072
Pressure Step	Q	6069	6212	4433	4523	3319	3381
Pressure Step	q_f	539.1	544	760.7	764.5	859.7	869.1

Table 6.13: MPC State Variable Energy

Controller input energy reduces for Q_{valve} as load goes up during a pressure step, but increases during a level step. Controller input energy for FW_{valve} increases as load goes up for pressure steps, but decreases for level steps. This is most likely due to the weighting between the R and Q matrices.

CHAPTER 7

COMPARISON OF CONTROL METHODS

This chapter is a compilation of the results from the previous chapters. No new control methodologies are introduced.

7.1 Simulation Results

The simulation results from Chapter 4, 5, and 6 are compiled here to show the different controllers directly compared to each other. Chapter 4 results are generated using equations (4.1)-(4.4). Chapter 5 results are generated using equations (2.1)-(2.3) and (5.1)-(5.2). Chapter 6 results are generated using equations (2.4)-(2.22) and (6.1)-(6.3) in conjunction with algorithm (2.1).

Each of the controllers was designed to meet the following parameters:

- 15% Overshoot for a Drum Level step at High load
- 450 seconds of Settling Time for a Drum Level step at High Load
- Drum Pressure will remain stable
- Drum Level will remain stable for other disturbances (such as a Drum Pressure Step)

Due to the fact that the system cannot be decoupled, conventional PID tuning techniques are not applicable and a heuristic trial and error approach was used. While more advanced tuning techniques can be used for calculating LQR weightings, like pole placement, none can directly guarantee a settling time and overshoot. As such a heuristic trial and error method was used to determine the weightings.

The following simulations use the initial condition at the high load setting as defined in (3.14). An initial reference signal is then created based off of the stable initial condition ($r_0 = y_0$). Simulations using the low and medium loads can be seen in the appendix.

$$\begin{aligned}
 \begin{matrix} x_0 \\ u_0 \end{matrix} &= \left\{ \begin{array}{ll} & \textit{High units} \\ V_{wt0} & = 57.1 \text{ m}^3 \\ p_0 & = 10.2 \text{ MPa} \\ \alpha_{r0} & = 0.0561 \text{ -} \\ V_{sd0} & = 4.854 \text{ m}^3 \\ Q_0 = Q_{valve} & = 76.84 \text{ MW} \\ q_{f0} = FW_{valve} & = 46.12 \text{ kg/s} \end{array} \right. \\
 r_0 = y_0 &= \left\{ \begin{array}{ll} & \textit{High units} \\ l_0 & = -0.051 \text{ } \Delta m \\ p_0 & = 10.2 \text{ MPa} \end{array} \right.
 \end{aligned}$$

The reference signal $r(t)$ will be applied, and r_1 will vary based on the step command.

$$r(t) = \begin{cases} r_0 & \textit{for } t < t_{step} \\ r_1 & \textit{for } t > t_{step} \end{cases}$$

The controlled outputs are each compared to their reference as a step change is applied. This system has two controlled variables therefore four steps are required to show the controllers response; variable 1 (Drum Pressure) step up, variable 1 (Drum Pressure) step down, variable 2 (Drum Level Deviation) step up, variable 2 (Drum Level Deviation) step down. When one variable is

being stepped the other has its reference held constant. The two variables are coupled together and when a reference is held constant it becomes a disturbance rejection response.

Controller performance will be defined using percent overshoot, settling time, and signal energy; which are defined in Chapter 4.2. These metrics will be used to compare the various controller types in a later chapter.

7.1.1 Level Step Increase Figures

The step command for this set of simulations is was calculated as follows:

$$r_1 = r_0 + \Delta r_{command} \quad \Delta r_{command} = \begin{bmatrix} \Delta l_{ref} \\ \Delta p_{ref} \end{bmatrix} = \begin{bmatrix} 0.1 \\ 0.0 \end{bmatrix}$$

$$r_1 = \begin{cases} & \text{High units} \\ l_{ref_0} & = 0.049 \quad \Delta m \\ p_{ref_0} & = 10.2 \quad MPa \end{cases}$$

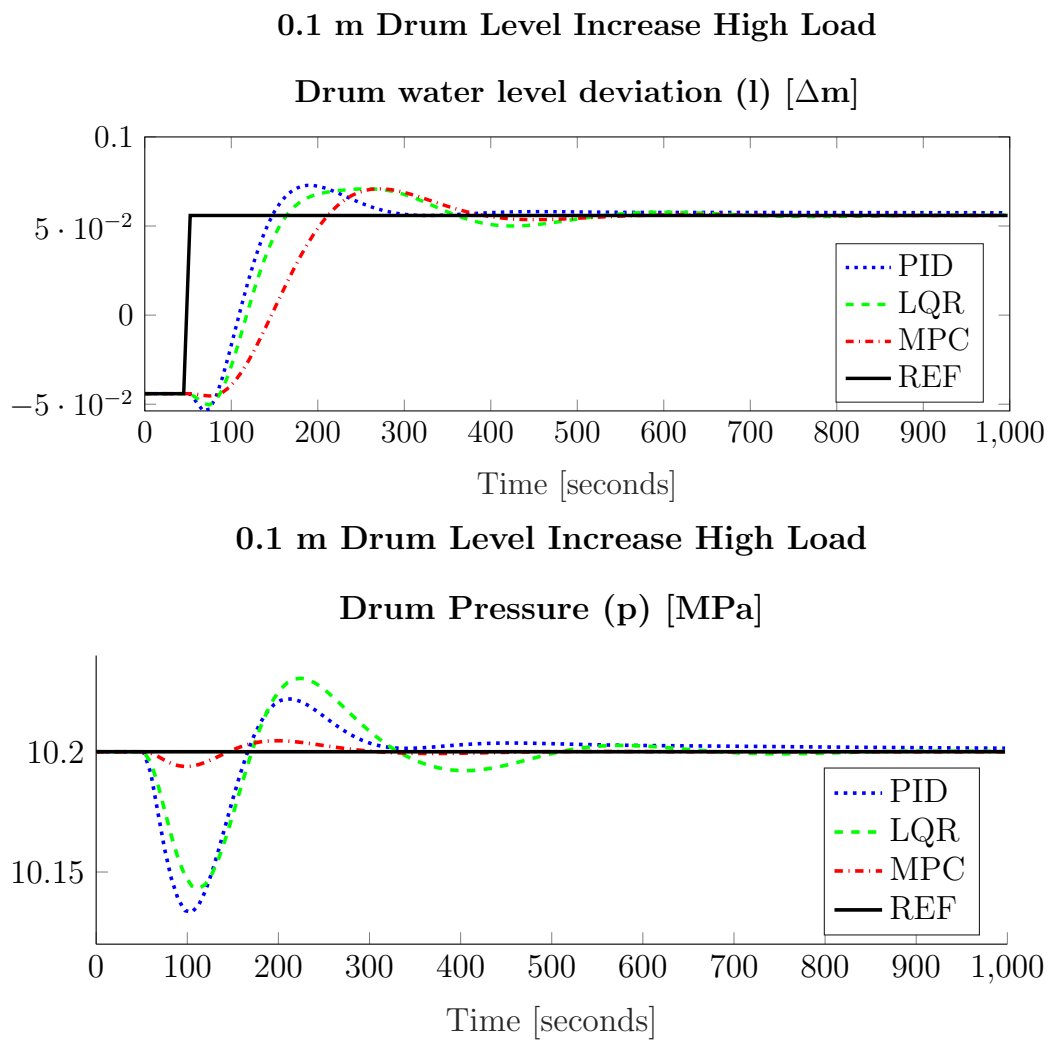


Figure 7.1: Controlled Variables Response to Drum Level step of 0.1 at High Load

			Low	Medium	High	Average
Level	Percent Overshoot	PID	26.89 %	21.76 %	15.68 %	21.45 %
Level	Percent Overshoot	LQR	43.74 %	23.75 %	14.97 %	27.49 %
Level	Percent Overshoot	MPC	26.9 %	20.23 %	14.99 %	20.71 %
Level	Settling Time	PID	580 s	520 s	450.5 s	516.8 s
Level	Settling Time	LQR	632.5 s	595.5 s	450 s	559.3 s
Level	Settling Time	MPC	669.5 s	492 s	433 s	531.5 s
Pressure	Disturbance Rejection Energy	PID	0.1864	0.3724	0.5285	0.3624
Pressure	Disturbance Rejection Energy	LQR	0.3215	0.4458	0.4857	0.4177
Pressure	Disturbance Rejection Energy	MPC	0.01159	0.007251	0.006173	0.008339

Table 7.1: Controller Performance Parameters: Level Step Increase

Figure 7.1 shows the response of drum pressure and drum level to a drum level step. This is the same data found in Figures 4.1, 5.3, and 6.1 (green dashed line for high load in each), however in Figure 7.1 the absolute values are compared instead of the change from initial conditions. Additional figures were added to the appendix to show the difference between the controllers at different loads. Figure B.1 shows the low load comparison and Figure B.9 shows the medium load. Table 7.1 shows the performance characteristics of these simulations as defined in Chapter 2.4. It can be seen that using these tuning parameters, the design goal is achieved.

Graphically in Figure 7.1 it can be seen that drum pressure is controlled to a much finer degree with the MPC controller than the others during a level step increase. Both MPC and LQR offer the advantage of a quickly dissipated transience response, while the PID takes a long time to return to set point. The drum level deviation graph shows that the PID response is the most aggressive, with desired short term response, but it takes a considerable amount of time to reach set point compared to the other controllers, but it is not a steady state error.

Numerically in Table 7.1 it can be seen that while drum level is controlled to the specified design parameters, the energy shown by drum pressure to reject disturbances varies by controller. Energy in this sense is an indirect measurement of signal transients, with lower energy being a signal with less deviation. The MPC controller out performs both LQR and MPC in this sense.

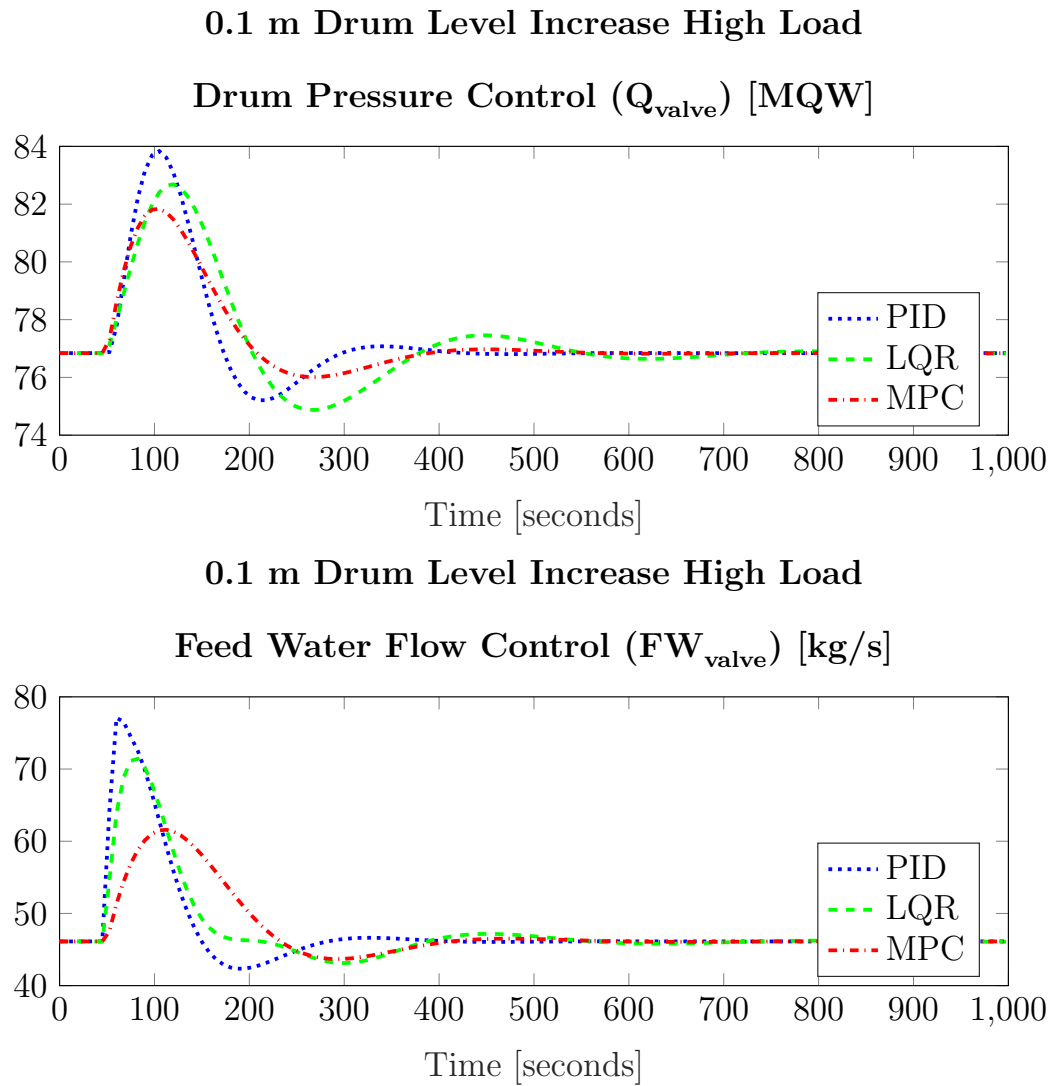


Figure 7.2: Controller Input Response to Drum Level step of 0.1 at High Load

	Controller	Low Load	Medium Load	High Load	Average
Q_{valve}	PID	1958	3893	5512	3787
Q_{valve}	LQR	1900	4315	5503	3906
Q_{valve}	MPC	1698	2821	3573	2697
FW_{valve}	PID	1.1e+5	9.546e+4	8.089e+4	9.545e+4
FW_{valve}	LQR	1.546e+05	9.241e+04	6.373e+04	1.036e+05
FW_{valve}	MPC	5.75e+04	4.827e+04	4.047e+04	4.874e+04

Table 7.2: Controller Input Performance Parameters: Level Step Increase

Figure 7.2 shows the controller inputs for the simulations shown in Figure 7.1. This is the same data found in Figures 4.2, 5.4, and 6.2 (green dashed line for high load in each), however in Figure 7.2 the absolute values are compared instead of the change from initial conditions. Additional figures were added to the appendix to show the difference between the controllers at different loads. Figure B.2 shows the low load comparison and Figure B.10 shows the medium load. Table 7.1.1 shows the performance characteristics of these simulations as defined in Chapter 2.4.

It should be noted the MPC controller uses less energy than either PID or LQR across all load levels, and that the MPC controller reacts less drastically than the other controllers.

7.1.2 Level Step Decrease Figures

The step command for this set of simulations is was calculated as follows:

$$r_1 = r_0 + \Delta r_{command} \quad \Delta r_{command} = \begin{bmatrix} \Delta l_{ref} \\ \Delta p_{ref} \end{bmatrix} = \begin{bmatrix} -0.1 \\ 0.0 \end{bmatrix}$$

$$r_1 = \begin{cases} & = \textit{High units} \\ l_{ref0} & = -0.151 \quad \Delta m \\ p_{ref0} & = 10.2 \quad MPa \end{cases}$$

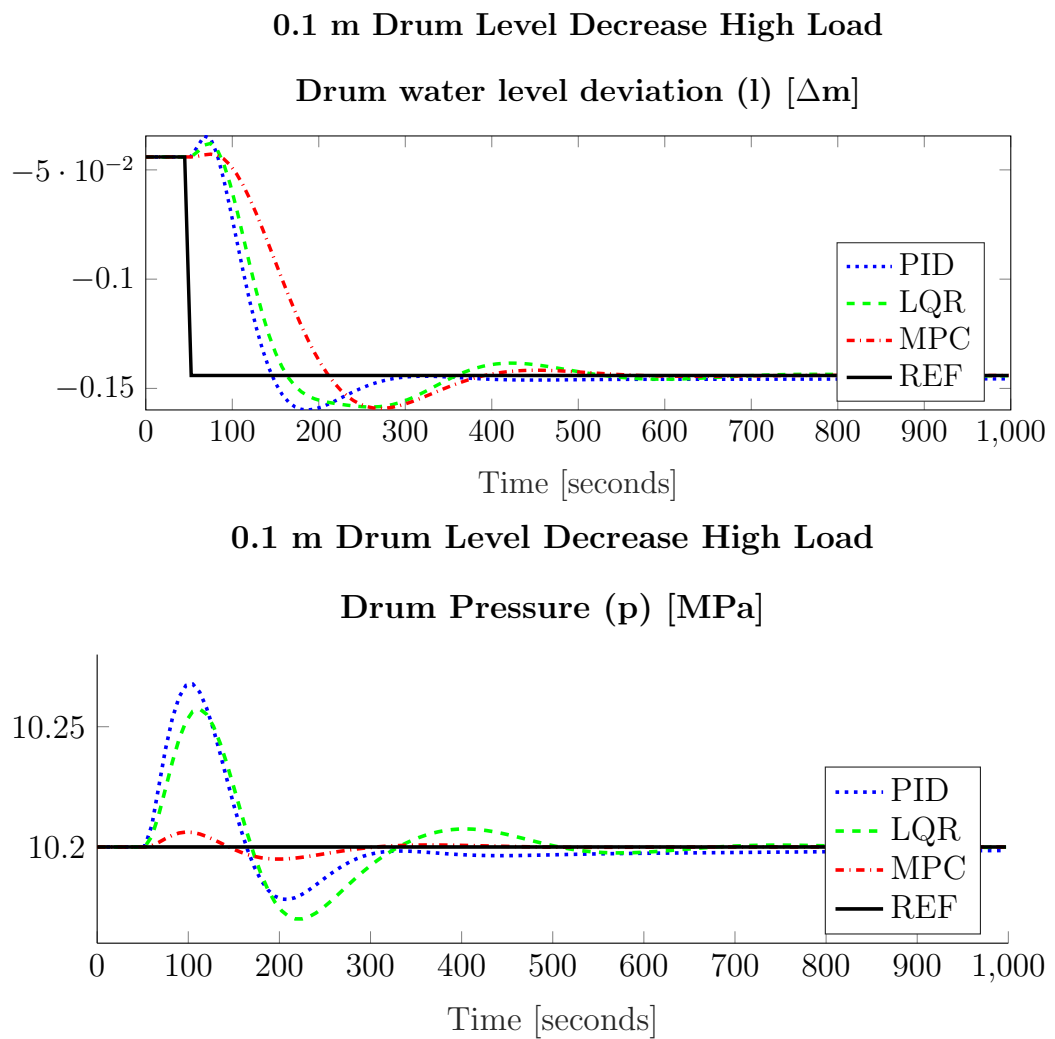


Figure 7.3: Controlled Variables Response to Drum Level step of -0.1 at High Load

			Low	Medium	High	Average
Level	Percent Overshoot	PID	26.96 %	20.99 %	14.5 %	20.82 %
Level	Percent Overshoot	LQR	44.94 %	23.42 %	14.43 %	27.6 %
Level	Percent Overshoot	MPC	26.9 %	20.32 %	15.08 %	20.77 %
Level	Settling Time	PID	565.5 s	508.5 s	436.5 s	503.5 s
Level	Settling Time	LQR	627.5 s	582.5 s	447 s	552.3 s
Level	Settling Time	MPC	671.5 s	492.5 s	434 s	532.7 s
Pressure	Disturbance Rejection Energy	PID	0.1909	0.3756	0.5292	0.3652
Pressure	Disturbance Rejection Energy	LQR	0.3299	0.4419	0.4779	0.4165
Pressure	Disturbance Rejection Energy	MPC	0.01262	0.008445	0.006847	0.009303

Table 7.3: Controller Performance Parameters: Level Step Decrease

Figure 7.3 shows the response of drum pressure and drum level to a drum level step. This is the same data found in Figures 4.4, 5.5, and 6.3 (green dashed line for high load in each), however in Figure 7.3 the absolute values are compared instead of the change from initial conditions. Additional figures were added to the appendix to show the difference between the controllers at different loads. Figure B.3 shows the low load comparison and Figure B.11 shows the medium load.

Figure 7.3 shows near identical performance to Figure 7.1, which is a set of simulations run with a step of the same magnitude in the opposite direction. Aside from the near symmetrical response for an increase and decrease in level steps, no new information can be seen from this set of figures, or the associated control inputs. Similarly, Table 7.3 shows near identical performance to Table 7.1, and no new information can be gained based off of these trends.

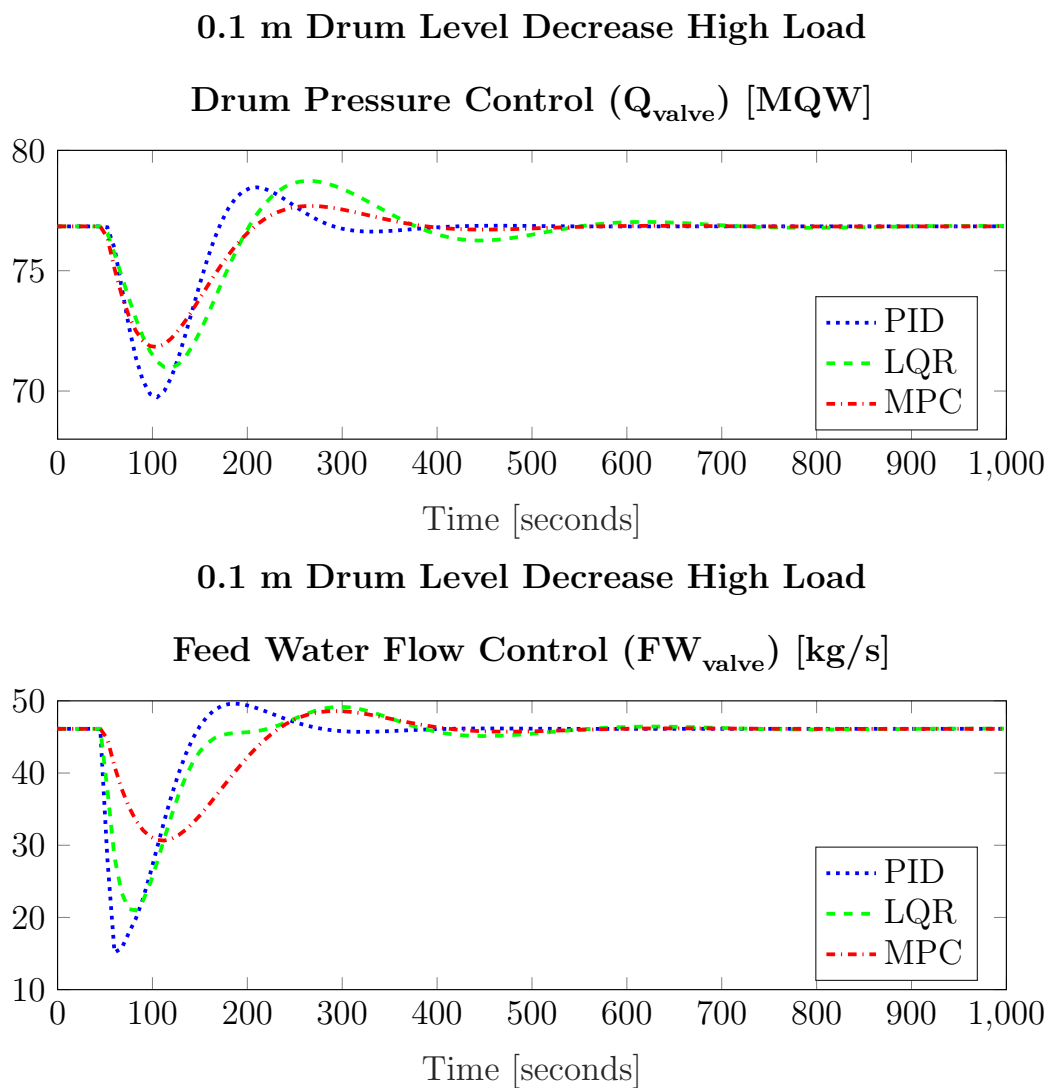


Figure 7.4: Controller Input Response to Drum Level step of -0.1 at High Load

Figure 7.4 shows the controller inputs for the simulations shown in Figure 7.3. This is the same data found in Figures 4.5, 5.6, and 6.4 (green dashed line for high load in each), however in Figure 7.4 the absolute values are compared instead of the change from initial conditions. Additional figures were added to the appendix to show the difference between the controllers at different loads. Figure B.4 shows the low load comparison and Figure B.12 shows the medium load.

	Controller	Low Load	Medium Load	High Load	Average
Q_{valve}	PID	2003	3924	5517	3815
Q_{valve}	LQR	1951	4274	5416	3880
Q_{valve}	MPC	1778	2877	3603	2753
FW_{valve}	PID	1.094e+5	9.41e+4	7.955e+4	9.436e+4
FW_{valve}	LQR	1.534e+05	9.026e+04	6.248e+04	1.02e+05
FW_{valve}	MPC	5.753e+04	4.845e+04	4.059e+04	4.886e+04

Table 7.4: Controller Input Performance Parameters: Pressure Step Decrease

As stated previously with Figure 7.3 and Table 7.3, Figure 7.4 and Table 7.1.2 shows near identical performance to Figure 7.2 and Table 7.1.1 no new information can be gained based off of these trends.

7.1.3 Pressure Step Increase Figures

The step command for this set of simulations is was calculated as follows:

$$r_1 = r_0 + \Delta r_{command} \quad \Delta r_{command} = \begin{bmatrix} \Delta l_{ref} \\ \Delta p_{ref} \end{bmatrix} = \begin{bmatrix} 0 \\ 0.1 \end{bmatrix}$$

$$r_1 = \begin{cases} & \text{High units} \\ l_{ref0} & = -0.051 \quad \Delta m \\ p_{ref0} & = 10.3 \quad MPa \end{cases}$$

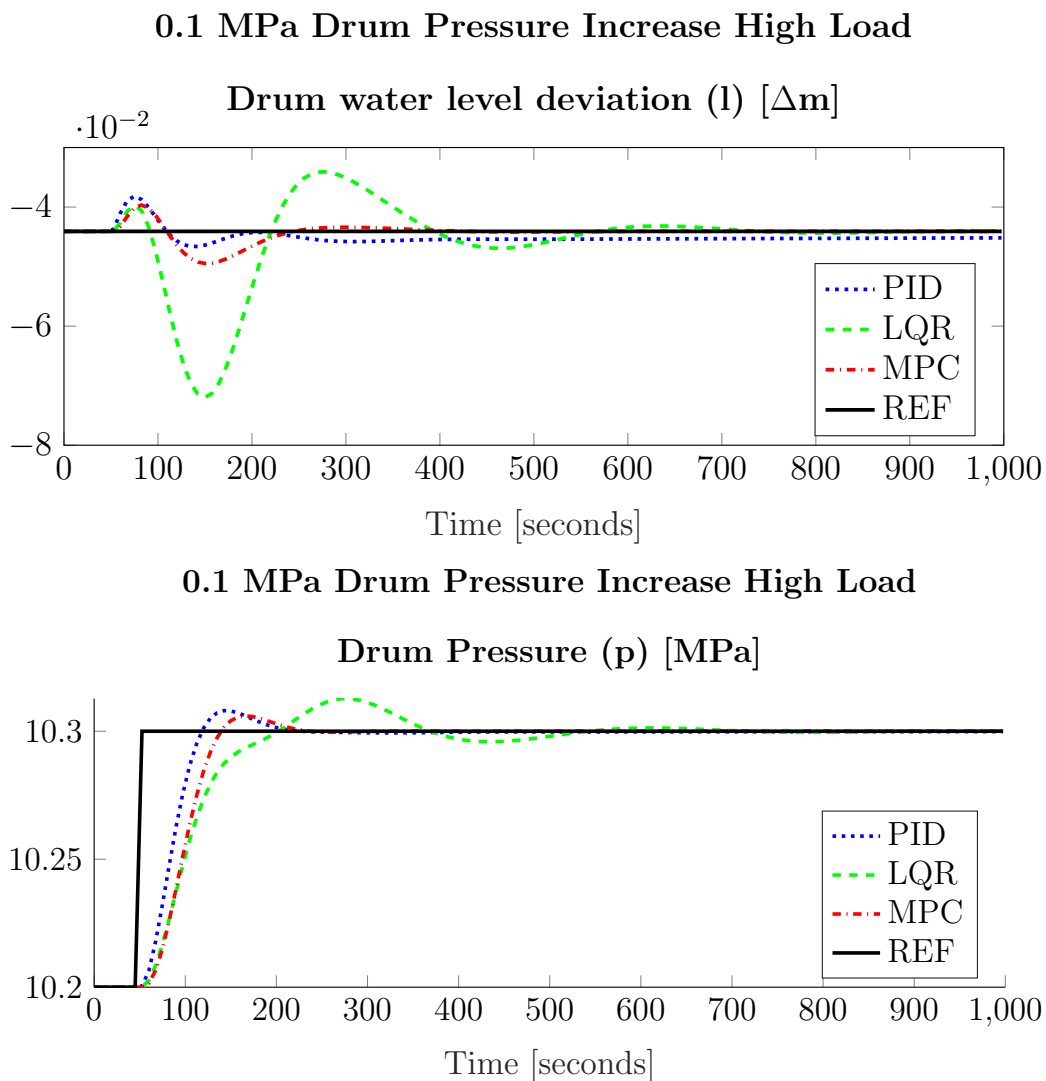


Figure 7.5: Controlled Variables Response to Drum Pressure step of 0.1 at High Load

	Controller	Low Load	Medium Load	High Load	Average
Percent Overshoot	PID	3.275 %	4.437 %	8.151 %	5.288 %
Percent Overshoot	LQR	16.47 %	15.77 %	12.76 %	15 %
Percent Overshoot	MPC	5.837 %	5.93 %	5.977 %	5.915 %
Settling Time	PID	244 s	173 s	143.5 s	186.8 s
Settling Time	LQR	619 s	599 s	450.5 s	556.2 s
Settling Time	MPC	186 s	170 s	158 s	171.3 s
Disturbance Rejection Energy	PID	0.01878	0.007735	0.005868	0.01079
Disturbance Rejection Energy	LQR	0.5229	0.2108	0.1089	0.2809
Disturbance Rejection Energy	MPC	0.009109	0.00566	0.004351	0.006373

Table 7.5: Controller Performance Parameters: Pressure Step Increase

Figure 7.5 shows the response of drum pressure and drum level to a drum pressure step at high load. This is the same data found in Figures 4.7, 5.7, and 6.5 (green dashed line for high load in each), however in Figure 7.5 the absolute values are compared instead of the change from initial conditions. Additional figures were added to the appendix to show the difference between the controllers at different loads. Figure B.5 shows the low load comparison and Figure B.13 shows the medium load. Table 7.5 shows the performance characteristics of these simulations as defined in Chapter 2.4.

From both Figure 7.5 and Table 7.5 show that the MPC controller offer the best performance, having the lowest values on the table for all performance characteristics. The PID response has a nonzero error after a reasonable amount of time, and while tuning would be able to remove this it would not be able to meet the design criterion. The LQR response does not perform as well as the MPC or PID, but it does not have that error component. The LQR design may be improved upon with more tuning of the Q and R matrices, however since overshoot and settling time do not correlate directly to the weighting matrices and a set of weighting matrices were found that met the design criterion, no further tuning is necessary.

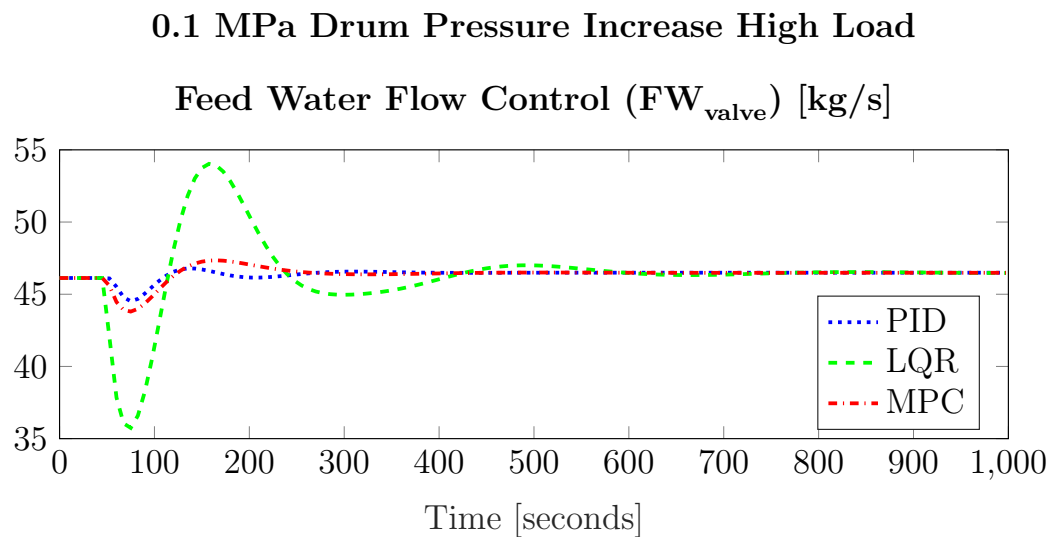
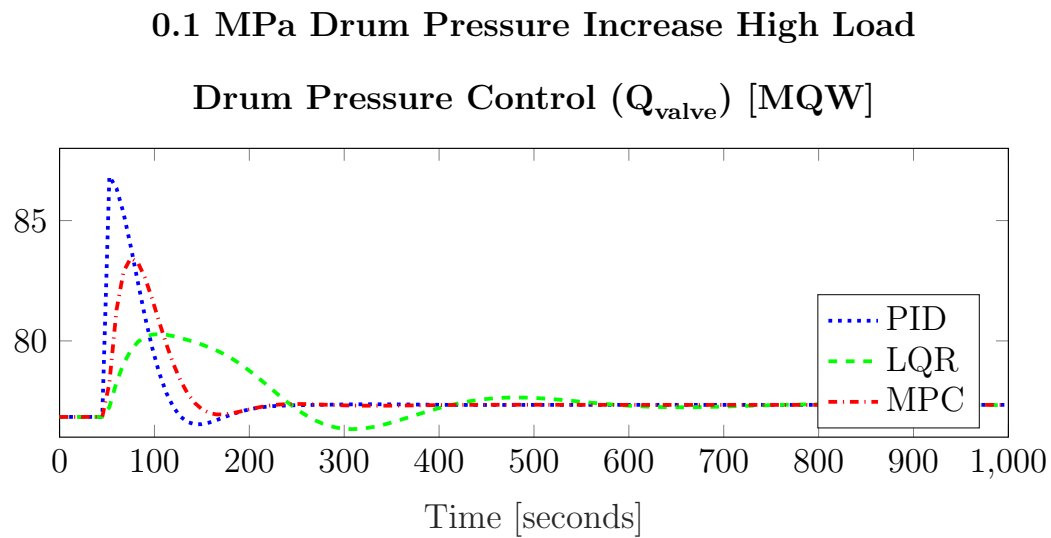


Figure 7.6: Controller Input Response to Drum Pressure step of 0.1 at High Load

	Controller	Low Load	Medium Load	High Load	Average
Q_{valve}	PID	8006	6800	5959	6922
Q_{valve}	LQR	7114	4666	3203	4995
Q_{valve}	MPC	7296	5441	4158	5631
FW_{valve}	PID	1416	648.9	504.8	856.7
FW_{valve}	LQR	6.975e+04	2.83e+04	1.501e+04	3.769e+04
FW_{valve}	MPC	544.8	774.4	879.5	732.9

Table 7.6: Controller Input Performance Parameters: Pressure Step Increase

Figure 7.6 shows the controller inputs for the simulations shown in Figure 7.5. This is the same data found in Figures 4.8, 5.8, and 6.6 (green dashed line for high load in each), however in Figure 7.6 the absolute values are compared instead of the change from initial conditions. Additional figures were added to the appendix to show the difference between the controllers at different loads. Figure B.6 shows the low load comparison and Figure B.14 shows the medium load.

It should be noted that the PID feed water energy is lower than the MPC feed water energy. The LQR controller does not behave similarly and may not be directly compared, however the design criterion was met so this is an acceptable LQR controller.

7.1.4 Pressure Step Decrease Figures

The step command for this set of simulations is was calculated as follows:

$$r_1 = r_0 + \Delta r_{command} \quad \Delta r_{command} = \begin{bmatrix} \Delta l_{ref} \\ \Delta p_{ref} \end{bmatrix} = \begin{bmatrix} 0 \\ -0.1 \end{bmatrix}$$

$$r_1 = \begin{cases} & \textit{High units} \\ l_{ref0} & = -0.051 \quad \Delta m \\ p_{ref0} & = 10.1 \quad MPa \end{cases}$$

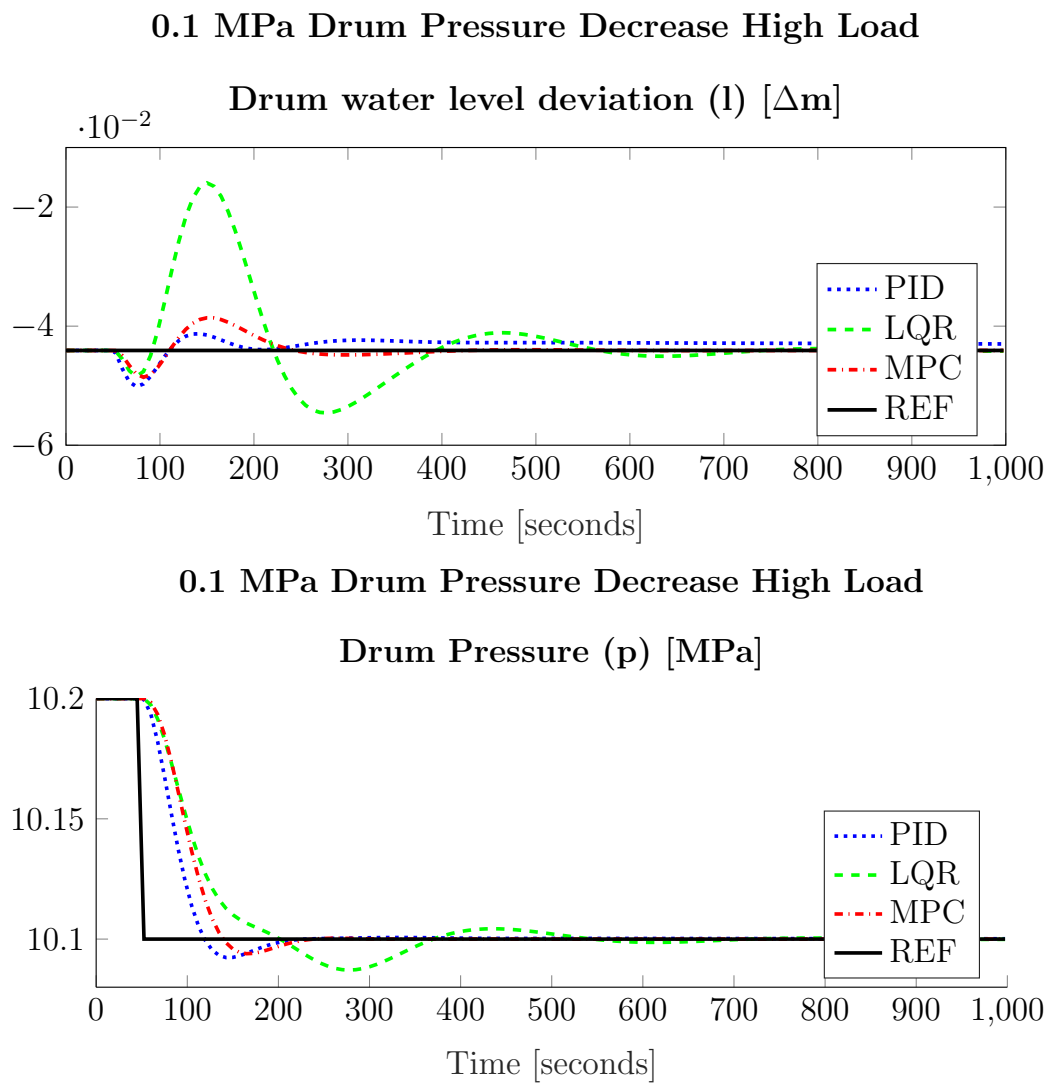


Figure 7.7: Controlled Variables Response to Drum Pressure step of -0.1 at High Load

	Controller	Low Load	Medium Load	High Load	Average
Percent Overshoot	PID	3.005 %	4.106 %	7.811 %	4.974 %
Percent Overshoot	LQR	15.6 %	15.76 %	12.88 %	14.75 %
Percent Overshoot	MPC	5.993 %	6.051 %	6.087 %	6.044 %
Settling Time	PID	246 s	169 s	143.5 s	186.2 s
Settling Time	LQR	621 s	605 s	453 s	559.7 s
Settling Time	MPC	189 s	172 s	159.5 s	173.5 s
Disturbance Rejection Energy	PID	0.01949	0.008199	0.006146	0.01128
Disturbance Rejection Energy	LQR	0.5669	0.2222	0.1127	0.3006
Disturbance Rejection Energy	MPC	0.009546	0.00586	0.004503	0.006636

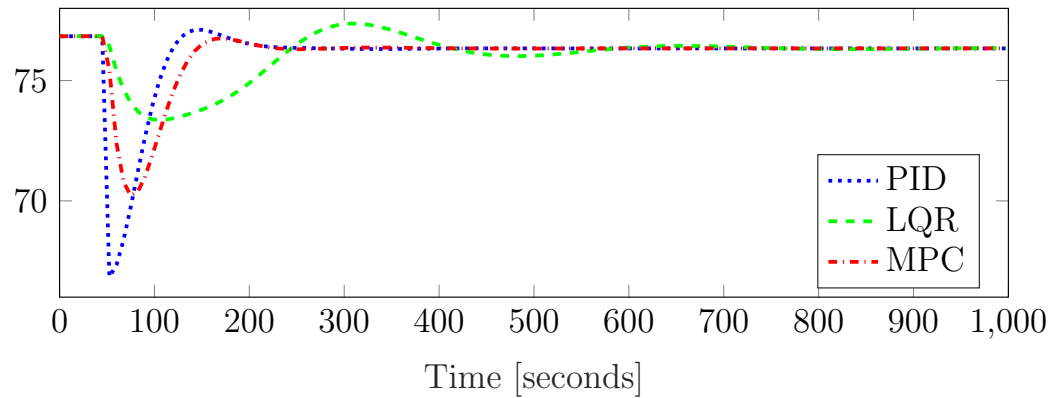
Table 7.7: Controller Performance Parameters: Pressure Step Decrease

Figure 7.7 shows the response of drum pressure and drum level to a drum pressure step at high load. This is the same data found in Figures 4.10, 5.9, and 6.7 (green dashed line for high load in each), however in Figure 7.7 the absolute values are compared instead of the change from initial conditions. Additional figures were added to the appendix to show the difference between the controllers at different loads. Figure B.7 shows the low load comparison and Figure B.15 shows the medium load.

Figure 7.7 shows similar simulations to Figure 7.5, the various simulations have similar initial conditions and controllers, however the step command applied is of opposite magnitude. What can be seen is near identical performance. Minor variations are expected due to the nonlinear nature of the system, and how at a lower load the shrink/swell effect is more pronounced, however these are negligible at this level of graphical zoom. Little new information can be seen from this step graph that could not be seen in previously.

0.1 MPa Drum Pressure Decrease High Load

Drum Pressure Control (Q_{valve}) [MQW]



0.1 MPa Drum Pressure Decrease High Load

Feed Water Flow Control (FW_{valve}) [kg/s]

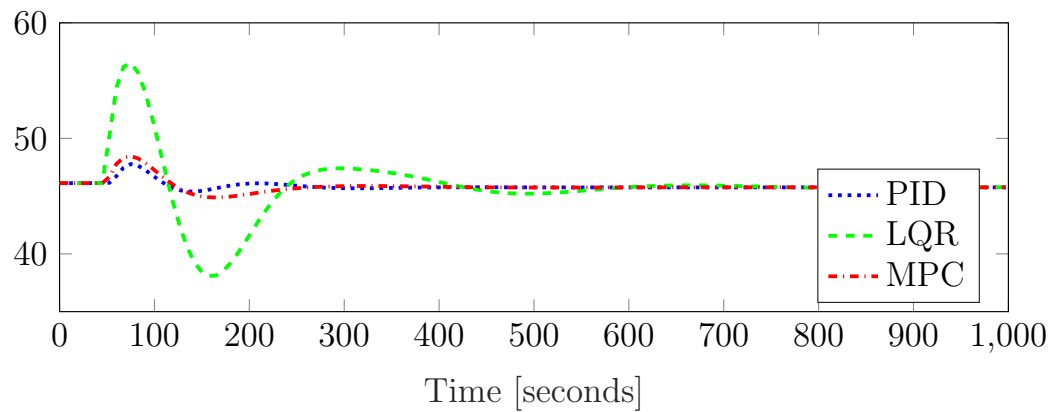


Figure 7.8: Controller Input Response to Drum Pressure step of -0.1 at High Load

	Controller	Low Load	Medium Load	High Load	Average
Q_{valve}	PID	8057	6836	5984	6959
Q_{valve}	LQR	7307	4788	3278	5124
Q_{valve}	MPC	7449	5540	4227	5739
FW_{valve}	PID	1464	680.8	524.2	889.8
FW_{valve}	LQR	7.581e+04	2.962e+04	1.544e+04	4.029e+04
FW_{valve}	MPC	550.2	778.5	889.1	739.3

Table 7.8: Controller Input Performance Parameters: Pressure Step Decrease

Figure 7.8 shows the controller inputs for the simulations shown in Figure 7.7. This is the same data found in Figures 4.11, 5.10, and 6.8 (green dashed line for high load in each), however in Figure 7.8 the absolute values are compared instead of the change from initial conditions. Additional figures were added to the appendix to show the difference between the controllers at different loads. Figure B.8 shows the low load comparison and Figure B.16 shows the medium load. Little new information can be seen from this step graph that could not be seen in previously.

7.2 Controller Performance

The following tables, Table 7.9-7.12, shows the controller performance as a result of the step functions. Percent overshoot, Settling Time, and Signal Energy are all listed below. Each of these values were shown with their proper figure in the previous section. The averages of the different load cases was also included.

			Low Load		Medium Load		High Load		Average	
Step		Con	Inc	Dec	Inc	Dec	Inc	Dec	Inc	Dec
Level Step	Level	PID	26.89	26.96	21.76	20.99	15.68	14.5	21.45	20.82
Level Step	Level	LQR	43.74	44.94	23.75	23.42	14.97	14.43	27.49	27.6
Level Step	Level	MPC	26.9	26.9	20.23	20.32	14.99	15.08	20.71	20.77
Pressure Step	Pressure	PID	3.275	3.005	4.437	4.106	8.151	7.811	5.288	4.974
Pressure Step	Pressure	LQR	16.47	15.6	15.77	15.76	12.76	12.88	15	14.75
Pressure Step	Pressure	MPC	5.837	5.993	5.93	6.051	5.977	6.087	5.915	6.044

Table 7.9: MPC Controller Percent Overshoot

			Low Load		Medium Load		High Load		Average	
Step		Con	Inc	Dec	Inc	Dec	Inc	Dec	Inc	Dec
Level Step	Level	PID	580	565.5	520	508.5	450.5	436.5	516.8	503.5
Level Step	Level	LQR	632.5	627.5	595.5	582.5	450	447	559.3	552.3
Level Step	Level	MPC	669.5	671.5	492	492.5	433	434	531.5	532.7
Pressure Step	Pressure	PID	244	246	173	169	143.5	143.5	186.8	186.2
Pressure Step	Pressure	LQR	619	621	599	605	450.5	453	556.2	559.7
Pressure Step	Pressure	MPC	186	189	170	172	158	159.5	171.3	173.5

Table 7.10: MPC Controller Settling Time

It should be noted that as load increases percent overshoot increases for both level and pressure. Settling time improves for the pressure steps but performance degrades as load increases for level steps. The controllers designed to meet criterion of a level step also perform well under a pressure step, however both LQR and PID have drawbacks to their responses.

Signal energy for the other signals was included to show which controller has the best disturbance rejection and which controller uses less control energy or effort. For all table entries, the lower the value is the better the system performance.

			Low Load		Medium Load		High Load	
Step		Ctrlr	Inc	Dec	Inc	Dec	Inc	Dec
Level	Pressure	PID	0.1864	0.1909	0.3724	0.3756	0.5285	0.5292
Level	Pressure	LQR	0.3215	0.3299	0.4458	0.4419	0.4857	0.4779
Level	Pressure	MPC	0.01159	0.01262	0.007251	0.008445	0.006173	0.006847
Level	Level	PID	1.623	1.614	1.402	1.381	1.181	1.161
Level	Level	LQR	1.865	1.874	1.54	1.522	1.338	1.32
Level	Level	MPC	2.314	2.305	1.986	1.976	1.733	1.724
Pressure	Pressure	PID	0.01878	0.01949	0.007735	0.008199	0.005868	0.006146
Pressure	Pressure	LQR	0.5229	0.5669	0.2108	0.2222	0.1089	0.1127
Pressure	Pressure	MPC	0.009109	0.009546	0.00566	0.00586	0.004351	0.004503
Pressure	Level	PID	0.6238	0.6257	0.5483	0.5495	0.4979	0.4986
Pressure	Level	LQR	1.023	1.032	0.8732	0.8795	0.7804	0.7845
Pressure	Level	MPC	0.8489	0.8503	0.7793	0.7804	0.7247	0.7256

Table 7.11: Controlled Variable Energy

It should be noted that the signal energy for pressure during a level step change increases for PID and LQR but decreases for MPC. For a pressure step, the signal energy of the level deviation decreases as load increases.

Lower signal energy as defined for controlled variables (2.26) directly correlates to smaller transient responses in a controller. It should be noted that the PID signal has the lowest energy for the level controlled variable during a level step at high load. While it meets the design parameters with the smallest transients, the PID responses for the coupled controller makes this a less than desirable choice.

			Low Load		Medium Load		High Load	
Step		Ctrlr	Inc	Dec	Inc	Dec	Inc	Dec
Level	Q_{valve}	PID	1958	2003	3893	3924	5512	5517
Level	Q_{valve}	LQR	1900	1951	4315	4274	5503	5416
Level	Q_{valve}	MPC	1698	1778	2821	2877	3573	3603
Level	FW_{valve}	PID	1.1e+5	1.094e+5	9.546e+4	9.41e+4	8.089e+4	7.955e+4
Level	FW_{valve}	LQR	1.546e+05	1.534e+05	9.241e+04	9.026e+04	6.373e+04	6.248e+04
Level	FW_{valve}	MPC	5.75e+04	5.753e+04	4.827e+04	4.845e+04	4.047e+04	4.059e+04
Pressure	Q_{valve}	PID	8006	8057	6800	6836	5959	5984
Pressure	Q_{valve}	LQR	7114	7307	4666	4788	3203	3278
Pressure	Q_{valve}	MPC	7296	7449	5441	5540	4158	4227
Pressure	FW_{valve}	PID	1416	1464	648.9	680.8	504.8	524.2
Pressure	FW_{valve}	LQR	6.975e+04	7.581e+04	2.83e+04	2.962e+04	1.501e+04	1.544e+04
Pressure	FW_{valve}	MPC	544.8	550.2	774.4	778.5	879.5	889.1

Table 7.12: Controller Inputs Energy

Controller input energy can be seen as usually much high for PID responses,

however the LQR controller during a pressure step produces some outlying numbers. This is due to the design parameters and how the LQR controller was tuned.

As defined the signal energy for controller inputs (2.27) defines the controller effort being used, and a system with optimal control will use the least amount of control effort. It should be noted that in almost all cases the MPC controller uses less control energy to stabilize the system after a reference step.

Step		Ctrlr	Low Load		Medium Load		High Load	
			Inc	Dec	Inc	Dec	Inc	Dec
Level	V_{wt}	PID	1.598e+4	1.594e+4	1.58e+4	1.576e+4	1.564e+4	1.561e+4
Level	V_{wt}	LQR	1.562e+04	1.557e+04	1.536e+04	1.532e+04	1.517e+04	1.515e+04
Level	V_{wt}	MPC	1.498e+04	1.498e+04	1.484e+04	1.484e+04	1.474e+04	1.474e+04
Level	p	PID	0.1864	0.1909	0.3724	0.3756	0.5285	0.5292
Level	p	LQR	0.3215	0.3299	0.4458	0.4419	0.4857	0.4779
Level	p	MPC	0.01159	0.01262	0.007251	0.008445	0.006173	0.006847
Level	α_r	PID	0.0002076	0.000215	0.0004804	0.0004939	0.0008013	0.0008225
Level	α_r	LQR	0.000213	0.000224	0.0005359	0.0005436	0.0008706	0.0008789
Level	α_r	MPC	0.000237	0.0002481	0.0005121	0.0005283	0.0008241	0.000845
Level	V_{sd}	PID	503.9	498.1	393.2	381.1	275.1	264.6
Level	V_{sd}	LQR	660.2	664.7	398	384	241.5	232
Level	V_{sd}	MPC	358.1	357.6	263	263.2	179.1	179.1
Level	Q	PID	1698	1726	3272	3274	4488	4458
Level	Q	LQR	1714	1750	3813	3762	4815	4728
Level	Q	MPC	1541	1610	2508	2557	3126	3153
Level	q_f	PID	1.068e+5	1.062e+5	9.221e+4	9.085e+4	7.767e+4	7.632e+4
Level	q_f	LQR	1.517e+05	1.505e+05	9.045e+04	8.831e+04	6.222e+04	6.098e+04
Level	q_f	MPC	5.716e+04	5.719e+04	4.792e+04	4.81e+04	4.014e+04	4.027e+04
Pressure	V_{wt}	PID	6.382	6.526	0.76	0.7595	0.2998	0.2845
Pressure	V_{wt}	LQR	243.9	263.7	106.4	111	60.48	62.07
Pressure	V_{wt}	MPC	5.64	6.424	2.365	2.497	1.785	1.829
Pressure	p	PID	27.89	27.88	28.04	28.03	28.2	28.19
Pressure	p	LQR	28.14	28.15	28.02	28.02	27.95	27.95
Pressure	p	MPC	27.76	27.77	27.87	27.87	27.95	27.95
Pressure	α_r	PID	0.001432	0.001415	0.001741	0.001719	0.002175	0.002143
Pressure	α_r	LQR	0.001657	0.001645	0.001898	0.001881	0.002274	0.002247
Pressure	α_r	MPC	0.001426	0.001416	0.001706	0.001689	0.002111	0.002084
Pressure	V_{sd}	PID	31.54	32.48	7.076	7.27	1.803	1.829
Pressure	V_{sd}	LQR	364.5	404	121	130.7	49.07	51.9
Pressure	V_{sd}	MPC	22.82	25.39	5.346	5.901	1.908	2.072
Pressure	Q	PID	6110	6164	4895	4935	4035	4065
Pressure	Q	LQR	6587	6763	4338	4451	2981	3051
Pressure	Q	MPC	6069	6212	4433	4523	3319	3381
Pressure	q_f	PID	1378	1425	631.6	662.6	493.9	512.7
Pressure	q_f	LQR	6.842e+04	7.44e+04	2.759e+04	2.89e+04	1.453e+04	1.496e+04
Pressure	q_f	MPC	539.1	544	760.7	764.5	859.7	869.1

Table 7.13: Controller State Variables Energy

The Controller state variables energies are of interest, as they show an account of several things. If a state deviates slightly from its initial condition at the start of a simulation the energy will be low, and if it deviates a significant amount the energy will be high. This can be seen in the following: for a level step V_{wt} (a partial analog for drum level) has three orders of magnitude more than a pressure step. Conversely for a pressure step p has two orders of magnitude more energy than a level step. Other Controller state variables energies are easy to understand: Q and q_f are similar to Q_{valve} and FW_{valve} , but this is due to the linear approximations used in (3.12). States α_r and V_{sd} vary only across steps, but do not appear to vary across loads or controllers. It should be noted that pressure (p) is on both Table 7.11 and Table 7.13 however they are defined differently, once being compared to the reference and one being compared to the initial conditions.

CHAPTER 8

CONCLUSIONS

8.1 Summary of Results

Industrial boiler systems are used worldwide, however most use basic control schemes even though the system is highly nonlinear and complex. The nonlinearities come into play from the Shrink/Swell effect which causes the variables most desired to be controlled to initially go in the opposite direction of how they will eventually stabilize. In this research a model was tested, expanded upon, and used to test three different types of controllers showcasing each ones limitations.

The advantage of using Three Element Control is that it is an extension of classical control schemes where every signal used is directly measurable or controllable. It is easy to troubleshoot this style of controller in an industrial setting. The PID controller was tuned using trial and error to meet the design criterion, but was not able to offer acceptable performance when a different control variable was stepped. The design criterion may be able to be reduced to allow for better performance of the entire system. Three element control is a proven method to control boiler level and works in conjunction with a (PID) pressure controller in many industrial settings.

The Linear Quadratic Regulator is well known in research, but it's application in nonlinear systems in industry is lacking. The LQR controller

was designed and tuned by varying diagonal elements in its weighting matrices, placing more weight on the error signals than the other states, as well as placing more weight on heat flux than feed water flow. The design criterion were met however compared to the PID and MPC controllers, the performance of the controller when the opposite control variable being stepped was lacking. Alternative weighting may be able to more tightly control this variable, however it is still a valid controller based on the design criterion. Additionally, a LQR controller can have boundary conditions defined in the cost function that can change the dynamics of the controller. An example of a boundary condition would be control saturation, where feed water flow into the boiler could not go below zero or above maximum flow rate for the pump. It should be noted that as load increases the performance of the LQR controller improves for both controlled variables. A major drawback to this control method is that it uses full state feedback, which is not directly implementable. Several states in the model are not measurable, and to use in a control calculation an observer must be used.

Model Predictive Control theory has its roots in similar optimizations as LQR has, and as such MPC has some similar advantages and drawbacks. The MPC controller requires full state feedback or the use of an observer, but it can be made more robust with additional boundary conditions set into it's cost function. The MPC controller in this research was weighted to favor the states over the controls, but no weighting was introduced to weigh particular states over another. The control horizon and prediction horizon may not be the most optimal choices, and smaller horizon choices will improve processing time. The key feature of the MPC controller's is the linearization at each time step, which is what allowed this controller to perform optimally in all scenarios, and is what allowed for the nonlinearities to be controlled properly. This linearization could be limited to every other or every third sample to improve processing time at a cost to performance.

This research has shown through Figures 7.5-7.4 and Tables 7.9-7.12 that the nonlinear MPC control strategy drastically outperforms both the LQR

control strategy and the Three Element control strategy in all cases. Further tuning can be done to the PIDs and the LQR Q and R matrices, but due to how the nonlinear MPC is designed, it is unlikely that better results will be found. Both the LQR and MPC controllers were designed off of a model, and knowing key performance parameters of the boiler itself is critical for these controllers to work. An observer must also be designed for industrial implementation. Both of these setbacks are not the case in the three element controller, however the performance gains shown here make the nonlinear MPC a valid path to start designing towards.

8.2 Further Research

Further research can be done on implementing a full state or partial state observer. The design of an observer is a separate task from the design of a controller, [17] which is not a trivial task and is why it was out of the scope of this research. The role of an observer is to ensure the error between the estimated and the actual state variables are minimized. An observer is necessary for the LQR and MPC controllers designed as they were designed as full state feedback controllers. If the states are not available, the estimated states are suggested to be used for control. The Three Element Control methodology does not require an observer because it was designed around using measurable signals.

Control saturation should be introduced into the model, it was seen in several examples that the simulation assumed that feed water flow could go negative. In a physical system feed water flow is controlled by a valve that will be considered a certain percentage open. In this model FW_{valve} was designed as the flow demand of the valve after a command was given. Scaling and saturation to not allow the FW_{valve} signal to stay between 0-100% would give a more realistic approach. If input saturation is introduced, an anti-windup function should be introduced on the cascaded Three Element controller. Input saturation can also be introduced into the cost functions of the MPC and LQR

as seen in [17] 3.8.

A more complex model of the input heat transfer system can be created. This model takes thermal energy as an input, however this is not a measurable or directly controllable quantity. The thermal energy model will vary based on the method used to heat the boiler, from natural gas to geothermal the energy input will be different based on the application. A more complex model for feed water can also be implemented, however a first order system may be sufficient for a pump and valve combination. The steam valve model from [13] can also be expanded upon to include a turbine/generator combination.

A Simulink model can also be built to show the system; how the states and inputs flow, which will make it easier to add the previously suggested research. All simulations were done in MatLab and the code itself is not as visually intuitive as a Simulink model can be.

REFERENCES

- [1] Robert Allen Feng Zheng, Zhu Jimao. Design of continuous and discrete lqi control systems with stable inner loops. *Journal of Shanghai Jiaotong University*, E-12 No.6:787–792, 2007.
- [2] Jingwen Huang Jia Wang Hao Zang, Hongguang Li. A composite model predictive control strategy for furnaces. *Chinese Journal of Chemical Engineering*, 22.7:788–794, July 2014.
- [3] Chris Hardy. Process control integration blog: Three element drum level control.
- [4] Magnus Holmgren. X steam for matlab, 2006-01-20.
- [5] Allen D. Houtz. Cascade, feed forward and three-element control.
- [6] Mihai Iacob. Re: Linkedin followup message to robert a. borzellieri, March 19, 2018.
- [7] Rodney D. Bell Karl Johan Åström. Drum-boiler dynamics. *TFRT*, 7577, 1998.
- [8] Spirax Sarco Limited. Learn about steam: The boiler house.
- [9] Jobert H. A.Ludlage Siep Weiland Paul M. J.Van den Hof M. Bahadr Saltk, Leyla zkan. Model predictive control in industry: Challenges and opportunities. *Journal of Process Control*, 61:77–102, January 2018.

- [10] The MathWorks. lqi linear-quadratic-integral control.
- [11] S.R.Nekoo M.H.Korayem. Finite-time state-dependent riccati equation for time-varying nonaffine systems: Rigid and flexible joint manipulator control. *ISA Transactions*, 54:125–144, January 2015.
- [12] Hamza Hamadah R. Bhushan Gopaluni Michael G. Forbes, Rohit S. Patwardhan. Model predictive control in industry: Challenges and opportunities. *IFAC-PapersOnLine*, 48.8:531–538, 2015.
- [13] Gheorghe-Daniel Andreescu Mihai Iacob. Drum-boiler control system employing shrink and swell effect remission in thermal power plants. *3rd International Congress on Ultra Modern Telecommunications and Control Systems and Workshops (ICUMT)*, 2011.
- [14] T.U. Bhatt P. Panwar, S. Mukhopadhyay and A.P. Tiwari. Design of decentralized pi and lqr controllers for level and pressure regulation of steam drum of advanced heavy water reactor. *Indian Control Conference (ICC)*, 2018.
- [15] B. Wayne Bequette Sambit Ghosh. A framework for the control room of the future: Human-in-the-loop mpc. *IFAC-PapersOnLine*, 51.34:252–257, 2019.
- [16] Marcelo Farenzena Luis Gustavo S. Longhi Antnio Carlos Zanin Herbert Campos G.Teixeira Ricardo Guilherme Duraiski Viviane Rodrigues Botelho, Jorge Otvio Trierweiler. Model assessment of mpcs with control ranges: An industrial application in a delayed coking unit. *Control Engineering Practice*, 84:261–273, March 2019.
- [17] Liuping Wang. *Model Predictive Control System Design and Implementation Using MATLAB*. Springer-Verlag London Limited, London, England, 2009.

- [18] Guoliang Wei Jianhua Wang Yan Song, Kaiqun Zhu. Distributed mpc-based adaptive control for linear systems with unknown parameters. *Journal of the Franklin Institute*, 356:2606–2624, March 2019.

APPENDIX A

ADDITIONAL INFORMATION FROM SOURCES

Åström-Bell Figures [7]

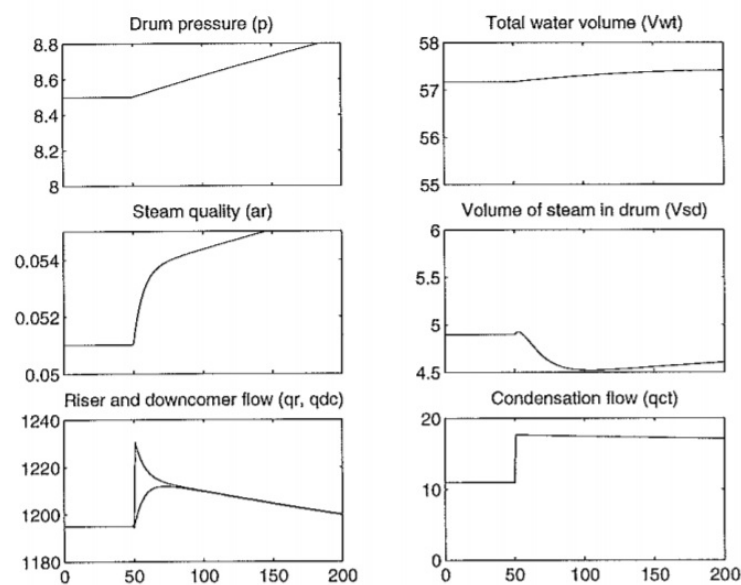


Figure 4 Responses to a step corresponding to 10 MW in fuel flow rate at medium load.

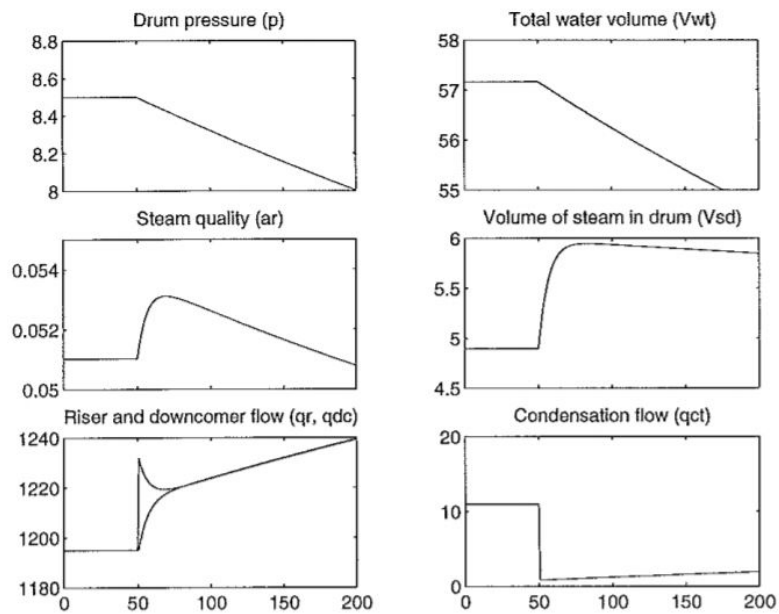


Figure 5 Responses to a step of 10 kg/s in steam flow rate at medium load.

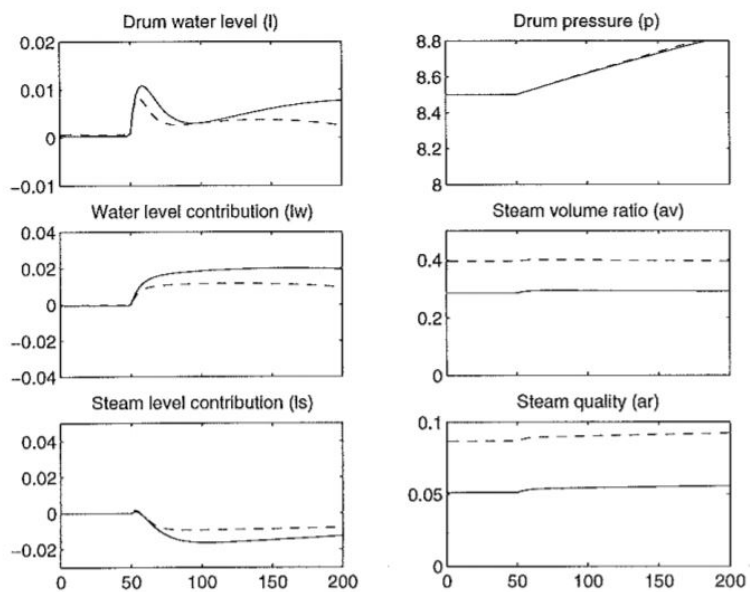


Figure 6 Responses to a step change corresponding to 10 MW in fuel flow rate at medium (solid) and high (dashed) loads.

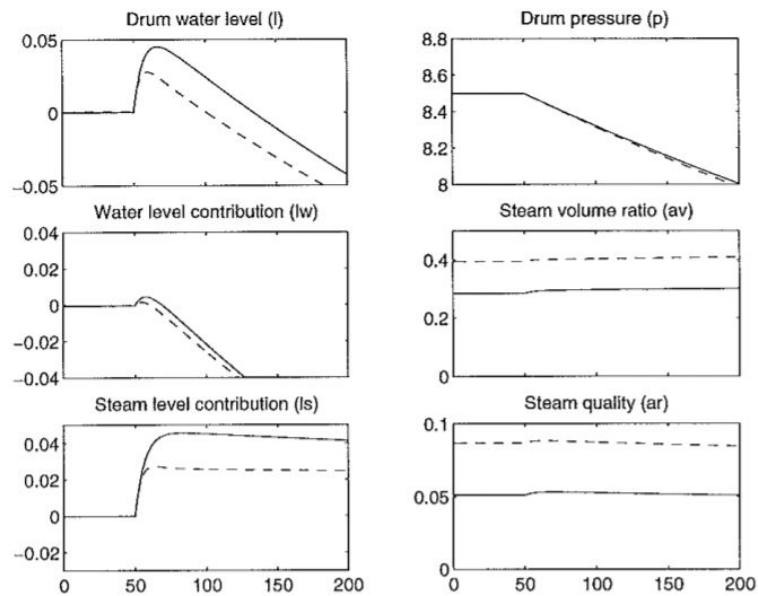


Figure 7 Responses to a step change of 10 kg/s in steam flow rate at medium (solid) and high (dashed) loads.

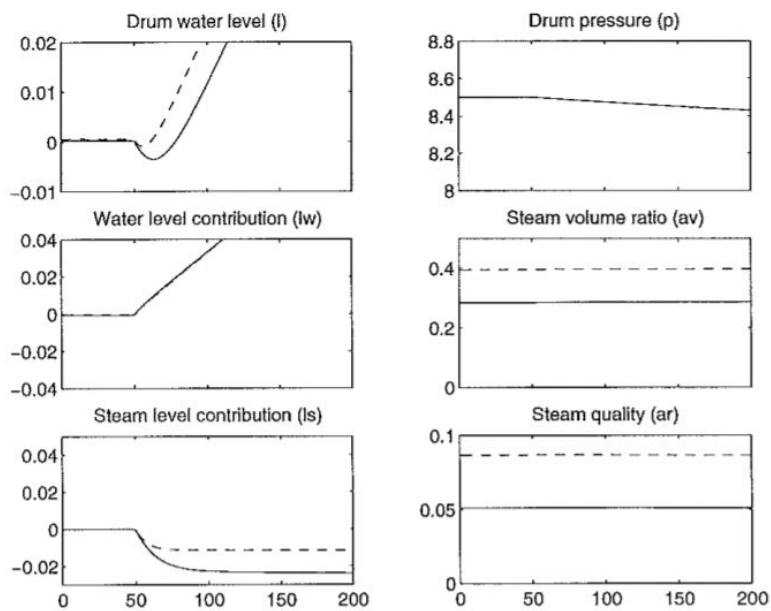


Figure 8 Responses to a step change of 10 kg/s in feedwater flow rate at medium (solid) and high (dashed) loads.

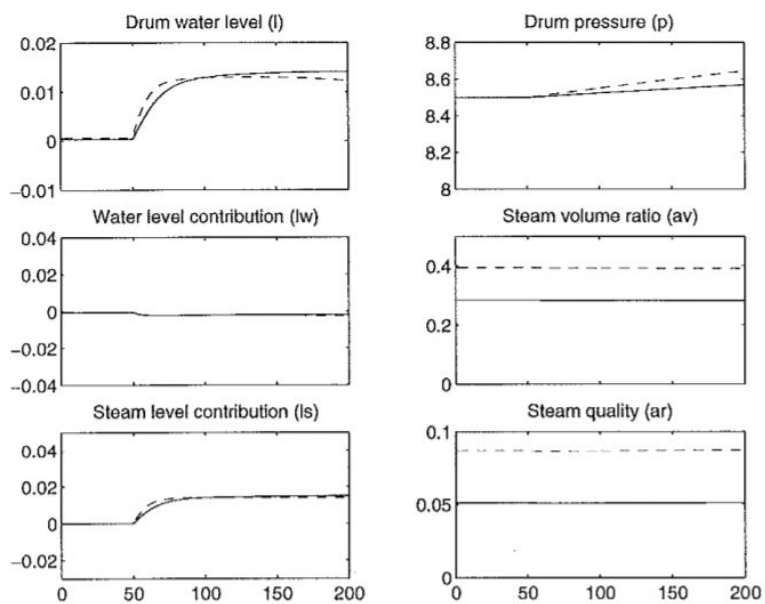


Figure 9 Responses to a step change of 10° C in feedwater temperature at medium (solid) and high (dashed) loads.

APPENDIX B

CONTROLLER

COMPARISON GRAPHICS

Low Load Figures

Low Load Level Step Increase Response

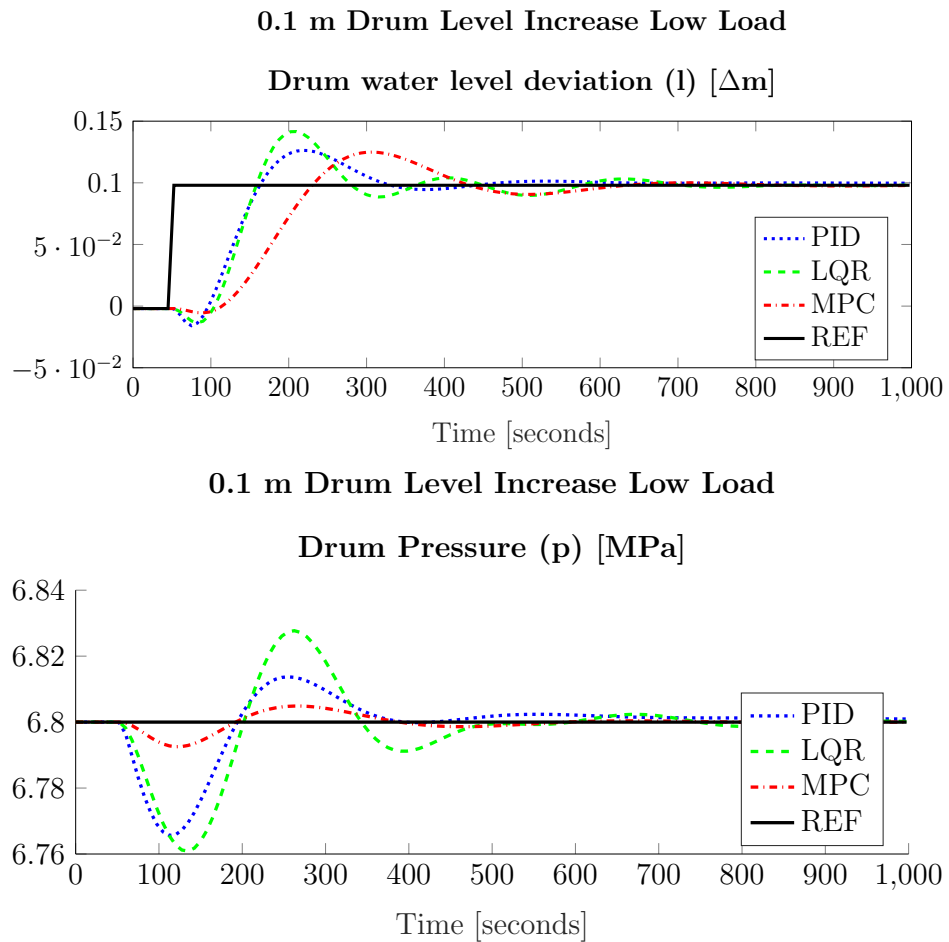


Figure B.1: Controlled Variables Response to Drum Level step of 0.1 at Low Load

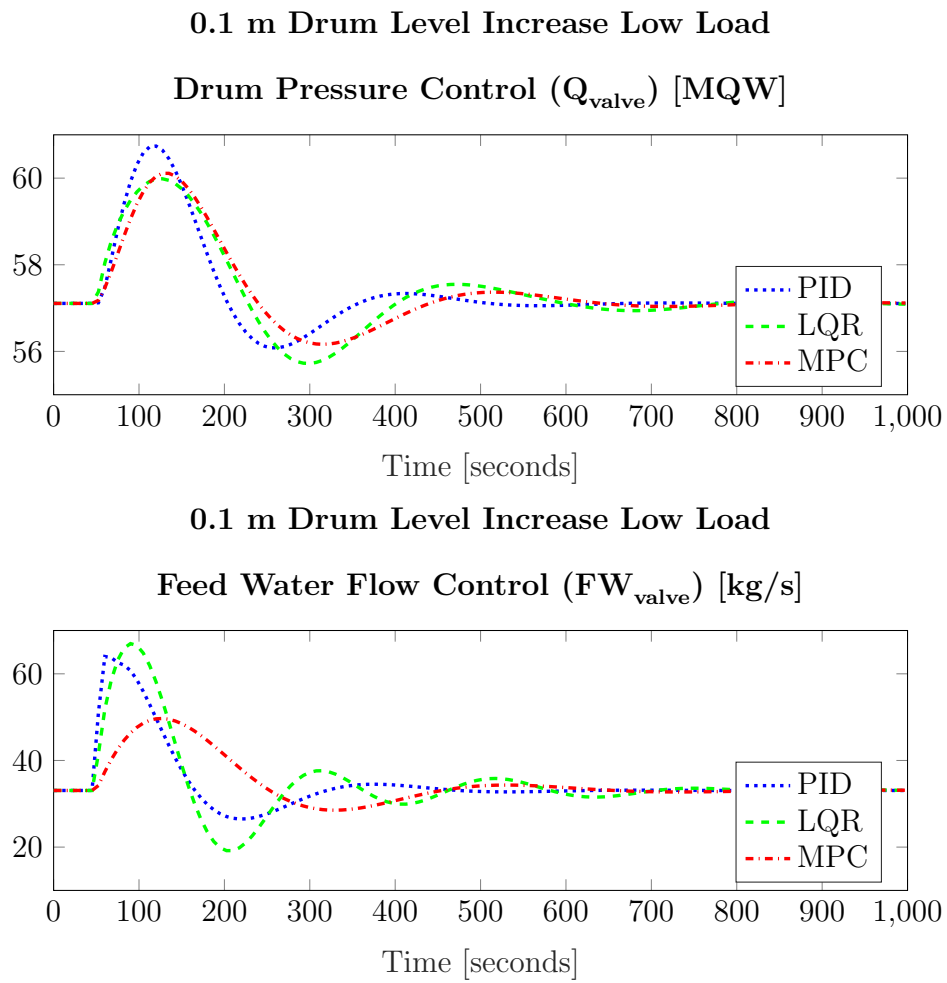


Figure B.2: Controller Input Response to Drum Level step of 0.1 at Low Load

Low Load Level Step Decrease Response

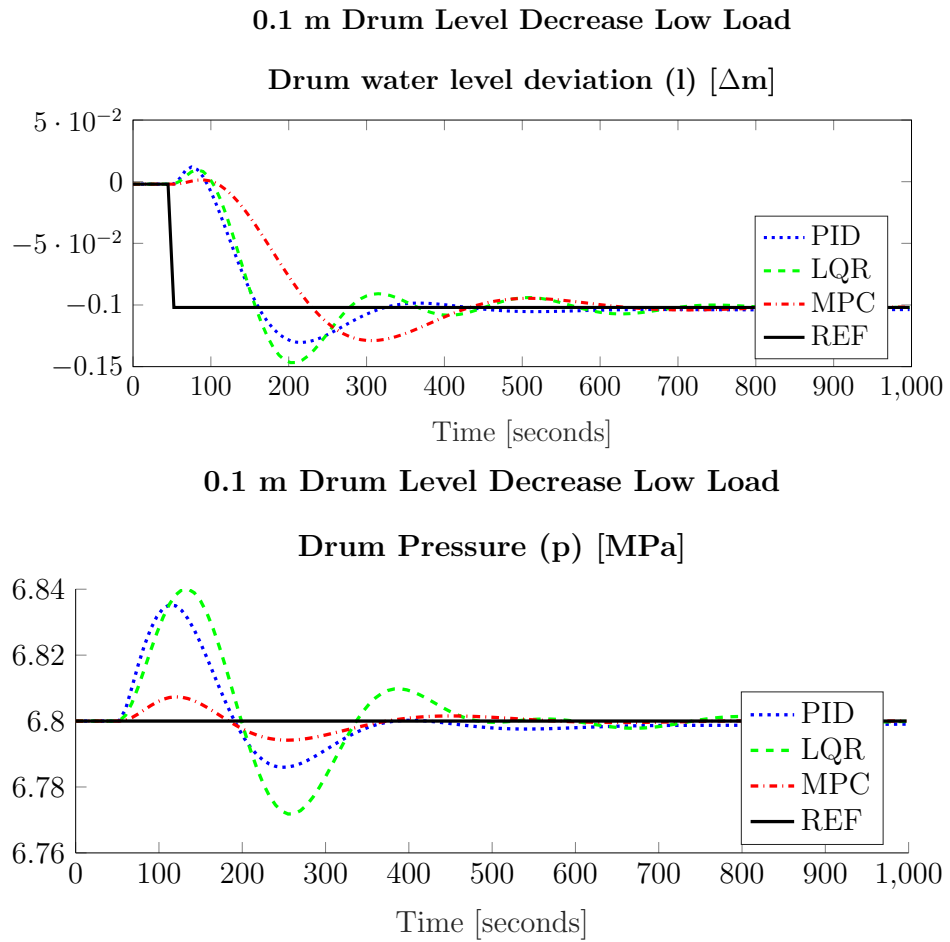


Figure B.3: Controlled Variables Response to Drum Level step of -0.1 at Low Load

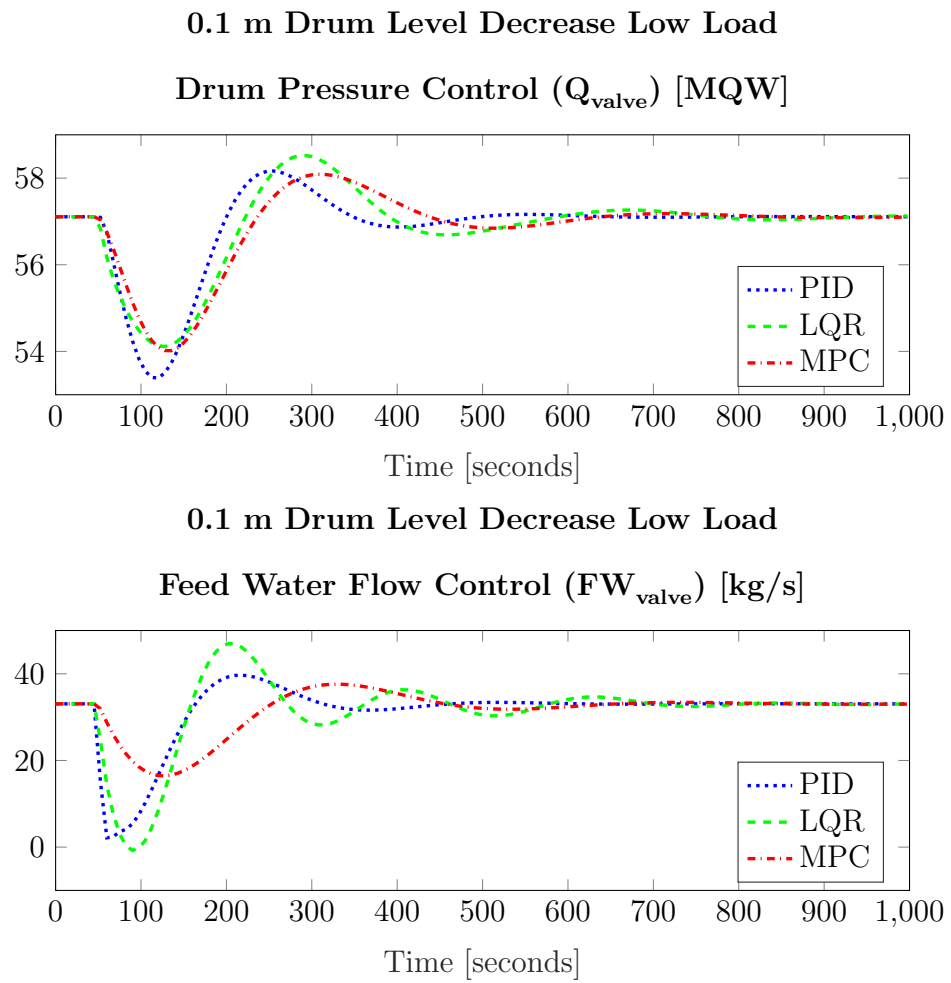


Figure B.4: Controller Input Response to Drum Level step of -0.1 at Low Load

Low Load Pressure Step Increase Response

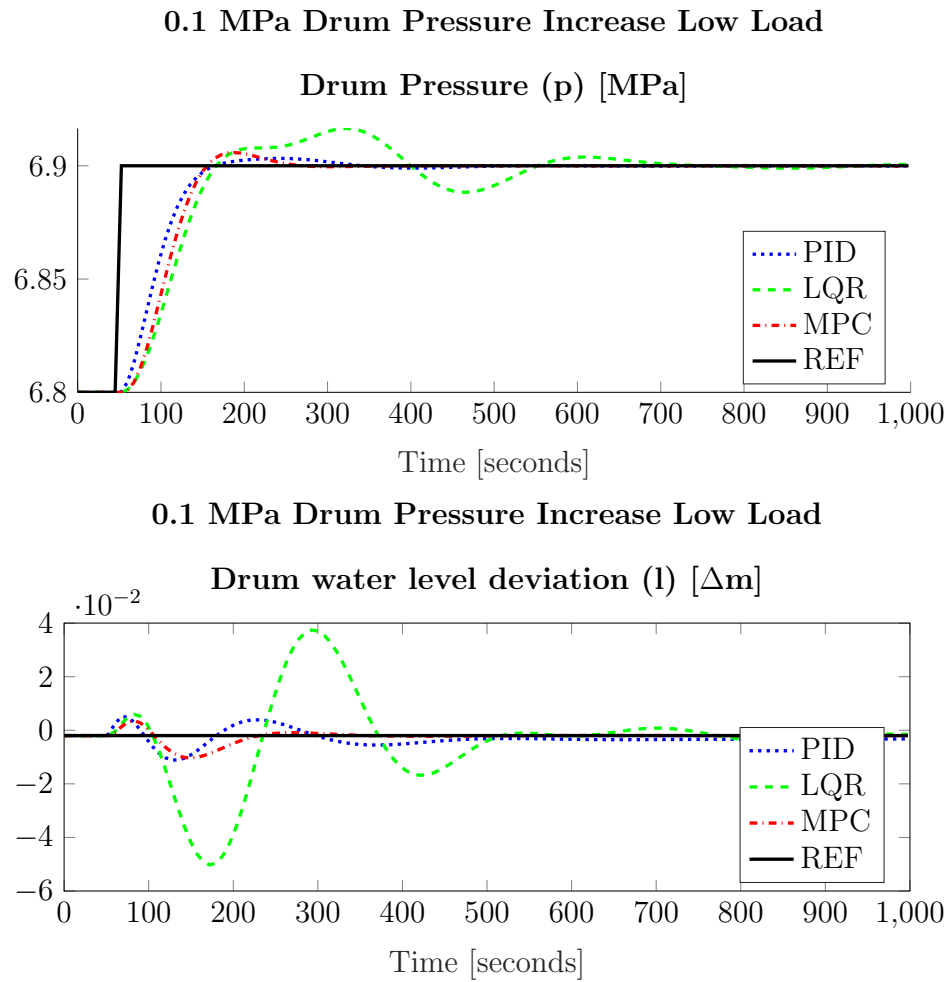


Figure B.5: Controlled Variables Response to Drum Pressure step of 0.1

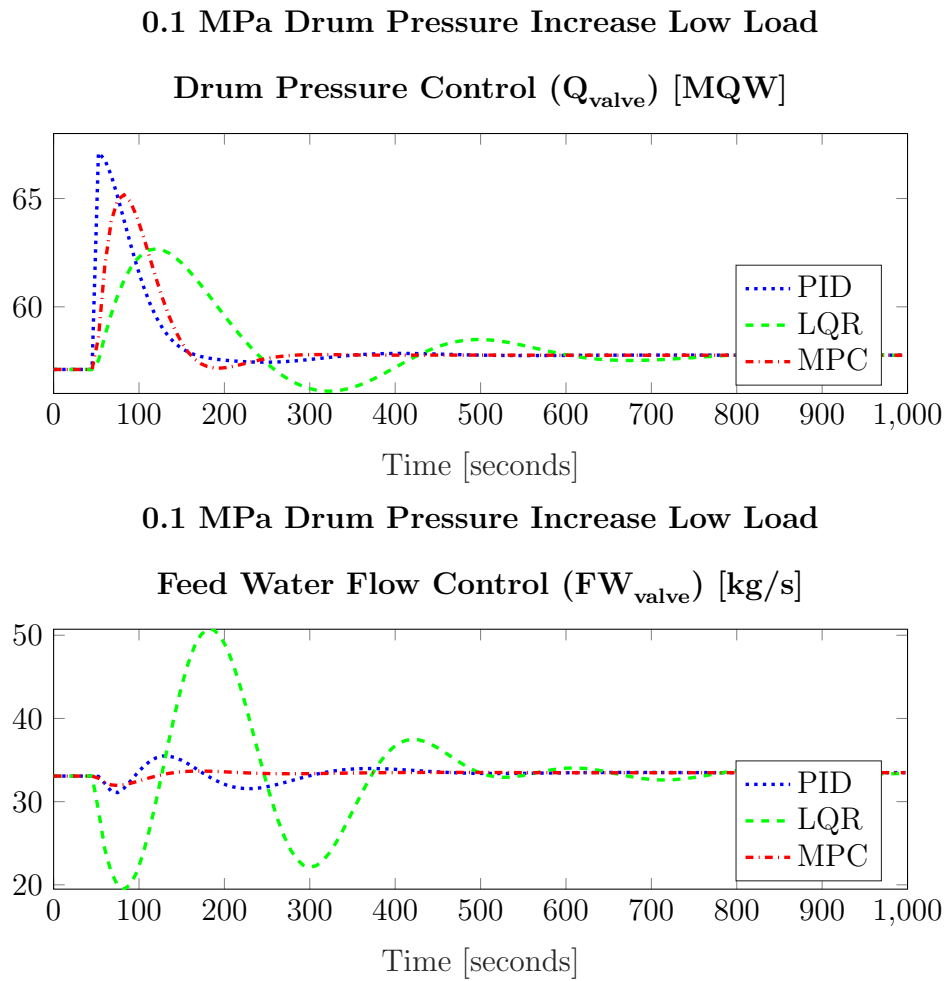


Figure B.6: Controller Input Response to Drum Pressure step of 0.1 at Low Load

Low Load Pressure Step Decrease Response

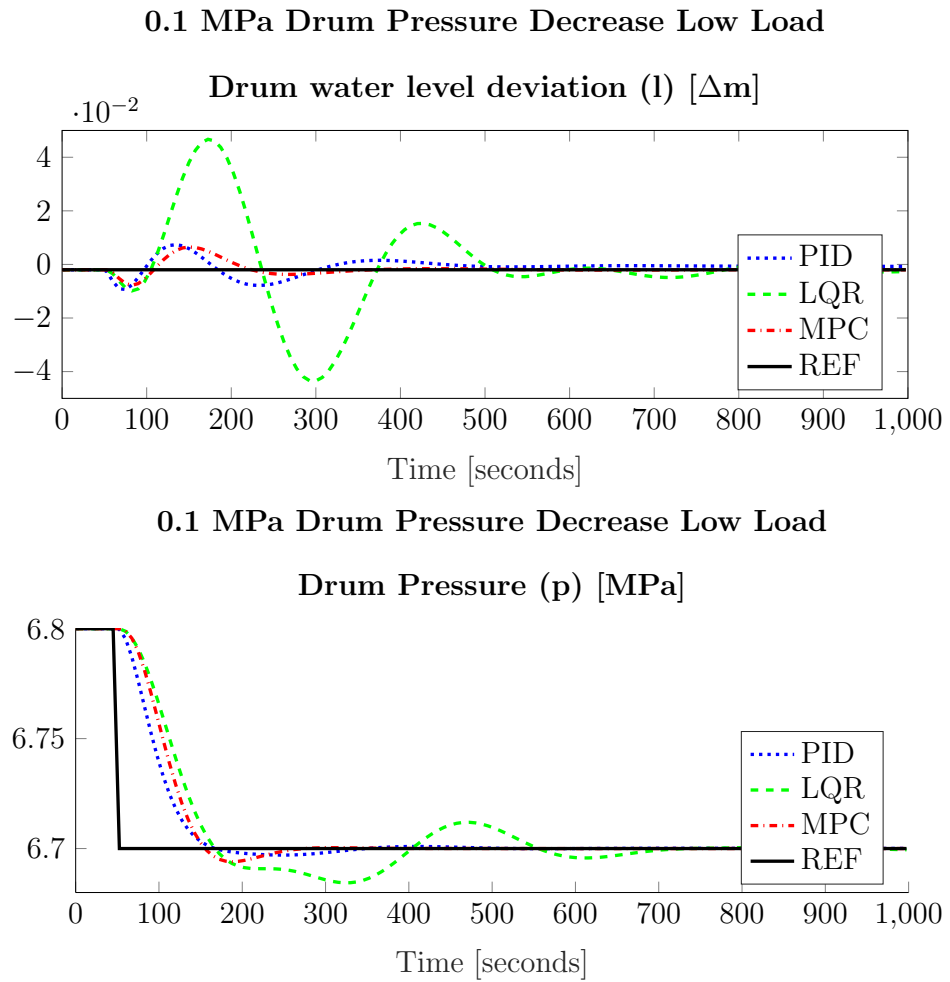


Figure B.7: Controlled Variables Response to Drum Pressure step of -0.1 at Low Load

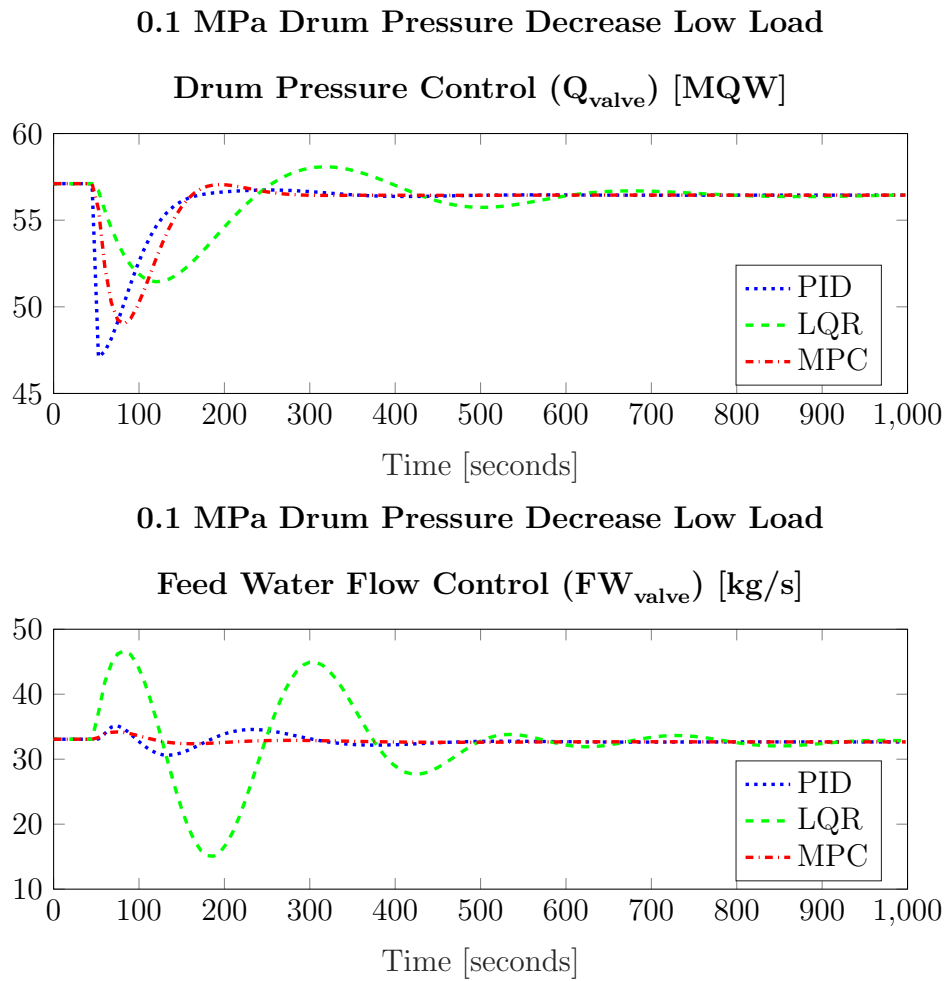


Figure B.8: Controller Input Response to Drum Pressure step of -0.1 at Low Load

Medium Load Figures

Medium Load Level Step Increase Response

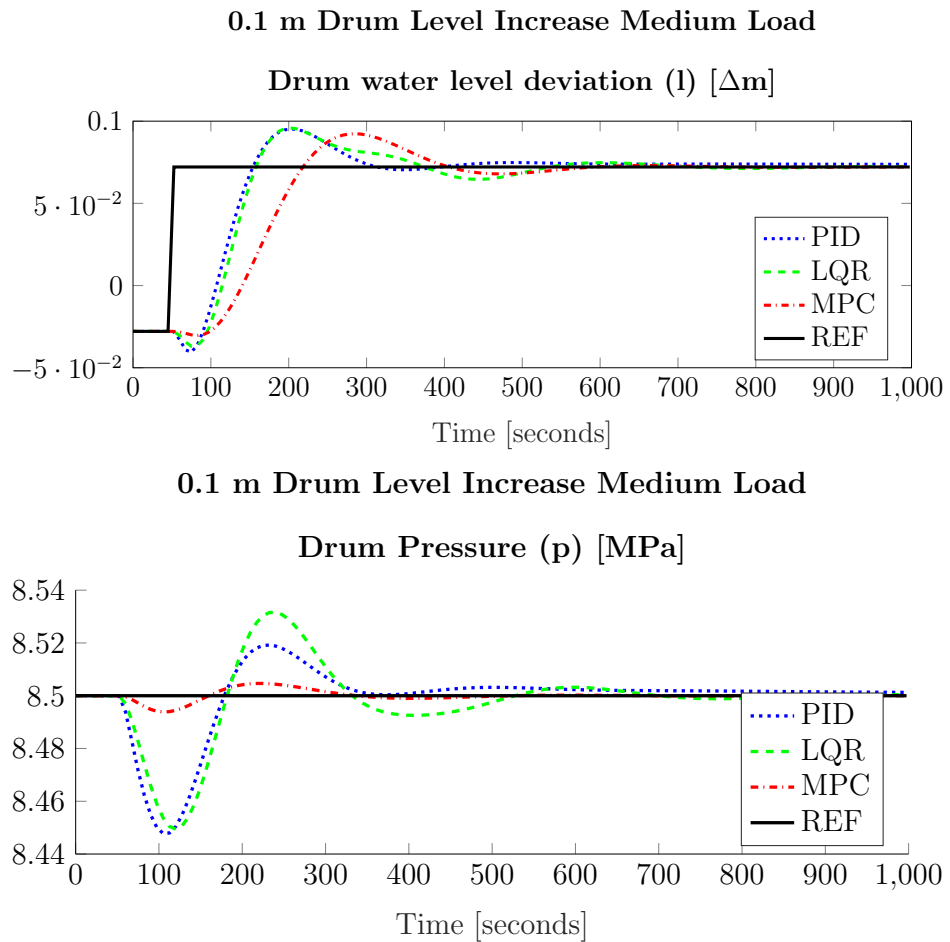


Figure B.9: Controlled Variables Response to Drum Level step of 0.1 at Medium Load

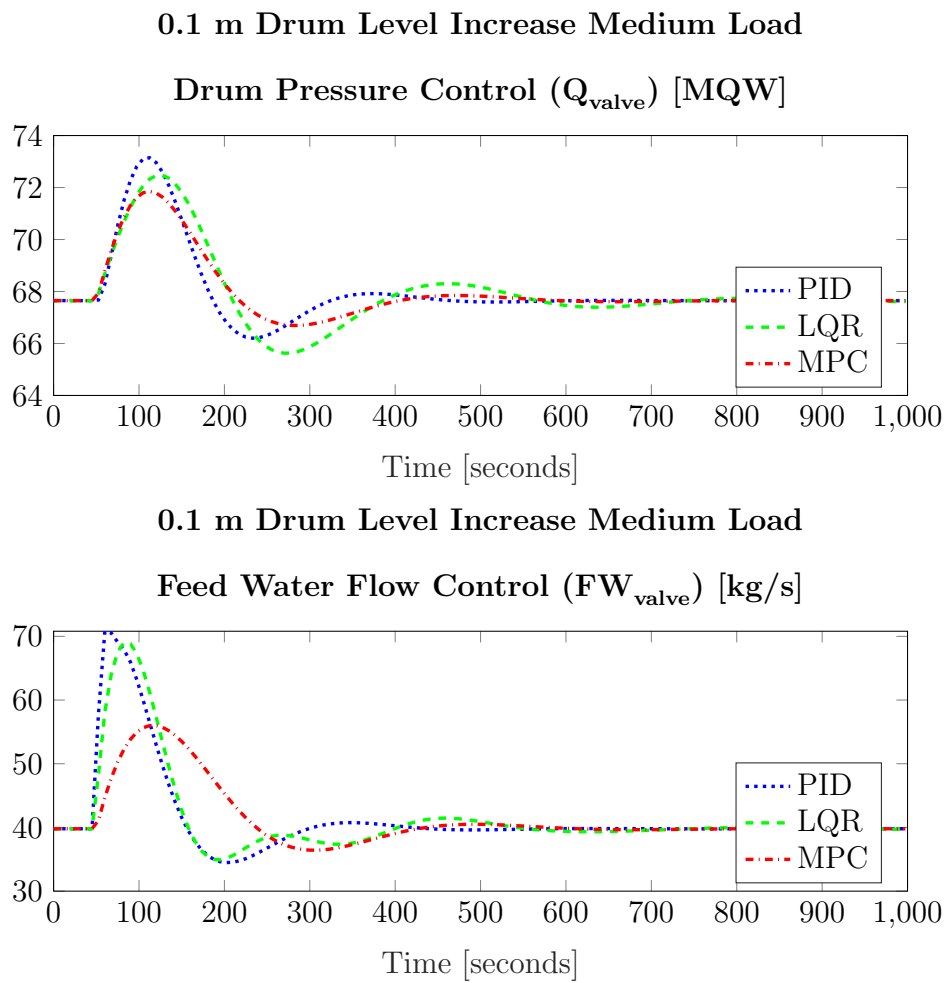


Figure B.10: Controller Input Response to Drum Level step of 0.1 at Medium Load

Medium Load Level Step Decrease Response

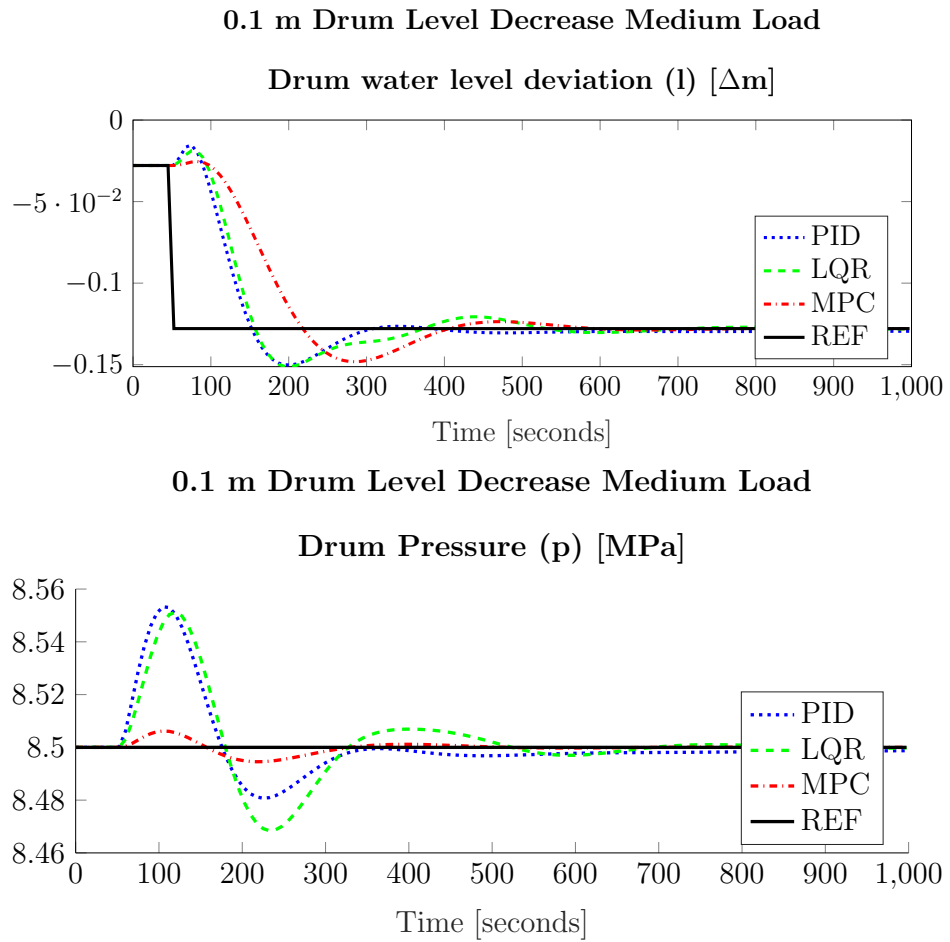


Figure B.11: Controlled Variables Response to Drum Level step of 0.1 at Medium Load

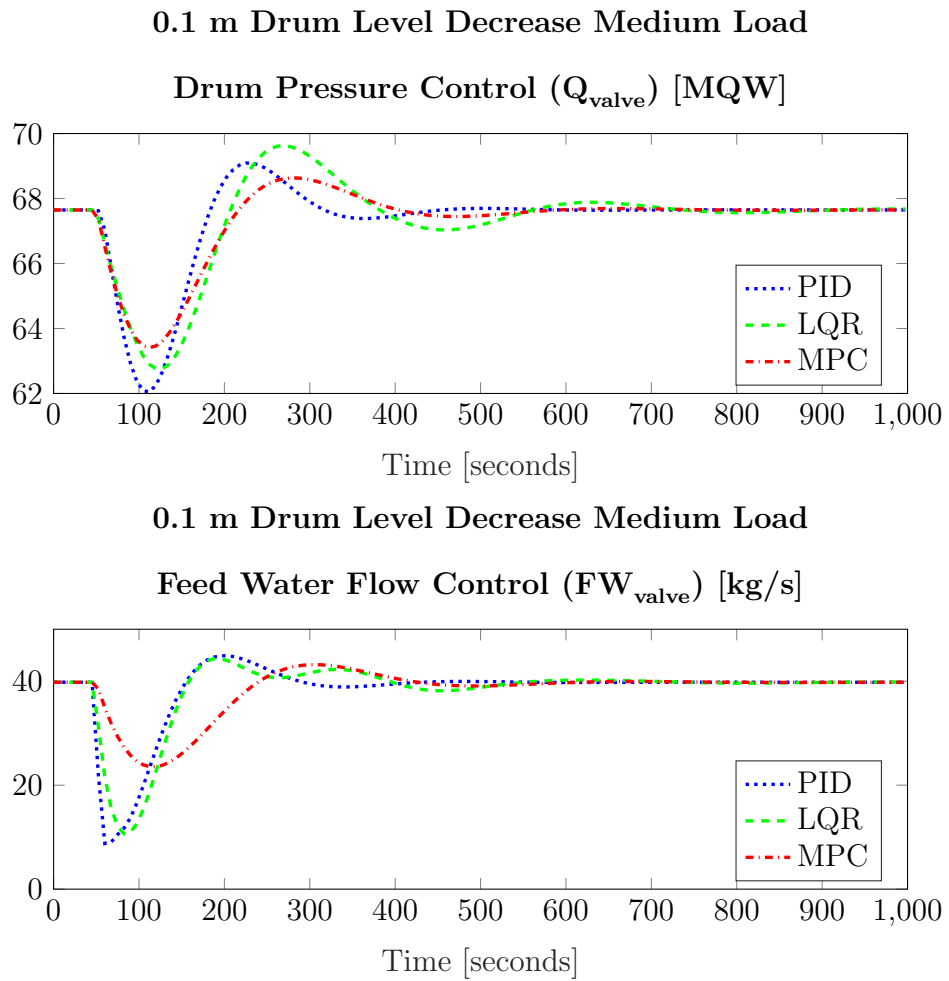


Figure B.12: Controller Input Response to Drum Level step of -0.1 at Medium Load

Medium Load Pressure Step Increase Response

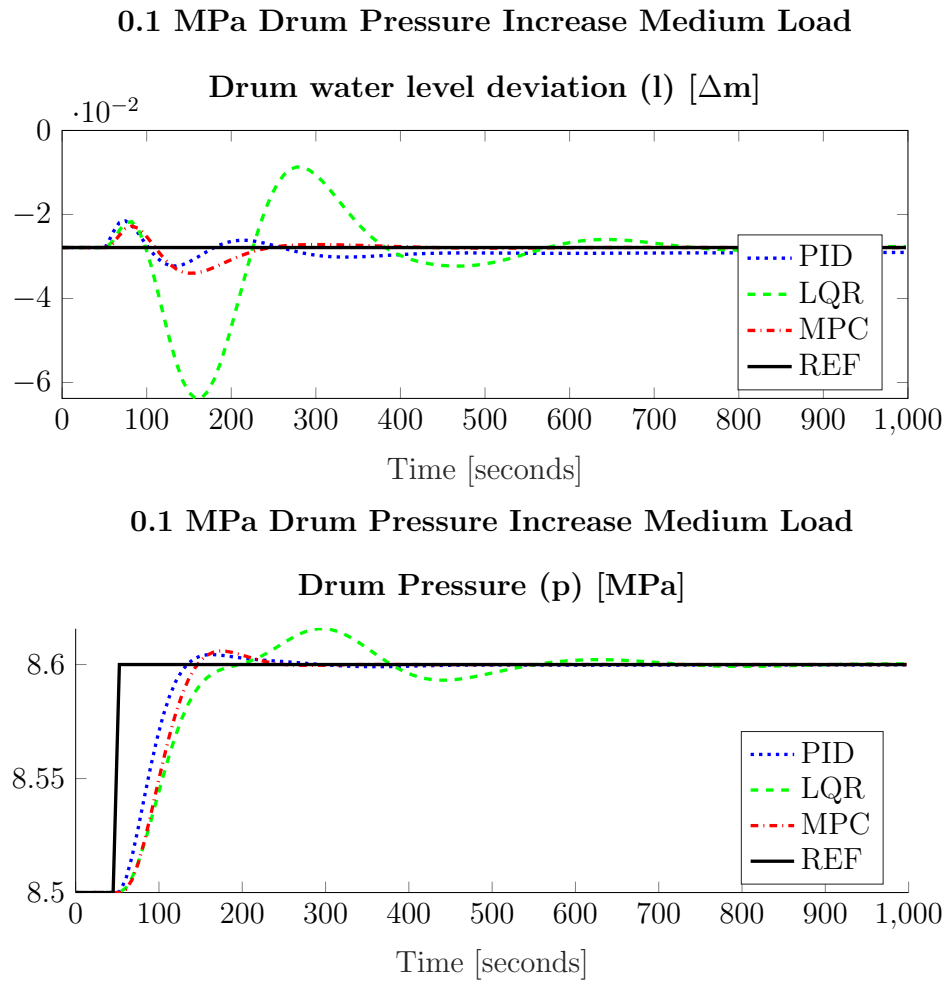


Figure B.13: Controlled Variables Response to Drum Pressure step of 0.1 at Medium Load

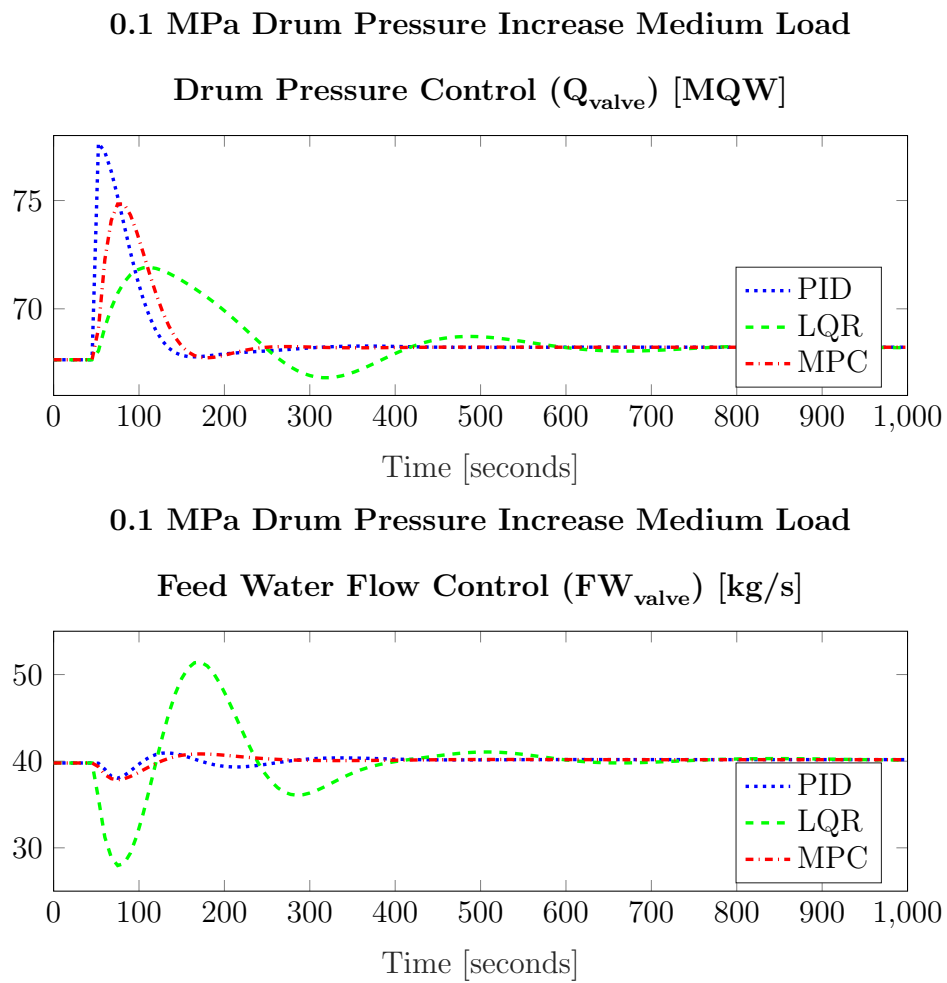


Figure B.14: Controller Input Response to Drum Pressure step of 0.1 at Medium Load

Medium Load Pressure Step Decrease Response

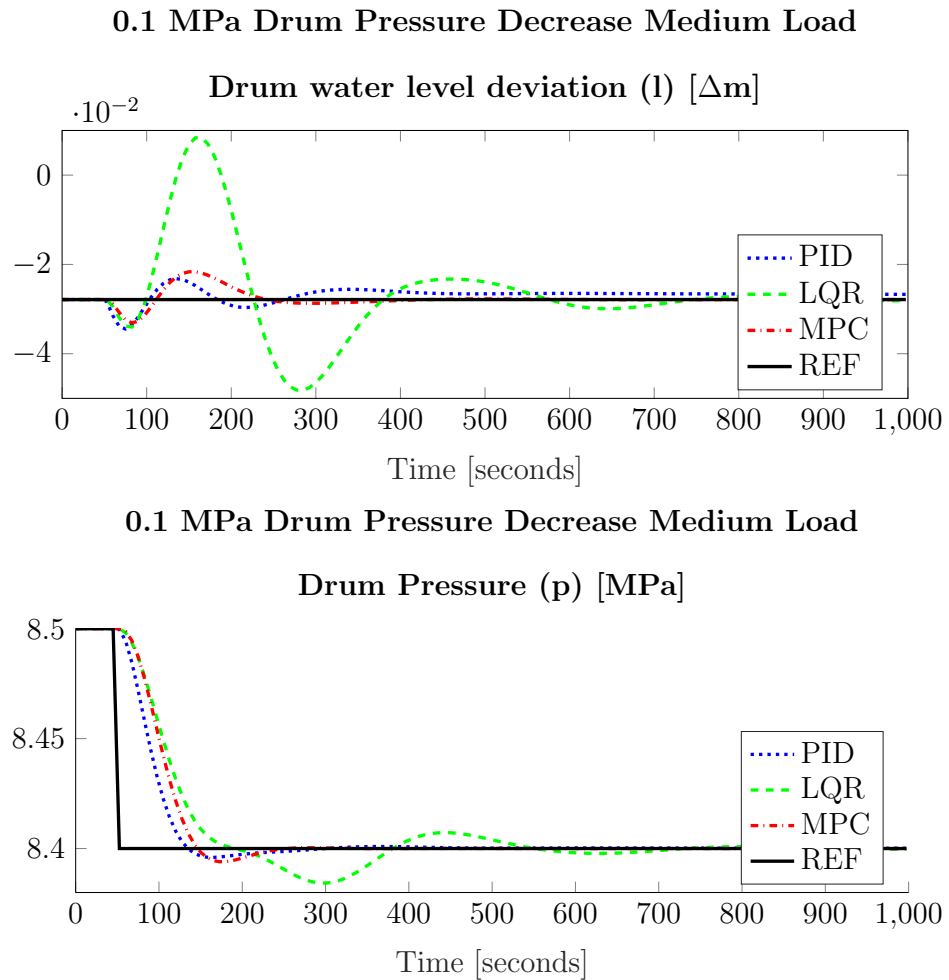


Figure B.15: Controlled Variables Response to Drum Pressure step of 0.1 at Medium Load

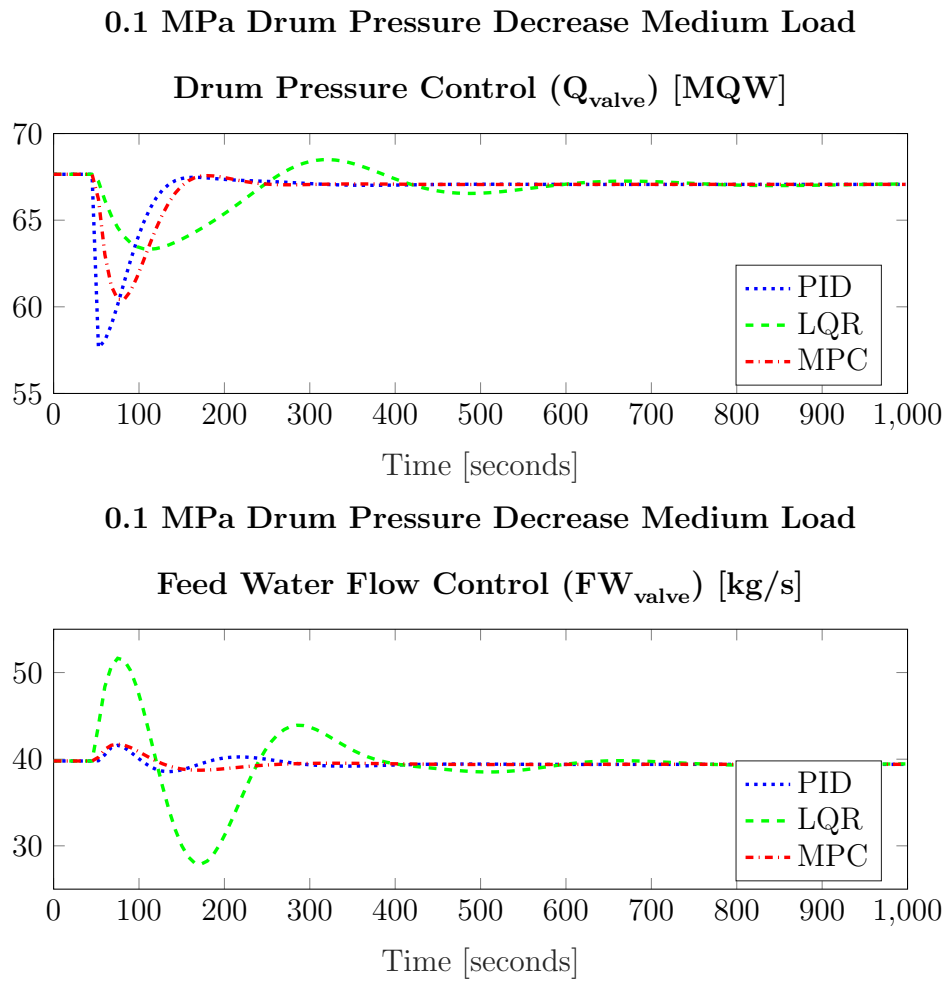


Figure B.16: Controller Input Response to Drum Pressure step of -0.1 at Medium Load

APPENDIX C

MATLAB FILES

X-Steam.m [4]

The code used in XSteam.m is available for download from the following link:

<https://www.mathworks.com/matlabcentral/fileexchange/9817-x-steam-thermodynamic-properties-of-water-and-steam>

A document detailing the functions can be found here:

<http://assets.openstudy.com/updates/attachments/4e134b420b8b56e555996beb-slnkktn-1310012884358-xsteamformatlab.pdf>

Borzellieri_Thesis.m

To save paper please contact me directly at Robert.A.Borzellieri@gmail.com for a copy of the MatLab script used. The code is entirely contained in a single script file, except for the XSteam functions noted above.